Genomic analyses for feed efficiency traits in American mink

by

Pourya Davoudi

Submitted in partial fulfillment of the requirements
for the degree of Doctor of Philosophy

at

Dalhousie University
Halifax, Nova Scotia
December 2023

Table of Contents

List of Tables

List of Figures

Abstract

Feed efficiency is a key factor in the economic outcomes of mink production systems, as the cost of feed accounts for the largest portion of their variable expenses. So far, the Canadian mink industry has relied solely on phenotypic selection as its main method of selection. Phenotypic data from 1,038-2,288 American mink with growth and feed efficiency traits were recorded in two different farms. In chapter 3, phenotypic and genetic parameters for growth and feed efficiency traits were estimated. The moderate heritabilities of feed efficiency-related traits in American mink, coupled with high favorable genetic correlations among them, confirmed the potential inclusion of these traits in genetic/genomic selection programs to achieve significant genetic improvements. The other chapters aimed to display the genetic architecture underlying feed efficiency-related traits. To this end, all individuals were genotyped using Affymetrix Mink 70K single nucleotide polymorphism (SNP) array. In chapter 4, the characteristics of copy number variations (CNVs) within the genome of American mink were determined through the examination of whole-genome sequencing data of 100 individuals. Biological pathway analysis on candidate genes overlapped with identified CNV regions (CNVRs) revealed several pathways related to growth (regulation of actin cytoskeleton, and cAMP signaling pathways), behavior (axon guidance, circadian entrainment, and glutamatergic synapse), lipid metabolism (phospholipid binding, sphingolipid metabolism and regulation of lipolysis in adipocytes), and immune response (Wnt signaling, Fc receptor signaling, and GTPase regulator activity pathways). Further, chapter 5 evaluated the association between CNVRs and 27 economically important traits in American mink. The findings revealed several significant CNVRs, which overlapped with genes reported to have impacts on growth and feed efficiency (*ARID1B, APPL1, TOX,* and *GPC5*), reproduction (*GRM1, RNASE10, WNT3, WNT3A,* and *WNT9B*), pelt quality (*MYO10*, and *LIMS1*), and Aleutian disease tests (*IFNGR2, APEX1, UBE3A*, and *STX11*). Similarly, chapters 6 and 7 aimed to identify runs of homozygosity (ROH) and their associations with growth and feed efficiency traits. The outcome suggested potential selection footprint in alignment with the breeding goals for mink, which include improving body length, reproductive performance, and fur quality. Furthermore, the results of the GWAS in Chapter 8 contributed to the identification of 153 potential candidate genes, some of which were known to have roles on the development of body size and feed efficiency, such as *TUBB, CDKN1A, SRSF3, GPRC6A, RFX6,* and *KPNA5*. Overall, the findings from this thesis provided useful information about the genetics of feed efficiency measurements for the mink industry, and identified potential candidate genes underlying feed efficiency traits, making them valuable as genetic markers in genomic breeding programs.

Acknowledgement

First and foremost, I would like to express deep appreciation to my supervisor, Dr. Younes Miar, who has not only been a dedicated mentor but has also played the role of an older brother in my personal development. His guidance has significantly influenced my growth, not just academically, but also as an individual. I am profoundly thankful for the privilege of learning from Dr. Miar and for the profound impact he has had on my life.

I would also like to extend my gratitude to the members of my thesis committee, Dr. Bruce Rathgeber and Dr. Stefanie Colombo, for their time, expertise, and valuable insights. Their constructive feedback and thoughtful input have greatly enriched the quality of this work. I am also extremely grateful for the outstanding assistance provided by Dr. Duy Ngoc Do, a valued member of our research group. His support, expertise, and collaborative spirit played a crucial role in the successful completion of this thesis. I would like to extend special thanks to our lab members, Guoyu Hu and Persia Carol Thapa, with whom I learned the true meaning of friendship.

The full financial support provided by Natural Sciences and Engineering Research Council of Canada (NSERC), Mitacs, Canada Mink Breeders Association, Nova Scotia Mink Breeders Association, Nova Scotia Department of Agriculture, Mink Veterinary Consulting and Research Service Ltd, ACENET and the Digital Research Alliance of Canada are gratefully acknowledged. I am very grateful to the Canadian Center for Fur Animal Research, Millbank Fur Farm, North American Fur Auction, SAGA, Neogen, and Miar Lab staff for collecting and providing the data. Lastly, I want to say a heartfelt thank you to my wife, Zahra Alizadeh, whose unwavering support and understanding have been my rock throughout this journey. Your love and encouragement have been my constant inspiration.

CHAPTER 1. Introduction

1.1 Introduction

American mink (*Neogale vison*) has long been considered as one of the most valuable sources of pelt in the fur industry. Yet, the current mink industry faces numerous challenges, notably the increasing costs of production and the emerging diseases, both of which impede the progress toward achieving sustainability in mink breeding (Karimi et al. 2021a). An effective solution within the mink industry involves improving economically important traits like feed efficiency, growth, reproduction, and fur quality through breeding programs.

The profitability of livestock production depends on minimizing costs without reducing quality or production. Providing feed for animals represents a significant portion of the variable costs in mink production programs (Berg and Lohi, 1992; Sørensen et al. 2003). Feed efficiency is described as the association between animal intake (input) and production (output). Currently, the Canadian mink industry selects their breeding animals only based on phenotypic performance (Karimi et al. 2019); however, the genetic component of feed efficiency traits has not yet been investigated. Therefore, enhancing feed efficiency is the optimal approach to efficiently utilize limited resources and promote sustainability within the mink industry.

Before incorporating a novel trait into the breeding programs, the heritability of the trait and its genetic correlation with other breeding goal traits must be identified (Brito et al. 2020). Heritability is defined as the ratio of genetic variation to overall phenotypic

variation, and in turn helps us determine the degree to which the potential trait is under genetic control (Visscher et al. 2008). Published studies indicated that feed efficiency-related traits are moderately heritable traits, and there is a good potential for them to respond to selection (Arthur and Herd, 2005). Additionally, it is essential to understand the magnitude and direction of correlations between feed efficiency and other economically important traits for implementing a successful breeding program (Mu et al. 2016). Traits with high positive correlations tend to improve simultaneously, but high negative correlations between traits lead to the opposite direction of improvement.

Further genetic advancements have become possible due to the introduction of molecular genetics techniques (Andersson and Georges, 2004). Several genomic markers were produced by the application of gene identification and quantitative trait loci (QTL) discoveries in livestock, which were integrated into selection programs in many species (Misztal, 2006). As a result of significant progress in developing single nucleotide polymorphism (SNP) arrays, along with the advances in statistical and computational approaches in livestock, there has been a surge in the ability to apply genome-wide association studies (GWAS) and genomic selection (Sharma et al. 2015). Detecting genetic variants that contribute to economically important traits is critical in animal genetics (Sharma et al. 2015). Copy number variants (CNVs) and other forms of structural variation like runs of homozygosity (ROH) are crucial in understanding of the genetic architecture of traits (Peripolli et al. 2017; Goshu et al. 2018). The CNV refers to a structural variation in an individual's genome that changes the number of copies of a genomic region (Zhang et al. 2009). Therefore, CNVs play significant roles as genetic variation sources complementary to SNP data. The ROH can reveal the level of inbreeding, the genetic

relationships between individuals, selection pressure, mating schemes and the age of inbreeding (Purfield et al. 2012; Zavarez et al. 2015; Mastrangelo et al. 2018). Detecting ROH can also assist scientists in uncovering the genetic selection footprint within the genome (Peripolli et al. 2017).

Genomic selection can enhance the genetic gain for feed efficiency traits by reducing the generation interval and increasing the accuracy of selection (Brito et al. 2020). The information given within the genomic analyses will allow us to build a capable mapping tool for identifying extra loci underlying different biochemical pathways of feed efficiency traits in mink. Researchers have made several attempts to recognize genes that lead to the variation in these traits (Brito et al. 2020; Prakash et al. 2020). Moreover, integrating GWAS results with the genomic selection method enhances the power to identify genomic variation potentially useful in mink breeding. Although there has been significant development of genomic programs in other domestic animals, genomic methods have not yet been developed in mink breeding systems.

1.2 Objectives

The aim of this dissertation is to improve growth and feed efficiency traits in American mink. The specific objectives include:

a) Providing appropriate feed efficiency indicators in American mink.
b) Estimating heritability of feed efficiency traits in American mink.
c) Estimating genetic and phenotypic correlation of feed efficiency traits with each other in American mink.

d) Investigating the distribution and pattern of chromosomal segments of mink genome such as ROH and CNV.

e) Applying the CNV and ROH-based association studies with economically important traits in American mink.

f) Performing the genome-wide association studies for growth and feed efficiency traits in American mink.

g) Examining the potential impacts of CNV, ROH, SNP, and the overlapped genes on traits of economic interest for mink selection programs through in-depth functional annotation analyses.

CHAPTER 2. Literature review[1]

2.1 Introduction

Providing feed for an animal is one of the main input costs in any animal production system. The expenses associated with feed can account for 60-70% of total costs for mink production systems (Berg and Lohi, 1992; Sørensen et al. 2003). Feed efficiency (FE) can be defined as the association between feed intake (input) and production (output), and therefore, improving FE will reduce production costs. In order to relate feed intake to animal efficiency, it is necessary to apply comprehensive strategies for FE measurements. One of the most common measures of FE is feed conversion ratio (FCR) that is defined as the ratio of body weight gain to feed intake (Skinner-Noble and Teeter 2003). Another measure of FE is residual feed intake (RFI), as proposed by Koch et al. (1963). It is described as the difference between actual feed intake and expected intake based on an animal's body size and maintenance over a time period.

FE traits are economically important traits that are controlled by many genes and environmental factors. Several studies have been conducted to analyze these traits. Examples include, evaluation of breeding values for selection candidates (Miar et al. 2015; Garrick, 2017) or identifying candidate genes for FE (Do et al. 2014; Fu et al. 2020). Some studies successfully identified quantitative trait loci (QTLs) that are related to feed efficiency in different livestock species (Andersson et al. 1994; Georges et al. 1995),

[1] A version of this chapter has been published in Frontiers in Genetics. Davoudi et al. 2022 Application of genetic, genomic, and biological pathways in improvement of swine feed efficiency. 13:903733. doi: https://doi.org/10.3389/fgene.2022.903733

however, due to low resolution in QTL mapping analysis and complex genetic architecture in most QTLs, QTL mapping has not been very successful (Andersson, 2009). Genome-wide association studies (GWAS) is a powerful tool for identification of causal genes or regulatory elements for economically important traits such as FE traits in livestock. GWAS has some benefits, e.g. the power to identify genetic variants and the practical approach to evaluate genetic architecture of complex traits (Kronenberg, 2008). Genomic data are extensively accessible in the livestock industry and supply a profitable means of estimating genetic merit. This is helpful for selection decisions that enhance genetic gains. Genomic selection is now a widely used animal breeding program approach since it enhances the selection for difficult and expensive traits to measure, such as FE and growth traits (Meuwissen et al. 2013). The objective of this chapter is to provide a summary of different measurements of FE, then present the state of the art for genetic and genomic studies for FE. This is followed by an overview of the genomics tools that can be applicable to detect genetic variations associated with FE traits. Finally, there is a discussion of current and future methods and technologies that could improve FE traits.

2.2 Measures of feed efficiency

Body weight gain per unit of feed consumed by an animal is a general measurement of FE in most studies (Patience et al. 2015). Although FE has conventionally been described as the ratio of feed consumed compared to the growth achieved by an animal, other FE indicators have been proposed recently (Crowley et al. 2010; Berry and Crowley, 2012). Despite the importance of FE as a critical parameter in breeding programs, there is little consensus regarding the optimized approach to achieve ideal FE (Gaines et al. 2012). Firstly, this lack of concensus might be due to the fact that a complex biological process

affects FE (Cantalapiedra-Hijar et al. 2018). Secondly, there is controversy surrounding how to define and measure FE traits (Patience et al. 2015). Finally, it should be noted that measuring FE is remarkably difficult to measure; compared to growth traits, which can easily be obtained by weighing the animals at specific periods in a lifetime (Hoque and Suzuki, 2009).

2.2.1 Feed conversion ratio

Feed conversion ratio (FCR; feed to body weight gain ratio) has traditionally been investigated as a simple and relatively common indicator of FE (Hoque and Suzuki, 2009). Although FCR is considered an essential part of the goal in breeding programs, there are some definite issues with FCR. Selection based on FCR can lead to large-sized animals at a mature age that might have high energy requirements for maintenance (Smith et al. 2010). In addition, high genetic correlations with FCR, growth, body size and body composition, cause the changes in component traits in future generations (Gunsett, 1984). Finally, animals with similar FCR might vary in growth rate and feed intake (Smith et al. 2010). Thus, there is a need to define an indicator that negates the effect of body weight on FE of each animal.

2.2.2 Residual feed intake

Residual feed intake (RFI) is another FE measurement proposed as an alternative to FCR. RFI is defined as the difference between the observed feed intake and the expected feed intake. This was first proposed by Koch et al. (1963). They suggested that feed intake could be adjusted for body weight and weight gain. Since RFI is independent of body weight and average daily gain (ADG), selection for RFI can alter the energy of maintenance

requirements without changing the body size and production level. In addition, due to the RFI's mathematical independence to animal production, this method is notably suitable to investigate the biological mechanisms underlying the FE variation in each individual (Berry and Crowley, 2013). However, RFI calculation might be dependent on the predicted feed requirement for production and maintenance (Do et al. 2013), which might cause difficulty in comparing results of different studies. In addition, in the case where genetic correlation exists between FE and maintenance traits, the heritability estimation might be unreliable (Lu et al. 2015).

2.2.3 Other feed efficiency indicators

A wide variety of terms have been proposed to define FE, which can be applied as alternative measurement for FCR and RFI (Berry and Crowley, 2013). Kleiber ratio (KR), defined as growth rate/body mass$^{0.75}$, was suggested as an indirect selection parameter for feed conversion (Kleiber, 1947). It is acknowledged that KR is a useful indicator in selection for growth efficiency since it does not require the calculation of individual intake and enables ranking of individuals with high growth efficiency relative to body size (Köster et al. 1994). Another indicator of FE is partial efficiency of growth (PEG), described as the ratio of ADG per unit of feed intake consumed for growth. Studies reported that PEG has some advantages over FCR since it has considerably lower genetic and phenotypic correlation with ADG compared to ADG and FCR (Arthur et al. 2001; Nkrumah et al. 2004). Residual gain (RG) and residual feed intake and gain (RIG) are other alternative measures of FE (Crowley et al. 2010; Berry and Crowley, 2012). RG is defined as the difference between the actual ADG and the expected ADG and combines the measurements of growth and feed intake in a similar principle to RFI. However, for RFI,

feed intake is regressed on ADG and body weight, but in the calculation of RG, ADG is regressed on feed intake and body weight (Crowley et al. 2010). RIG, proposed by Berry and Crowley (2012), combines RFI and RG to identify efficient and fast-growing animals independent of their body weights. Therefore, the advantages of both reduced feed intake and greater ADG are represented in RIG.

2.3 Genetics of feed efficiency

2.3.1 Heritability

Generally, estimated heritability of traits (defined as the ratio of genetic variation to the overall phenotypic variation) is used to determine the degree to which traits are under genetic control. In order to have an accurate estimate of heritability, a well-established measure of FE, as well as complete and precise pedigree information on many individuals are required.

Although in few studies, heritability estimates for RFI in American mink have been reported within a range spanning from 0.13 to 0.49 (Shirali et al. 2015; Madsen et al. 2020). The diverse range of heritability estimates presented in the literature is due to evaluation of different populations, ages, diets, environments, and the number of animals in the study. A controversial subject related to RFI is that this term or other unspecified feed intake terms are referred to as FE. The residual might be associated with random errors, for example, prediction and measurement errors, inaccurate recording or feeding loss (Van der Werf, 2004). These errors can reflect the phenotypic variation, which might change the heritability of RFI. The heritability for FCR has not been reported in American mink, yet its mathematical inverse gain:feed ratio reported as 0.30 (Sørensen, 2002). The only

estimates of heritability reported in American mink for component traits (such as ADG and DFI) were 0.43 and 0.38 for ADG and DFI, respectively (Sørensen, 2002). It is well-documented that FE-related traits are moderately heritable traits, and therefore, have good potential to respond to selection.

2.3.2 Genetic correlation

Although heritability can provide information about the candidates' genetic merit for traits of interest, understanding the magnitude and direction of correlations between FE traits and other economically important traits is essential to establish a successful breeding program (Brito et al. 2020). Traits with high positive genetic correlations tend to improve simultaneously, but high negative genetic correlations between traits cause the opposite direction of improvement.

The FCR and RFI genetic improvement strategies are different and rely on their particular genetic correlations with other production traits. Although there is no study inverstigated the genetic correlation between FCR and RFI in American mink, the high and positive genetic correlation between FCR and RFI traits have been documented in other species, such as pig (Do et al. 2013), cattle (Brito et al. 2020), and chicken (Prakash et al. 2020). In mink, the genetic and phenotypic correlations of RFI and BW are relatively low and range between -0.08 to 0.12 (Madsen et al. 2020). Selection based on RFI is also associated with animal characteristics related to energy cost. Decreasing the maintenance energy requirements leads to decreased physical activity and reduced heat production, which could significantly contribute to higher energy efficiency (Gilbert et al. 2017). Therefore, low RFI individuals are desired since they spend less energy on feed consumption, interacting with others, heat production, and maintenance requirements (Gilbert et al. 2017). In mink,

RFI is reported to be highly correlated with DFI, indicating that selection against RFI can decrease DFI (Madsen et al. *2*020). Nevertheless, it is important to consider differences in body weight of animals using in genetic parameter estimation, since animals with different weights might have different maintenance requirements, and thereby have an impact on the estimated parameters, genetic correlations and prediction of FE traits (Patience et al. 2015).

2.4 Genomics applications

Genetic variation is a fundamental factor that outlines the foundation of heritable traits. Therefore, to gain a comprehensive understanding of genes, it is essential to investigate the genetic variations present, and how these variations may impact on gene function, and thereby, how they can shape the phenotype (Barnes, 2010). Single nucleotide polymorphisms (SNPs) represent the predominant form of genetic variation among individuals within a specific species, arising from mutations that introduce base-pair differences between chromosome sequences (Leaché and Oaks, 2017). The desire characteristics of the SNPs, including their genome-wide distribution and their substantial prevalence, render them as valuable sources of genetic variation.

Recently, a major scientific milestone in genomic analysis for American mink was achieved through the availability of the first chromosome-level genome assembly (Karimi et al. 2022). The high-quality mink reference genome assists in uncovering the genetic mechanisms within the American mink genome, ultimately enhancing genetic improvement through genomic breeding programs. In addition, it serves as the foundation for practical scientific advances for the SNP discovery and the design of SNP arrays, enabling researchers to conduct GWAS and implement genomic selection in American mink (Karimi et al. 2022). Notably, the use of SNP genotyping arrays to generate large

SNP data sets has become routine (Sharma et al. 2015). This method is widely applicable in diverse genomic studies, ranging from pinpointing the selection footprint, detecting the genetic variants associated with economically important traits to implementing genomic selection in livestock species (Kranis et al. 2013). To this end, our research group at Dalhousie University developed the first medium-density 70K SNP array for American mink, which in turn provided the basis of the genomic analyses for this species (Hu et al. 2023).

2.4.1 Copy number variation

Copy number variation (CNV) is a genomic phenomenon characterized by differences in the number of copies of a particular DNA segment within an individual's genome (Zhang et al. 2009). Unlike SNPs, which involve changes in single DNA bases, CNVs involve changes in larger segments of the genetic code, varying in size from one kilobase to several megabases (Mills et al. 2011). Because of thier greater size, CNVs cover broader chromosomal regions in contrast to SNPs, and as a result, they have the potential to influence gene expression, modify gene dosage, and disrupting coding sequence, which could ultimately impact economically important phenotypes (Saitou and Gokcumen, 2020). In the last decade, several studies attempted to map the CNVs in the genome of livestock species, including cattle (Lee et al. 2020), chicken (Wang et al. 2010), pig (Paudel et al. 2013), sheep (Fontanesi et al. 2011), and buffalo (Strillacci et al. 2021). It is well-documented that the CNVs are associated with different economically important traits, such as growth (Li et al. 2022), feed efficiency (Xu et al. 2019), reproduction (Zhou et al. 2018), and health traits (Estrada-Reyes et al. 2022). Despite the potential impact on the

traits of interest, there has been no research conducted to characterize CNV in the American mink genome and their potential effects on economically important traits.

2.4.2 Runs of homozygosity

Runs of homozygosity (ROH) are consecutive segments of homozygous genotypes within an individual, arising from selection processes, where parents pass on identical haplotypes to their offspring (Ceballos et al. 2018). The distribution of ROH throughout a population's genome, often referred to as ROH islands, reveals specific genomic areas that are impacted by selection footprint (Peripolli et al. 2017). This, in turn, offers valuable insights into the genetic adaptations and evolutionary mechanisms contribute to the shaping of populations (Peripolli et al. 2017). Using whole-genome sequencing data, Karimi et al. (2021b) reported high abundance of short ROH segments, indicating distant inbreeding approximately over 50 generation ago in American mink. Despite the importance of ROH islands and the possibility of using ROH in association studies to detect homozygous genomic regions associated with complex traits in livestock, this approach has yet to be investigated in American mink.

2.4.3 Genome-wide association analyses

Detection of causative mutations underlying QTLs has always been challenging in domestic animals (Zhang et al. 2012). Compared to conventional QTL mapping methods, GWAS has the power to identify genetic variants with even modest effects (Hirschhorn and Daly, 2005). In livestock species, the advancement of genomic technologies has enabled researchers to perform different GWAS to identify genomic regions and candidate genes associated with economically important traits, including meat quality and quantity,

reproductive traits, and FE traits. In several studies, numerous regions with minor effects have been detected for FE traits, indicating that feed efficiency is a polygenic characteristic (Onteru et al. 2013). Feeding is one of animals' most conserved activities, and a key mechanism for survival is to regulate feed intake (Bader et al. 2007). FE traits are quantitative traits with complex genetic architecture (Do et al. 2014). Therefore, an important field of research in livestock genetics and breeding is the discovery of candidate genes underlying these traits.

2.5 Future perspectives and opportunities

2.5.1 Phenotypic measures and genetic analyses

To date, several ratio and residual traits have been developed as FE measures. Although ratio traits have some advantages, such as the ease of calculation and interpretation, their main drawback is the strong correlations between ratio traits and their component traits (Berry and Crowley, 2013). On the other hand, FE can be measured independently of production level using residual measurements like RFI, which are based on the mathematical model considering energy requirements for body maintenance and production over a specific production time period. As the model implies in RFI, the feed intake and production correlation is assumed to be constant at all production and feed intake levels. However, the true biological efficiency depends on the degree of production and feed intake, which means that the correlation of maintenance requirement, production and feed intake varies over the growth period (Van Der Werf, 2004). In this context, it is suggested to apply a random regression model as it considers the variation within animals between different growth period stages (Veerkamp and Thompson, 1999).

Over recent decades, many feeding strategies have been introduced by breeding companies to facilitate the measuring feeding process in a precise way to achieve accurate measurement of individual FE on a large scale that can increase the genetic gain and productivity. Nowadays, a vast amount of data can be extracted from the state-of-the-art technologies such as sensors for precision feeding systems, machine vision sensors, infrared thermal imaging sensors, microphones, and radio frequency identification (RFID) tags. Introducing new traits for selection of FE can significantly improve the accuracy of prediction. Martinsen et al. (2015) introduced new FE traits like fat efficiency and lean meat efficiency. Their results indicated that these traits help breeders select animals with high genetic potential for efficient deposition of lean meat at low feed costs. Furthermore, measuring the components of FE such as net FE (digestibility, net energy, heat production, and methane energy output), activity and behaviour (feeding per day, total time spent eating per day, feed intake, and time spent eating per visit), and robustness, might help breeders select more efficient individuals in diverse breeding conditions. It was shown that there are positive phenotypic and genetic correlations between feeding behaviour and FE traits, indicating their possible role on selection of feed-efficient individuals (Von Felde et al. 1996; Lu et al. 2017). A deep understanding of the feeding behaviour can help breeders to improve feeding strategies, and thus, increase the productivity (Andretta et al. 2016).

2.5.2 Beyond genomics

Although significant progress has been achieved in understanding the complexities of genetic control of FE traits, the breeders are always seeking ways to improve FE in their breeding programs to obtain greater genetic progress. One practical way to enhance genetic gain is to maintain genetic variation. Gene editing technology, which generates progeny

with selected mutations, can add variation to the population (Wang et al. 2015). Modification of genes might allow breeders to confer the desired phenotypes to improve production traits or disease resistance. Likewise, by focusing on modification in the mink genome, researchers have the potential to enhance mink feed efficiency in the future. In recent years, numerous "omics" technologies such as proteomics, transcriptomics, metabolomics, epigenomics, and metagenomics have generated valuable data in the research of FE. Over time, integrating such technologies can give us more accurate selection of animals with better FE. The integration, joint modeling, and analyses of different "omics" data through system genetics would increase the power of identifying causal genes, regulatory networks and pathways that might lead to improve economically important traits like FE. Ultimately, the information derived from the integration such as biomarkers and gene networks or causal genes and variants can be incorporated into genomic selection programs to achieve higher accuracy and genetic gain.

CHAPTER 3. Genetic and phenotypic parameters for feed efficiency and component traits in American mink[1]

3.1 Introduction

The American mink (*Neogale vison*), a semi-aquatic species originated in North America, is one of the most widespread animals used in the fur industry. The domesticated farmed mink has been bred in fur farms in China, Russia, North Europe, and North America because of its high-quality fur, leading to a great economic profit for countries (Anistoroaei et al. 2009; Thirstrup et al. 2015). Recently, a large culling has been carried out in several countries due to spreading the Covid-19 pandemic in their infected farms (Oreshkova et al. 2020; Aguiló-Gisbert et al. 2021; Boklund et al. 2021). Feed cost has been known as the single largest expense, up to 60-70% of the total cost in mink production (Berg and Lohi, 1992; Sørensen et al. 2003). Therefore, efficiency in the use of feed resources of growing animals is a key criterion to improve economic sustainability in mink production.

The FE can be measured by RFI, which is defined as the difference between actual feed intake and predicted feed intake required for maintenance and growth estimated through a regression model involving metabolic body weight (BW) and average daily gain (ADG) (Koch et al. 1963). As a linear trait, RFI has been reported to be independent of growth rate and body weight (Herd et al. 2003). Therefore, the advantage of identifying animals with low RFI values is to decrease feed intake without having adverse effects on animal growth

[1] A version of this chapter has been published in Journal of Animal Science. Davoudi et al. 2022. Genetic and phenotypic parameters for feed efficiency and component traits in American mink. 13:903733. 100(8), skac216. doi: https://doi.org/10.1093/jas/skac216

and size. Even though RFI might be a good FE indicator, it might lead to a lower profit, as slow-growing animals with relatively low feed intake will receive an excellent RFI value (Berry and Crowley, 2012). Residual gain (RG) was then introduced to adjust the ADG relative to feed intake (Koch et al. 1963). Animals with positive RG could have faster growth rates but are not associated with feed intake (Crowley et al. 2010). Alternatively, residual intake and gain (RIG) was proposed by (Berry and Crowley, 2012) to combine the desired characteristics of both RFI and RG. In other words, RIG can select fast-growing individuals with low feed intake, while still being independent of BW.

Although there might be a possibility to achieve a substantial genetic improvement for FE traits through genetic improvement, there is still a need to collect large-scale feed intake records for calculating the FE indicators. This is possible in other livestock industries such as cattle (Esfandyari and Jensen, 2021) and pigs (Santiago et al. 2021), but can be an issue for mink industry, as it requires the state-of-the-art technologies for recording the feed intake data introducing substantial cost to this industry. Alternatively, Kleiber ratio (KR), which is the ratio of weight gain to metabolic BW, can be an appropriate indicator for efficiency of feed conversion as it does not require individual intake to be measured and allows classification of animals with high efficiency of growth relative to body size (Kleiber, 1947). In addition, studies reported a high genetic correlation between KR with other FE traits and growth traits, and thereby, the selection for KR might lead to improvement of FE and growth traits (Abegaz et al. 2005).

Feed efficiency in mink has been investigated in terms of gain:feed (Berg and Lohi, 1992), FCR (Nielsen et al. 2011; Nielsen et al. 2012), and RFI (Shirali et al. 2015; Madsen et al. 2020). To incorporate FE in mink production, the magnitude of correlations between ratio

traits and BW, and the independence of FE traits with BW should be considered. On the one hand, the price of pelt has been reported to have strong correlations with BW and body length (BL), but on the other hand, BW and BL have negative correlations with litter size (Nielsen et al. 2011), and fur quality traits (Lagerkvist et al. 1994). Madsen et al. (2020) has already shown the possibility of selecting RFI in Danish brown mink with no negative effects on BW. However, to the best of our knowledge, there is no comprehensive study that examined different FE traits and their correlations with component traits in American mink. Therefore, the focus of this chapter was to model five different measures of FE traits including FCR, KR, RFI, RG, and RIG, and to estimate the phenotypic and genetic correlations among these FE measures, and six component traits, including FBW, FBL, harvest weight (HW), harvest length (HL), daily feed intake (DFI) and ADG in American mink.

3.2 Materials and Methods

The proposed work was approved by the Dalhousie University Animal Care and Use Committee (certification# 2018-009, and 2019-012), and mink used in the current chapter were cared for according to the Code of Practice for the Care and Handling of Farmed Mink (Turner et al. 2013) guidelines.

3.2.1 Animals and traits

In this experiment, 1,088 animals from the Canadian Centre for Fur Animal Research (CCFAR) at Dalhousie University, Faculty of Agriculture (Truro, NS, Canada), and 1,477 animals from Millbank Fur Farm (Rockwood, ON, Canada), born in 2018 and 2019, were randomly selected for data collection. Mink were housed under standard farming

conditions, and diets were based on the by-products of human food production, which were adjusted according to animal requirements in each production period. The detail information regarding the feed ingredients, chemical composition, and metabolic energy of diet during the different time periods are provided by Do and Miar (2020). Each annual cycle of mink reproduction was started by mating between males and females at the beginning of March. Mink kits were born in late April or early May and weaned around the end of June. The experiment was designed during the growing-furring period, from August 1st to November 14th. In CCFAR farm, each animal was kept separately at different cages, and feed was distributed to each cage every day. Allocated feed to each cage was regulated up and down in case there was little or too much leftover in order to accurately meet the *ad libitum* access every day. Feed intake (FI) was then measured daily, subtracting the quantity of feed supplied by the amount of feed leftovers.

All animals were weighed individually at the beginning of the test period (August 1st), at the final day of the test period (November 14th), and at the harvest day (December 10th). Body length was measured at the final test day (November 14th) and at harvest day (December 10th). For the commercial farm (Millbank Fur Farm), due to extensive laboring requirements for recording, only harvest weight and harvest length (December 10) were measured, and FI was recorded only for year 2019. After merging the data from the two farms, 2,288 records were available for harvest weight (HW) and harvest length (HL), and 1,906 records for FI. Due to the lack of BW records on the test period for Millbank Fur Farm, the total number of calculated records for FE traits was limited to the number of BW and FI records from CCFAR farm.

Daily feed intake (DFI) was calculated based on the average FI values obtained during the test period. The average daily gain (ADG) was calculated as follows:

$$ADG = \frac{Final\ BW - Initial\ BW}{DOT},$$

where final BW is the BW at the final day of test period, Initial BW is the BW at the beginning of test period, and DOT is the number of days on the test.

The feed conversion ratio (FCR) was calculated as:

$$FCR = \frac{DFI}{ADG}$$

Mid-test metabolic BW ($BW^{0.75}$) and Kleiber ratio (KR) were computed as:

$$BW^{0.75} = \left(\frac{Initial\ BW + Final\ BW}{2}\right)^{0.75}$$

$$KR = \frac{ADG}{BW^{0.75}}$$

The following linear regression model was fitted to estimate the residual feed intake (RFI):

$$DFI = \beta_0 + \beta_1 ADG + \beta_2 BW^{0.75} + \varepsilon,$$

where β_0 is the intercept, ε is RFI, and β_1 and β_2 are the partial regression coefficients of DFI on ADG and $BW^{0.75}$, respectively.

To estimate the residual gain (RG), the following linear regression model was fitted as:

$$ADG = \beta_0 + \beta_1 DFI + \beta_2 BW^{0.75} + \varepsilon,$$

where β_0 is the intercept, ε is RG, and β_1 and β_2 are the partial regression coefficients of ADG on DFI and $BW^{0.75}$, respectively.

Residual intake and gain (RIG) was calculated based on the method proposed by (Berry and Crowley, 2012) as follows:

$$RIG = \left(-1 \times \left(\frac{RFI_i}{RFI_{sd}}\right)\right) + \left(\frac{RG_i}{RG_{sd}}\right),$$

where RFI_i, is the RFI for the individual animal, RFI_{sd} is the standard deviation of RFI for all animals, RG_i is the residual gain of the individual animal, and RG_{sd} is the standard deviation of RG for all animals.

3.2.2 Statistical and genetic analyses

For each trait, an optimal model was defined by testing the significance of fixed and random effects. The fixed effects were farm (CCFAR and Millbank Fur Farm), sex (male and female; 1~1 ratio), color-type (dark, demi, mahogany, pastel, and stardust), row-year (year: 2018 and 2019; row: 1, 4, 5, 7, 8, and 11), and age of animals (in days). The fixed effect of farm was tested for HW, HL, and DFI as the records were available for both farms. The fixed effects were statistically tested ($P < 0.05$) using univariate models in Asreml-R version 4 (Butler et al. 2018). The significance ($P < 0.05$) of random common litter effects was only tested for HW and HL, as repeated dams were used only for HW and HL in Millbank Fur Farm. The significance ($P < 0.05$) of different random effects for each trait was tested by comparing the full and reduced models as follows:

$$-2\ (logL_{reduced\ model} - logL_{full\ model}$$

$$\sim x^2_{df\ (full\ model) - df(reduced\ model)},$$

where logL and df are log-likelihood and degrees of freedom in each model, respectively.

The variance components were estimated for each trait using the following univariate model:

$$\boldsymbol{y} = \boldsymbol{Xb} + \boldsymbol{Za} + \boldsymbol{Sc} + \boldsymbol{Wm} + \boldsymbol{e},$$

in which $\boldsymbol{y}$ is the vector of phenotypic observations, $\boldsymbol{b}$ is the vector of fixed effects, $\boldsymbol{a}$ is the vector of random additive genetic effects, $\boldsymbol{c}$ is the vector of random common litter effects, $\boldsymbol{m}$ is the vector of random maternal effects, and $\boldsymbol{e}$ is a vector of residual effects. The $\boldsymbol{X}$, $\boldsymbol{Z}$, $\boldsymbol{S}$ and $\boldsymbol{W}$ are the incidence matrices associating the phenotypic observations to fixed, random additive genetic, random common litter effects, and random maternal effects, respectively. It was assumed that random effects were independent and normally distributed:

$$\begin{bmatrix} \boldsymbol{a} \\ \boldsymbol{c} \\ \boldsymbol{m} \\ \boldsymbol{e} \end{bmatrix} \sim \boldsymbol{N} \begin{bmatrix} \boldsymbol{A\sigma_a^2} & \mathbf{0} & \mathbf{0} & \mathbf{0} \\ \mathbf{0} & \boldsymbol{I\sigma_c^2} & \mathbf{0} & \mathbf{0} \\ \mathbf{0} & \mathbf{0} & \boldsymbol{A\sigma_m^2} & \mathbf{0} \\ \mathbf{0} & \mathbf{0} & \mathbf{0} & \boldsymbol{I\sigma_e^2} \end{bmatrix},$$

where σ_a^2, σ_c^2 σ_m^2, and σ_e^2 are the variances of random additive genetic, common litter, maternal, and residual effects, respectively; **I** is an identity matrix; and **A** is the numerator relationship matrix. Pedigree of phenotyped animals was traced back 16 generations comprising 25,041 individuals to construct the numerator relationship matrix. All analyses were performed using Asreml-R version 4 (Butler et al. 2018).

The model applied for bivariate analyses between each pair of traits was:

$$\begin{bmatrix} \boldsymbol{y_1} \\ \boldsymbol{y_2} \end{bmatrix} = \begin{bmatrix} \boldsymbol{X_1} & \mathbf{0} \\ \mathbf{0} & \boldsymbol{X_2} \end{bmatrix} \begin{bmatrix} \boldsymbol{b_1} \\ \boldsymbol{b_2} \end{bmatrix} + \begin{bmatrix} \boldsymbol{Z_{a1}} & \mathbf{0} \\ \mathbf{0} & \boldsymbol{Z_{a2}} \end{bmatrix} \begin{bmatrix} \boldsymbol{a_1} \\ \boldsymbol{a_2} \end{bmatrix} + \begin{bmatrix} \boldsymbol{Z_{c1}} & \mathbf{0} \\ \mathbf{0} & \boldsymbol{Z_{c2}} \end{bmatrix} \begin{bmatrix} \boldsymbol{c_1} \\ \boldsymbol{c_2} \end{bmatrix}$$

$$+ \begin{bmatrix} \boldsymbol{Z_{m1}} & \mathbf{0} \\ \mathbf{0} & \boldsymbol{Z_{m2}} \end{bmatrix} \begin{bmatrix} \boldsymbol{m_1} \\ \boldsymbol{m_2} \end{bmatrix} + \begin{bmatrix} \boldsymbol{e_1} \\ \boldsymbol{e_2} \end{bmatrix}$$

where $\boldsymbol{y_1}$ and $\boldsymbol{y_2}$ are the vectors of observations for the first and second trait; $\boldsymbol{b_1}$, $\boldsymbol{b_2}$, $\boldsymbol{a_1}$, $\boldsymbol{a_2}$, $\boldsymbol{c_1}$, $\boldsymbol{c_2}$, $\boldsymbol{m_1}$, $\boldsymbol{m_2}$, $\boldsymbol{e_1}$, and $\boldsymbol{e_2}$ are the vectors of fixed, random additive genetic, common litter, maternal, and residual effects for traits 1 and 2, respectively; and $\boldsymbol{X_1}$, $\boldsymbol{X_2}$, $\boldsymbol{Z_{a1}}$, $\boldsymbol{Z_{a2}}$, $\boldsymbol{Z_{c1}}$, $\boldsymbol{Z_{c2}}$, $\boldsymbol{Z_{m1}}$, and $\boldsymbol{Z_{m2}}$ are the incidence matrices associating observations to fixed, random additive genetic, common litter, and maternal effects for traits 1 and 2, respectively. The random effects were assumed to be normally distributed with a mean of zero and a (co)variance structure equal to:

$$\begin{bmatrix} \boldsymbol{a_1} \\ \boldsymbol{a_2} \end{bmatrix} \sim \left(\boldsymbol{0}, \boldsymbol{A} \otimes \begin{bmatrix} \boldsymbol{\sigma^2_{a1}} & \boldsymbol{\sigma_{a1a2}} \\ \boldsymbol{\sigma_{a1a2}} & \boldsymbol{\sigma^2_{a2}} \end{bmatrix} \right),$$

$$\begin{bmatrix} \boldsymbol{c_1} \\ \boldsymbol{c_2} \end{bmatrix} \sim \left(\boldsymbol{0}, \boldsymbol{I} \otimes \begin{bmatrix} \boldsymbol{\sigma^2_{c1}} & \boldsymbol{\sigma_{c1c2}} \\ \boldsymbol{\sigma_{c1c2}} & \boldsymbol{\sigma^2_{c2}} \end{bmatrix} \right),$$

$$\begin{bmatrix} \boldsymbol{m_1} \\ \boldsymbol{m_2} \end{bmatrix} \sim \left(\boldsymbol{0}, \boldsymbol{A} \otimes \begin{bmatrix} \boldsymbol{\sigma^2_{m1}} & \boldsymbol{\sigma_{m1m2}} \\ \boldsymbol{\sigma_{m1m2}} & \boldsymbol{\sigma^2_{m2}} \end{bmatrix} \right), \text{ and}$$

$$\begin{bmatrix} \boldsymbol{e_1} \\ \boldsymbol{e_2} \end{bmatrix} \sim \left(\boldsymbol{0}, \boldsymbol{I} \otimes \begin{bmatrix} \boldsymbol{\sigma^2_{e1}} & \boldsymbol{\sigma_{e1e2}} \\ \boldsymbol{\sigma_{e1e2}} & \boldsymbol{\sigma^2_{e2}} \end{bmatrix} \right),$$

where $\boldsymbol{A}$ is the numerator relationship matrix; $\boldsymbol{I}$ is an identity matrix; σ^2_{a1}, σ^2_{a2}, σ^2_{c1}, σ^2_{c2}, σ^2_{m1}, σ^2_{m2}, σ^2_{e1}, *and* σ^2_{e2} are the variances of random additive genetic, common litter, maternal, and residual effects for traits 1 and 2, respectively; σ_{a1a2}, σ_{c1c2}, σ_{m1m2}, and σ_{e1e2} are the covariances of additive genetic, common litter, maternal, and residual effects between traits 1 and 2, respectively.

The final reported heritability for each trait was calculated by the averages across the bivariate models. Phenotypic and genetic correlations among traits were estimated pairwise

in bivariate models. The significance of these estimates was tested using a Z-test with the null hypothesis that the estimates are equal to zero ($\alpha = 0.05$).

3.3 Results and discussion

The aim of this chapter was to estimate the genetic and phenotypic parameters for different FE and component traits in American mink. The descriptive statistics for FE and component traits in American mink are presented in Table 3.1. During the test period, the average values for FCR and KR were 31 and 5.4, respectively, but the mean values of RFI, RG, and RIG were close to zero, as expected by their definitions. The average values of HW, HL, FBW, and FBL were consistent with the values reported in our previous studies (Do et al. 2021) because the current data set is extracted from those studies with focus on feed efficiency and component traits. The HW (2.2kg) and FBW (2.1kg) values falls within the range of estimates (1.9 in females, and 3.6 in males) reported by Shirali et al. (2015), and (1.9 in females, and 3.7 in males) reported by Thirstrup et al. (2017).

3.3.1 Variance components estimation

Relevant fixed and random effects for estimation of genetic and phenotypic parameters of studied traits are given in Table 3.2. It was observed that sex had significant effects ($P < 0.05$) on all traits. Several studies reported that growth pattern varies between different gender in mink, with the slower growth and late mature for female (Sørensen et al. 2003; Do and Miar, 2020). It was indicated that the maintenance requirement is negatively associated with the animal weight in mink, thereby the difference in feed utilization between sexes is expected due to the differences in size between males and females (Burlacu et al. 1984). The effect of farm was significant ($P < 0.05$) for HW, HL and DFI,

but not tested for other traits as only one farm had data on all traits. Row-year also significantly ($P < 0.05$) affected most of the studied traits except for ADG, RG, and KR. Color-type had significant effects ($P < 0.05$) on FBL, DFI, FCR, RFI, and RIG. Several studies indicated the importance of color-type on reproductive performance and growth parameters in mink (Ślaska et al. 2009) Previous studies identified many candidate genes controlling the colors of mink (Song et al. 2017a; Manakhov et al. 2019). Therefore, the effect of color on FE traits might be due to the pleiotropic effects of genes controlling FE and colors in American mink. In addition, previous studies in mink showed high genetic differences among color types of farm mink (Belliveau et al. 2011; Thirstrup et al. 2015). The genetic differentiation between color types within each farm in the study of (Thirstrup et al. 2015) clearly suggested that mink from the same farm have been kept as separate (color) breeds, because specific color types at a given farm are selected in order to enhance fur quality and body size. (Do et al. 2021) reported a significant effect ($P < 0.05$) of color-type on HW and HL, which is in contrast with our results. This discrepancy might be due to the inclusion of harvest records (n=1240) from the commercial mink farm with only one color-type (dark) in this chapter.

The random common litter effect was significant ($P < 0.05$) for HW and HL, although it was not tested for other traits because common litter effect was not applicable for other traits as there were not repeated dams for other traits. The random maternal effect was significant ($P < 0.05$) for most of the studied traits except for HW and HL. These results were in agreement with previous studies that showed the importance of random maternal effects for different traits in mink, such as growth parameters (Do et al. 2021), reproduction traits (Karimi et al. 2018), and fur quality traits (Thirstrup et al. 2017). The estimates of

variance components, heritability, and proportion of variance explained by maternal and common litter effects for each trait obtained from univariate models are presented in Table 3.3.

3.3.2 Heritability estimates

The heritability (±SE) estimated obtained from bivariate models for all studied traits are presented in the diagonal elements of Table 3.4. These values were similar to those obtained through univariate analyses and the minor differences between these estimates can be due to the missing records for some traits. The estimated heritabilities (±SE) ranged from FCR (0.20±0.09) to HW and FBL (0.28±0.10). The heritability estimated for FE traits in the present chapter indicated that there might be a potential for their improvement using genetic/genomic selection.

The range of heritability estimates for body weight and length traits (HW, HL, FBW, and FBL) in the current chapter were in general agreement with the previously reported estimates (Socha et al. 2008; Koivula et al. 2010; Do et al. 2021). The heritability estimates (±SE) for HW (0.28±0.06) and FBW (0.28±0.10) are slightly lower than those reported for BW in furring periods (0.35 to 0.46) by (Do et al. 2021). Although some parts of the data sets from both studies overlapped, different statistical models and sample size might cause such differences. Regarding the body length traits in mink, the heritability estimates (±SE) for HL (0.23±0.06) and FBL (0.28±0.10) were in accordance with the literature cited (Lagerkvist et al. 1993; Liu et al. 2017; Thirstrup et al. 2017; Do et al. 2021). However, there was a large variation in the heritability estimates for body length in mink, from 0.19 to 0.53 (Hansen and Berg, 2008; Liu et al. 2017; Thirstrup et al. 2017; Do et al. 2021). This large variation might be due to the differences of breed, population or the differences in

model components, sample sizes, environmental factors, and also visual scoring of body length as it might be affected by the fatness of the animal (Koivula et al. 2010).

The estimated heritability (±SE) for ADG (0.25±0.09) and DFI (0.26±0.09) were lower than the heritability estimates reported by Sørensen, (2002) in mink (0.38 for DFI and 0.43 for ADG). This inconsistency may be due to the fact that they collected the data at the early growing period in mink as the chemical compositions and metabolic energy of mink diets were changed between different growing and furring periods (Do and Miar, 2020). In rabbits, (Piles and Sánchez, 2019) reported a heritability of 0.32 for DFI, and the estimated heritability for ADG ranged from 0.22 (Drouilhet et al. 2013) to 0.31 (Piles and Blasco, 2010), which were in agreement with our estimate. In addition, (Kempe et al. 2010) estimated the heritability for DFI (0.23) and ADG (0.28) in blue fox, which were similar to our results.

The heritability estimate (±SE) for FCR in this chapter was 0.20±0.09. To our knowledge, no study reported the heritability for FCR in American mink, though Sørensen (2002) reported a heritability of 0.30 for its mathematical inverse gain: feed ratio (G:F) in mink, which was higher than our estimate. This difference might be due to the fact that they estimated the heritability of G:F in the early growing period of mink. However, several studies found similar heritability of 0.19 (Drouilhet et al. 2013), 0.21 (Piles et al. 2004), and 0.22 (Garreau et al. 2016) for FCR in rabbits. The heritability (±SE) for RFI was 0.23±0.09, which falls within the range of estimates (0.25 in males, and 0.13 in females) reported by Madsen et al. (2020) for furring periods in mink, but lower than estimates (0.43 to 0.49 in males, and 0.39 to 0.46 in females) by Shirali et al. (2015). Different heritabilities have been reported previously in the literature for RFI in other livestock species, ranging

from 0.10 to 0.51 in pigs (Jiao et al. 2014; Hong et al. 2020c), 0.11 to 0.45 in sheep (Cammack et al. 2005; Tortereau et al. 2020), 0.10 to 0.49 in chickens (Pakdel et al. 2005; Begli et al. 2016), and 0.01 to 0.62 in cattle (Vallimont et al. 2011; Berry and Crowley, 2013). The diverse range of heritabilities estimates presented in the literature is due to including different populations, age, diet, breeding environment, sample size, and trait definition (Miar et al. 2014a; Miar et al. 2014b).

The heritability estimates for RG, RIG, and KR were 0.21±0.10, 0.25±0.10, and 0.26±0.10, respectively. To the best of our knowledge, this is the first estimated heritabilities presented for RG, RIG, and KR in American mink. (Berry and Crowley, 2013) applied a comprehensive meta-analysis for FE traits in dairy and beef cattle and reported a pooled heritability (±SE) of 0.28±0.03 for RG across all studies, which is similar to our estimate of 0.21. In addition, (Ndung'u et al. 2020) reported a pooled heritability of 0.30 for RG in indigenous chicken at 13 weeks of age among different studies, and considerably higher pooled heritability at younger ages (0.71 for 12 weeks of age, and 0.77 at 11 weeks of age). Our heritability estimate (±SE) for RIG (0.25±0.10) was lower than the estimated heritability of 0.36±0.06 reported by (Berry and Crowley, 2012) for the first time as an alternative index for FE trait in cattle. However, a wide range of heritabilities (±SE) were reported for RIG in livestock species, such as 0.13±0.06 in cattle (Novo et al. 2021), 0.18±0.01 to 0.57±0.03 in pigs (Lu et al. 2017), and 0.23±0.03 in turkey (Willems et al. 2013). These discrepancies are expected as RIG traits are linear combinations of the RFI and RG traits. Therefore, the trait definition might be different due to the different characteristics and adjustments for RFI and RG traits. The estimated heritability (±SE) of 0.26±0.10 for KR in this chapter was lower than a pooled heritability (±SE) of 0.35±0.03

calculated for KR from different studies in cattle (Berry and Crowley, 2013). However, these discrepancies could be due to the differences in the genetic backgrounds of different species, sample sizes, and statistical models.

3.3.3 Genetic correlations

Genetic and phenotypic correlations between FE and component traits are shown in Table 3.4. High genetic correlations (±SE) close to unity among HW and FBW (0.97±0.02) and HL and FBL (0.97±0.03) in this chapter were in agreement with most cited literature in mink (Shirali et al. 2015; Do et al. 2021). Do et al. (2021) reported high genetic correlations among BW traits in different time intervals in American mink, ranging from 0.72 to 0.98. Similarly, Shirali et al. (2015) reported moderate to high genetic correlations (from 0.39 to 0.99) among BW traits during the growing-furring period in Danish mink. The results suggested that breeders can select mink based on BW in different time periods in order to have the desire BW at harvest time. In this chapter, strong positive genetic correlations (±SE) were estimated between HW and HL (0.73±0.10), and between FBW and FBL (0.79±0.13). Our results are consistent with the results of Do et al. (2021), who found strong genetic correlations between BW and HL in different time periods (0.70 to 0.88) in American mink. These strong positive genetic correlations confirm the idea that selection for higher BW might lead to higher animal body length, which in turn helps breeders to reach larger pelt size and more profit. Daily feed intake had high genetic correlations (±SE) with HW (0.68±0.10), HL (0.79±0.12), FBW (0.61±0.20), and FBL (0.78±0.15). Similar findings were obtained by (Kempe et al. 2010), who reported strong genetic correlations between DFI and growth traits (0.56 to 0.95) in Finnish blue fox. Our results indicated that selection solely on body length traits might lead to an undesirable increase in feed intake,

which in turn leads to higher production costs. Although pelt size is one of the main factors in determining the price of pelt, negative correlations between BL and BW with fertility and fur quality traits must be considered in selection programs (Lagerkvist et al. 1994).

The FCR had high negative genetic correlations (±SE) with HW (-0.88±0.12), FBW (-0.64±0.21), and ADG (-0.87±0.09). Sørensen (2002) found strong genetic correlations between FE (gain:feed) with BW (0.59) and ADG (0.85) in Danish mink. The reason we observed negative values in our experiment compared to positive values in their study may be due to the fact that gain:feed is the mathematical inverse of FCR. In rabbits, the genetic correlations between FCR and growth rate were lower, ranging from – 0.38 to – 0.49 (Piles et al. 2004; Drouilhet et al. 2013). However, the strong negative genetic correlation between FCR and ADG is well documented in livestock species such as pigs (Akanno et al. 2013), chicken (Mignon-Grasteau et al. 2004), and beef cattle (Arthur et al. 2001). Our results revealed that selection for better FCR will lead to faster-growing but heavier animals over time. Thus, it should be pointed out that direct selection for such ratio traits like FCR might cause undesirable changes in related component traits, since direct selection for FCR emphasizes more on the information in the numerator in spite of the distributional properties of the component, and thereby causes selection pressure to be placed nonlinearly on weight gain (Gunsett, 1984). In addition, the non-significant ($P > 0.05$) genetic correlation of 0.29±0.39 between FCR and DFI in the current chapter indicated that improving the FCR has negligible impact on feed intake in American mink. However, selection for reducing FCR can be enhanced by selecting for BW and ADG and against feed intake in an optimum selection index weight (Kennedy et al. 1993; Quinton et al. 2007).

The genetic correlations (±SE) of RFI with ADG (-0.24±0.16), FBW (-0.20±0.30), and FBL (0.20±0.28) were low and non-significant (P > 0.05) in the current chapter. Madsen et al. (2020) reported low genetic correlation between RFI and BW (-0.08 to 0.12) across different gender in Danish mink population, which was in agreement with our results. Similar genetic correlations (±SE) were estimated between RFI and growth traits (-0.09±0.22 with ADG, and 0.19±0.19 with slaughter weight) in rabbits (Larzul and De Rochambeau, 2005). The RFI had a strong genetic correlation (±SE) with DFI (0.80±0.11), which was higher than the estimated value in Danish mink (from 0.41 to 0.55) (M D Madsen et al. 2020). These discrepancies might be due to differences in sample size, population, and statistical models. However, our results were in accordance with the most cited literature in other livestock species, such as dairy cattle (Manzanilla-Pech et al. 2016), pigs (Do et al. 2013), and chickens (Yuan et al. 2015). The results indicated that selection against RFI will be beneficial to reduce feed intake in the Canadian mink populations without negative impacts on growth traits. Reduced DFI of efficient animals might be associated with lower maintenance requirements, reduced energy content of body weight gain, and increased efficiency of animals in utilizing the energy for weight gain. Consequently, efficient animals apply energy efficiently to gain weight, which in turn do not add extra cost due to their maintenance. However, selection solely based on RFI might lower growth rates (ADG and BW) since animals with a small amount of body weight will eat less feed, which in turn will get a more favorable rank for their RFI values (Berry and Crowley, 2013). Additionally, the issue of RFI is more pronounced when the feed is restricted, as variation of RFI among animals is substantially decreasing due to feed restriction (Pitchford et al. 2018). It was reported that selection for RFI is leading to

increased body fatness and lower activity (Hebart et al. 2021). Selection for RFI might come across with other physical issues such as decreased heat loss, and thereby being more affected by high temperature, and decreased reproductive rate (Pitchford, 2004), which can be important for the farmers as the production might decrease due to more susceptible animals with impaired reproductive performance.

The RG had a moderate genetic correlation (±SE) with ADG (0.43±0.14) and non-significant ($P > 0.05$) genetic correlations with FBW (0.12±0.31), FBL (0.27±0.36), and DFI (-0.38±0.32). The RIG showed non-significant ($P > 0.05$) genetic correlations (±SE) with FBW (0.14±0.31) and FBL (-0.15±0.31), but favorable strong genetic correlations (±SE) with ADG (0.58±0.21) and DFI (-0.62±0.24). Genetic correlations for RG and RIG have not been investigated in mink in the literature. (Berry and Crowley, 2012) reported nearly zero non-significant ($P > 0.05$) genetic correlations (±SE) between RG with metabolic BW (0.06±0.12) and feed intake (-0.03±0.13), and a positive high genetic correlation between RG and ADG (0.82±0.05). This chapter was the first to propose RIG as a new FE measurement, and reported a moderate favorable genetic correlation (±SE) between RIG and feed intake (-0.35±0.10), and ADG (0.47±0.10), and non-significant ($P > 0.05$) genetic correlation with metabolic BW (0.11±0.10), which were in agreement with our results. Our results revealed that applying RG into the selection program would result in faster-growing mink without any impact on improving the feed intake. Alternatively, our results suggested that RIG can be included in mink selection programs to enhance the growth rate and reduce requirement on feed intake since it guarantees the reduced DFI and increased ADG. However, it should be pointed out that calculating the residual traits is

more difficult than ratio traits as they cannot be estimated for a single individual and require other animals to be included in the regression model (Berry and Crowley, 2013).

In this chapter, all residual traits had high genetic correlations (±SE) with HW (-0.50±0.23 with RFI, 0.84±0.19 with RG, and 0.85±0.16 with RIG). These results were expected, as none of the residual traits in our chapter were adjusted for HW in their models. Residual traits would be uncorrelated with HW, if they were included in the model. Nevertheless, it was not applicable in this chapter as there were no complete records for HW to be adjusted in residual traits.

In this chapter, KR was strongly and positively correlated with (±SE) HW (0.86±0.09), HL (0.76±0.19), FBL (0.68±0.17), FBW (0.88±0.11), and ADG (0.97±0.02), but had a non-significant ($P > 0.05$) genetic correlation with DFI (0.23±0.30). These reported correlations were in agreement with the correlations reported in other livestock species. For example, high genetic correlations (±SE) of 0.91±0.02 (Steyn et al. 2014) and 0.75±0.06 (Crowley et al. 2010) in cattle, and 0.91±0.03 (Mandal et al. 2015) in sheep were reported between KR and ADG. Berry and Crowley, (2013) reported a non-significant pooled genetic correlation (±SE) of -0.04±0.03 between KR and DFI, which was in accordance with our result. The results in the current chapter suggested that selection based on KR may increase the growth traits in American mink, but with no improvement in feed intake. Direct selection for FE traits might be difficult and expensive as measuring and recording individual feed intake is required, even when the animal is raised in groups. This may be applicable for livestock species such as pigs and cattle, due to their state-of-the-art recording feeding systems. However, the high cost of collecting such data will limit the number of feed intake records for breeding programs in American mink, as most mink

farms come from a rural condition with lack of automatic feed recording systems. Interestingly, KR might be an ideal trait to be included in mink breeding programs since it does not require the observations on feed intake, which in turn substantially reduces the cost. However, like FCR, as a ratio trait, KR must be included in the selection programs using a proper selection index with other component traits. The negative correlation among some FE traits is an artifact of the definition of the trait, as for some traits like RFI and FCR, the lower and negative values are preferable, while for other traits like RG, RIG, and KR, the positive values are more desirable.

The reported high genetic correlation (±SE) of 0.75±0.20 between RFI and FCR in the current chapter was in agreement with the estimated genetic correlation of 0.96±0.03 in rabbits (Drouilhet et al. 2013). As expected, RIG showed strong and favorable genetic correlations (±SE) with RFI (-0.84±0.12) and RG (0.92±0.06), because RIG was a linear combination of RFI and RG. The results were similar to the values reported by (Berry and Crowley, 2012), who reported high genetic correlations between RIG with RFI (-0.87±0.03), and RG (0.83±0.04). The KR showed high and favorable genetic correlations (±SE) with RG (0.74±0.14), RIG (0.80±0.12), and FCR (-0.93±0.05). Although KR is not a direct FE indicator as it does not include feed intake in its calculation (Berry and Crowley, 2013), the strong genetic correlations with other FE traits makes it an appealing measurement, that can lead to improvement of other traits, if implemented in mink breeding programs.

3.4 Conclusions

In conclusion, the current chapter evaluated the genetic and phenotypic parameters among FE and component traits in American mink. There is evidence of non-significant genetic

correlation between RFI and growth traits and of high genetic correlation between RFI and feed intake. This fact makes the trait applicable for selection for higher feed efficiency, with negligible effects on the animal growth. The RIG is recommended to be a robust measure of feed efficiency and can be included in the selection programs as it will improve the growth rate and reduce the feed intake, as well as avoid any negative effects on growth traits. The KR trait also appears to be a good indirect FE trait as it has positive genetic correlations with other component traits, and there is no need for collecting the feed intake records to calculate this trait. Overall, our results suggest that the estimates of genetic and phenotypic parameters of FE traits can be applied in American mink to develop an index for selection of feed-efficient mink and consequently reduce the cost of mink production.

Table 3.1 Descriptive statistics for feed efficiency and component traits in American mink. abbreviations, units, number of animals per trait, means, standard deviations (SD), minimum (Min), maximum (Max), and coefficient variation values.

Traits	Abbreviation	Unit	Numbers	Mean	SD	Min	Max	CV (%)
Harvest weight	HW	kg	2,288	2.2	0.7	0.7	4.1	33.3
Harvest length	HL	cm	2,288	45.4	5	33	59	11
Final Body length	FBL	cm	1,046	37.6	4	29	47	10.6
Final Body weight	FBW	kg	1,046	2.1	0.6	1	3.8	31.1
Average daily gain	ADG	g/d	1,046	8.3	3.8	1.2	19.6	45.6
Daily feed intake	DFI	g	1,906	212.4	52	49	366.8	24.5
Feed conversion ratio	FCR	-	1,038	31	11.3	11	78.2	36.5
Residual feed intake	RFI	g/d	1,044	0	36.6	-86.5	169.4	-
Residual gain	RG	g/d	1,042	0	1.3	-5.7	5.3	-
Residual intake and gain	RIG	g/d	1,043	0	1.5	-5.6	5	-
Kleiber ratio	KR	-	1,046	5.4	1.5	1.1	9.7	28.6

Table 3.2 Significance of fixed and random effects included in the univariate models for analyses of feed efficiency and component traits in American mink.

	Fixed effects					Random effects		
Traits	**Farm**	**Sex**	**Color-type**	**Row-Year**	**Age of animal (days)**	**Animal**	**Maternal**	**Common litter**
Harvest weight	*	*	NS[1]	*	NS	✓	NS	*
Harvest length	*	*	NS	*	*	✓	NS	*
Final Body length	NT[2]	*	*	*	NS	✓	*	NT
Final Body weight	NT	*	NS	*	NS	✓	*	NT
Average daily gain	NT	*	NS	NS	*	✓	*	NT
Daily feed intake	*	*	*	*	NS	✓	*	NT
Feed conversion ratio	NT	*	*	*	*	✓	*	NT
Residual feed intake	NT	*	*	*	NS	✓	*	NT
Residual gain	NT	*	NS	NS	*	✓	*	NT
Residual intake and gain	NT	*	*	*	*	✓	*	NT
Kleiber ratio	NT	*	NS	NS	*	✓	*	NT

[1] NS = Non-significant.

[2] NT = Not tested.

* $P < 0.05$.

Table 3.3 Variance components and heritability estimates (±SE) for feed efficiency and component traits in American mink.

	Parameters[1]						
Traits[2]	σ^2_a	σ^2_m	σ^2_c	σ^2_e	Heritability	c^2_m	c^2_c
HW	2.31E-02±6.29E-03	NE[3]	1.05E-02±2.91E-03	6.01E-02±3.95E-03	0.25±0.06	NE	0.11± 0.03
HL	1.05 ±0.32	NE	1.05±0.32	3.52±0.21	0.21± 0.09	NE	0.11± 0.03
FBL	0.93±0.39	0.43±0.17	NE	2.12±0.23	0.27±0.13	0.12±0.04	NE
FBW	1.97E-02±9.05E-03	1.27E-02±4.21E-03	NE	4.40E-02±5.17E-03	0.26±0.11	0.17±0.05	NE
ADG	1.00±0.43	0.60±0.21	NE	2.64±0.26	0.24±0.11	0.14± 0.04	NE
DFI	296.09±11.39	168.37±50.80	NE	653.91±63.78	0.26±0.10	0.15± 0.04	NE
FCR	12.62±6.53	6.20±3.01	NE	46.80±4.14	0.19±0.06	0.08±0.04	NE
RFI	104.73±43.55	40.10±20.29	NE	313.81±28.07	0.23± 0.07	0.09±0.04	NE
RG	0.37±0.18	0.38±0.10	NE	0.95±0.10	0.22± 0.11	0.22± 0.05	NE
RIG	0.37±0.18	0.31±0.09	NE	0.90±0.10	0.24± 0.11	0.19± 0.05	NE
KR	0.27±0.11	0.18±0.05	NE	0.65±0.07	0.25± 0.11	0.16± 0.04	NE

[1]σ^2_a = Additive genetic variance; σ^2_m = Maternal genetic variance; σ^2_c = Common litter genetic variance; σ^2_e = Residual variance; c^2_m = Proportion of variance explained by maternal effects; c^2_c = Proportion of variance explained by common litter effects.

[2]HW = Harvest weight; HL = Harvest length; FBL = Final body length; FBW = Final body weight; ADG = Average daily gain; DFI = Daily feed intake; FCR = Feed conversion ratio; RFI = Residual feed intake; RG = Residual gain; RIG = Residual intake and gain; KR = Kleiber ratio.

[3]NE: not estimated.

Table 3.4 Estimates of heritabilities (diagonal), genetic correlations (above diagonal), and phenotypic correlations (below diagonal) and their SE for feed efficiency and component traits in American mink.

Trait[1]	HW	HL	FBL	FBW	ADG	DFI	FCR	RFI	RG	RIG	KR
HW	0.28±0.06	0.73±0.10	0.85±0.11	0.97±0.02	0.96±0.04	0.68±0.10	-0.88±0.12	-0.50±0.23	0.84±0.19	0.85±0.16	0.86±0.09
HL	0.56±0.02	0.23±0.06	0.97±0.03	0.93±0.07	0.94±0.04	0.79±0.12	-0.68±0.22	-0.02±0.27	0.07±0.28	0.12±0.29	0.76±0.19
FBL	0.38±0.03	0.56±0.05	0.28±0.10	0.79±0.13	0.65±0.21	0.78±0.15	-0.38±0.17	0.20±0.28	0.27±0.36	-0.15±0.31	0.68±0.17
FBW	0.79±0.01	0.50±0.03	0.51±0.03	0.27±0.11	0.90±0.06	0.61±0.20	-0.64±0.21	-0.20±0.30	0.12±0.31	0.14±0.31	0.88±0.11
ADG	0.70±0.02	0.38±0.03	0.36±0.03	0.89±0.01	0.25±0.09	0.37±0.26	-0.87±0.09	-0.24±0.16	0.43±0.14	0.58±0.21	0.97±0.02
DFI	0.32±0.03	0.27±0.03	0.42±0.03	0.65±0.02	0.54±0.03	0.26±0.09	0.29±0.39	0.80±0.11	-0.38±0.32	-0.62±0.24	0.23±0.30
FCR	-0.50±0.03	-0.24±0.04	-0.18±0.04	-0.59±0.02	-0.72±0.02	-0.08±0.04	0.20±0.09	0.75±0.20	-0.74±0.18	-0.81±0.15	-0.93±0.05
RFI	-0.22±0.04	-0.05±0.04	0.01±0.04	-0.18±0.04	-0.24±0.04	0.77±0.02	0.47±0.03	0.23±0.09	-0.59±0.23	-0.84±0.12	-0.53±0.24
RG	0.33±0.03	0.02±0.04	-0.02±0.04	0.37±0.04	0.73±0.02	0.05±0.04	-0.63±0.02	-0.37±0.03	0.21±0.10	0.92±0.06	0.74±0.14
RIG	0.37±0.04	0.04±0.04	-0.04±0.04	0.36±0.04	0.66±0.02	-0.29±0.04	-0.69±0.02	-0.71±0.02	0.90±0.01	0.25±0.10	0.80±0.12
KR	0.58±0.03	0.28±0.04	0.22±0.04	0.72±0.02	0.94±0.01	0.43±0.04	-0.82±0.01	-0.25±0.04	0.85±0.01	0.76±0.02	0.26±0.10

[1]HW = Harvest weight; HL = Harvest length; FBL = Final body length; FBW = Final body weight; ADG = Average daily gain; DFI = Daily feed intake; FCR = Feed conversion ratio; RFI = Residual feed intake; RG = Residual gain; RIG = Residual intake and gain; KR = Kleiber ratio.

CHAPTER 4. Genome-wide detection of copy number variation in American mink using whole-genome sequencing[1]

4.1 Introduction

Copy number variations (CNVs), mainly refer to deletion or duplication of DNA segments, are a particular form of genomic structural variation ranging from 50 bp to several megabases (Mb) (Mills et al. 2011). Although CNVs are less frequent compared to single nucleotide polymorphisms, due to their greater size, they might have large effects as a result of altering gene dosage, disrupting coding sequence and modifyng gene expression (Saitou and Gokcumen, 2020), leading to significant impacts on phenotypes of economic interest (Liu and Bickhart, 2012; Wang et al. 2012; Bickhart and Liu, 2014). In addition, CNVs are associated with disease susceptibility (Henrichsen et al. 2009; Zhang et al. 2009; Long et al. 2013; Kendall et al. 2019; Warland et al. 2019; Sahajpal et al. 2022), and might contribute to substantial part of missing heritability (Manolio et al. 2009). It was shown that CNVs play a critical role in regulating several complex diseases in human including autism (Zhang et al. 2009), breast cancer (Long et al. 2013), schizophrenia (Warland et al. 2019), depression (Kendall et al. 2019), and susceptibility to Coronavirus (Sahajpal et al. 2022). Similarly, CNVs have been suggested to be responsible for traits and diseases in domesticated animals, such as polled intersex syndrome in goats (Pailhoux et al. 2001), susceptibility to melanoma in horses (Rosengren Pielberg et al. 2008), osteopetrosis in cattle (Meyers et al. 2010), and dominant white color in pigs (Giuffra et al. 2002).

[1] A version of this chapter has been published in BMC Genomics. Davoudi et al. 2022. Genome-wide detection of copy number variation in American mink using whole-genome sequencing. 23:649. doi: https://doi.org/10.1186/s12864-022-08874-1

The decreasing costs of whole-genome sequencing (WGS) have made it feasible to map CNV with high resolution and accuracy (Zhao et al. 2013). Multiple approaches have been developed for WGS-based CNV detection, which use paired-end mapping, read-depth, and split-read (Zhao et al. 2013). The paired-end mapping method is applicable to paired-end reads and performs better in detection of CNVs in low-complexity regions (Zhao et al. 2013). On the other hand, the read-depth method relies on the depth of coverage in genomic regions and utilizes the changes in read depth to detect the CNV (Abyzov et al. 2011), and can identify large CNVs in complex genomic regions (Yoon et al. 2009). The split-read method refers to sequences that map to the reference genome only at one end, with other partially or unmapped reads providing the location of the breakpoint (Zhao et al. 2013).

Characterisation of CNV has been widely studied in livestock species such as cattle (Letaief et al. 2017; Strillacci et al. 2018; Butty et al. 2020), sheep (Salehian-Dehkordi et al. 2021; Yuan et al. 2021; Ladeira et al. 2022), goat (Guo et al. 2020; Guan et al. 2021; Nandolo et al. 2021), pig (Bovo et al. 2020; Zheng et al. 2020; Qiu et al. 2021), chicken (Strillacci et al. 2017; Lin et al. 2018; Seol et al. 2019), turkey (Strillacci et al. 2019; Maria Giuseppina Strillacci et al. 2021), buffalo (Maria G. Strillacci et al. 2021), yak (Zhang et al. 2016; H. Wang et al. 2019), and rabbit (Fontanesi et al. 2012), indicating that CNVs might have significant impacts on the economically important traits (Fontanesi et al. 2011; Upadhyay et al. 2017; Stafuzza et al. 2019; Feng et al. 2020). However, to our knowledge, there is no genome-wide CNV study in American mink. Therefore, the objectives of the current chapter were to: 1) provide the first large-scale CNV map in American mink using whole-genome sequence data; 2) define sets of high confidence CNV regions (CNVR) by incorporating multiple approaches; and 3) examine the potential impacts of CNVR and their overlapped genes on traits of economic interest for mink selection programs through in-depth functional annotation analyses.

4.2 Methods

4.2.1 Animals and sampling

All procedures applied in this chapter were approved by the Dalhousie University Animal Care and Use Committee (certification# 2018-009, and 2019-012), and mink used were cared for according to the Code of Practice for the Care and Handling of Farmed Mink guidelines (Turner et al. 2013).

All individuals were raised through standard farming condition and were euthanized in December 2018 (Do and Miar, 2019). Tongue samples were collected from two different farms, the Canadian Center for Fur Animal Research (CCFAR) at Dalhousie Faculty of Agriculture (Truro, NS, Canada) and Millbank Fur Farm (Rockwood, ON, Canada). All mink from Millbank Fur Farm were Black in color (n = 15), and individuals from CCFAR varied in color types, including Demi (n = 32), Mahogany (n = 20), Black (n = 16), Pastel (n = 10), and Stardust (n = 7). To keep the relationship between individuals low, we checked the pedigree information and selected individuals with the lowest degree of kinship for the further analyses (median = 0.015; 1st–3rd quantile of relatedness = 0.008–0.039). More details were provided about the studied individuals by Karimi et al. (2021a).

4.2.2 Quality control and read alignment

Using the DNeasy Blood and Tissue Kit (Qiagen, Hilden, Germany), we extracted genomic DNA from tongue tissue samples in accordance with the manufacturer's protocol. Sequencing (100 bp pair-end reads) was performed by BGISEQ-500 platform at Beijing Genomics Institute (BGI, Guangdong, China). Low-quality reads and adapter sequences were removed by using the SOAPnuke software version 2.1.5 (Chen et al. 2018). Then, high-quality reads were aligned to the latest American mink reference genome (Karimi et al. 2022) using Burrows-Wheeler Aligner version 0.7.17 (Li, 2013) with default parameters. The conversion of aligned files to binary alignment map (BAM) format and subsequent sorting was performed with SAMtools version 1.11 (Li et al. 2009). Duplicates were then removed using the MarkDuplicates command tool of Picard version 2.0.1 (Toolkit, 2019). Finally, the BAM files were indexed by SAMtools software version 1.15 (Li et al. 2009).

4.2.3 Identification of CNV

To increase the accuracy of CNV detection, we employed three software programs, including CNVpytor version 1.2.1 (Suvakov et al. 2021), DELLY version 0.9.1 (Rausch et al. 2012), and Manta 1.6.0 (Chen et al. 2016). The CNVpytor software applies a read-depth approach, and both DELLY and Manta use paired-end and split-read methods. For each individual, the sorted BAM file was processed by CNVpytor (Suvakov et al. 2021), which is a Python version of its ancestor CNVnator (Abyzov et al. 2011). Although both perform the same procedures, we applied CNVpytor as it is considerably faster in computational time (Suvakov et al. 2021). The CNV calling was carried out by setting a bin size of 100 bp, following the recommendation of Abyzov et al. (2011). For improving the CNV detection accuracy, the following criteria were set to filter false positive candidates: the CNV calls with P-value<0.01, sizes greater than 1 kb, fraction of mapped reads with zero quality (q0) > 50%, fraction of N bases (i.e., unassembled reference genome) within call region (pN) > 5%, and the distance to nearest gap in reference genome (dG) > 100,000. In the current chapter, we removed CNVs smaller than 1 kb to avoid noises, since most of the CNVs calling algorithms had low accuracy for small CNVs. DELLY (Rausch et al. 2012) and Manta (Chen et al. 2016) were performed with default parameters. The calls were filtered by removing the following 1) calls that were flagged IMPRECISE, 2) calls that did not pass the quality filters as suggested by DELLY and Manta (flag PASS), and 3) calls that had sizes smaller than 1 kb. Although DELLY and Manta had the ability to detect translocations and inversions events, we only considered deletions and duplications to have comparable results with the CNVpytor software. Only deletions and duplications were kept for further analyses. To generate a high-confident consensus call from different software, we implemented SURVIVOR version 1.0.3 (Jeffares et al. 2017) with default parameters, which merged the calls together with a maximum allowed distance of 1 kb, and CNVs with at least two out of three callers were kept for further analyses. This procedure cut down the false positive rate, yet without significantly reducing the sensitivity (Jeffares et al. 2017).

4.2.4 Determination of CNVR

The CNVR were obtained by the CNVruler software version 1.2, merging CNVs among individuals with at least 50% reciprocal overlap in their genomic coordinates. For instance, considering two CNVs, CNV1 starts at position **X** and ends at position **Y**, and CNV2 from **Z** to **W**, with **X** < **Z** < **Y** < **W**. Then if the reciprocal overlap between the two CNVs is at least 50%, the software merges them as a CNVR that runs from **X** to **W** on the genome. To reduce the false positive rate, only the CNVR found in more than two samples were considered for further analyses (Pierce et al. 2018). The CNVR were categorized as gain or loss. The overlapping "loss" and "gain" CNVR were merged into single regions and called "mixed" CVNRs.

4.2.5 Functional enrichment analysis of candidate genes overlapped with CNVR

A list of genes in the mink genome was downloaded from the NCBI website and Bedtools version 2.30.0 (function:intersect) (Quinlan and Hall, 2010) and was used to catalogue genes in corresponding regions. The Gene Ontology (GO) terms for molecular function, biological process, and cellular component, as well as metabolic pathway analyses, were conducted using the Kyoto Encyclopedia of Genes and Genomes (KEGG) database by the g:Profiler (Raudvere et al. 2019). Analyses were performed using R packages including gprofiler2 version 0.2.1 (Peterson et al. 2020), clusterProfiler version 3.0.4 (Yu et al. 2012), enrichplot version 1.16.1 (Yu, 2022), and org.Hs.eg.db version 2.7.1 (Carlson, 2019). All enrichment functions were selected through false discovery rate corrections and pathways with adjusted P-values<0.05 were considered to be significant.

4.3 Results

4.3.1 Detection of CNVs

We employed different software including CNVpytor, DELLY, and Manta to detect CNVs in 100 American mink using WGS data. After merging the results of these methods, we retrieved a total of 164,733 CNV events (including 144,517 deletion and 20,216 duplication events) (Table 4.1), with an average number of 1,647.3 per animal. The length size of identified CNVs ranged from 1 kb to 4255

kb with an average size of 7.4 kb. The CNVs were distributed over 14 autosomes with varying numbers in each autosome (Figure 4.1).

4.3.2 Number and distribution of CNVR

A total of 5,378 CNVR were obtained by merging overlapping CNVs across all individuals that covered 47.3 Mb of mink genome corresponding to 1.9% of autosomal genome sequence (Table 4.2). The CNVR included 4,073 losses, 625 gains, and 680 mixed (loss and gain) events (Figure 4.2). To achieve high-confident CNVR, we only considered CNVR identified in two or more samples. The size of CNVR varied from 1 to 3171.5 kb with an average of 8.9 kb. The largest number of CNVR were on chromosome 1 (683) and the lowest number were observed on chromosome 14 (82), which is in accordance with chromosome lengths.

In total, 4,103 out of 5,378 CNVR (76.3%) had sizes within 1–5 kb interval, following by 1,060 (19.71%) within 5–10 kb, 91 (1.69%) within 10–20 kb, 56 (1.04%) within 20–50 kb, and 68 (1.26%) greater than 50 kb in length (Figure 4.3).

The number of individuals supporting the CNVR varied from 2 to 98 out of 100 individuals, concentrating at 40.2% with 2-10 individuals, and only 5.6% of detected CNVR were observed in more than 90 individuals. Furthermore, the physical locations of CNVR across the mink genome are presented in Figure 4.4.

4.3.3 Functional annotation and gene enrichment analyses

Analysis of the CNVR gene content revealed 1,391 genes within or partially overlapped with 1,878 (34.9%) detected CNVR. The enrichment analyses revealed 279 significant Gene Ontology (GO) terms and 21 significant pathways using KEGG. The results of GO analysis revealed that CNVR were significantly enriched (P-value<0.05) in different biological functions e.g., axon guidance, phospholipid binding, Fc receptor signaling pathway, and GTPase regulator activity. The top ten significant GO terms enriched in CNVR-harbored genes were listed in the following GO categories (biological process, cellular component, molecular function) as depicted in Figure 4.5.

In addition, the pathway analysis using KEGG revealed 21 significantly enriched pathways (Figure 4.6). These genes are mainly related to the axon guidance, glutamatergic synapse, regulation of actin cytoskeleton, cAMP signaling pathway, sphingolipid metabolism, and regulation of lipolysis in adipocytes (Figure 4.6). The results of GO enrichment and pathway analysis using KEGG revealed the biological functions of several genes associated with fur characteristics and development (*MYO5A, RAB27B, FGF12, SLC7A11*, and *EXOC2*), and immune system processes (*SWAP70, FYN, ORAI1, TRPM2*, and *FOXO3*).

4.4 Discussion

American mink (*Neogale vison*) is well-known as one of the most important sources of fur across the world (Karimi et al. 2020). It is essential for the mink industry to implement highly efficient breeding plans to meet sustainable production requirements (Karimi et al. 2021a). Genome-wide identification of CNVs can provide new insights into genomic variations, which can assist in developing genomic breeding strategies for American mink. Numerous studies have been performed to identify CNVR in other species e.g., cattle (Strillacci et al. 2018), pig (Stafuzza et al. 2019), goat (Guo et al. 2020), sheep (Yuan et al. 2021), chicken (Zhao et al. 2013), and buffalo (Strillacci et al. 2021). Several studies indicated that CNVs could be highly associated with economically important traits in these species (Da Silva et al. 2016; Liu et al. 2020; Fernandes et al. 2021; Qiu et al. 2021). To our knowledge, the current chapter provides the first genome-wide CNV detection in American mink.

We performed CNV analyses on mink genome using WGS data. In total, we identified 164,733 CNV events (144,517 deletions and 20,216 duplications) with the average number of 1,647.3 per mink. Similar results were reported in other livestock species e.g., dairy cattle (182,823 CNVs) (Hu et al. 2020), yak (98,441 CNVs) (Zhang et al. 2016), Nellore cattle (195,873 CNVs) (Antunes et al. 2018), and goat (208,649 CNVs) (Guo et al. 2020). Some other studies reported a wide range of CNVs from 12 CNVs in chicken (Griffin et al. 2008) to 1,747,604 CNVs in sheep (Yuan et al. 2021). This discrepancy might be due to the differences in the sample size, algorithms used for CNV calling, and

sequencing technology (Locke et al. 2015). A considerable number of detected CNVs were deletions (88.7%) in our chapter, which was expected because of the limited ability of the current algorithms in detection of insertions (Teo et al. 2012). In addition, the detection of insertion is more diffucult in end mapping methods, since they only detect the duplications when mapped reads are shorter than the fragmented length (Teo et al. 2012).

The results showed that 5,378 CNVR covered around 47.3 Mb (1.9%) of the mink genome, which falls within the range of several studies reported in other species, such as pig (1.72%) (Wang et al. 2015), cattle (2.5%) (Upadhyay et al. 2017), chicken (1%) (Strillacci et al. 2017), quail (1.6-1.9%) (Khatri et al. 2019), horse (1.3%) (Ghosh et al. 2014), and buffalo (2%) (Strillacci et al. 2021). The CNVR covered the genome in different ranges in other species, including cat (0.3%) (Genova et al. 2018), pig (0.9%) (Keel et al. 2019), yak (6.2%) (Wang et al. 2019), goat (10.8%) (Guo et al. 2020), chicken (12.8%) (Fernandes et al. 2021), and cattle (13%) (Antunes et al. 2018). Several reasons might affect the quantity of CNVR detection such as the detection algorithm, population size, genetic background, the quality of applied technology, and the differences in genome size (Redon et al. 2006; Locke et al. 2015).

The results showed that 1,391 genes in the mink genome were harbored within the detected CNVRs (34.9% of the total detected CNVRs). The GO and pathway analysis using KEGG enrichment results suggested that the CNVs might contribute to various biological processes related to growth (regulation of actin cytoskeleton, and cAMP signaling pathway), lipid metabolism (phospholipid binding, sphingolipid metabolism, and regulation of lipolysis in adipocytes), behavior (axon guidance, circadian entrainment, and glutamatergic synapse), and immune response (Wnt signaling pathway, Fc receptor signaling pathway, and GTPase regulator activity). For instance, the most significantly enriched GO terms and pathway analysis using KEGG results were related to axon guidance known as the key step in the formation of the neuronal network (Negishi et al. 2005). Interestingly, it was reported that CNVs might contribute to axonal growth, which has been connected with autism spectrum disorders (McFadden and Minshew, 2013). The enrichment of several pathways

related to lipid metabolism implied that CNVs might contribute to the fur growth and quality as fat metabolism is an important process during furring (Ding et al. 2019). Circadian entrainment is an essential part of behavior and adaptation since it plays a fundamental role to assists organisms in adapting to daily environmental cycles (Emerson et al. 2008). Several studies demonstrated that the annual reproductive cycle in mink is under photoperiodic control, and is initiated by decreasing the daylength (Martinet et al. 1992; Jallageas and Mas, 1996). It is well-documented that photoregulation of reproductive activity is associated with the circadian rhythm of photosensitivity, leading to a proper photoperiodic response in mink (Boissin-Agasse et al. 1982; Boissin-Agasse and Boissin, 1985). Boissin-Agasse et al. (1982) identified that seasonal testis activity in mink initiated in the Fall when the daily light period is decreasing and exposure to light at this period inhibited testicular development. Zschille et al. (2010) reported different circadian activity rhythm in male and female mink, and observed active males during the night, and females with high activity during the day. Gender differences in circadian activity rhythms of wild American mink increases the female hunting successes as it allows females to be in a patch in different time than males to avoid the competitive pressure from the males (Zschille et al. 2010). In addition, several studies in mink have shown that decreasing the photoperiod in the Fall initiates winter fur growth and starting the hair growth in summer is associated with increasing photoperiod in spring (Rose et al. 1984; Rose et al. 1987; Martinet et al. 2011). Recently, Nandolo et al. (2021) reported enrichment of circadian entrainment pathway among genes detected across the CNVs in African goats, supporting the importance of circadian entrainment in goats during the adaptation to unstable environment. Notably, it is well-documented that Wnt signaling pathway plays a key role in hair growth and development of hair follicles (Millar et al. 1999; Rishikaysh et al. 2014). The maintenance of Wnt signaling pathway is a critical part to hair-inducing activity of dermal papilla through regulating the β-catenin pathway, and thereby required for follicle regeneration and growth of the hair shaft (Kishimoto et al. 2000; Shimizu and Morgan, 2004). Interestingly, Yuan et al. (2021) demonstrated the contribution of Wnt signaling

pathway to the hair follicle development process in Alpine Merino sheep by identifying Wnt-related signaling pathways associated with CNVR-harboring genes (Yuan et al. 2021).

In addition, GO enrichment and pathway analysis using KEGG analyses identified several key genes (*MYO5A*, *RAB27B*, *FGF12*, *SLC7A11*, and *EXOC2*) participating in a wide range of pathways associated with fur characteristics and development. In this chapter, the *MYO5A* gene (CNVR_Chr13:75.88–75.89 Mb), a class of actin-based motor proteins, was enriched in several pathways such as actin filament organization, actin-based cell projection, calmodulin binding, actin binding, and cytoskeletal motor activity. The *MYO5A* gene is found in pigment-producing cells, which produce melanin and eventually provides the pigment required for normal color of hair, skin, and eye (Mermall et al. 1998). It has been suggested that *MYO5A* gene plays a key role in the industrial Silverblue coat color in American mink (Manakhov et al. 2019). Several studies reported that the *MYO5A* gene can cause diluted (grey) coat color phenotype in different species, e.g., rabbit (Fontanesi et al. 2012), horse (Bierman et al. 2010), dog (Christen et al. 2021), and mice (Zhang et al. 2021). The *RAB27B,* which overlapped with CNVR_Chr3:143.66–143.67 Mb, is part of the small GTPase Ras-associated binding family that regulates the membrane trafficking and secretion of exosomes. It was indicated that *RAB27B* and its paralogue (the *RAB27A*), played some roles in the transport of melanosomes, and the knockout of this gene might cause silvery gray hair (Chen et al. 2002; Ménasché et al. 2003; Westbroek et al. 2004). Recently, Ku et al. (2020) reported that *RAB27A/B* played a regulating role for hair growth during the hair cycle in human. The *FGF12* gene overlapped with CNVR (Chr6:114.36–114.37 Mb), was related to hair growth development. Fibroblast growth factors (FGF) are a family of growth factors that are involved in the regulation of hair morphogenesis and cycle hair growth (Lin et al. 2015; Ornitz and Itoh, 2015). Lv et al. (2020) reported a regulating role of *FGF12* gene in the sheep hair follicle development process. In addition, our finding supported by Wang et al. (Wang et al. 2021) study that reported the role of *FGF12* gene in hair follicle development in cashmere goats. The *SLC7A11* gene (CNVR_Chr7:73.54–73.57 Mb) is an amino acid transporter which mediates the extracellular cysteine in exchange for glutamate

(Jyotsana et al. 2022). It is well documented that the *SLC7A11* gene plays a critical role in changing the fur and skin color formation in animals through regulating the production of pheomelanin pigment (He et al. 2012; Tian et al. 2015; Chen et al. 2019; Wang et al. 2019). The amino acid cysteine is necessary for the formation of disulfide bonds and crosslinking between cysteines in the keratins and hair keratin-associated proteins is proved to be as an important step in forming the fineness, length, flexibility and other physical properties of hair and wool fibers (Deb-Choudhury, 2018). Thus, it was shown that the differences in the cysteine content leads to various structure of the hair fiber among species (Shimomura and Ito, 2005). Cysteine is an integral part of the pheomelanin synthesis to construct yellow or red hair color in humans and animals as it regulates the conversion of dopaquinone to pheomelanin in hair follicle melanocytes (Granholm et al. 1996; Ito and Wakamatsu, 2003). Chintala et al. (Chintala et al. 2005) found that the subtle gray mouse pigmentation mutant is under the genetic control of a mutation form of *SLC7A11* gene as it affects the rate of extracellular cystine transport into melanocytes, which reduces pheomelanin production and consequently, the loss of yellow pigment. Moreover, Song et al. (2017b) identified the *SLC7A11* gene as one of the key genes associated with the development of black and white coat color in farmed mink. The *EXOC2* gene (CNVR_Chr1:123.59–123.60 Mb) has been previously found to be associated with pigmentary phenotypes such as hair color and skin pigmentation (Han et al. 2008; Li et al. 2017; Guo et al. 2018). Our results suggested that these CNVR-harboring genes might be the potential candidate genes for fur characteristics and development in American mink.

Our results also revealed several CNVR-harbored genes related to the immune system process (*SWAP70*, *FYN*, *ORAI1*, *TRPM2,* and *FOXO3*). The *SWAP70* gene (CNVR_Chr11:157.8–157.9 Mb), is essential for normal B-cell migration that immobilizes F-actin filaments on phagosomes, contributing to immune regulation such as maturation and differentiation of immune cells (Baranov et al. 2016; Qian et al. 2021). Interestingly, Karimi et al. (2021a) reported the *SWAP70* gene as a potential candidate gene for response to Aleutian mink disease virus infection. The *FYN* gene (CNVR_Chr1:20.84–20.85 Mb), which is involved in various signaling pathways, plays a critical role

in apoptosis and immune response by regulating neuronal development and signaling in T and B cells (Picard et al. 2002; Comba et al. 2020). Zanella et al. (2015) suggested the *FYN* gene as a functional candidate gene associating with immune response to vaccinated pigs against influenza virus. The *ORAI1* gene (CNVR_Chr3:234.70–234.71 Mb) was the other gene associated with immune response, which is an important signaling component required for T cell activation and function (Feske et al. 2010). The *ORAI1* gene plays a role in maintaining a tick resistance status during the cattle tick infection (Bagnall et al. 2009). Recently, Xue et al. (2022) reported that the *ORAI1* might have regulating functions in the immune response, exacerbates inflammation and endoplasmic reticulum stress in bovine hepatocytes.

The *TRPM2* gene (CNVR_Chr6:1.82–1.83 Mb), which is a Ca^{2+}-permeable cation channel, is highly expressed in immune cells, primarily polymorphonuclear leukocytes, monocytes/macrophages, and T-cells (Beck et al. 2006; Yamamoto et al. 2008). It was revealed that *TRPM2*-deficient mice were highly susceptible to listeriosis infection, showing an ineffective innate immune response (Knowles et al. 2011). The *FOXO3* gene (CNVR_Chr1:23.49–23.50 Mb), which significantly enriched in Wnt signaling pathway, has been found to have therapeutic potential in chronic and autoimmune diseases (Hartwig et al. 2021). Aleutian mink disease virus causes autoimmune disorders in mink, stimulating the immune responses to provide antibodies, and consequently forming the immune complexes (Jepsen et al. 2009; Karimi et al. 2021b). Taking into account that most of mink farms are challenged by Aleutian mink disease virus, the most prevalence disease in the worldwide mink industry, suggesting that these genes, and related pathways, might substantially contribute to the modulation of immune responses to Aleutian mink disease virus infection. Nevertheless, the above functional inference of CNVs is based on enrichment analyses of their annotated genes and mostly based on the results from studies in other species, therefore, further functional validation of these CNVs is required to confirm their functions in mink.

4.5 Conclusions

In this chapter, we present the first CNV map of American mink using WGS data. We identified 5,378 CNVR covering 1.9% of the mink autosome. Functional annotation revealed CNVR enriched for genes related to natural behavior, lipid metabolism, and immune response. Our results revealed several CNVR that harbor genes related to fur quality *(MYO5A*, *RAB27B*, *FGF12*, *SLC7A11*, and *EXOC2*), and immune system response (*SWAP70*, *FYN*, *ORAI1*, *TRPM2*, and *FOXO3*). Overall, the results of the current chapter may facilitate our further understanding of the genetic control of different characteristics of fur in American mink and immune responses to Aleutian mink disease virus infection, which is the most prevalence disease in the worldwide mink industry.

Table 4.1 Descriptive statistics of CNVs detected in American mink genome.

CNV		Length (bp)		
	Number	Mean	Minimum	Maximum
Deletion	144,517	6,432.2	1,000	3,171,151
Duplication	20,216	14,655.3	1,003	4,254,987
Overall	164,733	7,441.3	1,000	4,254,987

Table 4.2 Distribution of CNVR across autosomal chromosomes of American mink genome.

Chromosome	Chromosome length (bp)	CNVR count	Length of CNVR (bp)	Coverage (%)	Max size (bp)	Average (bp)	Min size (bp)
1	317,036,279	683	4,071,099	1.3	371,616	5,960.6	1,003
2	240,416,976	522	4,470,485	1.9	858,878	8,564.1	1,016
3	235,645,773	508	3,550,404	1.5	1,786,562	6,988.9	1,003
4	231,359,643	433	2,209,544	1	234,143	5,102.9	1,003
5	167,246,402	324	4,406,049	2.6	3,171,454	13,598.9	1,019
6	224,559,537	543	2,456,160	1.1	150,398	4,523.3	1,004
7	207,076,058	417	2,699,685	1.3	664,002	6,474.1	1,012
8	144,012,018	273	2,135,038	1.4	955,355	7,820.7	1,009
9	101,698,841	224	1,068,011	1.1	229,614	4,767.9	1,004
10	75,573,270	189	2,509,561	3.3	1,866,663	13,278.1	1,005
11	220,349,319	569	11,245,345	5.1	2,939,814	19,763.4	1,003
12	148,690,698	319	1,804,339	1.2	652,086	5,656.2	1,003
13	152,771,447	292	4,030,656	2.6	1,986,383	13,803.7	1,004
14	46,742,321	82	633,928	1.4	367,849	7,730.9	1,018
Overall	2,513,178,582	5,378	47,290,304	1.9	3,171,454	8859.5	1003

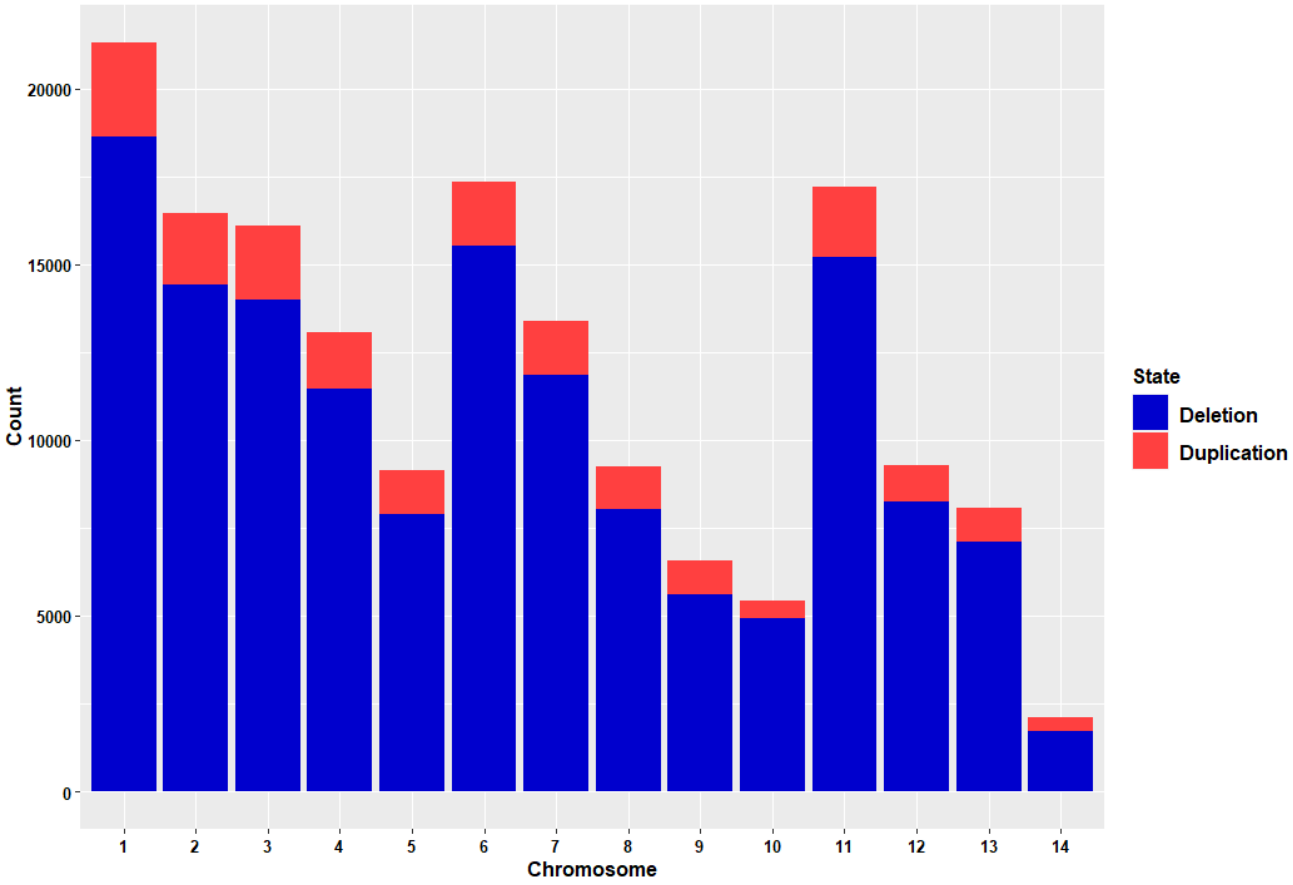

Figure 4-1 Numbers of CNVs identified across autosomal chromosomes of American mink.

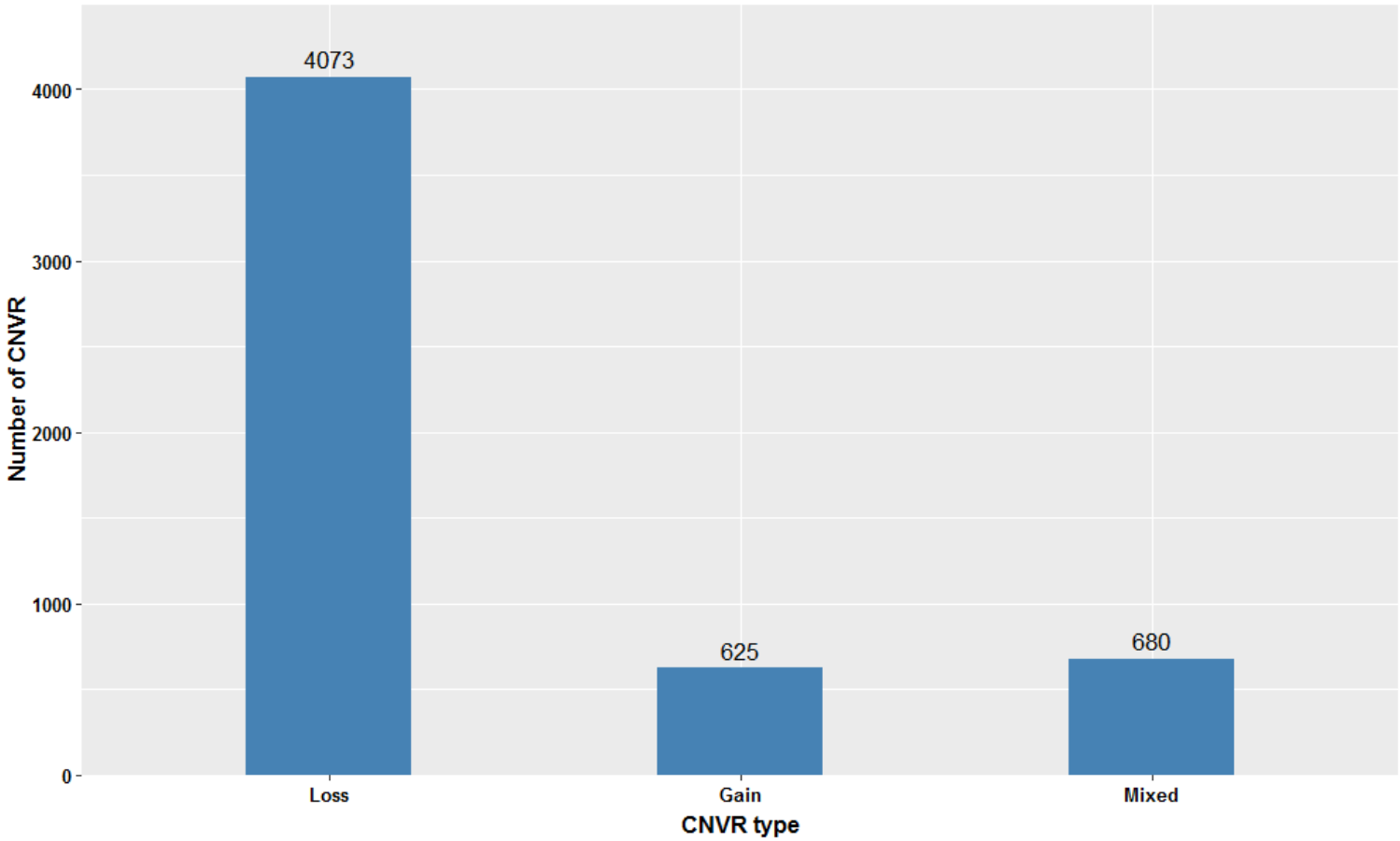

Figure 4-2 Distribution of CNVR types in American mink.

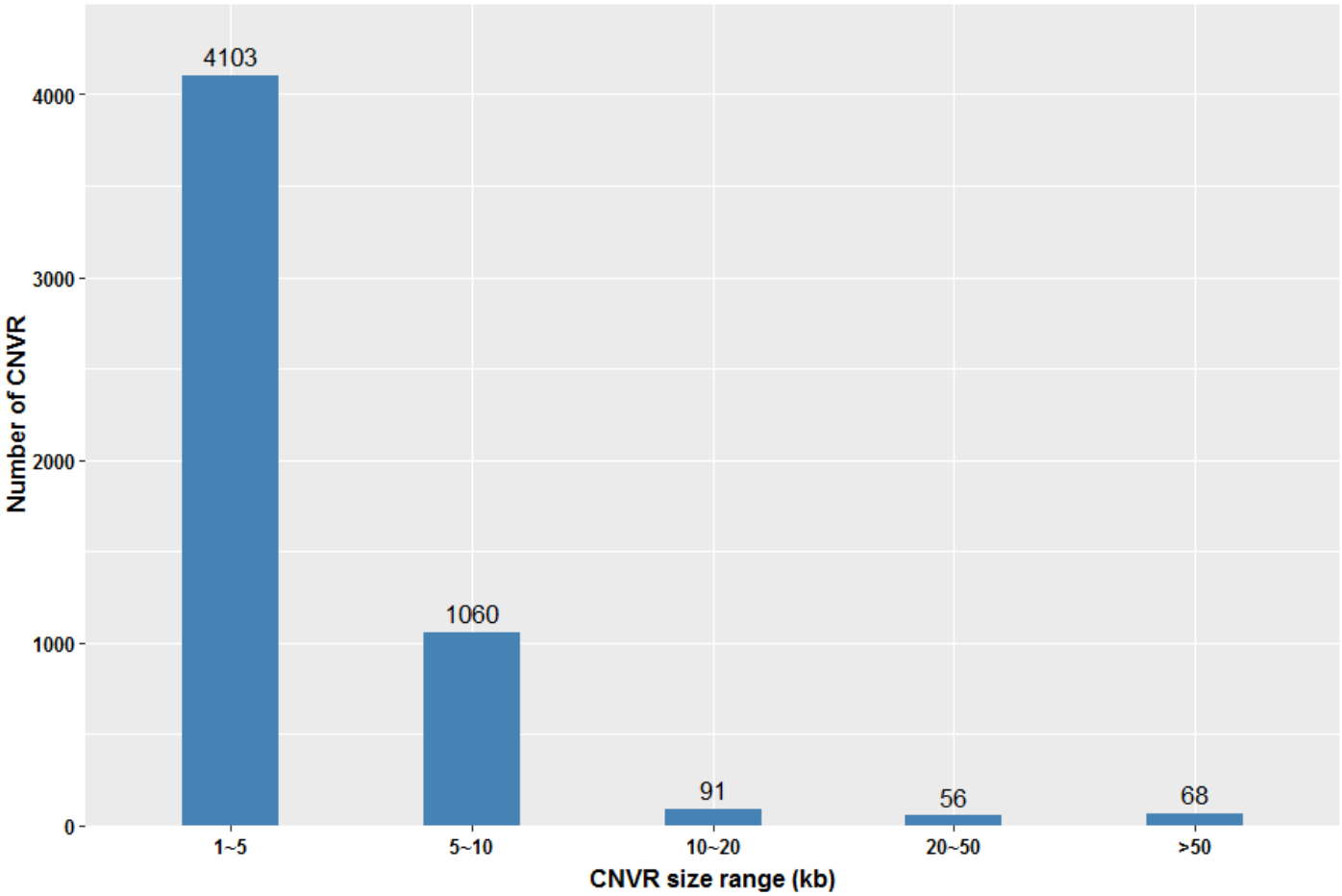

Figure 4-3 Distribution of CNVR sizes in American mink.

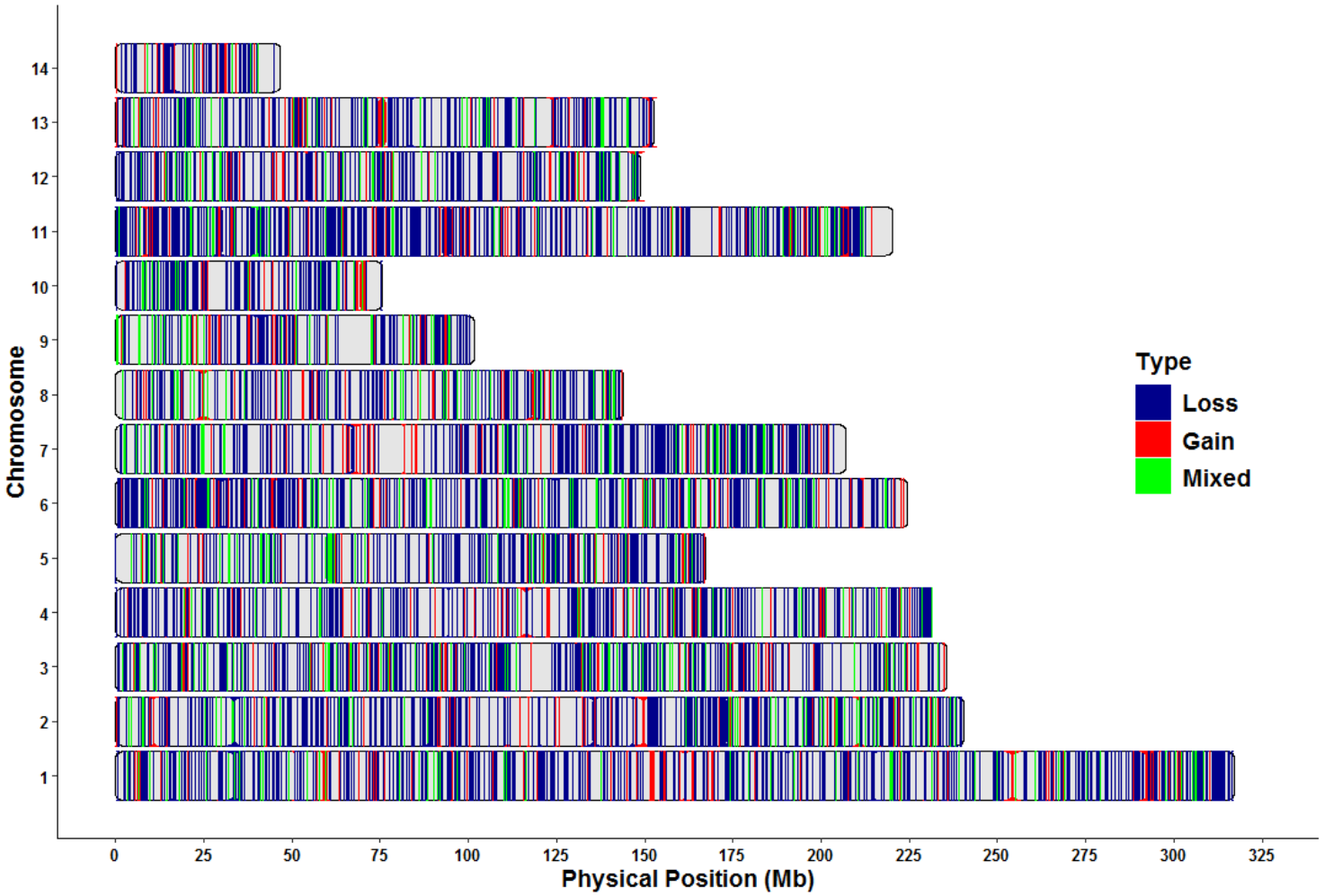

Figure 4-4 Genomic landscape of CNVR in American mink.

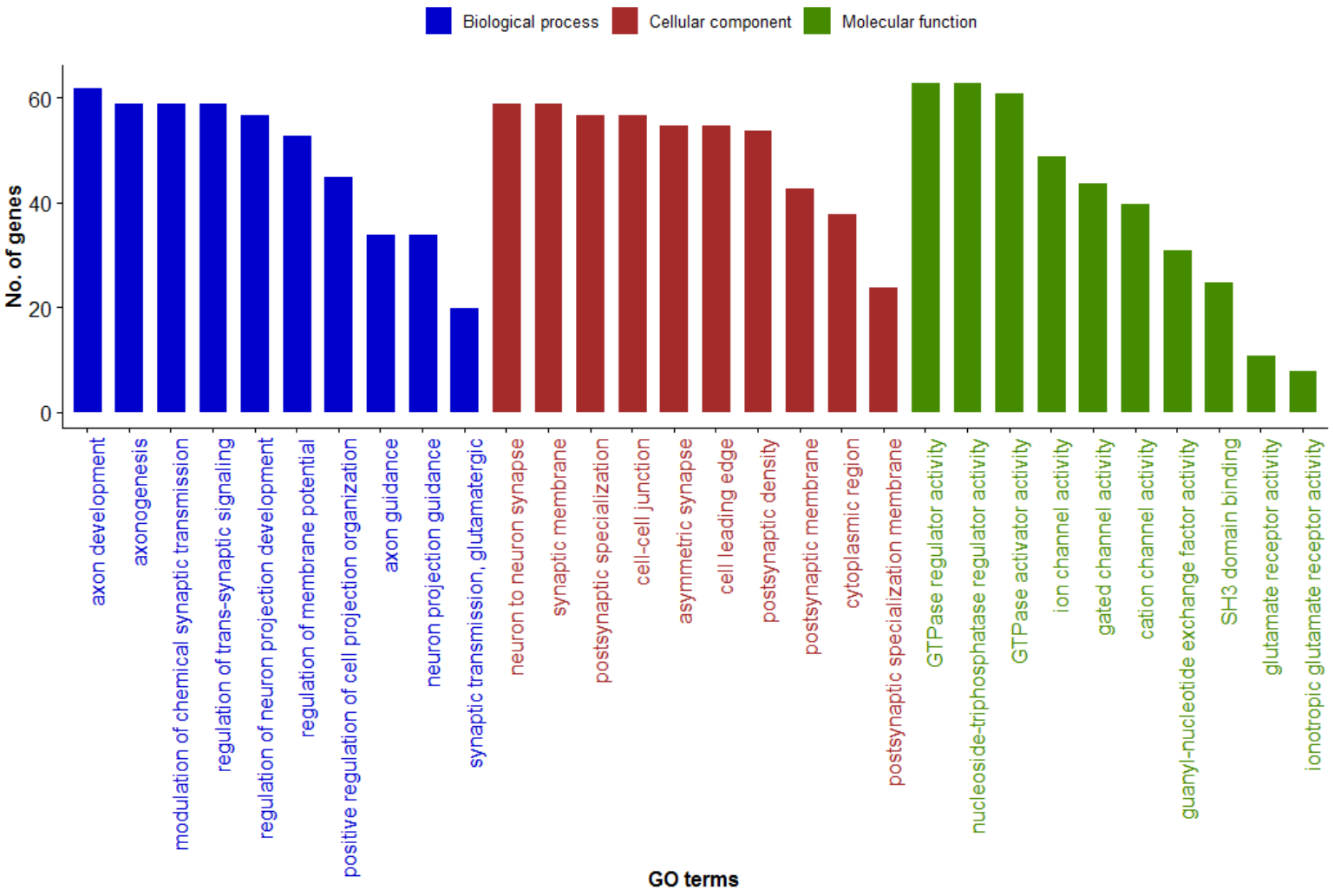

Figure 4-5 The top ten significant Gene Ontology terms enriched in CNVR-harbor genes in the three main GO categories (biological process (blue), cellular component (red), molecular function (green)).

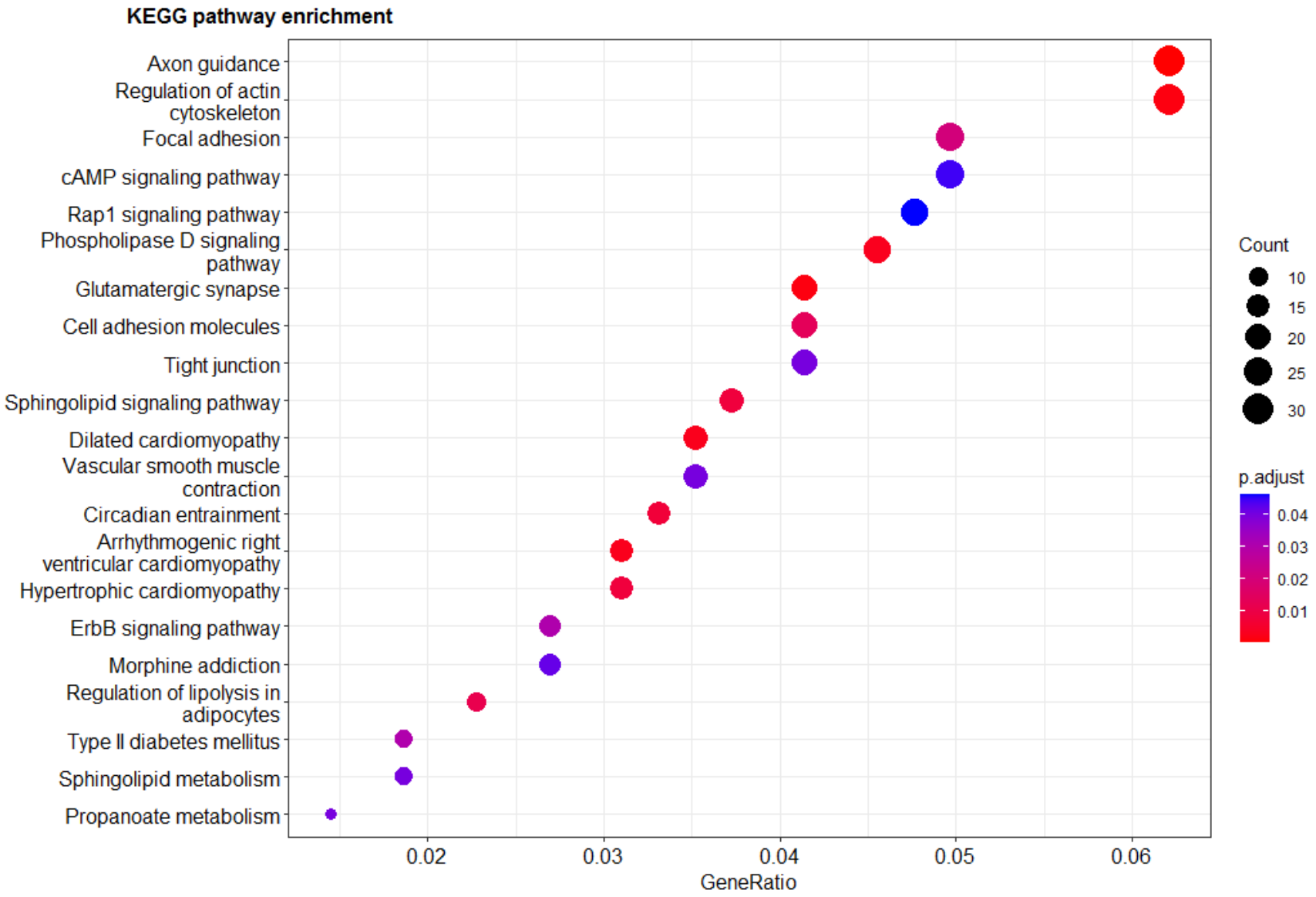

Figure 4-6 The metabolic pathways using KEGG enriched in CNVR-harbor genes.

CHAPTER 5. Genome-wide association studies for economically important traits in mink using copy number variation[1]

5.1 Introduction

American mink (*Neogale vison*) is one of the most important animals in the global fur industry, yet requires highly efficient breeding programs to deal with challenges faced in mink production systems (Karimi et al. 2022). Several studies have been carried out to discern the genetics of complex traits affecting the sustainability of mink production, including growth (Madsen et al. 2020; Do et al. 2021), feed efficiency (Shirali et al. 2015; Davoudi et al. 2022a), disease resistance (Farid et al. 2018; Hu et al. 2021; Karimi et al. 2021a; Hu et al. 2022a), pelt quality (Thirstrup et al. 2017; Valipour et al. 2022a; Valipour et al. 2022b), and reproduction traits (Hansen et al. 2010; Kołodziejczyk and Socha, 2011; Karimi et al. 2018). Understanding the genetic architecture underlying such traits using genome-wide association studies (GWAS) might contribute to expediting the genetic progress through selection, and therefore enhance the production efficiency of the mink industry.

Copy number variations (CNVs) refer to frequently observed structural variations in the form of deletions or duplications greater than 50 base pairs (Mills et al. 2011), which cover more of the genome (total bases) and have a higher mutation rate than single nucleotide polymorphisms (SNPs) (Geistlinger et al. 2018). Similar to SNPs, CNVs can be applied to detect associations with traits of economic interest in livestock species, and therefore, are considered complementary sources to explain genetic variation contributing to differences in phenotypes (Hay et al. 2018). Over the past decade, multiple studies have been carried out to examine the

[1] A version of this chapter has been submitted to the Scientific Reports by Davoudi et al. 2023. Genome-wide association studies for economically important traits in mink using copy number variation.

association between CNVs with several important phenotypes in livestock species, such as reproduction (Liu et al. 2019c; Zheng et al. 2020), health (Schurink et al. 2018; Butty et al. 2021; Berton et al. 2022), feed efficiency and growth (Zhou et al. 2018; Wang et al. 2020; Li et al. 2022), and performance traits (Fernandes et al. 2021; Yang et al. 2021; Ding et al. 2022). The availability of a high-quality chromosome-based genome assembly (Karimi et al. 2022) and a genome-wide SNP array for American mink facilitates the identification of genetic variations underlying economically important traits. Recently, Davoudi et al. (2022a) characterized the CNVs in American mink using whole-genome sequencing data. However, up to now, the CNV-based GWAS with economically important traits has not been reported in mink. Therefore, this chapter aimed to identify CNV in a large sample of genotyped mink and perform CNV-based GWAS analyses for Aleutian disease tests, growth and feed efficiency, reproduction and pelt quality traits. In addition, we performed functional annotation of the associated CNV regions (CNVRs) to identify the potential candidate genes for these key traits.

5.2 Materials and Methods

All procedures applied for this chapter were approved by the Dalhousie University Animal Care and Use Committee, and we adhered to the Code of Practice for the Care and Handling of Farmed Mink guidelines (Turner et al. 2013) throughout all phases of the research.

Initially, the Axiom™ Analysis Suite (Affymetrix®) was applied to perform quality control of raw intensity files and filter genotypes based on dish QC (DQC) values less than 0.82, and a minimum call rate of 97%, following the '*Best Genotyping Practices'* Workflow described in Axiom™ Genotyping Solution Data Analysis Guide (Thermofisher Scientific, 2017). The SNPs in sex chromosomes were excluded and only those that passed the quality control were kept for further analyses. The final data set contained 47,644 SNPs that were located on autosomal chromosomes.

The CNV detection was performed with PennCNV v.1.0.5 software (Wang et al. 2007), using the signal intensity ratios (Log R Ratio, LRR) and allelic frequencies (B Allele Frequency, BAF) obtained from the Axiom® CNV Summary Tool software (Affymetrix®). Then, the PFB (Population Frequency of B allele) file was compiled based on the BAF of each marker in the whole population, using the PennCNV *'compile_pfb.pl'* function. The GC content around each SNP marker is known to affect the signal strength through the potential interference of genomic waves (Marioni et al. 2007). Therefore, we first estimated the percentage of GC content of 1-Mb genomic regions surrounding each marker (500 kb on each side) using faToTwoBit and hgGcPercent tools provided by UCSC Genome Browser (Kuhn et al. 2013) and the FASTA information of the American mink genome assembly (Karimi et al. 2022). Next, the GC content file was implemented in PennCNV by *'-gcmodel'* function, which applies a regression model for adjusting the high GC content and recovers samples affected by genomic waves (Diskin et al. 2008). To achieve high-confidence CNV calls, quality control was applied with the following criteria: standard deviations for LRR<0.35, BAF drift<0.01, and waviness factor value between −0.05 and 0.05. We only retained those CNVs longer than 1 kb in length including at least three consecutive SNPs located on autosomal chromosomes. Finally, 2,063 high-quality samples were kept for subsequent analyses.

5.2.1 Phenotypic and deregressed EBV values

The deregressed estimated breeding values (dEBVs) were calculated for 27 economically important traits, including 11 growth and feed efficiency traits, eight reproduction traits, five pelt quality traits, and three Aleutian disease tests. The growth and feed efficiency traits include harvest weight (HW), harvest length (HL), final body weight (FBW), final body length (FBL), daily feed intake (DFI), average daily gain (ADG), feed conversion ratio (FCR), residual feed intake (RFI), residual gain (RG), residual intake and gain (RIG), and Kleiber ratio (KR). The reproduction traits include gestation length (GL), total number of kits born (TB), number of

kits alive at birth (LB), number of kits alive at weaning (LW), survival rate at birth (SB), average kit weight per litter at birth (AWB), average kit weight per litter at weaning (AWW), and survival rate at weaning (SW). The pelt quality traits include dried pelt size (DPS), overall quality of dried pelt (DQU), dried pelt nap size (DNAP), live grading overall quality of fur (LQU), and live grading nap size (LNAP). The Aleutian disease tests include counterimmunoelectrophoresis (CIEP), the Aleutian mink disease virus (AMDV) capsid protein-based enzyme-linked immunosorbent assay (ELISA-P), and the AMDV antigen-based enzyme-linked immunosorbent assay (ELISA-G). Breeding values were estimated for all individuals using different animal models for growth and feed efficiency described in detail by (Davoudi et al. 2022a), for reproduction traits described in detail by (Karimi et al. 2018), for pelt quality traits described in detail by (Valipour et al. 2022a), and for Aleutian disease tests described in detail by (Hu et al. 2021).

The EBV reliabilities were calculated using the following formula:

$$EBV\ reliabilities\ = 1 - \frac{prediction\ error\ variance}{additive\ genetic\ variance\ of\ the\ trait}$$

Next, the EBV reliabilities were applied to calculate the dEBVs using the method proposed by (Garrick et al. 2009). The calculations were performed by the '*wideDRP'* function in DRP package (Lopes, 2017) in the R environment (R Core Team, 2022), by setting the estimated heritability and the default value of 0.5 for the c parameter, which indicates the proportion of genetic variance not explained by markers. The descriptive statistics of the dEBVs for all traits are summarized in Table 5.1. We removed the animals with dEBV reliability lower than 0.20. The dEBVs were used as the pseudo-phenotype for the association analyses.

5.2.2 CNV association analysis

ParseCNV2 software (Glessner et al. 2022), which integrates PLINK (Chang et al. 2015) for association analyses, was used to detect the association between CNV and dEBVs of the studied traits. ParseCNV2 software converts the CNV events into probe-based statistics for individual CNVs (Glessner et al. 2022). Since CNV boundaries differ among individuals, it may be difficult to determine the exact start and end points of CNVs, which makes it challenging to classify different CNVs. Therefore, the CNV association tests were conducted for deletions or duplications separately at the probe level. The following model was applied for association testing:

$$\boldsymbol{y} = \boldsymbol{X}\boldsymbol{b} + \boldsymbol{e},$$

where $\boldsymbol{y}$ is the vector of dEBVs, $\boldsymbol{X}$ is the design matrix relating dEBVs to fixed effect of one CNV at a time, $\boldsymbol{b}$ is the fixed effect of CNV, and $\boldsymbol{e}$ is the vector of random residual effects. The association test output was used to merge neighboring SNPs in proximity (less than 1 Mb apart) with comparable association significance (±1 log P-value) into CNV regions (CNVRs), which constitute a genomic span of at least two consecutive probes. The local lowest P-value for identified probes was chosen to indicate the significant level of the whole CNVRs. To consider multiple testing correction, a threshold less than 5×10^{-4} was applied to consider a CNVR significantly associated with the phenotypes, as proposed by the ParseCNV2 developers (Glessner et al. 2013; Glessner et al. 2022).

5.2.3 Gene annotation

The list of genes in the latest American mink reference genome (ASM_NN_V1) (Karimi et al. 2022) was downloaded from the NCBI and the *'intersect'* function in Bedtools (Quinlan and Hall 2010) was used to detect the genes that overlapped with significant CNV regions. Finally, an extensive review of the literature was performed to investigate the biological function of identified candidate genes.

5.3 Results

5.3.1 CNV identification and distribution

Using the PennCNV software based on the Hidden Markov Model method (Wang et al. 2007), a total of 10,137 CNV events were identified from 2,063 individuals that passed the quality control criteria. While PennCNV is extensively utilized for CNV detection in genotyping array data, it is essential to note its limitations. The internal HMM model applied in the software specifically considers successive SNPs at each step, making it particularly sensitive to local noise. This sensitivity often results in false positives, over-segmentation (where a true CNV is incorrectly divided into smaller segments), and generally imprecise boundaries in the PennCNV calls (Montalbano et al. 2022). Among the total identified CNVs, 6,968 (68.74%) were duplications and 3,169 (31.26%) were deletions, with a deletions/duplications CNV ratio of 0.45. The length of the CNV events ranged from 1.05 to 6,148.34 kb, with an average size of 109.69 kb. Table 5.2 presents the descriptive statistics of the identified CNVs in the American mink genome. Analysis of the distribution of CNV size showed that approximately half of the CNVs ranged from 1 to 50 kb, with relatively rare CNV events (3.97%) larger than 500 kb (Figure 5.1a). The number of CNVs on each chromosome and the chromosome length showed a strong positive linear correlation (Figure 5.1c, r=0.78), such that 1,282 CNVs were identified for the largest chromosome (Chromosome 1) and 225 CNVs for the smallest chromosome (chromosome 14; Figure 5.1b).

5.3.2 Association analyses

In order to explore the effect of CNVs on the complex phenotypes, CNV-based association analyses were carried out for the 27 economically important traits in American mink. Association analyses revealed that 250 CNVRs (71 deletions and 179 duplications) were significantly associated with at least one of the studied traits ($P<0.0005$). Manhattan plots for significant CNVRs across the autosomes associated with all studied traits are shown in Figures

5.2-5.5. These significant regions were identified across all 14 autosomes, while chromosome one showed the largest number (n=53).

The overview of the top significant CNVRs associated with each studied trait is shown in Table 5.3. The highest number of significant CNVRs (n=27) were associated with TB, compromising the most significant region (ID: CNVR54) with a P-value of 3.58×10^{-14}. In addition, the average length of significant CNVRs was 66.2 kb, ranging from 1.23 to 444.54 kb.

5.3.3 Candidate genes within the significant CNVR

We further investigated the candidate genes encompassing the significant CNVRs. The results revealed that a total of 320 potential candidate genes overlapped with significant CNVRs based on the annotation of the American mink genome. The duplication CNVR on chromosome 7 (ID: CNVR143) overlapped with the highest number of genes (n=13) while no genes identified within 80 significant CNVRs.

Using the information from the GeneCards database and an extensive literature review, several candidate genes were found to be related to growth and feed efficiency traits (*ARID1B, APPL1, TOX,* and *GPC5*), reproduction traits (*GRM1, RNASE10, WNT3, WNT3A,* and *WNT9B*), pelt quality traits (*MYO10,* and *LIMS1*), and Aleutian disease tests (*IFNGR2, APEX1, UBE3A,* and *STX11*).

5.4 Discussion

Genome-wide association studies using SNP markers have been instrumental in unraveling the underpinning of complex traits (Abdellaoui et al. 2023). In recent years, CNVs have gained widespread utilization as a supplementary tool in association studies, adding in the identification of genetic variants associated with economically important traits and shedding light on the elucidating the genetic basis of these traits across different livestock species (Xu et al. 2019; Fernandes et al. 2021; Salehian-Dehkordi et al. 2021; Ladeira et al. 2022;

Taghizadeh et al. 2022). To the best of our knowledge, there is no prior research had delved into the realm of CNV associations with diverse phenotypes in American mink.

We conducted the CNV-based association studies using Affymetrix Mink 70K SNP array to identify potential genetic variants associated with dEBVs of 27 different traits such as growth and feed efficiency, reproduction, Aleutian disease tests, and pelt quality traits. In total, 10,137 CNVs were identified, with an average number of five CNVs per sample. Although the average number of detected CNVs per individual is substantially less than our previous chapter using whole-genome sequencing data (average number of 1,647.3), it is in agreement with the results of other studies that used SNP genotyping data with a similar marker density (Liu et al. 2019d; Butty et al. 2021; Qiu et al. 2021; Wang et al. 2021). It is well-known that the SNP genotyping density affects the number and length of the identified CNVs (Butty et al. 2021). The average length of identified CNVs (109.69 kb) is much longer than our previous chapter with an average size of 7.4 kb, showing differences in resolution and coverage of genome between SNP array and whole-genome sequencing data, yet falls within the range of other studies using comparable SNP array data sets (Butty et al. 2020; Strillacci et al. 2021). A total of 250 significant CNVRs were associated with at least one of the studied traits ($P<0.0005$), overlapping with 320 potential candidate genes.

For growth and feed efficiency traits, we identified 86 CNVRs associated with eleven traits. Within these significant CNV segments, we identified *ARID1B, APPL1, TOX,* and *GPC5* genes, which might have large impacts on growth rate and feed efficiency in American mink. The *ARID1B* gene is overlapped with the duplication CNVR1 (Chr1:10,430,780–10,527,641), which was significantly associated with traits such as FBW, ADG, FCR, KR, and RIG. The *ARID1B* gene, which plays a key role in controlling the maturation of neurons during brain development (Ka et al. 2016), is the commonly mutated gene in Coffin-Siris syndrome, a genetic disorder characterized by intellectual disability, developmental delay, and growth

impairment (Tsurusaki et al. 2012; Celen et al. 2017). Yu et al. (2015) reported that the *ARID1B* gene overlapped with identified CNVs in patients with short stature and developmental disorder, indicating the critical function of *ARID1B* mutations in human height regulation. Interestingly, Bovo et al. (2020) detected a region being targeted by selection pressure, harboring the *ARID1B* gene in different pig breeds that grouped by their size, supporting the effect of this gene on body size. The *APPL1* gene located on duplication CNVR125 (Chr6:198,790,330–198,804,380) interacts with several proteins such as adiponectin receptors, AMPK, and Rab5 (a small GTPase downstream of *APPL1*) to regulate apoptosis, cell proliferation, metabolism and insulin sensitivity in energy homeostasis, resulting in increased glucose uptake and fatty acid oxidation (Deepa and Dong, 2009). Schweer et al. (2018) reported that the *APPL1* gene is associated with feed efficiency traits in beef cattle through the regulation of glucose.

The *TOX* gene, located in the duplication CNVR75 (Chr4:75,332,844,330–75,473,471), which overlapped with the identified CNVR in chapter 4 (Davoudi et al. 2022c), was significantly associated with FBW and ADG. The *TOX* gene is a family member of high-mobility group box proteins and serves as a regulator of gene expression, mostly through modifying the density of the chromatin structure (Wilkinson et al. 2002). In cattle, numerous studies demonstrated that the *TOX* gene is associated with feed efficiency (Seabury et al. 2017), growth (Martínez, 2014), carcass traits (Lee et al. 2013; Bhuiyan et al. 2018; De Las Heras-Saldana et al. 2020), and development of puberty (Fortes et al. 2012). Furthermore, it is shown that the *TOX* gene is associated with weight gain, obesity, and metabolic syndrome-related phenotypes in humans (Li et al. 2017). The *GPC5* gene, which mediates several functions in the control of cell division and growth regulation (Baranzini et al. 2009), is found within a deletion CNVR96 (Chr5:149,166,233– 149,199,404), associating with ADG, RIG, and KR. Congruent with these findings, *GPC5* was reported as a candidate gene located within a significant SNP with a

pleiotropic effect on RIG, RFI, and efficiency of intake in beef cattle (Serão et al. 2013). Moreover, other GWAS indicated the association of the *GPC5* gene with human height (Lango et al. 2010), body mass index (Wang et al. 2012), and body size/body weight in chicken (Gu et al. 2011; Wang et al. 2016).

Regarding the female reproduction traits, we found 168 significant CNVRs, overlapping with several functional genes, among which *GRM1, RNASE10, WNT3, WNT3A,* and *WNT9B* might be the candidate genes related to female reproduction in mink. The *GRM1* gene, which was previously identified in a CNV study in American mink (Davoudi et al. 2022c), was located within the duplication CNVR15 (Chr1: 56,870,177–56,925,961), associated with AWB trait. The *GRM1* was a gene of interest reported in several studies to be associated with female reproduction in different livestock species, such as seasonal reproduction in sheep (Zhu et al. 2022a), litter size in goats (Dong et al. 2023), number of teats and litter traits in pig (Verardo et al. 2015), and fertility-related traits in cattle (Tahir et al. 2021). Interestingly, it was reported that the *GRM1* gene located within structural variations and runs of homozygosity regions associated with litter traits in pigs (Liu et al. 2019a; Chen et al. 2022), highlighting the hypothesis that this gene might be a candidate gene for female reproduction in American mink. It was suggested that *RNASE10* gene action in the proximal epididymis is vital for the acquisition of spermatozoa adhesiveness, eventually affecting the mode of sperm transport in the female reproductive tract (Krutskikh et al. 2012).

In the current chapter, several *WNT* family genes were identified to be associated with reproduction traits in American mink, including *WNT3* and *WNT9B* (both found within the duplication CNVR118), and *WNT3A* (overlapped with the deletion CNVR23). It is well-documented that the expression of *WNT3* during the early pregnancy mediates the stromal cell proliferation and trophoblast invasion, eventually affecting the embryonic development (Kaloğlu et al. 2020). Comparably, the *WNT9B* gene has been reported as one of the key genes

associated with inducing the gonadotropin-releasing hormone secretion during follicular development in sheep (Chen et al. 2021). Another gene, *WNT3A*, is known as the main regulator of reproductive behavior and follicular activity associated with estrus, which in turn may contribute to the reproductive efficiency in cattle (Aloqaily et al. 2018).

The gene annotation within significant CNVRs for pelt quality traits identified some functional candidate genes affecting fur characteristics, such as *MYO10* and *LIMS1*. The *MYO10* gene is an integral member of the myosin family, which is involved in various cellular processes such as dynamic actin remodeling, cell migration and adhesion, and filopodia formation (Bohil et al. 2006; Mattila and Lappalainen, 2008). Our findings are in accordance with previous studies indicating that the *MYO10* gene plays a key role in mediating skin pigmentation through regulating melanosome transportation in the skin (Singh et al. 2010; Heimsath et al. 2017; Tokuo et al. 2018). It was demonstrated that the melanocytes present in the skin control the quantity and types of melanosomes, ultimately determining the coat color (Hirobe 2011). Notably, it was shown that the *MYO10* gene mutation altered the coat color pigmentation pattern in mice, further supporting its role in facilitating melanoblast migration (Liakath-Ali et al. 2019). Interestingly, another member of the myosin superfamily, the *MYO5A* gene, has been widely documented for its impact on coat color phenotype in different species (Bierman et al. 2010; Fontanesi et al. 2012; Christen et al. 2021), and specifically in American mink (Manakhov et al. 2019; Davoudi et al. 2022c). The *LIMS1* gene is located within the duplication CNVR170 (Chr8: 65,501,492–65,735,953), associated with the DQU trait.

The *LIMS1* gene involved in the control of cell signaling, adhesion, migration, proliferation, and survival (Kovalevich et al. 2011). Several studies demonstrated that the *LIMS1* gene regulates cell adhesion and spreading through the ternary protein complex of integrin-linked kinase (ILK), PINCH, and parvin (Legate et al. 2006). To this end, ILK has been reported as a crucial factor for hair morphogenesis (Lorenz et al. 2007). Interestingly, Endo et al. (2018)

reported that the *LIMS1* gene was associated with hair morphology and density in East Asians. Furthermore, it was shown that the loss of *LIMS1* gene expression from mouse keratinocytes resulted in impaired hair follicle growth (Karaköse et al. 2015), supporting the importance of this gene on fur development in mink.

Aleutian mink disease virus causes autoimmune disorders in mink by stimulating their immune response to produce antibodies and form immune complexes (Jepsen et al. 2009; Karimi et al. 2021a). For CIEP, ELISA-P, and ELISA-G, we identified 9, 12, and 22 significant CNVRs, respectively, which overlapped with several immune-related genes such as *IFNGR2, APEX1, UBE3A,* and *STX11*. The *IFNGR2* gene encodes IFNγR2, which is part of the IFN-γ receptor complex that is overexpressed in an inflammatory environment (Regis et al. 2006). It is well established that *IFNGR2* is an important regulator for IFN-γ-STAT1 signaling in T cells (Schroder et al. 2004), in turn, the dysregulation of the *IFNGR2* gene is associated with a variety of autoimmune diseases (Holzer et al. 2013). The *APEX1* and *UBE3A* genes overlapped with the duplication CNVR236 (Chr13: 96,258,171–96,346,188) and the deletion CNVR237 (Chr13: 125,264,701–125,304,748), respectively, both associated with ELISA_G, GL and AWB traits. In agreement with our results, Hu et al. (2021) indicated a favorable genetic correlation between Aleutian disease test and reproduction traits in American mink, which suggested the potential for genetic selection of Aleutian disease test traits to alleviate the adverse impact caused by Aleutian disease in mink farms.

The *APEX1* gene (also called *APE1*) encodes a multifunctional protein that regulates the DNA base excision repair and redox activities, the latter demonstrated to be involved in mediating the T helper cell 1 (Th1) response (Akhter et al. 2016). In addition, it is well-documented that the *APEX1* gene plays a proinflammatory function in stimulating cytokine and chemokine expression, eventually contributing to innate and adaptive immunity processes (Oliveira et al. 2022). It has been confirmed that the *UBE3A* gene, present in both glutamatergic and

GABAergic neurons in the brain, functions as a transcriptional regulator of the immune system within the brain (Furumai et al. 2019). Recently, Zhang et al. (2022) revealed that the *UBE3A* gene within a deletion CNV is associated with the enrichment levels of immune signaling pathways, eventually enhancing antitumor immunity and immunogenicity. The *STX11* gene, which is a member of the SNARE family, is highly expressed in immune tissues such as the thymus, spleen, and lymph nodes, regulating the IFN-γ secretion from natural killer cells, consequently mediating the immune cell function (Prekeris et al. 2000; D'Orlando et al. 2013).

5.5 Conclusion

For the first time in American mink, the CNV-based GWAS were applied for economically important traits using the Affymetrix Mink 70K SNP array. We identified 10,137 CNVs, including 6,968 duplications and 3,169 deletions, among which 250 CNVRs were significantly associated with at least one trait. From this, we identified several candidate genes contributing to the growth and feed efficiency (*ARID1B, APPL1, TOX,* and *GPC5*), reproduction (*GRM1, RNASE10, WNT3, WNT3A,* and *WNT9B*), pelt quality (*MYO10,* and *LIMS1*), and Aleutian disease tests (*IFNGR2, APEX1, UBE3A,* and *STX11*). Overall, the associated CNVRs and respective candidate genes in the current chapter supply additional information, complementary to GWAS analyses solely based on SNP markers, further helping reveal the genetic basis of traits of economic interest in American mink.

Table 5.1 Descriptive statistics of the deregressed EBV (dEBVs) for growth, feed efficiency, Aleutian disease tests, pelt quality and reproduction traits in American mink.

Trait	Abbreviations	Numbers	dEBVs			
			Mean	SD	Min.	Max.
Harvest weight	HW	1985	-0.01	0.30	-1.82	1.92
Harvest length	HL	1921	0.10	2.03	-7.92	9.91
Final body weight	FBW	1037	0.00	0.30	-1.15	1.37
Final body length	FBL	1038	-0.08	1.98	-6.59	5.83
Daily feed intake	DFI	1872	0.01	0.07	-0.15	0.23
Average daily gain	ADG	1044	-0.02	2.19	-10.14	9.18
Feed conversion ratio	FCR	1036	0.34	8.60	-23.39	61.52
Residual feed intake	RFI	1044	0.00	0.02	-0.12	0.14
Residual gain	RG	1042	-0.04	1.51	-7.19	5.70
Residual intake and gain	RIG	1043	-0.04	1.48	-6.76	6.43
Kleiber ratio	KR	1044	-0.01	1.15	-6.05	4.64
Counterimmunoelectrophoresis test	CIEP	1356	0.00	0.12	-0.63	0.34
VP2 based enzyme-linked immunosorbent assay test	ELISA-P	1356	0.04	2.12	-5.16	10.34
AMDV-G based enzyme-linked immunosorbent assay test	ELISA-G	1356	-0.10	2.23	-6.39	10.83
Gestation length	GL	1321	-0.44	2.74	-29.01	25.43
Total number of kits born	TB	1321	0.25	1.37	-6.51	11.10
Number of kits alive at birth	LB	1319	0.35	1.26	-5.15	9.14
Number of kits alive at weaning	LW	1314	-0.04	1.20	-8.51	7.39
Survival rate at birth	SB	1169	2.39	7.77	-61.69	46.51
Average kit weight per litter at birth	AWB	1168	0.01	0.83	-4.90	5.98
Average kit weight per litter at weaning	AWW	1167	0.95	23.02	-168.37	132.25
Survival rate at weaning	SW	1166	-0.27	14.26	-86.29	51.27
Dried pelt size	DPS	1169	0.02	0.70	-7.20	8.24
Overall quality of dried pelt	DQU	1148	-0.01	0.56	-3.92	2.17
Dried pelt nap size	DNAP	1159	0.17	1.10	-4.91	4.94
Live grading overall quality of fur	LQU	1260	0.05	0.56	-3.96	3.79
Live grading nap size	LNAP	1260	0.14	0.79	-3.84	3.60

Table 5.2 Descriptive statistics of CNVs detected in American mink genome.

CNV	Number	Length (bp)		
		Mean	Minimum	Maximum
Deletion	3,169	98,984.12	1,049	2,956,427
Duplication	6,968	114,555.32	1,128	6,148,335
Overall	10,137	109,687.54	1,049	6,148,335

Table 5.3 Overview of the top significant CNVRs associated with all studied traits in American mink.

CNVR ID	Type	Chromosome	Start position	End position	Length (bp)	Associated traits[1]	P-value	Candidate genes
CNVR54	Duplication	2	76,047,394	76,080,498	33,104	TB	3.58E-14	-
CNVR112	Deletion	5	45,720,950	45,756,856	35,906	DPS	1.26E-13	*ITGA3, LOC122907723*
CNVR203	Duplication	11	119,613,197	119,626,953	13,756	AWW	1.44E-13	*LOC122890709, LOC122889431*
CNVR126	Duplication	6	143,324,461	143,377,043	52,582	HW	3.48E-13	-
CNVR1	Duplication	1	10,430,780	10,527,641	96,861	FCR	5.35E-13	*ARID1B*
CNVR113	Deletion	5	158,304,905	158,351,587	46,682	DQU	6.26E-13	*METTL21C, BIVM, CCDC168*
CNVR200	Duplication	11	208,363,505	208,379,126	15,621	AWB	2.24E-12	*DLGAP2*
CNVR56	Duplication	2	51,828,542	51,834,524	5,982	LW	2.95E-12	-
CNVR20	Duplication	1	48,882,466	48,894,690	12,224	GL	3.08E-12	*BCKDHB*
CNVR54	Duplication	2	76,047,394	76,080,498	33,104	LQU	8.35E-12	-
CNVR216	Deletion	11	71,374,870	71,389,512	14,642	SW	5.42E-10	*TBC1D9*
CNVR90	Duplication	4	201,592,245	201,635,594	43,349	SB	1.71E-09	*KCND2*
CNVR238	Duplication	13	139,238,384	139,379,378	140,994	RFI	7.32E-09	-
CNVR235	Duplication	13	26,765,710	26,829,160	63,450	CIEP	1.98E-07	-
CNVR40	Duplication	2	237,951,459	238,012,681	61,222	ELISA_G	5.81E-07	-
CNVR159	Deletion	7	130,788,259	130,823,564	35,305	LNAP	1.9E-06	*PIWIL4*
CNVR2	Duplication	1	133,977,608	134,011,851	34,243	KR	2.64E-06	*SYCP2L*
CNVR13	Duplication	1	75,139,496	75,250,132	110,636	RIG	3.97E-06	-
CNVR1	Duplication	1	10,430,780	10,527,641	96,861	ADG	6.29E-06	*ARID1B*
CNVR179	Duplication	9	12,654,424	12,657,997	3,573	DNAP	6.66E-06	*TTLL11*
CNVR70	Duplication	3	46,223,063	46,323,843	100,780	LB	7.80E-06	*NDUFA10*
CNVR9	Duplication	1	282,031,840	282,086,441	54,601	HL	9.33E-06	-
CNVR192	Duplication	11	56,914,479	56,922,804	8,325	ELISA_P	4.19E-05	*LOC122890225*
CNVR4	Duplication	1	119,299,899	119,337,598	37,699	DFI	1.53E-04	*HSD17B8, SLC39A7, RXRB, COL11A2*
CNVR75	Duplication	4	75,332,844	75,473,471	140,627	FBW	1.81E-04	*TOX*
CNVR12	Duplication	1	11,780,319	11,833,194	52,875	RG	2.84E-04	*NOX3*
CNVR125	Duplication	6	198,790,330	198,804,380	14,050	FBL	4.27E-04	*ASB14, DNAH12, APPL1*

[1] TB: Total number of kits born, DPS: Dried pelt size, AWW: Average kit weight per litter at weaning, HW: Harvest weight, FCR: Feed conversion ratio, DQU: Overall quality of dried pelt, AWB: Average kit weight per litter at birth, LW: Number of kits alive at weaning, GL: Gestation length, LQU: Live grading overall quality of fur, SW: Survival rate at weaning, SB: Survival rate at birth, RFI: Residual feed intake, CIEP: Counterimmunoelectrophoresis test, ELISA_G: AMDV-G based enzyme-linked immunosorbent assay test, LNAP: Live grading nap size, KR: Kleiber ratio, RIG: Residual intake and gain, ADG: Average daily gain,

DNAP: Dried pelt nap size, LB: Number of kits alive at birth, HL: Harvest length, ELISA_P: VP2 based enzyme-linked immunosorbent assay test, DFI: Daily feed intake, FBW: Final body weight, RG: Residual gain, FBL: Final body length.

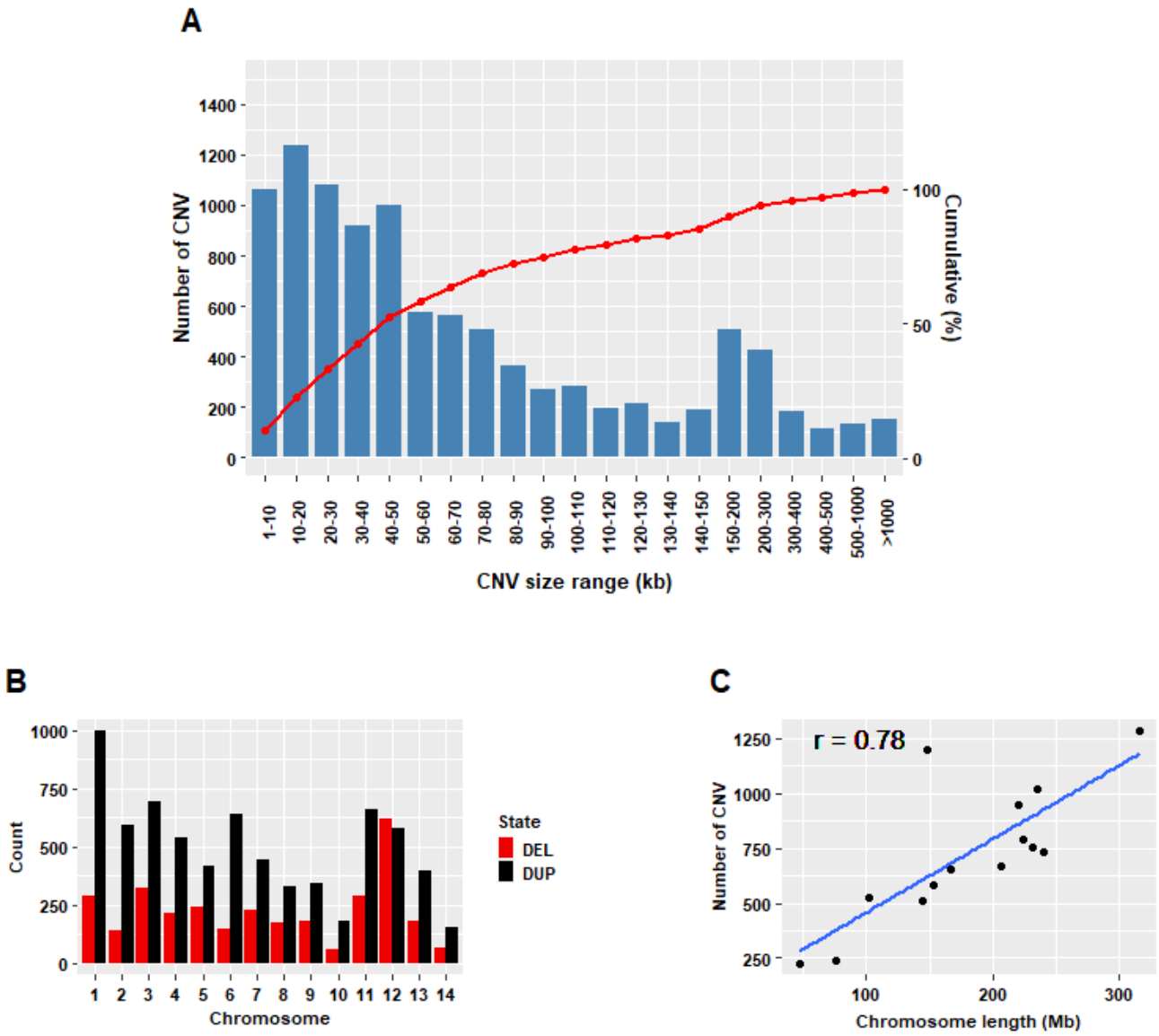

Figure 5-1 Graphical representation of identified CNVs. A) Distribution of CNV sizes B) Numbers of CNVs identified across autosomal chromosomes C) Correlation between CNV numbers and chromosome length.

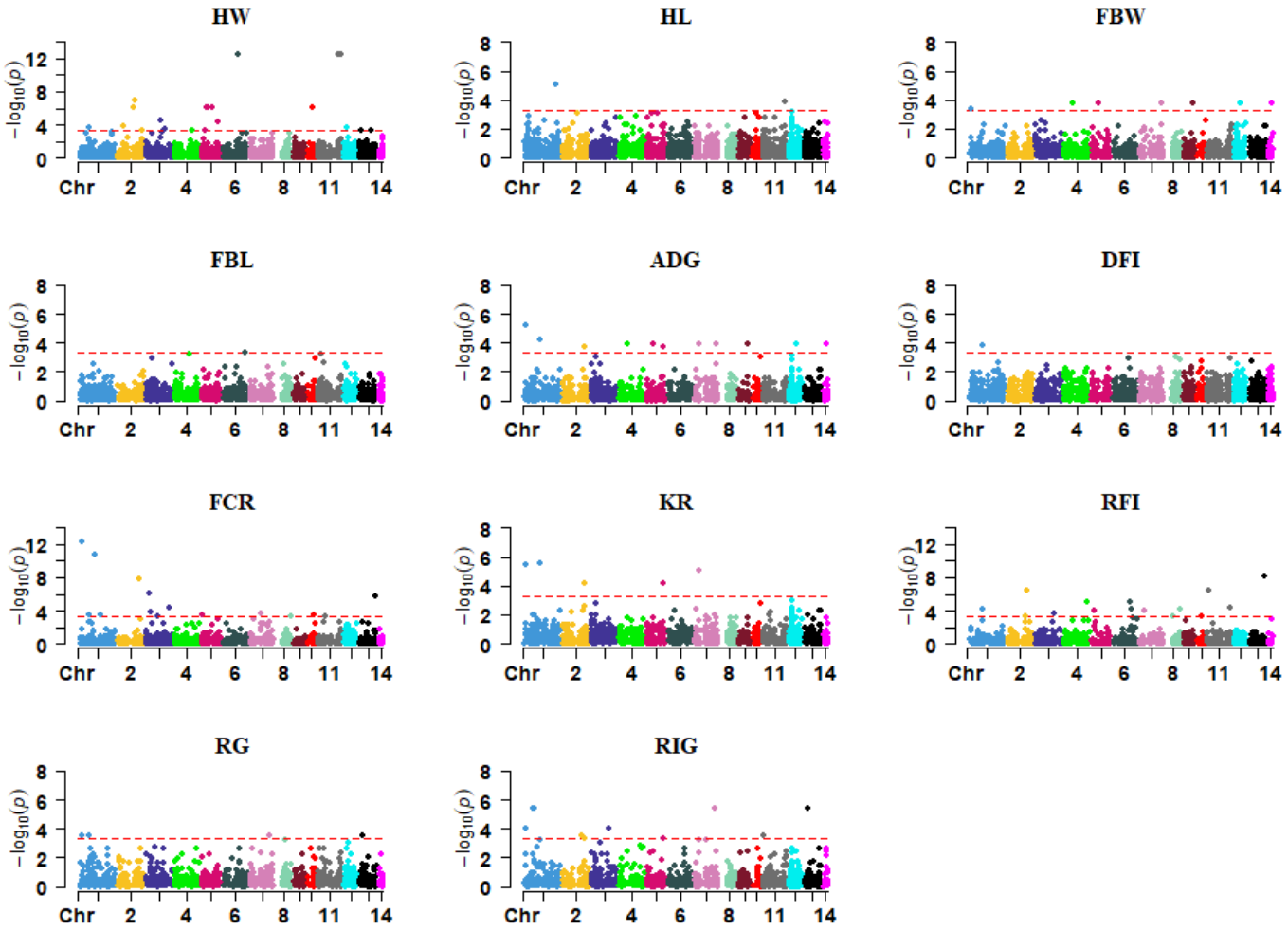

Figure 5-2 Manhattan plots for CNV regions across the 14 autosomal chromosomes associated with feed efficiency and growth traits. The horizontal line in each plot represents the threshold for significance (P< 0.0005) suggested by ParseCNV developers. HW: Harvest weight; HL: Harvest length; FBW: Final body weight; FBL: Final body length; ADG: Average daily gain; DFI: Daily feed intake; FCR: Feed conversion ratio; KR: Kleiber ratio; RFI: Residual feed intake; RG: Residual gain; RIG: Residual intake and gain.

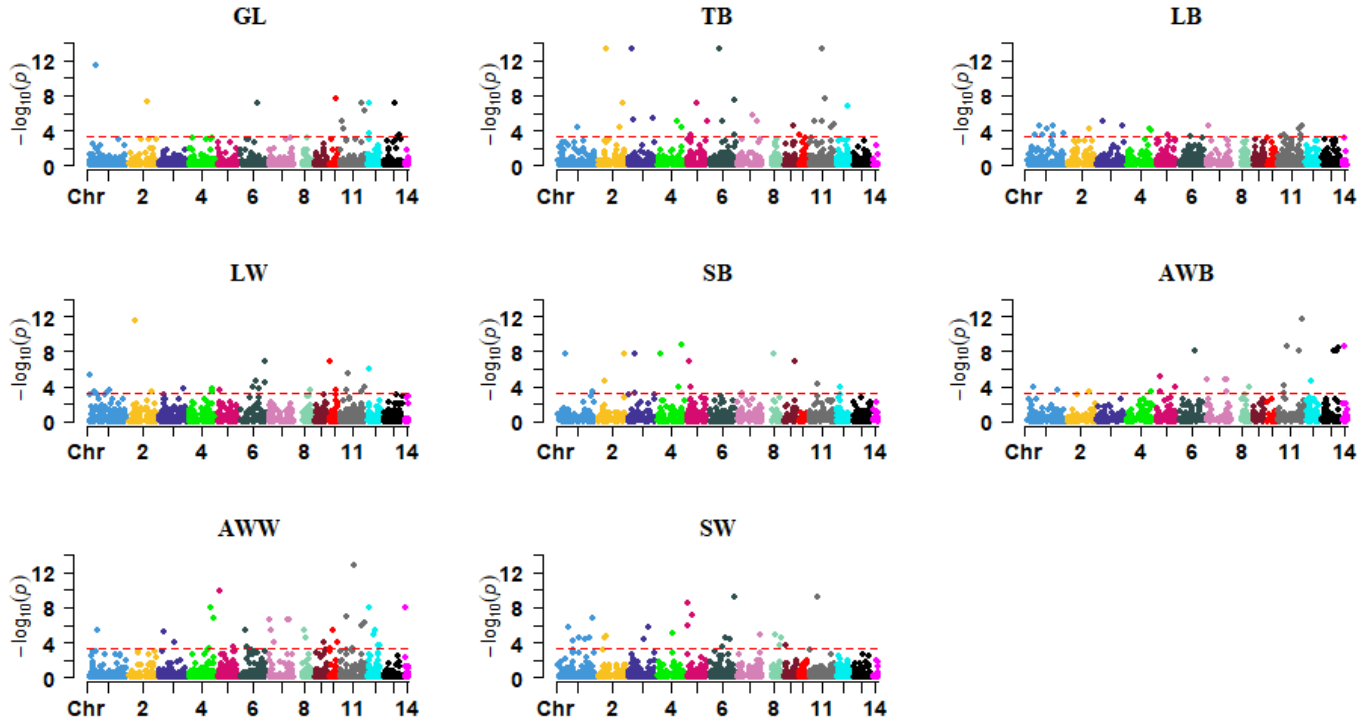

Figure 5-3 Manhattan plots for CNV regions across the 14 autosomal chromosomes associated with reproduction traits. The horizontal line in each plot represents the threshold for significance (P< 0.0005) suggested by ParseCNV developers. GL: Gestation length; TB: Total number of kits born; LB: Number of kits alive at birth; LW: Number of kits alive at weaning; SB: Survival rate at birth; AWB: Average kit weight per litter at birth; AWW: Average kit weight per litter at weaning; SW: Survival rate at weaning.

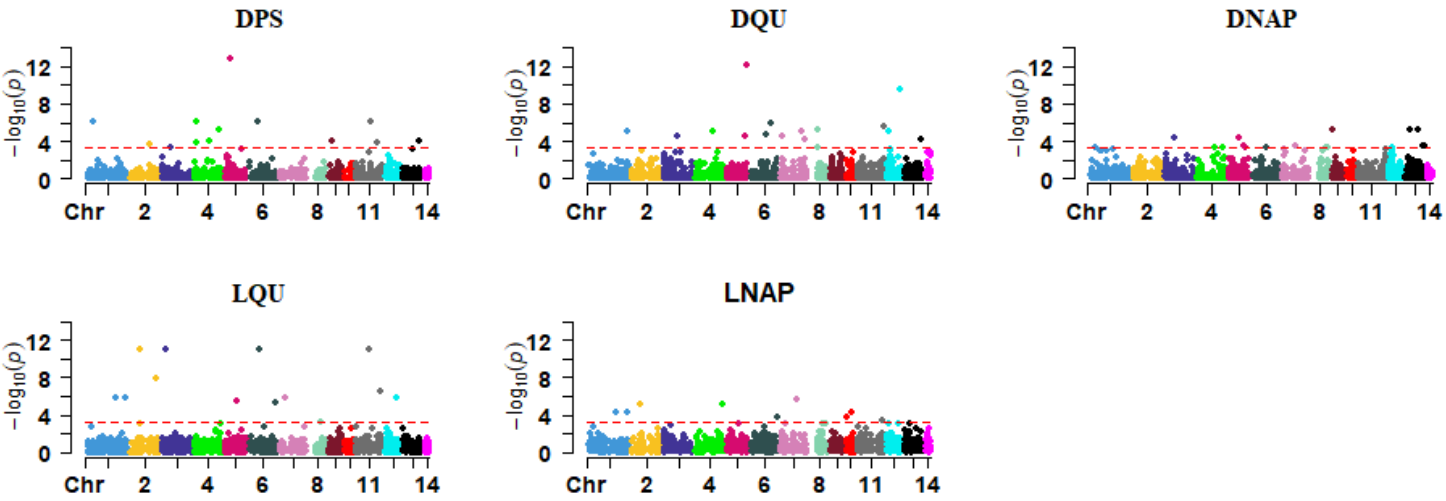

Figure 5-4 Manhattan plots for CNV regions across the 14 autosomal chromosomes associated with pelt quality traits. The horizontal line in each plot represents the threshold for significance (P< 0.0005) suggested by ParseCNV developers. DPS: Dried pelt size; DQU: Overall quality of dried pelt; DNAP: Dried pelt nap size; LQU: Live grading overall quality

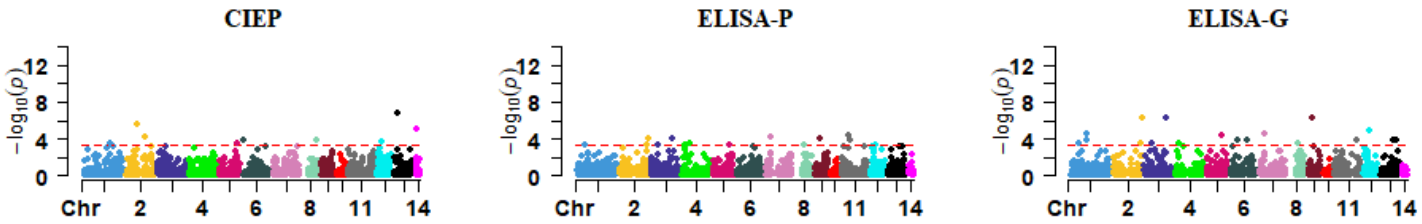

Figure 5-5 Manhattan plots for CNV regions across the 14 autosomal chromosomes associated with Aleutian disease tests. The horizontal line in each plot represents the threshold for significance (P< 0.0005) suggested by ParseCNV developers. CIEP: Counterimmunoelectrophoresis test; ELISA-P: VP2 based enzyme-linked immunosorbent assay test; ELISA-G: AMDV-G based enzyme-linked immunosorbent assay test.

CHAPTER 6. Characterization of runs of homozygosity islands in American mink using whole-genome sequencing data[1]

6.1 Introduction

With the advancements in whole-genome sequencing and analysis methods, there has been a growing scientific interest in discerning selection signatures in different farm animals species, such as cattle (Huang et al. 2023), pigs (Zhong et al. 2023), sheep (Dzomba et al. 2023), goats (Manunza et al. 2023), horse (Han et al. 2023), buffalo (Chen et al. 2023), rabbit (Ballan et al. 2022), and American mink (Karimi et al. 2021a; Valipour et al. 2022b). Runs of homozygosity (ROH) refer to contiguous segments of the genome where an individual inherits identical haplotypes from both parents due to shared ancestry (Ceballos et al. 2018). As its initial application, the ROH can be employed as a practical tool for estimating inbreeding (Curik et al. 2014). However, investigation of the occurrence of ROH across the genome of a population (i.e. ROH islands) displays the genomic regions subjected to selection pressure, which in turn provides valuable insights into the genetic adaptations and evolutionary processes shaping populations (Peripolli et al. 2017). Therefore, the identification of ROH islands can serve as a complementary approach to genome-wide association studies when aiming to detect population-specific major genes in animals (Gorssen et al. 2021).

[1] A version of this chapter has been submitted to the Journal of Animal Breeding and Genetics by Davoudi et al. 2023. Characterization of runs of homozygosity islands in American mink using whole-genome sequencing data.

Compared to major farm animals species, fewer genomic studies in mink have been perfomed to investigate selection footprint. Using genotyping by sequencing (GBS) data from 225 experimental black American mink, Karimi et al. (2021b) investigated the signatures of selection for response to Aleutian mink disease virus infection in American mink. Their findings revealed several potential candidate genes associated with immune response, liver development, and reproduction process, which provided a new insight into genetic mechanisms underlying the Aleutian disease phenotypes. Recently, Valipour et al. (2022b) reported the putative selection signals associated with fur characteristics, providing numerous regions possibly subjected to selection in American mink genome. In addition, Zhang et al. (2023) reported candidate genes with selection signatures enriched in pigmentation and melanogenesis, supporting the idea that improving fur characteristics was a direct target of selection in mink farming. In other species, several studies investigated the selection signals through examining the ROH islands; yet no studies aimed to reveal the potential candidate regions related to complex traits based on ROH islands detection. Therefore, the current chapter aimed to detect ROH patterns, ROH islands, and perform functional annotation analyses to detect the gene content and pathways involved in the candidate regions using whole-genome sequencing data of 100 American mink.

6.2 Materials and Methods

6.2.1 Ethics approval

All procedures used for the current chapter were approved by the Dalhousie University Animal Care and Use Committee, and all methods were carried out in line with the Code of Practice for the Care and Handling of Farmed Mink guidelines (Turner et al. 2013).

6.2.2 Sample collection

All individuals were reared under standard farming conditions and euthanized in December 2018. Tongue samples were collected from two distinct farms: the Canadian Center for Fur Animal Research (CCFAR) at Dalhousie Faculty of Agriculture in Truro, NS, Canada, and Millbank Fur Farm in Rockwood, ON, Canada. To ensure genetic diversity among the individuals, we carefully examined the pedigree information and selected individuals with the least amount of kinship for further analysis (median = 0.015; 1st–3rd quantile of relatedness = 0.008–0.039). More detailed information regarding the studied individuals can be found in the previous studies by Karimi et al. (2021b) and Davoudi et al. (2022c).

6.2.3 Whole-genome sequencing, reads alignment and variant calling

The whole-genome sequencing (WGS) data of 100 American mink is provided from chapter 4 (Davoudi et al. (2022c). A total of 8,373,854 bi-allelic variants from 100 individuals were retained, forming the final whole-genome single-nucleotide polymorphisms (SNPs) for subsequent analyses.

6.2.4 Detections of runs of homozygosity

The PLINK 1.9 (Purcell et al. 2007) with the '*--homozyg'* command was applied for the detection of ROH on the autosomes. The following setting were used to define ROH:

a) The minimum number of 50 SNP required to consider a ROH (*--homozyg-snp 50*);
b) The minimum length of 300 kb for a ROH segment (*--homozyg-kb 300*);
c) The maximum gap between consecutive SNPs could not be higher than 1000 kb (*--homozyg-gap 1000*);

d) Sliding windows of 50 SNPs (*--homozyg-window-snp 50*);

e) The minimum SNP density of one SNP per 50 kb (*--homozyg-density 50*);

f) Three heterozygous SNPs allowed in a ROH (*--homozyg-window-het 3*);

g) Five missing calls allowed in a ROH (*--homozyg-window-missing 5*); and

h) The rate in which a SNP was included in the sliding windows was at least 0.05 (*--homozyg-window-threshold 0.05*).

The identified ROH were specified according to the physical length into four categories: 0.3–1 Mb, 1–4 Mb, 4–8 Mb and above 8 Mb.

6.2.5 Runs of Homozygosity Islands

In order to determine the genomic regions that contained common ROH among the population, we employed the detectRUN (Biscarini et al. 2018) R package version 4.3.1 (R Core Team 2022) to calculate the percentage of the occurrences of a SNP in ROH by counting the number of times the SNP was identified in those ROH across individuals. Finally, we merged the genomic regions with the highest SNP occurrences, comprising the top 1% as a threshold to define 'ROH islands' (Yuan et al. 2022).

6.2.6 Functional Annotation

To gain insights into the biological mechanisms associated with complex traits, functional analysis was conducted to identify genes annotated within the detected ROH islands. To this end, the overlapped genes located within ROH islands were annotated from the American mink reference genome annotation file (Karimi et al. 2022) by 'intersect' function in Bedtools version 2.30.0 (Quinlan and Hall, 2010). To display the functions of candidate genes, the Gene Ontology (GO) terms for molecular function, biological process,

and cellular component, as well as metabolic pathway analyses, were conducted using the Kyoto Encyclopedia of Genes and Genomes (KEGG) database by the KOBAS 3.0 (Bu et al. 2021), and the significance of genes associated with each term was determined by applying a threshold of an FDR-corrected P-value<0.05.

6.3 Results

6.3.1 Runs of homozygosity

Using the whole-genome sequencing (WGS) data of 100 American mink with sliding window method in PLINK 1.9 software (Purcell et al. 2007), we have identified 34,652 ROH in the genome. Table 6.1 shows the summary of all ROH detected per chromosome and length classes. The results indicated that the average number of ROH segments per individual was 346.52, and the length of ROH segments ranged from 300 to 24,040.5 kb, with an average of 751.3 kb. In terms of the distribution of ROH lengths, the vast majority of the lengths were short (0.3–1 Mb), as they accounted for 84.39% of the total ROH length, while ROH segments longer than 8 Mb only accounted for 0.28% of the total length. The ROH density for different chromosomes across all individuals is shown in Figure 6.1. The number of ROH segments differed among chromosomes, with chromosome 1 had the highest count (n=4,807) while the chromosome 14 had the lowest count (n=617).

6.3.2 Runs of homozygosity islands

To identify the ROH islands, the top 1% SNPs, representing more than 38% of the samples, were selected. The Manhattan plot with the ROH islands over the 14 autosomes is presented in Figure 6.2. In total, 63 islands were detected among autosomes 1, 2, 4, 6, 8, 9,

11, 12, 13, and 14, of which autosome 1 and 11 showed the highest numbers of islands (n=17).

6.3.3 Functional Annotation

Table 6.2 shows the position of each ROH islands, along with the number of SNPs per ROH and their annotated genes. Within all of the ROH islands reported in the current chapter, 156 potential candidate genes were annotated. The ROH with length of 2.98 Mb and coordinate of 86,244,268–89,225,369 bp on chromosome 11 harbored the highest number of annotated genes (n=18).

The genes overlapped within ROH islands were associated with fur quality (*EDNRA, FGF2, FOXA2,* and *SLC24A4*), body size/weight (*MYLK4, PRIM2, FABP2, EYS,* and *PHF3*), immune capacity (*IL2, IL21, PTP4A1, SEMA4C, JAK2, CCNA2,* and *TNIP3*), and reproduction (*ADAD1, KHDRBS2, INSL6, PGRMC2,* and *HSPA4L*). The enriched annotation terms resulting from the ROH islands analysis were linked to diverse molecular functions, biological processes, and cellular components. Of interest, the GO (Figure 6.3) and pathway analysis using KEGG (Table 6.3) enrichment analyses revealed multiple significant terms (FDR-corrected P-value<0.05), among which cGMP-PKG signaling pathway, regulation of actin cytoskeleton, and calcium signaling pathway were highlighted due to their functional roles in growth and fur characteristics.

6.4 Discussion

Due to of its significant economic impact, American mink has been selectively raised for its valuable fur for several decades in North America (Bowman et al. 2017). Analyzing ROH islands might be valuable in identifying genomic regions undergone natural/artificial

selection, serving as a preliminary step to detect candidate genes associated with complex traits (Gorssen et al. 2021). In this chapter, the mean number of ROH per individual was reported as 346.52, which was higher than the mean number of 82 by Karimi et al. (2021b) and 102 per individuals by Karimi et al. (2022). However, such differences were expected as they set a threshold of 1000 kb and the current chapter applied a minimum ROH length of 300 kb in order to include the shorter ROH. The threshold of 300 kb was set considering that WGS data enable us to detect ROH with smaller sizes when compared to SNP array data due to their higher resolution (Almeida et al. 2019), which was demonstrated in other livestock species such as cattle (Zhang et al. 2015), sheep (Yang et al. 2016), and goat (Sun et al. 2022). The findings revealed 63 ROH islands, of which 156 genes were located within the identified ROH islands in the mink genome.

Enhancing fur quality stands out as the foremost breeding objective in mink farming (Thirstrup et al. 2017). In light of this, it was expected to detect multiple genes embedded in ROH islands, including *EDNRA, FGF2, FOXA2,* and *SLC24A4,* which were known to play essential roles in shaping fur characteristics. The *EDNRA* gene was located within the ROH islands on chromosome 11 (145,553,259-145,688,821 bp), which is encoding the endothelin A receptor, involved diverse biological processes such as branchial arch development, fetal muscle development and melanocyte functions (Sato et al. 2008; Menzi et al. 2016). Several studies demonstrated that *EDNRA* gene is associated with pigmentation, and in turn the coat color in several species such as goat (Menzi et al. 2016; Kumar et al. 2018; Wan et al. 2023), cattle (Dlamini et al. 2022), chicken (Liu et al. 2019b), and rabbit (Ballan et al. 2022). In a similar fashion, the *FGF2* gene has been reported to have regulatory roles on pigment cell proliferation and melanocyte (Zhang et al. 1997;

Dong et al. 2012). It was indicated that *FGF2* gene plays a crucial role in the extended cultivation of dermal papilla cells and the formation of spheres, which serves as a partial model representing an intact dermal papilla, and ultimately leading to hair follicle induction (Osada et al. 2007; Yamauchi and Kurosaka, 2009). The *FOXA2* gene (Chr8: 47,773,192-47,859,393 bp) known to be involved in numerous biological functions, through which it regulates the hair-inductive activity in hair follicles (Bak et al. 2020). Several lines of evidence implicate that the *SLC24A4* gene, which overlapped with ROH (Chr8: 44,072,167-44,396,621) bp, is a promising candidate associated with pigmentation, and thereby affecting the hair color (Sulem et al. 2007; Han et al. 2008; Meyer et al. 2020).

Mink farmers select animals that demonstrate superior growth features as they have direct impact on the value of the pelts (Do et al. 2022). Our results revealed that several candidate genes overlapped with ROH islands were associated with body size/weight such as *MYLK4, PRIM2, FABP2, EYS,* and *PHF3*. The *MYLK4* gene (Chr1: 126,022,318-126,118,167 bp), a member of the myosin light-chain kinase family, has been well-described to have a potential function for growth in various species, such as cattle (Zheng et al. 2019; Aytekin et al. 2020), pig (Fontanesi et al. 2014), goat (Shi et al. 2020b; Yang et al. 2022), sheep (Ibrahim et al. 2023), chicken (Yin et al. 2021), and goose (Tang et al. 2023). Similarly, the *PRIM2* gene was a gene of interest reported in a literature as a strong candidate gene related to body size and body weight in livestock species (Wang et al. 2014; An et al. 2020; Yin et al. 2023). The *FABP2* gene, which is highly expressed in intestinal epithelial cells, serves a strong regulatory function in the absorption and transportation of long chain fatty acids in small intestine, and ultimately mediates lipid metabolism (Huang et al. 2022). Shah et al. (2019) indicated up-regulation of *FABP2* in jejunum of feed-

efficient chickens, suggesting the role of this gene on proper energy utilization in the intestinal lumen through improving the transport of fatty acids. Interestingly, the *EYS* and *PHF3* genes, located in the ROH region on Chr1: 105,733,995-106,128,124 bp, have been recently reported as potential candidate genes involved in the signatures of selection for both body weight and body size in American mink (Do et al. 2022).

Among annotated candidate genes, we found several genes related to immune capacity, including *IL2, IL21, PTP4A1, SEMA4C, JAK2, CCNA2,* and *TNIP3*. The *IL2* gene (Chr8: 86,244,268-89,225,369 bp) is an essential factor in activating of T-cell-mediated immune responses, leading to the regulation and homeostasis of T- and natural killer cells (Chawla et al. 2020). Similarly, the *IL21* gene (located within the same ROH island as *IL2* gene), is widely known to play regulatory roles in the maturation and differentiation of B cells, along with its influence on the functionality of dendritic cells, affecting to both innate and adaptive immune responses (Spolski and Leonard, 2008). It was demonstrated that the *PTP4A1* gene is crucial for enhancing the innate immune response (Shirasaki et al. 2022). The *SEMA4C* gene, which is highly expressed in the regulatory and memory B cells, plays diverse roles in the regulation of migration of neural and immune cells, and ultimately contributing to the proper immune response (Maier et al. 2011; Yan et al. 2017). The *JAK2* gene is identified as an essential modulator of dendritic cells differentiation, maturation, and secretion of inflammatory cytokines (Hu et al. 2022b). It is notable, in this regard, that increasing the expression of *JAK2* was associated with the inflammation in autoimmune diseases (Li et al. 2013). Several studies have shown that the polymorphisms in *JAK2* gene are associated with mastitis resistance in dairy cattle (Usman et al. 2014; Khan et al. 2019; Ali et al. 2020). The *CCNA2* gene, recognized as a main positive regulator of the cell cycle

and DNA replication, has been frequently reported as a significant gene associated with immune infiltrating cells and cytokines, and thereby to be overexpressed in different cancers (Gao et al. 2014; Yang et al. 2016; Zhang et al. 2020). Evidence has shown that the *TNIP3* gene deficiency deteriorated the liver damage and inflammatory response during hepatic injury, rendering *TNIP3* gene as a strong candidate for inflammatory and immune events (Zhou et al. 2021).

Reproduction is a critically important trait in American mink as the economic success of mink production largely relies on their reproductive performance (Karimi et al. 2018). In the current chapter, numerous reproduction-related genes were identified such as *ADAD1, KHDRBS2, INSL6, PGRMC2,* and *HSPA4L.* It is well-documented that the *ADAD1* gene (Chr11: 86,244,268-89,225,369 bp), which is highly expressed in the testis, is essential for spermatogenesis and ultimately male fertility (Snyder et al. 2020; Dai et al. 2023). Of interest, several studies reported selection signals encompassing *ADAD1*, suggesting this gene as a potential candidate gene for reproduction in various livestock species, such as cattle (Zinovieva et al. 2020), pigs (Wang et al. 2022), and sheep (Nosrati et al. 2019). Several studies have identified that *KHDRBS2* gene (overlapped with three different ROH islands on chromosome 1) might affect different reproduction traits, such as pregnancy status in cattle (Reverter et al. 2016), teats number in pigs (Verardo et al. 2016), and litter size in goat (Islam et al. 2020). In addition, Macciotta et al. (2021) reported that *KHDRBS2* gene mapped to the ROH island in river and swamp buffalo, reinforcing this gene could be involved in biology of reproduction. The *INSL6* gene, which is highly expressed in germ cells of the testis, plays a key role in mediating the process of spermatogenesis (Burnicka-Turek et al. 2009). It was demonstrated that the insufficiency of *INSL6* can lead to different

degrees of male infertility (Lok et al. 2000; Ivell and Grutzner, 2009). It has been confirmed that the *PGRMC2* gene has a crucial function in the formation and development of ovarian follicle, and thereby in female fertility (Griffin et al. 2014; Wu et al. 2019). Another gene involved in reproduction, the *HSPA4L* gene, is highly expressed in testis and plays an essential role in the regulation of male fertility and sperm motility (Held et al. 2006; Liu, Wang and Liu, 2019).

We also found 56 significantly over-represented GO terms and nine significant pathways using KEGG (FDR-corrected P-value<0.05), among which cGMP-PKG signaling pathway, regulation of actin cytoskeleton, and calcium signaling pathway were associated with growth and fur characteristics. Notably, it is well-documented that the cGMP-PKG signaling pathway involves in the mechanism of melanogenesis by upregulating the expression of tyrosinase (Choi et al. 2012). Moreover, it was demonstrated that the cGMP-PKG signaling pathway can impede the flow of Ca^{2+} currents, resulting in an accumulation of intracellular Ca^{2+}, which ultimately leads to the pigment aggregation (Aspengren et al. 2003; Sandoval et al. 2017). Interestingly, our results in chapter 4 (Davoudi et al. (2022c) reported that the copy number variations involved in regulation of actin cytoskeleton, suggesting its impact on biological processes related to growth in American mink. It is well established that the calcium signaling pathway was significantly associated with several economically important traits in livestock species, such as average daily gain in cattle (Rolf et al. 2012), feed efficiency in pig (Xu et al. 2021), and abdominal fat percentage in chicken (Zhu et al. 2022b).

6.5 Conclusion

In conclusion, the current chapter identified a total of 34,652 ROH segments across all individuals, with shorter segments (0.3–1 Mb) being notably abundant, constituting approximately 84.39% of all ROH. Within all segments, we detected 63 distinct ROH islands that housed 156 annotated genes associated with various important traits. Specifically, these genes were associated with fur quality (*EDNRA, FGF2, FOXA2,* and *SLC24A4*), body size/weight (*MYLK4, PRIM2, FABP2, EYS,* and *PHF3*), immune capacity (*IL2, IL21, PTP4A1, SEMA4C, JAK2, CCNA2,* and *TNIP3*), and reproduction (*ADAD1, KHDRBS2, INSL6, PGRMC2,* and *HSPA4L*). Our study further employed Gene Ontology and pathway analysis using KEGG, which revealed multiple statistically significant terms ($P \leq 0.05$), among which the cGMP-PKG signaling pathway, regulation of actin cytoskeleton, and calcium signaling pathway being particularly noteworthy due to their roles in growth and fur characteristics. This chapter presents the first ROH islands study in American mink, highlighting the candidate genes within these regions and their potential implications as signatures of selection in response to targeted breeding objectives, such as improving body length, reproductive performance, and fur quality. These findings significantly contribute to our understanding of the genetics of American mink, offering complementary information to the implementation of breeding strategies aiming at genetic improvement in this species.

Table 6.1 Summary of all runs of homozygosity (ROH) identified from whole-genome sequencing of 100 American mink per chromosome and length classes.

	ROH			
	Number	Percentage (%)	Average size (Kb)	Standard deviation (Kb)
[A] Chromosome				
1	4807	13.87	738.70	901.46
2	3373	9.73	600.32	470.43
3	2572	7.42	694.28	764.73
4	3326	9.60	620.93	530.57
5	2180	6.29	722.33	1028.08
6	3408	9.83	710.19	865.22
7	2371	6.84	770.03	992.44
8	2269	6.56	773.32	686.44
9	1168	3.37	656.44	575.98
10	739	2.13	579.08	698.23
11	3454	9.97	1024.6	1778.95
12	2303	6.65	1037.59	1319.03
13	2065	5.96	703.41	705.83
14	617	1.78	738.49	601.55
[B] Class				
0.3-1 Mb	292.44	84.39	490	170
1-4 Mb	49.29	14.22	1713.88	703.78
4-8 Mb	3.83	1.11	5354.04	1068.47
>8 Mb	0.96	0.28	12325.36	4171.74
Total	34652	100	751.29	974.62

Table 6.2 Characterization of runs of homozygosity (ROH) islands and their annotated genes found in different chromosomes of American mink genome.

Chromosome	Start	End	Length (bp)	Number of SNPs	Annotated genes
1	104721319	104741618	20299	60	*KHDRBS2*
1	125896255	125948082	51827	81	*LOC122907237*
1	126022318	126118167	95849	188	*MYLK4*
1	28753136	28826253	73117	288	-
1	106890674	107116623	225949	307	*LOC122918972, LOC122898288, LOC122909514, EYS*
1	102756600	102935491	178891	601	*LOC122909378, LOC122909368, BEND6, ZNF451, DST*
1	107242257	107340292	98035	626	*EYS*
1	104343810	104548862	205052	691	*KHDRBS2*
1	107116665	107241813	125148	772	*EYS*
1	105733995	106128124	394129	874	*PTP4A1, TRNAK-CUU, PHF3, EYS*
1	99942603	100273514	330911	883	*LOC122902495, LOC122909213*
1	104795572	105154995	359423	972	*LOC122899742, LOC122902762, KHDRBS2*
1	106317032	106883424	566392	1497	*LOC122909508, EYS*
1	108983646	109335972	352326	1539	*LOC122897603, LOC122899762, LOC122902965*
1	108257708	108558822	301114	1592	-
1	103129335	103506916	377581	2233	*LOC122898299, LOC122917650, PRIM2*
1	107341441	108027021	685580	2249	*LOC122896847, LOC122909519, LOC122902880, EYS*
2	170508861	170822055	313194	1437	*LOC122899240*
4	106439178	106768850	329672	23	-
4	106910978	107027350	116372	71	-
4	121888060	121956365	68305	198	-
4	107650342	108000740	350398	254	-
4	121957416	122350026	392610	854	-
4	113212606	113559379	346773	2690	*LOC122905573*
4	95449787	95782006	332219	4596	-
6	101923587	101989857	66270	165	*LOC122910106*
6	101815982	101923575	107593	468	-
6	102042097	102169954	127857	582	*KCNMB2*
8	68467318	69091604	624286	74	*FAM178B, SEMA4C, LOC122916438, LOC122915420, LOC122916439*
8	44041151	44067425	26274	77	*SLC24A3*
8	47773192	47859393	86201	143	*FOXA2, LOC122915650*
8	44072167	44396621	324454	669	*SLC24A3*
8	47204756	47728796	524040	1263	*TRNAS-GCU_9, LOC122915398*
9	96449058	96771900	322842	778	*LOC122916790, RLN1, LOC122917852, INSL6, CD274, PLGRKT, JAK2*
11	137897822	137973307	75485	80	-
11	127172488	127210155	37667	122	*PDGFC*
11	141280013	141328732	48719	252	-
11	145553259	145688821	135562	290	*PRMT9, TMEM184C, LOC122889604, EDNRA*
11	137122705	137208822	86117	366	*SPOCK3*
11	90176799	90329411	152612	400	*MAD2L1, LOC122889186*
11	127222314	127471326	249012	443	*PDGFC, GLRB*
11	81294671	81859772	565101	791	*LOC122890258*
11	82380955	82926255	545300	1450	*LOC122890636, PGRMC2, LARP1B*
11	137410953	137851916	440963	2157	*LOC122919090, LOC122919093*
11	89225480	90176675	951195	2348	*LOC122890692, LOC122890748, NDNF, TNIP3, PRDM5*
11	84032476	85046239	1013763	3464	*LOC122890680*
11	82929120	84032284	1103164	3653	*LOC122889111, MFSD8, PLK4, HSPA4L, SLC25A31, ABHD18, INTU*
11	85046496	86032038	985542	3967	*LOC122890261, FAT4*
11	90329439	92600878	2271439	6331	*LOC122890142, C11H4ORF3, FABP2, USP53, MYOZ2 SEC24D, METTL14, LOC122890146, PDE5A, SYNPO2, PRSS12, NDST3*
11	86244268	89225369	2981101	9463	*LOC122890682, SPRY1, IL2, NUDT6, IL21*

					ADAD1, BBS7, CCNA2, EXOSC9, ANXA5, LOC122890264, QRFPR, SPATA5, FGF2, BBS12, KIAA1109, TRPC3, SMIM43
11	92601129	96863025	4261896	12098	*TRAM1L1, LOC122890266, ARSJ, UGT8, CAMK2D, ANK2*
12	34225236	34271197	45961	182	*LOC122892700, TSPAN19*
12	37963657	38164038	200381	645	*ACSS3, LIN7A*
12	113548876	114497008	948132	1198	*LOC122892058, FZD8, GJD4, CCNY*
12	81625544	81971351	345807	1353	*DBX2, LOC122890943, ANO6, LOC122892277*
12	76289632	76632724	343092	1539	*LOC122892767, LOC122891569, ABCD2, KIF21A*
12	38308621	39287802	979181	3562	*LOC122892788, PAWR, PTPRQ, OTOGL, PPP1R12A*
13	130126142	130548999	422857	66	-
13	31798228	32068184	269956	1599	*CCDC177*
13	30674647	31009999	335352	1654	*SLC24A4, RIN3*
14	30841280	31167018	325738	1092	*UMOD, PDILT, ACSM5, ACSM1, GP2, LOC122895515*
14	30349873	30820417	470544	1956	*LOC122896111, KNOP1, VPS35L, GPRC5B, GPR139, IQCK*
14	27095071	27491338	396267	1985	*LOC122895388, NTAN1, BFAR, RRN3, PDXDC1, PARN*

Table 6.3 Significantly enriched (adjusted P-value<0.05) KEGG pathways in genes localized within ROH islands.

Term	Pathway ID	Adjusted P-value	N. of genes	Gene symbols
cGMP-PKG signaling pathway	hsa04022	0.035	6	*KCNMB, MYLK4, SLC25A31, PPP1R12A, EDNRA, PDE5A*
Proteoglycans in cancer	hsa05205	0.024	5	*FZD8, CAMK2D, ANK2, FGF2, PPP1R12A*
Vascular smooth muscle contraction	hsa04270	0.030	4	*EDNRA, MYLK4, KCNMB2, PPP1R12A*
EGFR tyrosine kinase inhibitor resistance	hsa01521	0.037	3	*PDGFC, JAK2, FGF2*
Calcium signaling pathway	hsa04020	0.020	4	*CAMK2D, EDNRA, MYLK4, SLC25A31*
Regulation of actin cytoskeleton	hsa04810	0.018	4	*MYLK4, PDGFC, FGF2, PPP1R12A*
Pathways in cancer	hsa05200	0.011	6	*FZD8, IL2, CAMK2D, JAK2, EDNRA, FGF2*
Human T-cell leukemia virus 1 infection	hsa05166	0.018	4	*SLC25A31, MAD2L1, CCNA2, IL2*
Th17 cell differentiation	hsa04659	0.028	3	*IL21, IL2, JAK2*

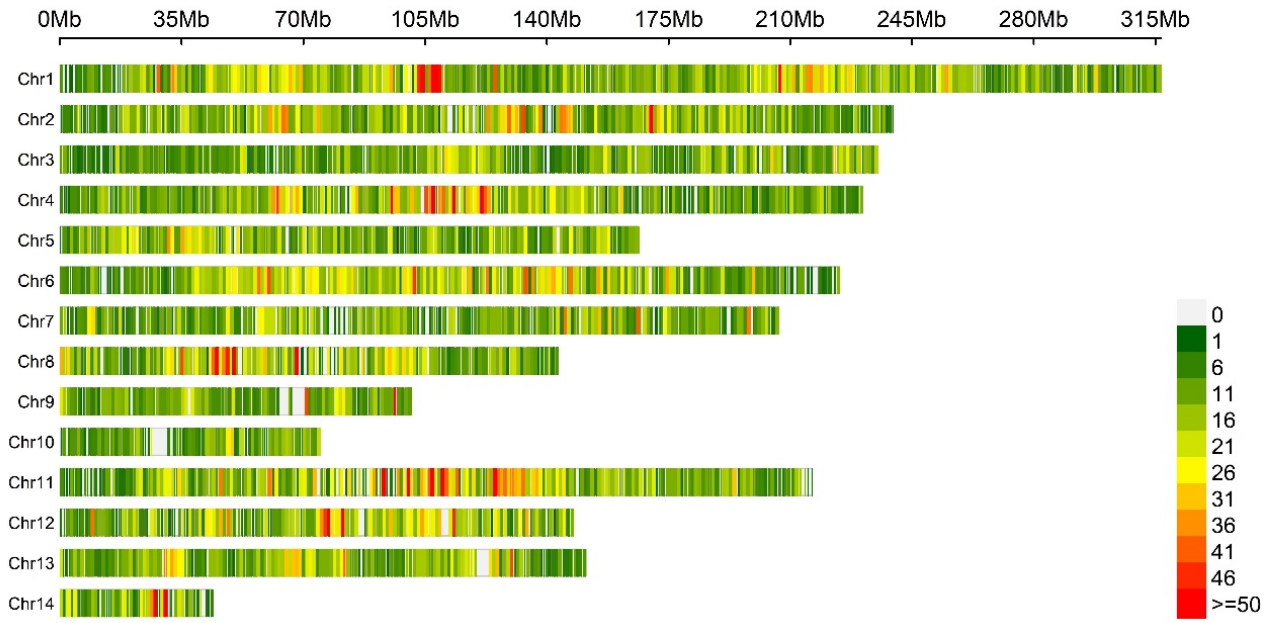

Figure 6-1 Genome-wide runs of homozygosity (ROH) density among all individuals within 1 Mb window size. The color gradient has been changed according to the ROH density, which is illustrated in the figure legend.

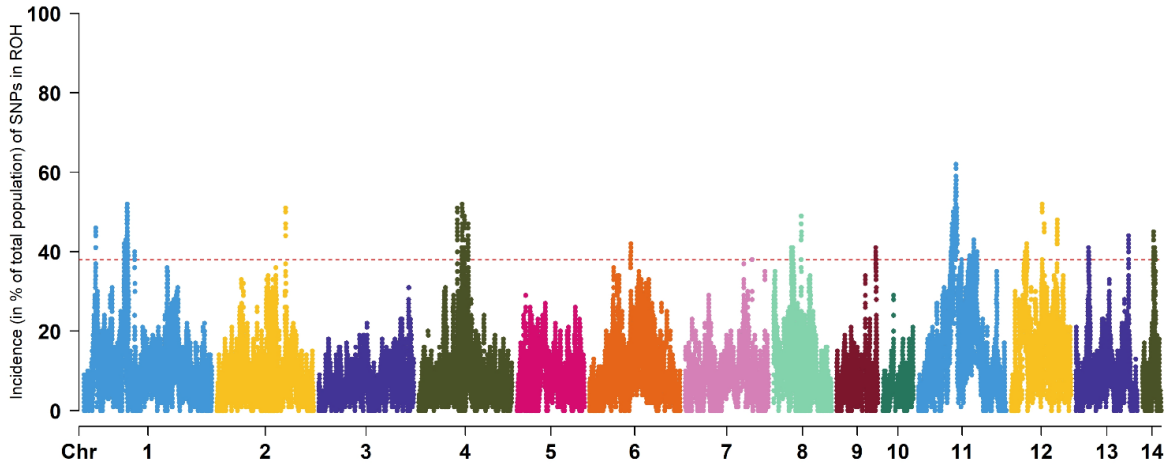

Figure 6-2 Manhattan plot of genome-wide frequency of SNPs occurrence into runs of homozygosity (ROH) identified in American mink. The red lines indicate the 1% SNPs with the highest occurrence in ROH, which represent the thresholds for identification of ROH islands.

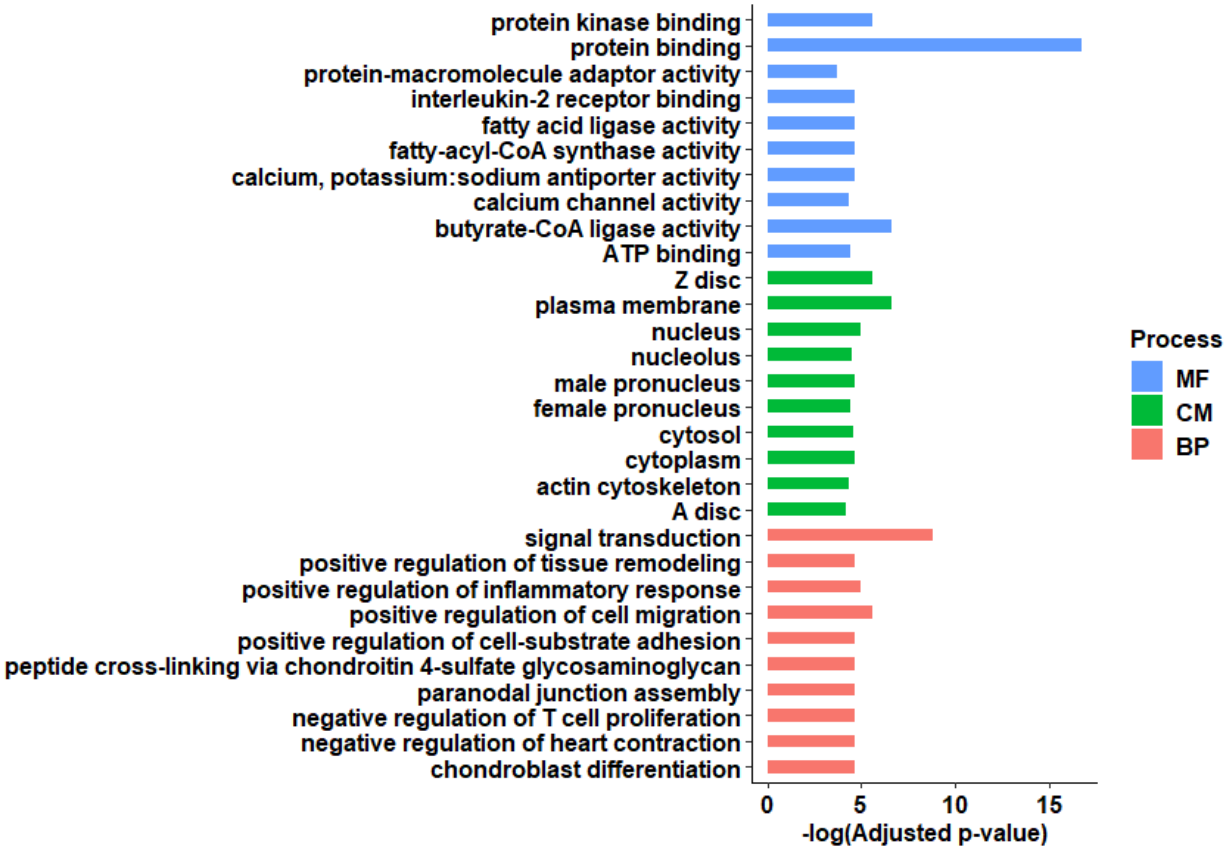

Figure 6-3 Top ten Gene Ontology terms under biological process, cellular components and molecular function enriched among the annotated genes overlapped with runs of homozygosity (ROH) islands.

CHAPTER 7. Identification of consensus homozygous regions and their associations with growth and feed efficiency traits in American mink[1]

7.1 Introduction

American mink breeding is entering the genomic era through the availability of a high-quality chromosome-based genome assembly (Karimi et al. 2022) and a genome-wide single-nucleotide polymorphisms (SNPs) array. Such technologies have paved the way for precise identification of homozygous segments in livestock species (Peripolli et al. 2017). Runs of homozygosity (ROH) are long homozygous regions, which are composed of two identical haplotypes inherited from a common ancestor (Ceballos et al. 2018). Characteristics of ROH in a population can be used as an indicator for estimation of inbreeding level in different species, such as cattle (Eriksson et al. 2023; Falchi et al. 2023), pigs (Jiang et al. 2022; Wu et al. 2022), chicken (Yuan et al. 2022; Wang et al. 2023), sheep (Ghoreishifar et al. 2019; Abdoli et al. 2023), goat (Manunza et al. 2023; Ziegler et al. 2023), and buffalo (Ghoreishifar et al. 2020; Liu et al. 2022).

Groups of several ROH within a specific region of the genome in a population are known as ROH islands (Nothnagel et al. 2010). It was reported that the analysis of ROH islands might reveal genomic regions under selection pressure, which in turn helps to identify candidate genes associated with traits of economic interest (Xie et al. 2019; Rocha et al. 2023). Furthermore, several studies have suggested the feasibility of performing association analyses using ROH to

[1] A version of this chapter has been submitted to PLOS One by Davoudi et al. 2023. Identification of consensus homozygous regions and their associations with growth and feed efficiency traits in American mink.

detect homozygous genomic regions associated with complex traits in livestock (Pryce et al. 2014). Sanglard et al. (2021) identified several regions of ROH significantly associated with antibody response to porcine reproductive and respiratory syndrome virus vaccination in pigs. In cattle, substantial numbers of ROH regions are reported to be associated with milk yield (Martikainen et al. 2020; Cesarani et al. 2021), fertility (Nani and Peñagaricano, 2020; Ghoreishifar et al. 2023), and production traits (Zhao et al. 2021), suggesting a complementary role of ROH in elucidating the genetic mechanisms underlying economically important traits.

Feed cost is the largest expense for mink production systems, and thereby, improving feed efficiency holds significant potential for increasing the profitability of mink farming through strategic breeding programs (Davoudi et al. 2022a). Several studies have reported moderate to high heritability for growth (Liu et al. 2017; Do et al. 2021) and feed efficiency traits (Shirali et al. 2015; Madsen et al. 2020; Davoudi et al. 2022a) in American mink, which highlighted a substantial genetic basis and presents opportunities for improvement by genetic and genomic breeding programs.

To the best of our knowledge, there is no study that examined homozygous segments in the American mink genome and their potential association with growth and feed efficiency traits. Therefore, the main objectives of this chapter were to 1) reveal the distribution and pattern of ROH within the genome of American mink; 2) identify highly frequent consensus ROH (ROH islands) and investigate the candidate genes within these regions; and 3) assess their associations with growth and feed efficiency traits.

7.2 Materials and Methods

7.2.1 Ethics approval

All animal procedures applied in this chapter were approved by the Dalhousie University Animal Care and Use Committee, and all methods were carried out in accordance with the Code of Practice for the Care and Handling of Farmed Mink guidelines (Turner et al. 2013).

7.2.2 Animals and traits

A detailed description of the phenotypic data used in this chapter can be found in Davoudi et al. (2022a). Briefly, a total of 2,288 American mink with growth and feed efficiency records were available. These traits were collected according to Davoudi et al. (2022a): final body weight (FBW), final body length (FBL), harvest weight (HW), harvest length (HL), daily feed intake (DFI), average daily gain (ADG), feed conversion ratio (FCR), Kleiber ratio (KR), residual feed intake (RFI), residual gain (RG), and residual intake and gain (RIG).

7.2.3 SNP genotyping and quality control

All mink were genotyped using the Affymetrix Mink 70K SNP array (Neogen, Lincoln, Nebraska, United States). Genotypes were pruned by PLINK 1.9 software based on the proportion of missing genotypes (>0.95), individual call rate (>0.90), and Hardy-Weinberg equilibrium ($P>10^{-6}$). In addition, SNPs located on sex chromosomes were removed, resulting in a final data set of 49,268 SNPs for further analyses.

7.2.4 Assessment of runs of homozygosity

We used PLINK 1.9 software (Purcell et al. 2007) to identify homozygous segments across autosomes of each individual's genome. The ROH were discovered based on the sliding window approach with the following parameters: (1) sliding window of 50 SNPs across the genome; (2) a

minimum ROH length of 1,000 kb; (3) the minimum SNP density was set to 50 kb/SNP; (4) maximum gap between consecutive homozygous SNPs was 1,000 kb; (5) only one heterozygous and one missing genotype were allowed; and (6) a minimum of 57 consecutive SNPs were included in an ROH, which was determined according to the formula proposed by Lencz et al. (2007), to control the false positive rate of the identified ROH:

$$The\ minimal\ number\ of\ SNPs\ in\ an\ ROH = \frac{log_e \frac{\alpha}{n_a n_s}}{log_e(1-het)},$$

where α is the percentage of false positive ROH (set to 0.05), n_s is the number of genotyped SNPs per individual, n_a is the number of individuals, and het is the proportion of heterozygosity across all SNPs.

7.2.5 Consensus regions and ROH islands

The '*homozyg-group*' function of the PLINK 1.9 software (Purcell et al. 2007) was applied to merge the individual ROH into different ROH groups in a pool containing the overlapping regions between all the individual ROH in the group i.e. the consensus homozygous region (Ku et al. 2011; Zhao et al. 2021). We retained the consensus ROH with a minimum of five SNPs and frequency of more than 5% for association analyses. In addition, to investigate the genomic regions with high frequency of ROH in the population (ROH islands), the threshold of higher than 80% was defined for consensus ROH (Signer-Hasler et al. 2022). The overlapped genes within ROH islands were annotated from the American mink reference genome annotation file (Karimi et al. 2022) through the '*intersect*' function in Bedtools version 2.30.0 (Quinlan and Hall 2010).

7.2.6 Association analyses between consensus ROH and phenotypes

According to the model described by Sanglard et al. (2021), we evaluated the association between consensus ROH with growth and feed efficiency traits using the linear model as follows:

$$y = \mu + Xb + Zu + e,$$

where $\boldsymbol{y}$ is the vector of phenotypic observation, μ is the grand mean, $\boldsymbol{b}$ is the vector of fixed effects, $\boldsymbol{X}$ and $\boldsymbol{Z}$ are the incidence matrices that relate the fixed and random effects with the dependent variable, respectively; $\boldsymbol{u}$ is the vector of random animal genetic effects and **e** is the vector of random residual effects. The random effects $\boldsymbol{u}$ and $\boldsymbol{e}$ were distributed as: $\boldsymbol{u} \sim N(0, \boldsymbol{G}\sigma_u^2)$ and $\boldsymbol{e} \sim N(0, \boldsymbol{I}\sigma_e^2)$, where σ_u^2 and σ_e^2 are the additive genetic and residual variances, respectively, **G** is the genomic relationship matrix, which was constructed by ASRgenomics package (Gezan et al. 2021) using the VanRaden equation (VanRaden 2008), and $\boldsymbol{I}$ is an identity matrix. The consensus ROH (n=196) were simultaneously fitted in the model as categorical fixed effects, coding as "yes" if the individual contained the ROH segment, or "no" otherwise. The other fixed effects, as described by (Davoudi et al. 2022a), were farm (two farms), sex (male and female), color type (dark, demi, mahogany, pastel, and stardust), row-year (year: 2018 and 2019; row: 1, 4, 5, 7, 8, and 11). The age of animals (in days) was included as a covariate in the model. The associations between each consensus ROH and studied traits were tested through linear mixed model analysis in ASReml 4.0 (Butler et al. 2017) with a statistical significance level ($P<0.01$).

7.3 Results

7.3.1 Assessment of runs of homozygosity

A total of 298,313 runs of homozygosity (ROH) were identified in the entire mink population studied. The results showed that the average number of ROH segments per individual was 99.90, spanning from 30 to 134, respectively, and the length of ROH segments ranged from 1.02 to 55.44 Mb, with an average of 4.16 Mb (Table 7.1). We classified ROH segments into five different length categories, including 1–2 Mb, 2–4 Mb, 4–8 Mb, 8–16 Mb, and >16 Mb (Figure 7.1A). The majority of detected ROH were classified as 2-4 Mb, representing 46.99% of all ROH (n=140,178),

followed by the length of 4–8 Mb and 1–2 Mb with 26.3% (n=78,451) and 17.42% (n=51,967), respectively. The percentage of ROH segments higher than 16 Mb were only 1.08% of all detected ROH (n=3,236). The distribution of ROH lengths across the genome is represented in Figure 7.1B. The largest ROH was located on chromosome 1 (55.44 Mb with 1563 SNPs), and the shortest ROH was identified on chromosome 3 (1.02 Mb with 79 SNPs). Further, the number of ROH segments varied across chromosomes, ranging from the lowest in chromosome 9 (n=5,728) to the highest in chromosome 1 (n=52,311). As shown in Figure 7.1C, the total length of the genome covered by ROH among individuals ranged from 84.78 Mb to 683.16 Mb, with an average of 414.81 Mb.

7.3.2 Consensus regions and ROH islands

To provide the shared homozygous regions for the association analyses, initially 6,980 consensus groups were formed using '*–homozyg-group'* function in PLINK 1.9 software, of which a total of 196 consensus ROH fulfilled the criteria of presenting in more than 5% individuals with a minimum of five SNPs. The chromosomal distribution map of identified ROH across mink autosomes and consensus ROH shared amoung individuals is shown in Figure 7.2.

The ROH islands were determined as regions where the consensus ROH presented in more than 80% of animals, with the aim of pinpointing the genes they encompass. The implementation of this approach resulted in the detection of ten ROH islands spanning 14 autosomes, most of which were located on chromosome six with seven ROH islands. These specific regions harbored 12 annotated genes, some with known effects on immune systems processes such as *DTX3L, PARP9, PARP14, CD86,* and *HCLS1* (Table 7.2). Notably, the three ROH islands on other chromosomes did not contain any known annotated genes.

7.3.3 Association analyses between consensus ROH and phenotypes

The association analysis revealed 13 consensus regions that were significantly (P<0.01) associated with growth and feed efficiency traits, of which four pleiotropic ROH affected more than one trait. The physical position of significant consensus ROH across the mink autosomes are shown in Figure 7.3. The frequency of the associated consensus regions ranged from 6.6 to 81.9% across all individuals. The average length of significant consensus ROH was 147.46 kb, ranging from 8.62 to 327.85 kb. Chromosome one exhibited the highest number of significant regions (n=5), followed by two significant regions on chromosome 13, and one significant region on chromosomes 2, 4, 5, 8, and 9. Detailed information regarding the consensus ROH significantly associated (P<0.01) with the studied traits, along with their annotated candidate genes can be found in Table 7.3. Notably, these significant consensus ROH encompassed 26 genes, including well-known candidates like *MEF2A, ADAMTS17, POU3F2,* and *TYRO3* which are recognized for their roles in growth and body size development.

7.4 Discussion

In this chapter, the mean number of ROH per individual was 99.9, which was in agreement with Karimi et al. (2022) who reported an average of 102 per animal using whole-genome sequencing data of 100 American mink. Yet, both studies reported higher numbers of ROH counts compared to the study of Karimi et al. (2021b), which identified 82 ROH segments per individual solely based on scaffolds. This discrepancy indicates that the recent chromosome-based reference genome in American mink has facilitated our capacity to detect homozygous segments. The distribution of detected ROH revealed that approximately more than 90% of ROH were shorter than 8 Mb, which was consistent with the results reported in other species, such as cattle (Mulim et al. 2022; Rocha et al. 2023), pigs (Shi et al. 2020a; Jiang et al. 2022), chicken (Marchesi et al.

2018; Cendron et al. 2020), sheep (Purfield et al. 2017; Signer-Hasler et al. 2019), and buffalo (Ghoreishifar et al. 2020; Macciotta et al. 2021). It is well-established that the large ROH (~10 Mb) represents recent inbreeding (up to five generations ago), whereas short ROH (~1 Mb) indicates more distant ancestral effects (up to 50 generations ago) (Howrigan et al. 2011; Keller et al. 2011). Considering the predominant of ROH with the length of 1 to 8 Mb, it is reasonable to hypothesize that the inbreeding events in American mink occurred approximately 5 to 50 generations ago. This timeline corresponds with the findings of Hu et al. (2023), who reported the rapid decline in the effective population size in American mink from 5 to 50 generations ago.

In recent years, the identification of ROH islands across the genome has gained popularity due to their capacity to reveal selection footprint in livestock species (Gorssen et al. 2021). The Aleutian disease, the most significant health concern for global mink farming, is an immune complex disease that causes autoimmune disorders in mink (Farid et al. 2022). Despite efforts to detect and eliminate infected animals using various immunological tests, these strategies have largely failed due to the high persistence nature of Aleutian disease in the breeding environment (Farid et al. 2012; Prieto et al. 2017). Intriguingly, our chapter uncovered several genes within ROH islands known to affect immune system processes, including *DTX3L, PARP9, PARP14, CD86,* and *HCLS1*. This implies that natural selection plausibly acts on immune-related genes in American mink.

The *DTX3L* gene, also known as *BBAP* (B-lymphoma and BAL-associated protein), plays regulatory functions on DNA damage signaling, tumor cell growth, and IFN signaling and antiviral response (Yan et al. 2013; Shen et al. 2017; Lo et al. 2018). Interestingly, Hong et al. (2020b) reported that inhibiting the *DTX3L* gene restrained the cell invasion and secretion of inflammatory factors, suggesting its potential as a therapeutic target for rheumatoid arthritis, a complex

autoimmune disease characterized by chronic synovitis of the joints in humans. The *PARP9* and *PARP14* genes, located within the ROH island on chromosome 6 (121,883,426:122,139,161 bp), belong to the PARP superfamily that regulate diverse biological processes such as DNA damage repair, cellular stress response, and antiviral innate immunity (Zhu and Zheng 2021). Research has demonstrated that *PARP9* gene, highly expressed in glioma, is correlated with checkpoint molecules involved in inflammatory and immune responses (Xu et al. 2020). Moreover, study has shown that knockdown of *PARP9* gene in human or mouse dendritic cells and macrophages resulted in substantial reduction of type I IFN production (*IFN-α* and *IFN-β*), highlighting its critical role in the antiviral immunity system (Xing et al. 2021). Similarly, *PARP14* knockout has shown therapeutic effects on tumors and allergic inflammation through mediating T-cell differentiation and action of cytokines (Cho et al. 2013; Mehrotra et al. 2013). Other genes of interest were *CD86* and *HCLS1* located within two different ROH islands on chromosome six (122,500,609:122,510,002 bp and 122,908,246:122,958,392 bp, respectively). Several lines of evidence indicated that *CD86*, which is one of the essential co-stimulatory molecules expressed on antigen presenting cells, plays a regulatory role in the immune response by mediating the activation of T-cells, B-lymphocytes, and macrophages (Nishimura et al. 2000; Liu et al. 2010). It was indicated that the *HCLS1* gene, which is expressed only in cells with lymphohematopoietic origin, plays a functional role in the regulation of T-cell immune synapses (Gomez et al. 2006).

It is well-documented that American mink is one of the most highly susceptible non-human species to severe acute respiratory syndrome coronavirus-2 (SARS-CoV-2) infection, leading to massive culls of many millions of mink across the world (Enserink, 2020; Koopmans, 2021; Adney et al. 2022). Intriguingly, most of the aforementioned genes, one way or another, have been reported to be associated with SARS-CoV-2, the virus that causes coronavirus disease-2019 (COVID-19). It

was indicated that in SARS-CoV-2 infection, the activation of macrodomain-sensitive ADP-ribosylation signal is mediated by *PARP9*/*DTX3L* complex, suggesting their critical role in interferon-mediated antiviral defence (Russo et al. 2021). Similarly, it was reported that the *PARP14* gene is essential for the optimal IFN expression, supporting the suggestion that *PARP14* is involved in antiviral immune response in CoV-infected cells (Grunewald et al. 2019). Several studies have shown that the expression of *CD86* on monocytes and dendritic cells was substantially decreased in patients with severe COVID-19 (Arunachalam et al. 2020; Wang et al. 2020; Zhou et al. 2020; Winheim et al. 2021). These findings merit further exploration of the functional role of the ROH islands-harbored genes revealed in the current chapter on Aleutian mink disease virus and COVID-19 infection in American mink.

In the present chapter, gene discovery performed on the 13 consensus regions that were significantly ($P<0.01$) associated with growth and feed efficiency traits, highlighted several candidate genes (i.e. *MEF2A, ADAMTS17, POU3F2,* and *TYRO3*) with potential impacts on growth rate and feed efficiency as reported in previous studies. The *MEF2A* and *ADAMTS17* were located within the consensus ROH on chromosome 13 (134,704,541:135,003,083 bp), which was significantly ($P<0.01$) associated with RFI. The *MEF2A* gene, which plays an important role in vertebrate skeletal muscle development and differentiation by activation of numerous muscle-specific and growth factor-induced genes (Wang et al. 2018), is known to be the candidate gene for muscle development and body growth in livestock species (Chen et al. 2010; Zhou et al. 2010; Juszczuk-Kubiak et al. 2012). Remarkably, a research conducted by Foroutan et al. (2021) revealed that *MEF2A* showed higher expression levels across all tested tissues (liver, muscle, and testis) in the offspring of low-RFI Angus bulls, as opposed to their high-RFI counterparts. The *ADAMTS17* gene, which is a member of ADAMTS proteins with numerous biological functions (Le Goff and

Cormier-Daire, 2011), has been previously reported as one of the height-associated variants in several species, such as horse (Metzger et al. 2018), cattle (Lee et al. 2020), dog (Hoopes et al. 2012; Bannasch et al. 2020), and human (Gudbjartsson et al. 2008; Lettre et al. 2008; Van Duyvenvoorde et al. 2014). Interestingly, the *ADAMTS17* gene was reported as a selective signal associated with animal height in the Shetland pony (Frischknecht et al. 2016), and Brazilian locally adapted taurine cattle (Peripolli et al. 2020), highlighting the potential impacts of *ADAMTS17* gene on body size.

The *POU3F2* gene located within a pleiotropic ROH on chromosome 11 (32,128,510: 32,316,405 bp), is associated with HW and FBW traits. The *POU3F2* gene, which is widely expressed in the central nervous system, has been well-described to play a key role in diverse neuronal functions and hormonal regulation (Lin et al. 2018; Westphal et al. 2018). Notably, Schönauer et al. (2023) reported a negative correlation of *POU3F2* gene expression with body mass index in human, suggesting the critical role of *POU3F2* in hyperphagic obesity in human. The *TYRO3* gene was found within the consensus ROH on chromosome 13 (85,787,981: 86,060,018 bp), significantly associated with KR trait. The *TYRO3* gene, which is expressed in neurons of the central nervous system, plays regulatory roles in cell proliferation and differentiation, associating with adipocyte size in moderately obese individuals (Rizkalla et al. 2012). A GWAS analysis by Sun et al. (2013) reported that *TYRO3* gene was associated with intramuscular fat content in the breast muscle of chicken. Interestingly, it was revealed that *TYRO3* was significantly differentially expressed in muscle between low and high RFI pigs, indicating that *TYRO3* might affect the body fat, and consequently increase feed efficiency in pigs (Vigors et al. 2019).

7.5 Conclusion

We characterized the distribution of ROH and ROH islands, and the association between the consensus ROH with growth and feed efficiency traits in American mink. In total, we identified 13 consensus regions significantly associated with the studied traits, harboring several candidate genes that are known to be associated with growth and body size development, such as *MEF2A, ADAMTS17, POU3F2,* and *TYRO3*. In addition, ten ROH islands were identified across the genome, harboring genes related to immune systems processes such as *DTX3L, PARP9, PARP14, CD86,* and *HCLS1*. Overall, the results revealed the impact of homozygosity in the mink genome on growth and efficiency traits. These findings have import implications for the evaluation and selection of American mink in genetic improvement programs, offering valuable insights for enhancing the breeding and sustainability of this species.

Table 7.1 Descriptive statistics of runs of homozygosity (ROH) number and length by ROH length class.

Class	Number	Percentage (%)	Average size (Mb)	Standard Deviation (Mb)
1-2 Mb	51,967	17.42	1.59	0.28
2-4Mb	140,178	46.99	2.89	0.56
4-8 Mb	78,451	26.3	5.44	1.14
8-16 Mb	24,481	8.21	10.49	2.02
>16 Mb	3,236	1.08	21.03	4.87
Total	298,313	100	4.16	3.12

Table 7.2 Characterization of consensus ROH shared by more than 80% of the mink population and the annotated genes in the corresponding regions.

Chr	Start	End	Length (bp)	Frequency (%)[a]	No. SNPs	Annotated genes
6	122,500,609	122,510,002	9,394	86.24	5	*CD86*
6	122,846,667	122,881,153	34,487	84.63	6	*GOLGB1*
6	122,908,246	122,958,392	50,147	84.33	5	*FBXO40; GOLGB1; HCLS1*
6	100,386,881	100,611,871	224,991	82.92	14	-
6	121,883,426	122,139,161	255,736	82.02	6	*SLC49A4; PARP9; DTX3L; LOC122908877; PARP14; HSPBAP1; LOC122911033*
2	45,138,611	45,265,052	126,442	81.92	19	-
2	45,100,650	45,130,801	30,152	81.88	6	-
6	120,478,852	120,531,357	52,506	81.41	6	*KALRN*
6	120,546,042	120,564,621	18,580	81.41	5	*KALRN*
1	217,785,451	217,894,574	109,124	80.17	5	*LOC122897674*

[a] Percentage of the population presented this ROH.

Table 7.3 Regions of runs of homozygosity (ROH) significantly associated with growth and feed efficiency traits in American mink.

Chr	Start	End	Length (bp)	Associated traits	P-value[a]	Frequency (%)[b]	No. SNPs	Candidate genes
1	233,051,034	233,378,886	327,853	RFI	0.0038	47.9	20	*PPP2R2B*
1	84,492,422	84,643,650	151,229	RG; RIG	0.0094; 0.0084	69.6	5	*MDGA1*
1	268,594,555	268,631,729	37,175	HW	0.0064	39.3	7	*THG1L*
4	20,9695,778	209,720,164	24,387	FBL	0.00027	66.6	5	*COPG2*
2	45,138,611	45,265,052	126,442	FBL; FBW; RFI	0.0014; 0.0016; 0.0065	81.9	19	-
5	42,989,622	43,198,887	209,266	FBL	0.0063	20.8	5	-
1	32,128,510	32,316,405	187,896	FBW; HW	0.0034; 0.0051	16.1	11	*POU3F2; FBXL4; LOC122913962*
5	130,209,831	130,237,085	27,255	DFI	0.0069	15.1	5	*KLHL1*
13	85,787,981	86,060,018	272,038	KR	0.0066	10.9	5	*MGA; OIP5; NUSAP1; RTF1; LTK; RPAP1; NDUFAF1; ITPKA; TYRO3; LOC122894302; LOC122894795; LOC122894805; LOC122894585*
9	10,609,898	10,786,369	176,472	RG	0.0023	10.9	6	*LHX2*
13	134,704,541	13,500,3083	298,543	RFI	0.0034	9.9	6	*LYSMD4; ADAMTS17; MEF2A*
8	134,262,073	134,331,827	69,755	HW	0.0062	6.6	5	-
1	69,893,506	69,902,125	8,620	HW; ADG	0.0047; 0.0065	55.1	7	*AKAP7*

[a] P-value<0.01.

[b] Percentage of the population presented this ROH.

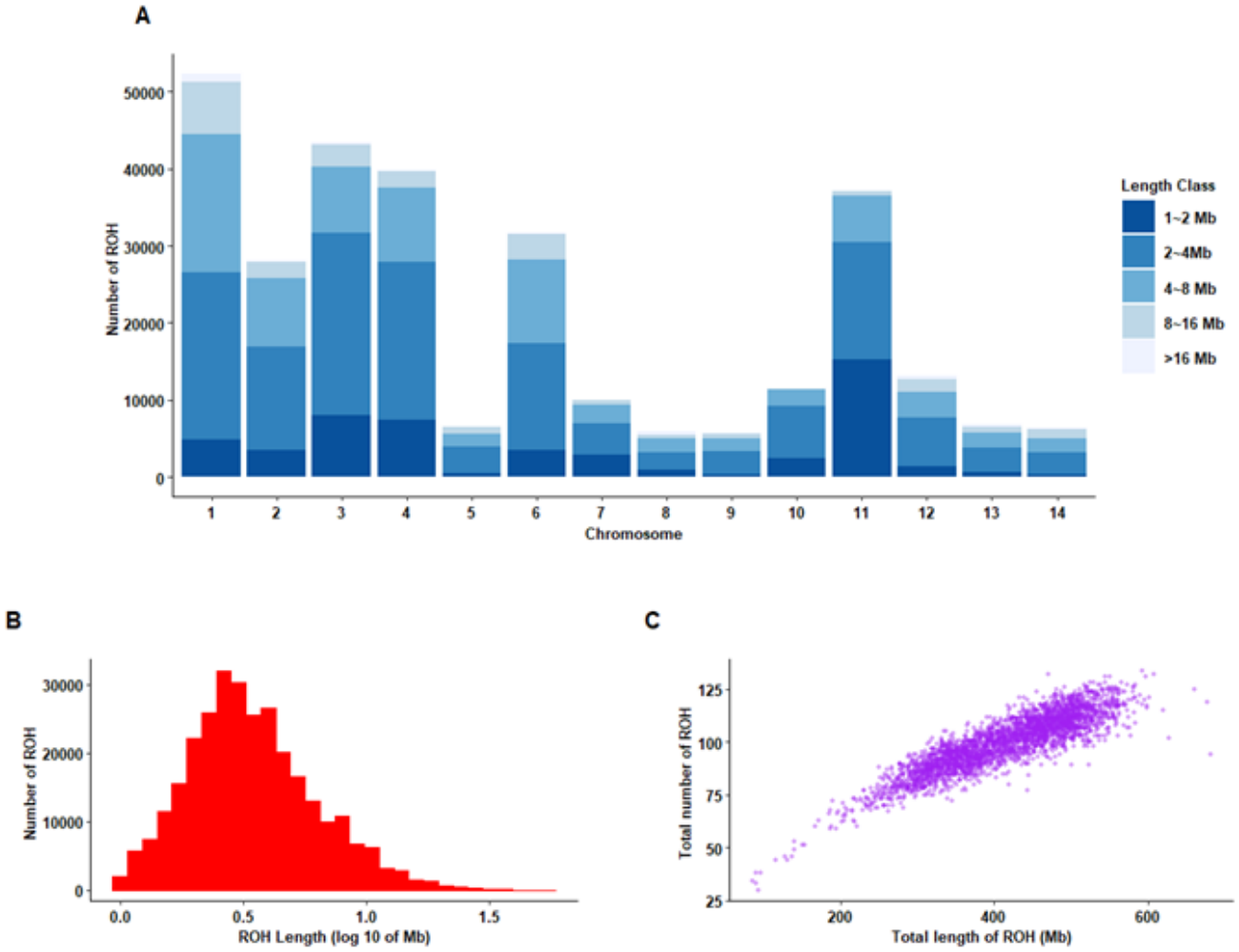

Figure 7-1 Characteristics of runs of homozygosity in American mink. **(A)** Frequency distribution of the average number of ROH in different length classes (Mb) in each chromosome. **(B)** Length distribution of ROH. X-axis shows the length of ROH (Mb) using a base-10 log scale. **(C)** Relationship between ROH number per animal and total length of the genome covered by them. Each point represents one individual.

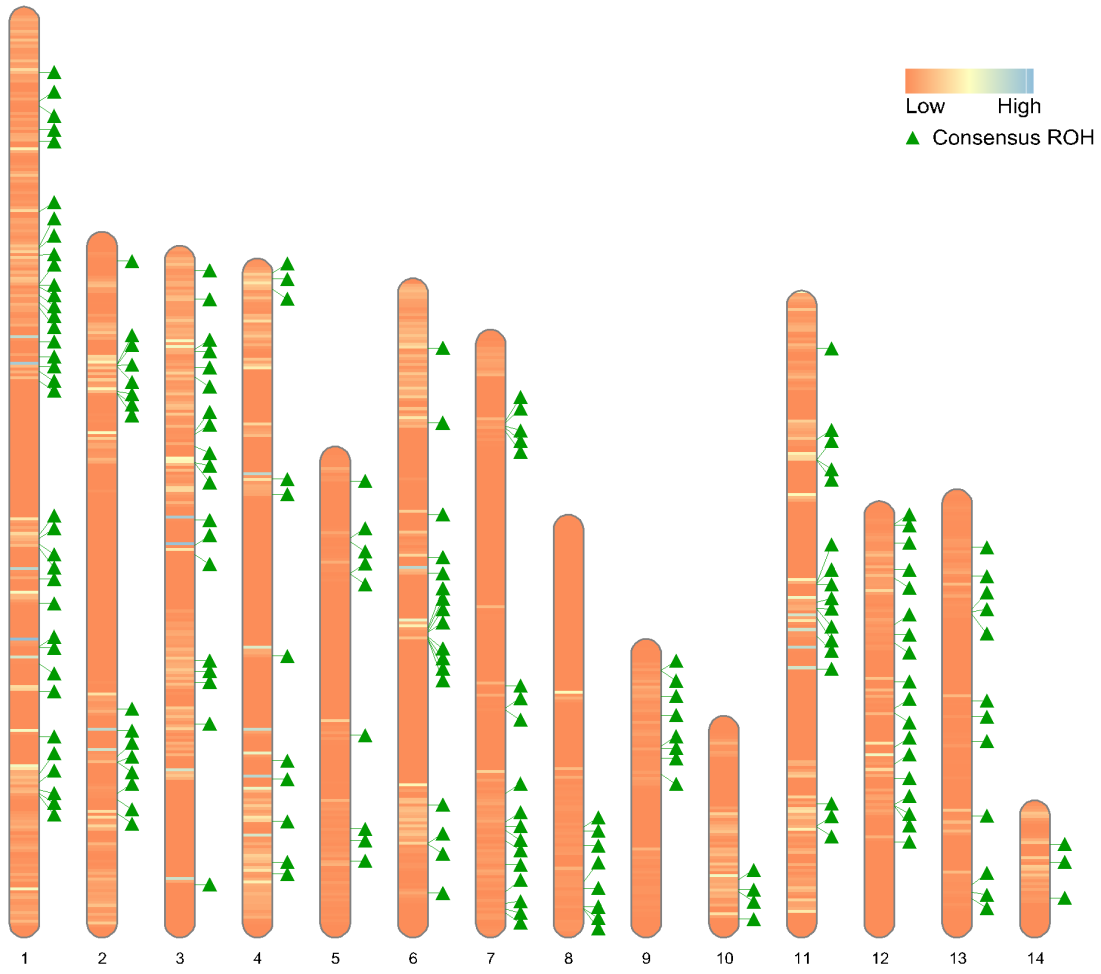

Figure 7-2 Chromosome ideograms showing the position of identified ROH and consensus ROH shared between individuals. The color scale within each chromosome represents the number of identified ROH, changing the gradient with more ROH detected in an area. The position of consensus ROH is marked with the green triangle next to the chromosome.

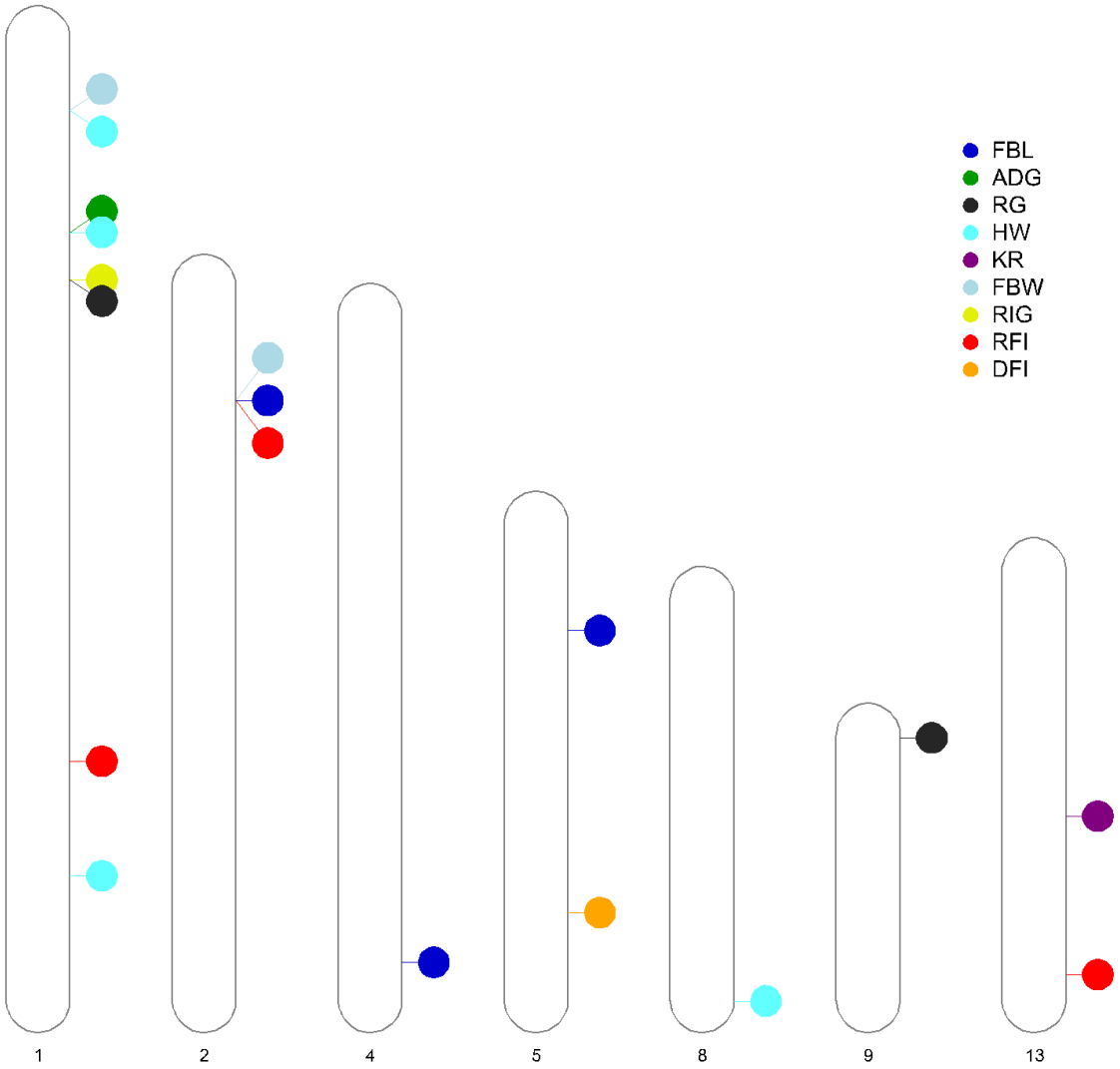

Figure 7-3 Physical position of significant consensus ROH across the mink autosomes.

CHAPTER 8. Genome-wide association studies for growth and feed efficiency traits in American mink[1]

8.1 Introduction

While American mink (*Neogale vison*) has served as a prominent species within the fur industry due to its remarkable fur characteristics, it is critical to recognize the existence of challenges such as increasing cost of production and emerging diseases, which hinder the achievement of sustainability in mink breeding (Karimi et al. 2021b). One of the methods to alleviate these challenges is to improve feed efficiency (FE), given that the expenses related to feed constitute a significant portion, accounting for around 60% to 70% of the overall expenses in mink production (Berg and Lohi, 1992; Sørensen et al. 2003). Consequently, the primary goals could revolve around the selection of animals with an enhanced ability to utilize feed resources.

The FE has been reported in American mink in the form of feed conversion ratio (FCR) (Nielsen et al. 2011), residual feed intake (RFI) (Shirali et al. 2015; Madsen et al. 2020), and more recently, residual gain (RG), residual intake and gain (RIG), and Kleiber ratio (KR) (Davoudi et al. 2022a). The FCR, a commonly used indicator for evaluating FE in several livestock species (Berry and Crowley, 2013; Prakash et al. 2020; Davoudi et al. 2022b), can be described as the amount of feed consumed per unit of body weight increase, and is a composite trait encompassing initial and final body weight and feed intake (Skinner-Noble and Teeter, 2003). The RFI is defined as the difference between the actual daily feed intake (DFI) of an individual and the expected DFI needed

[1] A version of this chapter has been submitted to Canadian Journal of Animal Science by Davoudi et al. 2023. Genome-wide association studies for growth and feed efficiency traits in American mink.

to attain an average daily gain (ADG) and the body weight (BW) (Koch et al. 1963). The RG is the other FE indicator that has been proposed to identify differences in feed use among growing animals, defining as the residual from a multiple regression of ADG on BW and DFI, which aids in pinpointing the individuals with the highest rate of weight gain (Crowley et al. 2010). The RIG indicator is suggested to combine the RFI and RG, allowing for the identification of efficient and fast-growing animals independent of their body weights. In addition, KR is another ratio measurement, which can be as desirable alternative to other FE traits as it does not require individual intake to be measured, showing the high KR values as individuals with efficient users of feed (Ghafouri-Kesbi et al. 2011).

Several studies have documented moderate heritabilities for FE traits in American mink (Shirali et al. 2015; Madsen et al. 2020; Davoudi et al. 2022a), indicating a significant genetic basis that holds the potential for improvement through genetic and genomic breeding programs. Genome-wide association studies (GWAS) are applied to uncover genomic regions associated with economically important traits as it is well-known that the genetic variants identified from GWAS might increase the accuracy of genomic prediction (Van den Berg et al. 2016). Over the years, GWAS have assisted scientists to identify numerous single nucleotide polymorphisms (SNPs) and candidate genes associated with FE traits in different species, such as cattle (Seabury et al. 2017), pigs (Do et al. 2014), chicken (Mebratie et al. 2019), and rabbit (Sánchez et al. 2020).

The recent advancement of chromosome-based genome assembly (Karimi et al. 2022) and 70K SNP array in American mink have opened up the possibilities to detection of genetic variants associated with traits of interest in this species, yet no association studies have been performed to evaluate the genetic architecture of FE traits in American mink. Therefore, the aim of this chapter was to identify the genomic regions associated with eight growth and feed efficiency traits in

American mink, including BW, ADG, DFI, FCR, RFI, RG, RIG, and KR. In addition, we applied functional annotation and gene enrichment analyses to understand the biological meaning underlying the identified regions/genes.

8.2 Materials and Methods

8.2.1 Ethics approval

All procedures used for the current chapter were approved by the Dalhousie University Animal Care and Use Committee, and all methods were performed in accordance with the Code of Practice for the Care and Handling of Farmed Mink guidelines (Turner et al. 2013).

8.2.2 Phenotypic and deregressed EBV values

In this chapter, the deregressed estimated breeding values (dEBVs) were calculated for eight growth and feed efficiency traits, including BW, ADG, DFI, FCR, RFI, RG, RIG, and KR. A detailed description regarding the phenotypic data and animal models utilized to obtain dEBVs in the current chapter is available in the work by Davoudi et al. (2022a). According to the trait, an optimal model with specific fixed and random effects were fit to calculate the EBVs, which is comprehensively explained in the chapter 5 (Davoudi et al. 2022a). The reliabilities of EBVs for each phenotype were calculated as follows:

$$\text{Reliability} = 1 - \frac{PEV}{\sigma_a^2},$$

where *PEV* is the prediction error variance; and σ_a^2 is the additive genetic variance of the trait. We used the 'wideDRP' function in the DRP package (Lopes 2017), which applies the EBV reliabilities following the method described by Garrick et al. (2009) to calculate the dEBVs.

Finally, the dEBVs were applied as the pseudo-phenotype for association analyses. Table 8.1 shows the descriptive statistics of the dEBVs for the studied traits.

8.2.3 SNP genotyping and Quality Control

Genomic DNA of 1,872 mink with feed intake measurement were genotyped using Affymetrix Mink 70K SNP array. The quality control of genotypic data was performed using PLINK 1.9 software (Purcell et al. 2007) as follows: minor allele frequency smaller than 0.01, a call rate lower than 90%, individuals with a call rate lower than 90%, and SNPs with significant deviation from Hardy-Weinberg equilibrium ($p<10^{-5}$) were excluded. In total, 25,793 autosomal SNPs remained for further analyses.

8.2.4 Genome-wide association studies

GCTA software (Yang et al. 2011) was used to perform the mixed linear model (MLM) to detect the association between each SNP and pseudo-phenotypes, including polygenic effects to account for the shared genetic effects of related individuals. Additionally, to control for the potential confounding effect of population structure, the first five principal components computed by the GCTA software (Yang et al. 2011) and were included as covariates in the association models (Price et al. 2006). The statistical model was as follows:

$$\boldsymbol{y} = \mathbf{1}\mu + \boldsymbol{W\alpha} + \boldsymbol{Xb} + \boldsymbol{Zu} + \boldsymbol{e},$$

where $\boldsymbol{y}$ is the vector of dEBVs for each growth and feed efficiency traits; μ is the overall mean and 1 is a vector of ones; $\boldsymbol{W}$ is a matrix containing the top five eigenvectors of principal components analyses and included as covariates; $\boldsymbol{\alpha}$ is the vector of corresponding coefficients with the intercept; $\boldsymbol{X}$ represents the vector of all marker genotypes, with coded 0, 1, 2 for genotypes AA, AB and BB, respectively; $\boldsymbol{b}$ stands for the corresponding effect size of the SNP; $\boldsymbol{u}$ is a vector

of additive polygenic effect with a normal distribution ($\boldsymbol{u} \sim N\,(0,\ \boldsymbol{G}\sigma_u^2)$, in which σ_u^2 is the additive polygenic variance, and **G** is the genomic-based relationship matrix (GRM); $\boldsymbol{Z}$ is an incidence matrix associating the dEBVs to the corresponding random polygenic effects; and $\boldsymbol{e}$ is the random residual effect, following a normal distribution as $\boldsymbol{e} \sim N\,(0,\ \boldsymbol{I}\sigma_e^2)$, in which σ_e^2 is the residual variance and $\boldsymbol{I}$ is the identity matrix of appropriate dimension. Because the Bonferroni correction sets an extremely stringent threshold for multiple testing (Johnson et al. 2010), false discovery rate (FDR) was used to determine the threshold P-values (Benjamini and Hochberg, 1995). The FDR was set as 0.01, and the threshold P-value was calculated as follows:

$$p = FDR \times \frac{n}{m},$$

where n shows the number of SNPs with p<0.01 in the GWAS results, and m is the number of SNPs qualified from the population. The estimations of phenotypic variance explained (PVE) by each significant SNP were performed using the GCTA software (Yang et al. 2011).

8.2.5 Annotation of candidate genes, Gene Ontology and pathway analysis

The annotated genes overlapped between the 0.5 Mb downstream and upstream region harboring significant SNPs were identified by using the American mink reference genome annotation file (Karimi et al. 2022) and Bedtools version 2.30.0 (Quinlan and Hall, 2010). The Gene Ontology (GO) terms for molecular function, biological process, and cellular component, as well as metabolic pathway analyses, were conducted using the Kyoto Encyclopedia of Genes and Genomes (KEGG) database by the ClueGO plug-in (Bindea et al. 2009) using Cytoscape 3.1.0 (Kohl et al. 2011). The ClueGO cut-off for the statistical assessment of the enriched terms was through false discovery rate corrections (FDR<0.05).

8.3 Results

8.3.1 Genome-wide association studies

The quantile-quantile (Q–Q) plots assessed the impact of population structure on GWAS, indicating no deviation from the observed -log10 P-values of the MLM to the expected -log10 P-values, and therefore, no evidence of any systematic bias in the current chapter (Figure 8.1). Considering all growth and feed efficiency traits, the empirical P-values of a multiple testing for BW, DFI, ADG, FCR, RFI, RG, RIG, and KR were 8.20×10^{-5}, 9.67×10^{-5}, 8.74×10^{-5}, 9.46×10^{-5}, 7.47×10^{-5}, 8.62×10^{-5}, 8.47×10^{-5}, 9.88×10^{-5}, respectively.

The Manhattan plots of GWAS for the studied traits are illustrated in Figure 8.2. A total of five, nine, six, 12, four, and six SNPs were significantly associated with BW, DFI, ADG, FCR, RG, and KR, and correspondingly explained 0.40, 1.47, 0.34, 0.92, 0.48, and 0.35% of the additive genetic variances, respectively. Notably, there were no significant associations for RFI and RIG traits. It is worth noting that six SNPs on chromosomes 1, 6, 8, and 13 were identified with pleiotropic effects on BW, ADG, FCR, and KR, respectively.

8.3.2 Candidate genes and functional enrichments

The information of significant SNPs associated with growth and feed efficiency traits and their annotated candidate genes within 1 Mb interval is provided in Table 8.2. A total of 153 functional genes located within 1 Mb surrounding the most significant SNPs were identified based on the latest American mink genome assembly. Among which, several candidate genes have been previously reported to have functional roles on growth and feed efficiency, such as *TUBB, CDKN1A, SRSF3, GPRC6A, RFX6,* and *KPNA5*. In order to gain a more comprehensive understanding of the candidate genes associated with pathways and biological functions, we

utilized these genes to perform an analysis of pathway analysis using KEGG and GO. The findings from these analyses pointed towards the primary involvement of the candidate genes in lipid metabolism (glycerophospholipid metabolism, ether lipid metabolism, arachidonic acid metabolism), hormone signaling and regulation (GnRH signaling pathway, type B pancreatic cell differentiation, and endocrine pancreas development), and muscle development (actin filament depolymerization, actin filament capping, and regulation of muscle cell apoptotic process) (Figure 8.3).

8.4 Discussions

Growth and feed efficiency have been considered as traits of interests in American mink as they directly related to the economic profit of the mink industry because of two main reasons: better growth might reach to larger pelt size and in turn higher profit (Thirstrup et al. 2017; Do et al. 2021), and also the feed is the largest cost for the mink production (Shirali et al. 2015; Madsen et al. 2020). It is well-known that the identification of genetic markers associated with growth and feed efficiency traits would assist to unveil the genetic basis underlying these traits, and therefore their inclusion in genomic breeding strategies (Higgins et al. 2018). To this end, numerous GWAS have detected SNPs that significantly associated with growth and feed efficiency traits (Sell-Kubiak et al. 2017; Brito et al. 2020; Davoudi et al. 2022b). To the best of our knowledge, the currents chapter performed the first GWAS on growth and feed efficiency traits in American mink. In this chapter, we performed GWAS for growth and feed efficiency traits in American mink using the MLM approach, which resulted in identification of 42 significant genetic markers, of which six SNPs had pleiotropic effects.

The AX-647632532 (at 122.7 Mb of chromosome 1) is the marker with the highest pleiotropic effect, associated with ADG, BW, FCR, and KR. The highest number of genes (n=26) were

annotated from 1-Mb flanking of this SNP, among which the *TUBB* gene was highlighted as a promising candidate gene affecting the growth and feed efficiency in American mink. It was reported that the expression of *TUBB* gene was higher in rumen tissue of low RFI (feed efficient) beef cattle, which supports the impact of this gene on feed efficiency traits (Kong et al. 2016; Lindholm-Perry et al. 2022). The AX-647628511 (at 83.1 Mb of chromosome 1) was another SNP of interest that was significantly associated with FCR. Several genes with known effects on growth and feed efficiency were annotated in 0.5 Mb upstream and downstream of this SNP, such as *CDKN1A, SRSF3, GPRC6A, RFX6,* and *KPNA5*. The *CDKN1A* gene, which encodes a cyclin-dependent kinase inhibitor 1A, plays functional roles on cell motility, DNA repair, and muscle cell proliferation and differentiation (Semenova et al. 2022; Ticli et al. 2022). It has been confirmed that *CDKN1A* was associated with FCR (Miao et al. 2021), ADG (Fontanesi et al. 2014), and intramuscular fat content (Martínez-Montes et al. 2017) in pigs, carcass traits in beef cattle (Karisa et al. 2013), and obesity in human (Liu et al. 2021). Using GWAS, it was reported that the *SRSF3* gene was significantly associated with FCR and carcass length in pigs (Guo et al. 2015; Falker-Gieske et al. 2019). In a similar fashion, it was revealed that the *GPRC6A*, RFX6, and *KPNA5* genes were associated with dry matter intake in cattle (Olivieri et al. 2016). Using copy number variation-based association studies, Fernandes et al. (2021) indicated the association between *GPRC6A* gene and body weight gain in broilers. In addition, other work has shown that *RFX6*, and *KPNA5* genes were strongly associated with feed efficiency (the inverse of FCR) and RIG traits (Brunes et al. 2021), supporting these genes as strong candidate genes for growth and feed efficiency in American mink.

The GO and pathway analysis using KEGG analyses revealed several biological processes that are significantly enriched among the candidate genes, involving in lipid metabolism

(glycerophospholipid metabolism, ether lipid metabolism, arachidonic acid metabolism), hormone signaling and regulation (GnRH signaling pathway, type B pancreatic cell differentiation, and endocrine pancreas development), and muscle development (actin filament depolymerization, actin filament capping, and regulation of muscle cell apoptotic process), and in turn leading to have impacts on growth and feed efficiency in American mink. The importance of lipid metabolism for growth and feed efficiency has been indicated by several studies in farmed animals (Fu et al. 2020; Mota et al. 2022; He et al. 2023). Of interest, the phospholipase A family (*PLA2G4B, PLA2G4D, PLA2G4E,* and *PLA2G4F*) acted in most of the enriched pathways. Because of their phospholipase A2 activity, these genes are known to be involved in regulating phospholipid and arachidonate metabolism (Long and Cravatt, 2011). It is notable, in this regard, that the *PLA2G4B* gene was reported as strong candidate gene affecting the intramuscular fat in domestic rabbit (Sosa-Madrid et al. 2020). In addition, it was shown that the *PLA2G4B* gene, along with other detected genes from this family (*PLA2G4D, PLA2G4E,* and *PLA2G4F*), was associated with growth traits in cattle (Grigoletto et al. 2019) and pigs (Hong et al. 2020a). Congruent with these findings, Davoudi et al. (2022c), in a copy number variation discovery, indicated many biological pathways related to lipid metabolism, which reinforce the physiological connection between lipid metabolism and growth and feed efficiency in American mink.

Other interesting biological pathways enriched in the current chapter were related to hormone secretion. Several studies have demonstrated the potential association of hormone secretion with feed efficiency in livestock species (Do et al. 2014; Ding et al. 2018; Taussat et al. 2020). It was shown that the GnRH signaling pathway plays a key role in the characterization of various growth phases in cattle (Widmann et al. 2013). Similarly, the GnRH signaling pathway was associated with RG, FCR, and RFI traits in cattle (Rolf et al. 2012; Taussat et al. 2020), rendering the

importance of this pathway in growth and feed efficiency regulation. The synthesis, storage, and secretion of insulin are key functions of type B pancreatic cells (Beck, 2006), which in turn might impact the feed efficiency of animals by maintaining glucose homeostasis in the body (Taussat et al. 2020). It is well-known that the proper working of actin filament, along with myosin in the myofilaments is essential for muscle cells to enhance their mobility and dynamics (Gokhin and Fowler, 2011; Mancin et al. 2022). Using proteomic analysis of high-FE and low-FE pigs, Wu et al. (2020) indicated that differentially expressed proteins between two FE divergent groups were mostly enriched in actin filament-based process, which supports the importance of actin filament pathways as a regulator of feed efficiency. Therefore, the enrichment of numerous actin pathways in the current chapter indicated its critical role on cytoskeleton and muscle development, which ultimately leads to better growth in American mink.

8.5 Conclusion

In conclusion, we performed the first genome-wide associations between SNPs and growth and feed efficiency traits in American mink. The GWAS results identified 42 SNPs reaching statistical significance (FDR<0.01), of which six were pleiotropic with effects on more than one trait. The annotation of genes surrounding significant SNPs identified 153 genes, some of which were known to have roles on growth and feed efficiency, such as *TUBB, CDKN1A, SRSF3, GPRC6A, RFX6,* and *KPNA5*. In addition, the enrichment analyses showed that pathways were mostly involved in lipid metabolism, hormone regulation and muscle development, which ultimately might lead to better growth in American mink. Overall, our results identified multiple genes involved in regulating growth and feed efficiency traits in mink, that can be implemented in genomic selection programs to select more efficient mink.

Table 8.1 Descriptive statistics of the deregressed EBV (dEBV) for growth and feed efficiency traits in American mink.

			dEBVs			
Trait	Abbreviations	Numbers	Mean	SD	Min.	Max.
Final body weight	FBW	1037	0.00	0.30	-1.15	1.37
Daily feed intake	DFI	1872	0.01	0.07	-0.15	0.23
Average daily gain	ADG	1044	-0.02	2.19	-10.14	9.18
Feed conversion ratio	FCR	1036	0.34	8.60	-23.39	61.52
Residual feed intake	RFI	1044	0.00	0.02	-0.12	0.14
Residual gain	RG	1042	-0.04	1.51	-7.19	5.70
Residual intake and gain	RIG	1043	-0.04	1.48	-6.76	6.43
Kleiber ratio	KR	1044	-0.01	1.15	-6.05	4.64

Table 8.2 Significant SNPs and positional candidate genes for growth and feed efficiency traits in American mink.

Traits[1]	Chr[2]	SNPs[3]	Position	Beta[4]	P-value	PVE (%)[5]	Candidate genes
ADG	1	**AX-647631147**	108686101	-0.89	3.14E-05	0.03	-
	1	**AX-647632532**	122729223	-0.90	2.76E-06	0.09	*POU5F1, PSORS1C2, CDSN, C1H6ORF15, MUC21, SFTA2, GTF2H4, IER3, TUBB, MDC1, NRM, PPP1R18, C1H6orf136, MRPS18B, GNL1, RPP21, TCF19, CCHCR1, VARS2, DHX16, ATAT1, PPP1R10, PRR3, FLOT1, ABCF1, DDR1*
	4	AX-647741010	206936126	-0.85	3.36E-05	0.09	*GCC1, ARF5, FSCN3, ZNF800, PAX4, GRM8, SND1*
	8	**AX-647794228**	130312171	-0.55	3.15E-05	0.03	*OSR1, RDH14, NT5C1B*
	13	**AX-647683777**	85473817	0.55	4.15E-05	0.03	*JMJD7, TYRO3, ITPKA, ZNF106, GANC, VPS39, PLA2G4F, PLA2G4E, SPTBN5, PLA2G4B, RPAP1, LTK, RTF1, CAPN3, TMEM87A, PLA2G4D, EHD4, MAPKBP1, MGA*
	13	**AX-647686472**	123955159	0.50	1.59E-05	0.08	*MKRN3, NDN, MAGEL2*
BW	1	**AX-647631147**	108686101	-0.17	4.53E-09	0.19	-
	1	**AX-647632532**	122729223	-0.13	1.39E-06	0.10	*POU5F1, PSORS1C2, CDSN, C1H6orf15, MUC21, SFTA2, GTF2H4, IER3, TUBB, MDC1, NRM, PPP1R18, C1H6orf136, MRPS18B, GNL1, RPP21, TCF19, CCHCR1, VARS2, DHX16, ATAT1, PPP1R10, PRR3, FLOT1, ABCF1, DDR1*
	8	**AX-647794228**	130312171	-0.08	1.64E-05	0.03	*OSR1, RDH14, NT5C1B*
	13	**AX-647683777**	85473817	0.08	2.56E-05	0.04	*JMJD7, TYRO3, ITPKA, ZNF106, GANC, VPS39, PLA2G4F, PLA2G4E, SPTBN5, PLA2G4B, RPAP1, LTK, RTF1, CAPN3, TMEM87A, PLA2G4D, EHD4, MAPKBP1, MGA*
	13	**AX-647686472**	123955159	0.07	1.53E-05	0.04	*MKRN3, NDN, MAGEL2*
DFI	5	AX-647754701	155604252	0.01	8.90E-05	0.03	*GPR18, ZIC5, ZIC2, GPR183, UBAC2, TM9SF2, CLYBL, DOCK9*
	5	AX-647754738	155838880	0.01	2.76E-06	0.04	*GPR18, ZIC5, ZIC2, GPR183, UBAC2, TM9SF2, CLYBL, DOCK9, PCCA*
	6	AX-647756101	5748971	-0.02	7.53E-05	0.28	*B3GALT5, HMGN1, PSMG1, PCP4, IGSF5, LCA5L, GET1, BRWD1, DSCAM*
	6	AX-647756105	5765827	-0.02	4.91E-05	0.30	*B3GALT5, HMGN1, PSMG1, PCP4, IGSF5, LCA5L, GET1, BRWD1, DSCAM*
	6	AX-647756116	6005779	-0.02	4.27E-05	0.33	*B3GALT5, HMGN1, PSMG1, IGSF5, LCA5L, ETS2, BRWD1*
	6	AX-647756120	6011312	-0.02	4.27E-05	0.33	*B3GALT5, HMGN1, PSMG1, IGSF5, LCA5L, GET1, ETS2, BRWD1*
	6	AX-647769366	187090448	-0.01	6.06E-05	0.05	*MDFIC2, MITF, FRMD4B*
	10	AX-647647582	44029128	0.02	4.96E-05	0.07	*FAM71A, BATF3, DTL, PPP2R5A, NENF, ATF3, NSL1, TATDN3, FLVCR1, VASH2, INTS7, PACC1, SPATA45, ANGEL2, RPS6KC1*
	11	AX-647664634	198100038	-0.01	7.30E-05	0.04	*TRAPPC11, RWDD4, ING2, ENPP6, STOX2, WWC2*
FCR	1	AX-647628511	83111136	3.62	1.60E-05	0.11	*SRSF3, CDKN1A, GPRC6A, KPNA5, ZUP1, RSPH4A, RWDD1, CALHM4, KCTD20, STK38, FAM162B, PXT1, RFX6*
	1	**AX-647631147**	108686101	3.70	6.94E-06	0.12	-

	1	**AX-647632532**	122729223	3.45	2.55E-06	0.10	*POU5F1, PSORS1C2, CDSN, C1H6ORF15, MUC21, SFTA2, GTF2H4, IER3, TUBB, MDC1, NRM, PPP1R18, C1H6orf136, MRPS18B, GNL1, RPP21, TCF19, CCHCR1, VARS2, DHX16, ATAT1, PPP1R10, PRR3, FLOT1, ABCF1, DDR1*
	6	**AX-647758743**	32817838	2.54	1.18E-05	0.05	*ROBO1*
	6	AX-647764338	70252701	3.60	3.25E-05	0.11	*DIPK2A, SLC9A9*
	6	AX-647765320	89892337	3.41	1.33E-05	0.10	*SLITRK3, SI*
	6	AX-647773071	200544009	2.42	5.96E-06	0.05	*WNT5A, LRTM1, ERC2, CACNA2D3*
	8	AX-647790363	98284517	-2.19	1.38E-05	0.04	-
	8	**AX-647794228**	130312171	2.73	5.98E-08	0.06	*OSR1, RDH14, NT5C1B*
	9	AX-647798852	33147281	2.85	3.23E-06	0.07	*FOXE1, ALDH1B1, NANS, ANP32B, TRMO, XPA, TSTD2, TDRD7, IGFBPL1, TRIM14, HEMGN, NCBP1, TMOD1, CCDC180*
	12	AX-647669973	21729074	2.85	7.11E-05	0.07	*FAM71C, UHRF1BP1L, ANKS1B*
	13	**AX-647686472**	123955159	-2.19	7.38E-07	0.04	*MKRN3, NDN, MAGEL2*
KR	1	**AX-647631147**	108686101	-0.44	8.16E-05	0.08	-
	1	**AX-647632532**	122729223	-0.52	2.70E-07	0.11	*POU5F1, PSORS1C2, CDSN, C1H6orf15, MUC21, SFTA2, GTF2H4, IER3, TUBB, MDC1, NRM, PPP1R18, C1H6orf136, MRPS18B, GNL1, RPP21, TCF19, CCHCR1, VARS2, DHX16, ATAT1, PPP1R10, PRR3, FLOT1, ABCF1, DDR1*
	2	AX-647704560	169992751	-0.31	6.96E-06	0.04	*PCDH15*
	6	**AX-647758743**	32817838	-0.33	4.10E-05	0.05	*ROBO1*
	8	**AX-647794228**	130312171	-0.30	1.20E-05	0.04	*OSR1, RDH14, NT5C1B*
	13	**AX-647686472**	123955159	0.28	3.88E-06	0.03	*MKRN3, NDN, MAGEL2*
RG	4	AX-647741874	214079096	-0.64	3.37E-05	0.12	*AGBL3, TMEM140, CYREN, WDR91, STRA8, NUP205, STMP1, FAM180A, CNOT4, SLC13A4, MTPN*
	4	AX-647741879	214083831	-0.63	3.54E-05	0.12	*TMEM140, CYREN, WDR91, STRA8, NUP205, STMP1, FAM180A, CNOT4, SLC13A4, MTPN*
	4	AX-647741887	214162040	-0.64	3.47E-05	0.12	*TRNAC-GCA, STRA8, NUP205, STMP1, FAM180A, CNOT4, SLC13A4, MTPN*
	4	AX-647741891	214170873	-0.63	3.54E-05	0.12	*TRNAC-GCA, STRA8, NUP205, STMP1, FAM180A, CNOT4, SLC13A4, MTPN*

[1] BW: Body weight, ADG: Average daily gain, DFI: Daily feed intake, FCR: Feed conversion ratio, KR: Kleiber ratio, RG: Residual gain.
[2] Chr: Chromosome.
[3] SNP ID in boldface represents the SNP with pleiotropic effects on growth and feed efficiency traits.
[4] The allele substitution effect (beta).
[5] Percentage of phenotypic variation explained.

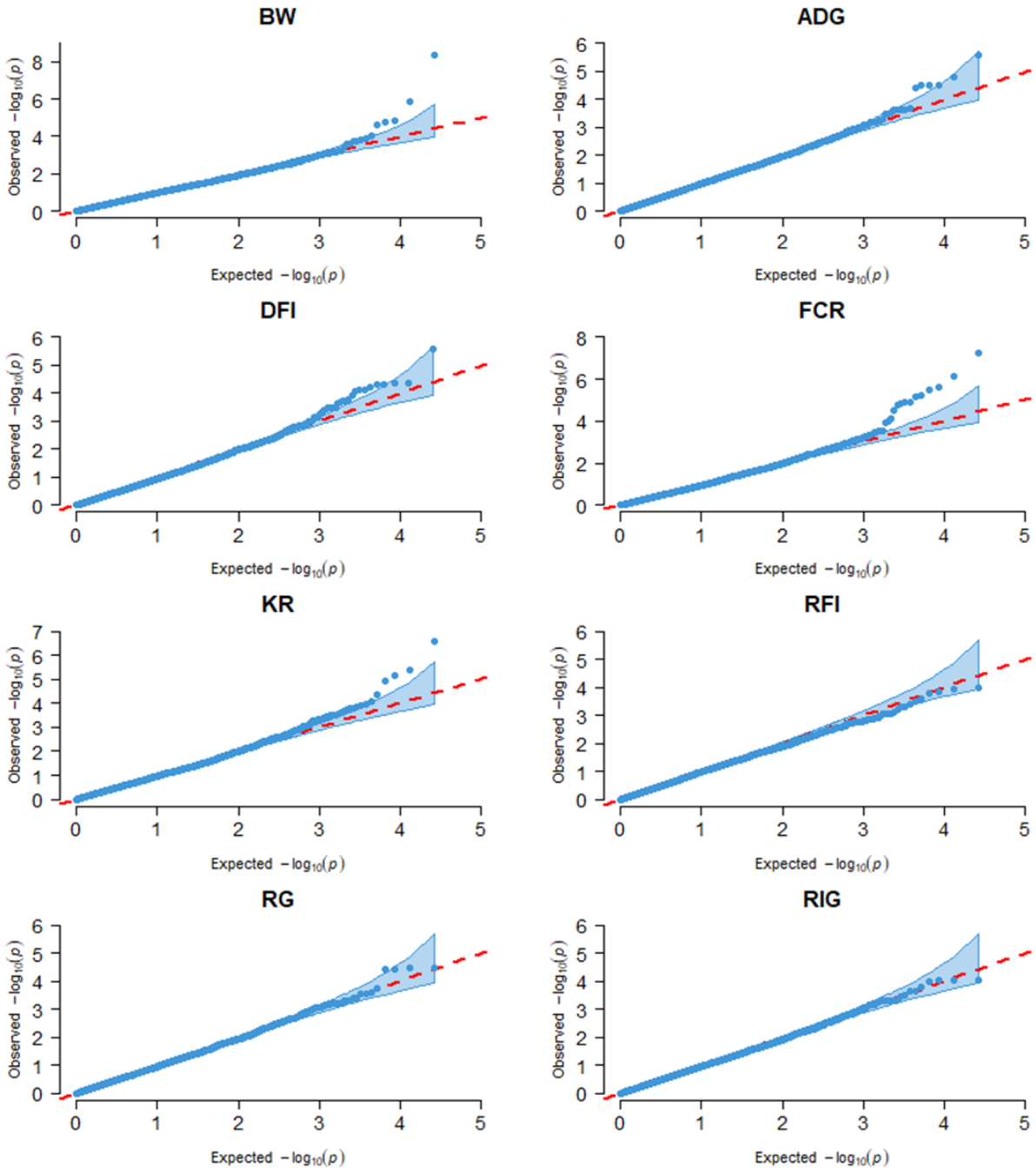

Figure 8-1 Q-Q plots for growth and feed efficiency traits using MLM model. BW: Body weight, ADG: Average daily gain, DFI: Daily feed intake, FCR: Feed conversion ratio, KR: Kleiber ratio, RFI: Residual feed intake, RG: Residual gain, RIG: Residual intake and gain.

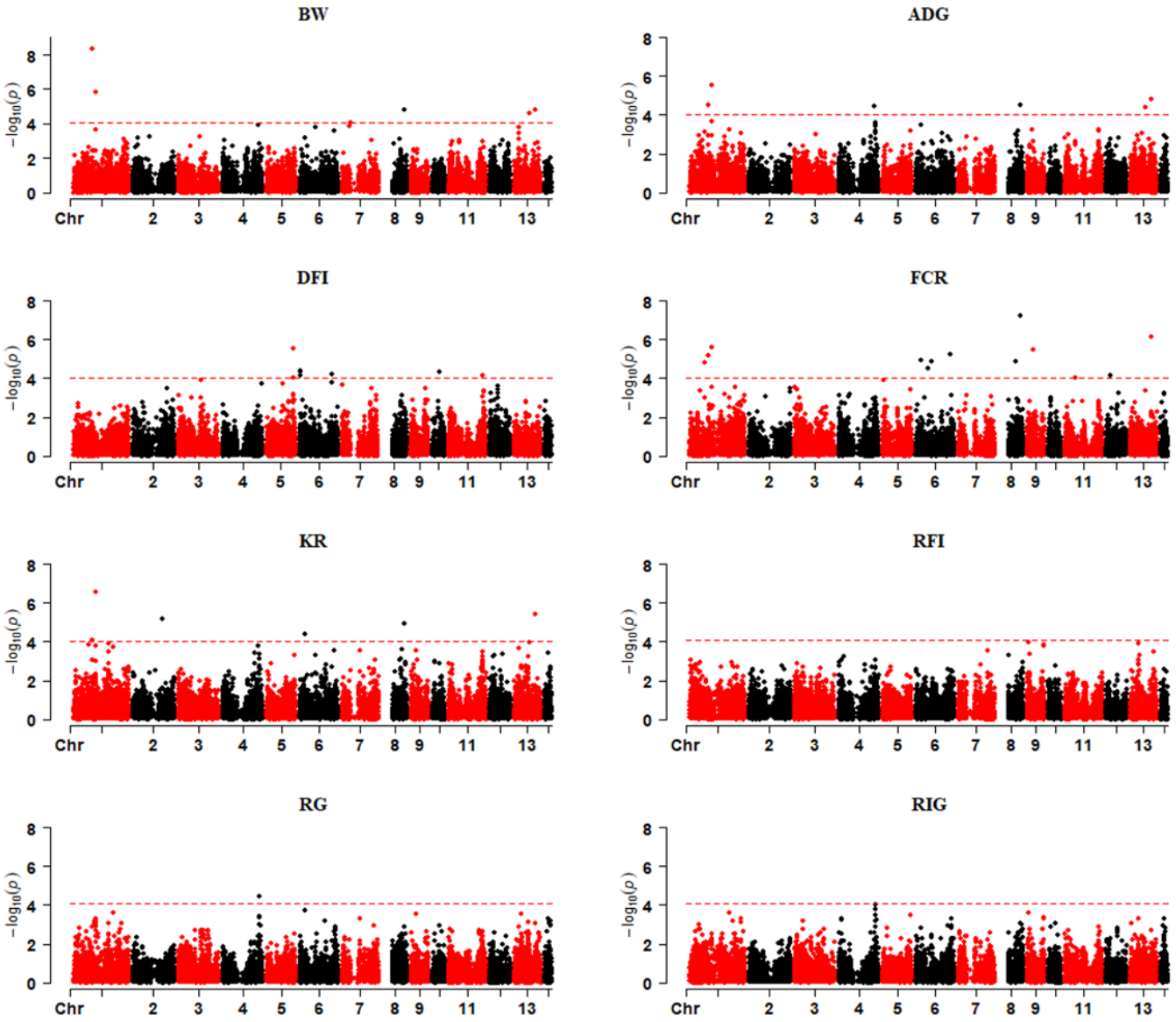

Figure 8-2 Manhattan plots of genome-wide association studies for growth and feed efficiency traits. BW: Body weight, ADG: Average daily gain, DFI: Daily feed intake, FCR: Feed conversion ratio, KR: Kleiber ratio, RFI: Residual feed intake, RG: Residual gain, RIG: Residual intake and gain.

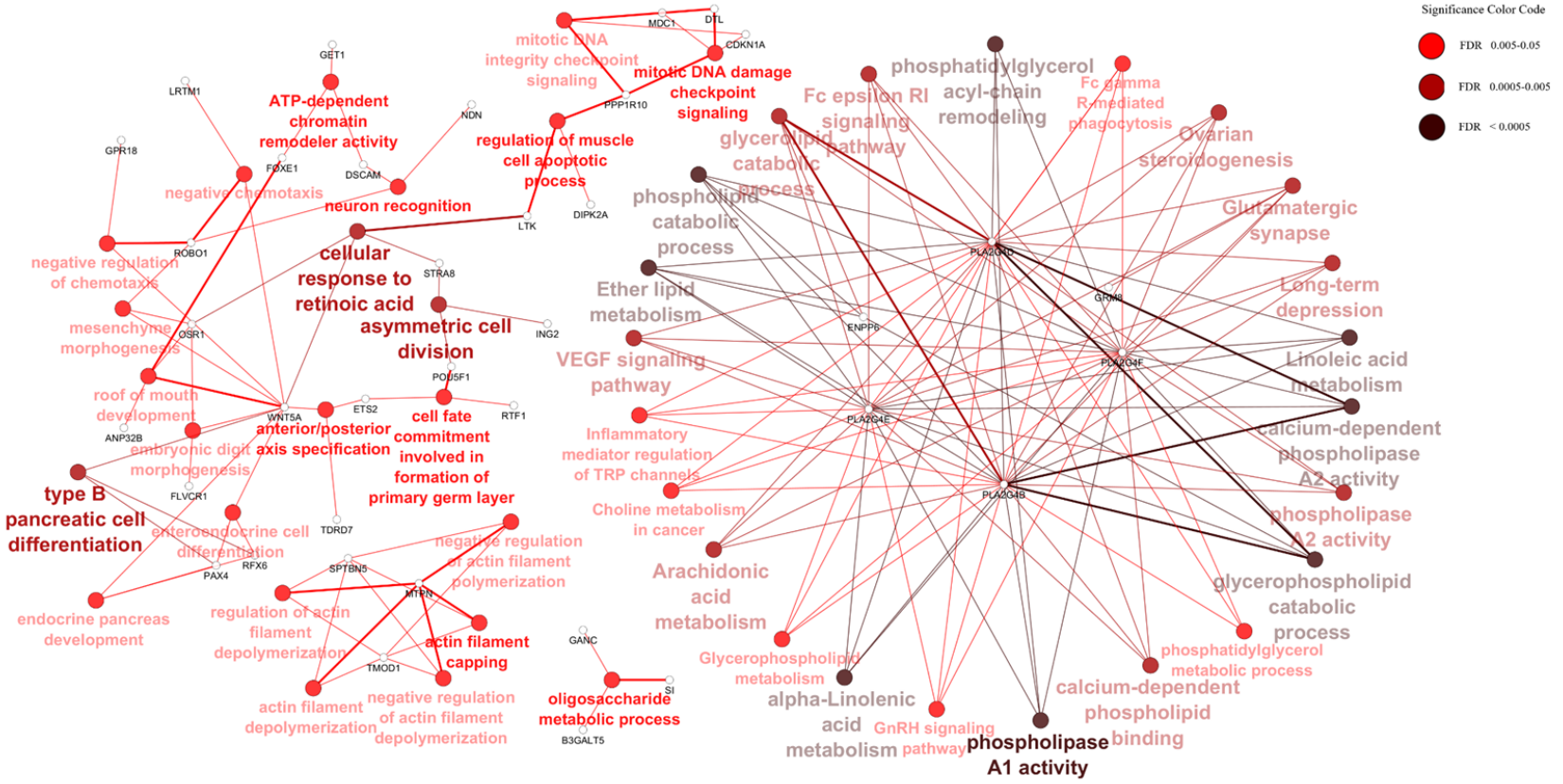

Figure 8-3 The Gene Ontology and metabolic pathways using KEGG enriched for the candidate genes surrounding the significant SNPs.

CHAPTER 9. General discussion and conclusion

9.1 Summary and general discussion

Improving feed efficiency in American mink is of utmost importance since it offers significant cost-saving potential for mink production systems, which primarily revolve around feed expenses. Until now, the Canadian mink industry has exclusively utilized phenotypic selection as their primary selection method, and it is important to highlight that feed efficiency has not been incorporated into their selection programs. The literature review, as discussed in chapter 2, showed that feed efficiency-related traits are moderately heritable traits, suggesting a significant genetic basis, which in turn, opens the door to potential enhancements through genetic and genomic breeding programs. In addition, chapter 2 elaborates on the progress achieved through the development of a chromosome-based reference genome and the creation of a 70K SNP array for the American mink. These advancements were crucial for genomic analyses of this species, essentially providing the infrastructure for the completion of this thesis.

9.1.1 Genetic parameters

The objectives of the first study in chapter 3 were to estimate 1) heritabilities for different feed efficiency and component traits, and 2) phenotypic and genetic correlations among these traits. The chapter introduced novel discoveries by providing the knowledge of the genetic parameters for feed efficiency and its component traits in American mink. The estimates of heritabilities (±SE) for feed efficiency and component traits were moderate, including 0.28±0.06, 0.23±0.06, 0.28±0.10, 0.27±0.11, 0.25±0.09, 0.26±0.09, 0.20±0.09,

0.23±0.09, 0.21±0.10, 0.25±0.10, and 0.26±0.10 for HW, HL, FBL, FBW, ADG, DFI, FCR, RFI, RG, RIG, and KR, respectively. The findings revealed non-significant genetic correlations between RFI and growth traits (-0.24±0.16 with ADG, and -0.20±0.30 with FBW), yet high genetic correlation with feed intake (0.80±0.11), showing the possibility of including RFI in the selection program for higher feed efficiency, with negligible effects on the animal growth. Another recommended feed efficiency measurement was RIG, since it enhances the growth rate and reduces the feed intake. According to the results, KR can be a desirable indicator trait for feed efficiency in the mink industry, given that it eliminates the necessity of recording feed intake data for its calculation.

9.1.2 Copy number variation

The main objective of the chapters 4 and 5 was to assess the potential of genome-wide CNVs as complementary genetic markers for the analysis of economically important traits in American mink. In chapter 4, the distribution and pattern of CNV in the American mink genome were mapped using whole-genome sequencing data of 100 individuals. This characterization involved a variant calling process, along with the use of several complementary software to detect CNV events. The results of this chapter revealed a total of 5,378 CNVR (4,073 losses, 625 gains, and 680 mixed events) covering 1.9% of the mink autosomes. Notably, the identified CNVRs overlapped with numerous annotated genes with known effects on fur characteristics and development, and immune system processes. In addition, the functional annotation analyses confirmed the genes involved in pathways were related to growth, behavior, lipid metabolism, and immune response. For instance, it is well-known that circadian entrainment is a crucial aspect of behavior and adaptation, as it plays a fundamental role in helping organisms adjust to daily environmental cycles.

Similarly, the identification of enriched immune response pathways in this chapter confirms the role of immune response modulation in Aleutian mink disease virus infection, a prevalent disease within the global mink industry.

Expanding upon the insights gained in chapter 4, chapter 5 delved into the examination of the association between CNVs and complex traits in American mink. Notably, this chapter involved a much larger, but different genomic data set, comprising 2,986 American mink genotyped with the Affymetrix Mink 70K SNP array. To perform the association analyses, the deregressed estimated breeding values of 27 economically important traits were included in the model as pseudophenotypes. Several significant CNVRs overlapped with genes reported to have impacts on growth and feed efficiency traits, reproduction, Aleutian disease, and pelt quality traits. In summary, these findings offer new tools for examining the mink genome and stand as a reference for forthcoming investigations that involve the presence of genomic structural variations.

9.1.3 Runs of homozygosity

In chapter 6, as the first study of ROH, we aimed to investigate the 1) genome-wide patterns of homozygosity, 2) ROH islands, and 3) annotated genes from those candidate regions using whole-genome sequencing data of 100 American mink. After performing quality control on the whole-genome sequencing data in chapter 4, we identified 8,373,854 bi-allelic variants retained for ROH analyses. A total of 34,652 ROH segments were identified in all individuals, among which shorter segments (0.3–1 Mb) were abundant throughout the genome, approximately accounting for 84.4% of all ROH. In this chapter, we were able to identify higher mean number of ROH per individual (n=346.5) in comparison to the means of 82 and 102 per individual reported in the studies by Karimi et al. (2021b; 2022),

respectively. The higher detection of ROH segments resulted from the improved resolution of whole-genome sequencing data, which allowed for the identification of smaller ROH sizes.

The genome-wide analysis of ROH islands can be an effective strategy to detect the variants shared among the individuals of a population, and thereby to reveal important genomic regions for complex traits. The Gene Ontology and pathway analysis using KEGG revealed several pathways with key roles on growth and fur characteristics, such as cGMP-PKG signaling pathway, regulation of actin cytoskeleton, and calcium signaling pathway. It is worth noting that the prior chapter demonstrated significant enrichment in the regulation of the actin cytoskeleton, highlighting its influence on biological processes associated with growth in American mink. The candidate genes from ROH islands and functional enrichment analysis suggest the possible signatures of selection in response to the mink breeding targets, such as increased body length, reproductive performance and fur quality.

The second study of ROH (chapter 7) aimed to evaluate the association between consensus ROH with growth and feed efficiency traits in American mink. To this end, the ROH-based association studies were carried out with linear mixed models for 11 growth and feed efficiency traits, which ultimately resulted in identification of 13 consensus ROH regions significantly associated with these complex traits. These regions were overlapped with several candidate genes with known functions on growth and body size development.

9.1.4 Genome-wide association studies

Lastly, in chapter 8, we aimed to identify potential genetic variants and positional candidate genes associated with growth and feed efficiency traits in American mink. To this end, GWAS were performed using deregressed estimated breeding values of 1,037-1,872 mink (as pseudophenotypes), genotyped with the Affymetrix Mink 70K SNP array. Association analyses were performed using the mixed linear model in GCTA software, resulted in finding 42 SNPs located on 11 different chromosomes significantly associated with six growth and feed efficiency traits, among which six SNPs had pleiotropic effects on at least two analyzed traits. The functional analyses of the annotated genes revealed that these genes were involved in lipid metabolism (glycerophospholipid metabolism, ether lipid metabolism, arachidonic acid metabolism), hormone signaling and regulation (GnRH signaling pathway, type B pancreatic cell differentiation, and endocrine pancreas development), and muscle development (actin filament depolymerization, actin filament capping, and regulation of muscle cell apoptotic process). In this chapter, the detection of a large number of SNPs, despite capturing only a small proportion of additive genetic variance, suggested a polygenic architecture of growth and feed efficiency in American mink.

9.2 Conclusion

In conclusion, the research conducted for this thesis successfully provided appropriate feed efficiency measurements in American mink, and the estimates of genetic and phenotypic parameters indicated the possibility of including these traits in mink breeding programs to develop an index for selection of feed-efficient mink and consequently reduce the cost of mink production. To the best of our knowledge, our findings offered the first genomic

analyses to identify genetic variants and biological mechanisms underlying growth and feed efficiency traits in American mink, which in turn provided a biological foundation for improving these traits using genomic selection programs to select more efficient mink.

9.3 General recommendations

In light of the findings in this thesis, there are several steps that need to be taken in the future to support the improvement of feed efficiency traits in American mink:

a) Future investigations on genetic parameters of feed efficiency in mink could benefit from the inclusion of diverse mink populations from various farms in order to increase the accuracy of genetic evaluation.

b) To address the limitations of custom SNP arrays, such as their limited capacity to capture a significant portion of heritability, it is recommended that future research employ a substantial number of individuals with whole-genome sequencing or imputation to the whole genome level. In the future, it is foreseeable that it will become economically viable to directly acquire all genetic variants from sequence-level data for all animals within a large population.

c) The significant regions and candidate genes associated with economically important traits in this thesis can be validated through fine mapping, thereby confirming the impact of these genes on these key traits in mink.

d) It is advisable that future studies include additional multi-omics approaches, such as transcriptomics and metabolomics, to identify biomarkers for economically important traits in mink, as their capacity to enhance genetic progress in complex traits has been demonstrated in other farm animals.

References

Abdellaoui, A., Yengo, L., Verweij, K. J., & Visscher, P. M. (2023). 15 years of GWAS discovery: Realizing the promise. *The American Journal of Human Genetics*, *110*, 179-194.

Abdoli, R., Mirhoseini, S. Z., Ghavi Hossein-Zadeh, N., Zamani, P., Moradi, M. H., Ferdosi, M. H., & Gondro, C. (2023). Runs of homozygosity and cross-generational inbreeding of Iranian fat-tailed sheep. *Heredity*, *130*, 358-367.

Abegaz, S., Wyk, J. B., & Olivier, J. J. (2005). Model comparisons and genetic and environmental parameter estimates of growth and the Kleiber ratio in Horro sheep. *South African Journal of Animal Science*, *35*, 30-40.

Abyzov, A., Urban, A. E., Snyder, M., & Gerstein, M. (2011). CNVnator: an approach to discover, genotype, and characterize typical and atypical CNVs from family and population genome sequencing. *Genome Research*, *21*, 974-984.

Adney, D. R., Lovaglio, J., Schulz, J. E., Yinda, C. K., Avanzato, V. A., Haddock, E., & Munster, V. J. (2022). Severe acute respiratory disease in American mink experimentally infected with SARS-CoV-2. *JCI Insight*, *7*. e159573.

Aguiló-Gisbert, J., Padilla-Blanco, M., Lizana, V., Maiques, E., Muñoz-Baquero, M., ChillidaMartínez, E., & Rubio-Guerri, C. (2021). First description of SARS-CoV-2 infection in two feral American mink (*Neovison vison*) caught in the wild. *Animals*, *11*, 1422.

Akanno, E. C., Schenkel, F. S., Quinton, V. M., Friendship, R. M., & Robinson, J. A. B. (2013). Meta-analysis of genetic parameter estimates for reproduction, growth and carcass traits of pigs in the tropics. *Livestock Science*, *152*, 101-113.

Akhter, N., Takeda, Y., Nara, H., Araki, A., Ishii, N., Asao, N., & Asao, H. (2016). Apurinic/Apyrimidinic endonuclease 1/redox factor-1 (Ape1/Ref-1) modulates antigen presenting cell-mediated T helper cell type 1 responses. *Journal of Biological Chemistry*, *291*, 23672-23680.

Ali, N., Niaz, S., Khan, N. U., Gohar, A., Khattak, I., Dong, Y., & Usman, T. (2020). Polymorphisms in gene are associated with production traits and mastitis resistance in dairy cattle. *Annals of Animal Science*, *20*, 409-423.

Ali, N., Niaz, S., Khan, N. U., Gohar, A., Khattak, I., Dong, Y., & Usman, T. (2020). Polymorphisms in gene are associated with production traits and mastitis resistance in dairy cattle. *Annals of Animal Science*, *20*, 409-423.

Aloqaily, B. H., Ferranti, E. M., Summers, A. F., Gifford, C. A., & Hernandez Gifford, J. A. (2018). Intraovarian WNT3A modulates estrogen-mediated estrus behavior in cattle. *Translational Animal Science*, *2*, 19-21.

An, B., Xu, L., Xia, J., Wang, X., Miao, J., Chang, T., & Gao, H. (2020). Multiple association analysis of loci and candidate genes that regulate body size at three growth stages in Simmental beef cattle. *BMC Genetics*, *21*, 1-11.

Andersson, L. (2009). Genome-wide association analysis in domestic animals: a powerful approach for genetic dissection of trait loci. *Genetica*, *136*, 341-349.

Andersson, L., & Georges, M. (2004). Domestic-animal genomics: deciphering the genetics of complex traits. *Nature Reviews Genetics*, *5*, 202-212.

Andersson, L., Haley, C. S., Ellegren, H., Knott, S. A., Johansson, M., Andersson, K., & Lundström, K. (1994). Genetic mapping of quantitative trait loci for growth and fatness in pigs. *Science*, *263*, 1771-1774.

Andretta, I., Pomar, C., Kipper, M., Hauschild, L., & Rivest, J. (2016). Feeding behavior of growing–finishing pigs reared under precision feeding strategies. *Journal of Animal Science*, *94*, 3042-3050.

Anistoroaei, R., Ansari, S., Farid, A., Benkel, B., Karlskov-Mortensen, P., & Christensen, K. (2009). An extended anchored linkage map and virtual mapping for the American mink genome based on homology to human and dog. *Genomics*, *94*, 204-210.

Antunes, M. V. A., Berton, M. P., de Camargo, G. M. F., Peripolli, E., de Oliveira Silva, R. M., Olivieri, B. F., & Baldi, F. (2018). Copy number variation regions in Nellore cattle: evidences of environment adaptation. *Livestock Science*, *207*, 51-58.

Arthur, P. F., Archer, J. A., Johnston, D. J., Herd, R. M., Richardson, E. C., & Parnell, P. F. (2001). Genetic and phenotypic variance and covariance components for feed intake, feed efficiency, and other postweaning traits in Angus cattle. *Journal of Animal Science*, *79*, 2805-2811.

Arthur, P. F., & Herd, R. M. (2005). Efficiency of feed utilisation by livestock—Implications and benefits of genetic improvement. *Canadian Journal of Animal Science*, *85*, 281-290.

Arunachalam, P. S., Wimmers, F., Mok, C. K. P., Perera, R. A., Scott, M., Hagan, T., & Pulendran, B. (2020). Systems biological assessment of immunity to mild versus severe COVID-19 infection in humans. *Science*, *369*, 1210-1220.

Aspengren, S., Sköld, H. N., Quiroga, G., Mårtensson, L., & Wallin, M. (2003). Noradrenaline-and melatonin-mediated regulation of pigment aggregation in fish melanophores. *Pigment Cell Research*, *16*, 59-64.

Aytekin, İ., Bayraktar, M., Sakar, Ç. M., & Ünal, İ. (2020). Association between MYLK4 gene polymorphism and growth traits at different age stages in Anatolian black cattle. *Animal Biotechnology*, *31*, 555-560.

Bader, R., Colomb, J., Pankratz, B., Schröck, A., Stocker, R. F., & Pankratz, M. J. (2007). Genetic dissection of neural circuit anatomy underlying feeding behavior in Drosophila: Distinct classes of hugin-expressing neurons. *Journal of Comparative Neurology*, *502*, 848-856.

Bagnall, N., Gough, J., Cadogan, L., Burns, B., & Kongsuwan, K. (2009). Expression of intracellular calcium signalling genes in cattle skin during tick infestation. *Parasite Immunology*, *31*, 177-187.

Bak, S. S., Park, J. M., Oh, J. W., Kim, J. C., Kim, M. K., & Sung, Y. K. (2020). Knockdown of FOXA2 impairs hair-inductive activity of cultured human follicular keratinocytes. *Frontiers in Cell and Developmental Biology*, *8*, 575382.

Ballan, M., Bovo, S., Schiavo, G., Schiavitto, M., Negrini, R., & Fontanesi, L. (2022). Genomic diversity and signatures of selection in meat and fancy rabbit breeds based on high-density marker data. *Genetics Selection Evolution*, *54*, 1-18.

Bannasch, D. L., Baes, C. F., & Leeb, T. (2020). Genetic variants affecting skeletal morphology in domestic dogs. *Trends in Genetics*, *36*, 598-609.

Baranzini, S. E., Wang, J., Gibson, R. A., Galwey, N., Naegelin, Y., Barkhof, F., & Oksenberg, J. R. (2009). Genome-wide association analysis of susceptibility and clinical phenotype in multiple sclerosis. *Human Molecular Genetics*, *18*, 767-778.

Baranov, M. V., Revelo, N. H., Dingjan, I., Maraspini, R., Ter Beest, M., Honigmann, A., & van den Bogaart, G. (2016). SWAP70 organizes the actin cytoskeleton and is essential for phagocytosis. *Cell Reports*, *17*, 1518-1531.

Barnes, M. R. (2010). Genetic variation analysis for biomedical researchers: a primer. *Genetic Variation: Methods and Protocols*, 1-20.

Beck, A., Kolisek, M., Bagley, L. A., Fleig, A., Penner, R., Beck, A., & Penner, R. (2006). Nicotinic acid adenine dinucleotide phosphate and cyclic ADP-ribose regulate TRPM2 channels in T lymphocytes. *The FASEB Journal*, *20*, 962-964.

Begli, H. E., Torshizi, R. V., Masoudi, A. A., Ehsani, A., & Jensen, J. (2016). Longitudinal analysis of body weight, feed intake and residual feed intake in F2 chickens. *Livestock Science*, *184*, 28-34.

Belliveau, A. M., Farid, A., O'Connell, M., & Wright, J. M. (1999). Assessment of genetic variability in captive and wild American mink (Mustela vison) using microsatellite markers. *Canadian Journal of Animal Science*, *79*, 7-16.

Benjamini, Y., & Hochberg, Y. (1995). Controlling the false discovery rate: a practical and powerful approach to multiple testing. *Journal of the Royal statistical society: series B (Methodological)*, *57*, 289-300.

Berg, P., & Lohi, O. (1992). Feed consumption and efficiency in paternal progeny groups in mink. *Acta Agriculturae Scandinavica A-Animal Sciences*, *42*, 27-33.

Berry, D. P., & Crowley, J. J. (2012). Residual intake and body weight gain: a new measure of efficiency in growing cattle. *Journal of Animal Science*, *90*, 109-115.

Berry, D. P., & Crowley, J. J. (2013). Cell biology symposium: genetics of feed efficiency in dairy and beef cattle. *Journal of Animal Science*, *91*, 1594-1613.

Berton, M. P., da Silva, R. P., Banchero, G., Mourão, G. B., Ferraz, J. B. S., Schenkel, F. S., & Baldi, F. (2022). Genomic integration to identify molecular biomarkers associated with indicator traits of gastrointestinal nematode resistance in sheep. *Journal of Animal Breeding and Genetics*, *139*, 502-516.

Bhuiyan, M. S., Lim, D., Park, M., Lee, S., Kim, Y., Gondro, C., & Lee, S. (2018). Functional partitioning of genomic variance and genome-wide association study for carcass traits in Korean Hanwoo cattle using imputed sequence level SNP data. *Frontiers in Genetics*, *9*, 217.

Bickhart, D. M., & Liu, G. E. (2014). The challenges and importance of structural variation detection in livestock. *Frontiers in Genetics*, *5*, 37.

Bierman, A., Guthrie, A. J., & Harper, C. K. (2010). Lavender foal syndrome in Arabian horses is caused by a single-base deletion in the MYO5A gene. *Animal Genetics*, *41*, 199-201.

Bindea, G., Mlecnik, B., Hackl, H., Charoentong, P., Tosolini, M., Kirilovsky, A., & Galon, J. (2009). ClueGO: a Cytoscape plug-in to decipher functionally grouped gene ontology and pathway annotation networks. *Bioinformatics*, *25*, 1091-1093.

Biscarini, F., Cozzi, P., Gaspa, G., & Marras, G. (2018). detectRUNS: Detect runs of homozygosity and runs of heterozygosity in diploid genomes.

Bohil, A. B., Robertson, B. W., & Cheney, R. E. (2006). Myosin-X is a molecular motor that functions in filopodia formation. *Proceedings of the National Academy of Sciences*, *103*, 12411-12416.

Boissin-Agasse, L., & Boissin, J. (1985). Incidence of a circadian cycle of photosensitivity in the regulation of the annual testis cycle in the mink: a short-day mammal. *General and Comparative Endocrinology*, *60*, 109-115.

Boissin-Agasse, L., Boissin, J., & Ortavant, R. (1982). Circadian photosensitive phase and photoperiodic control of testis activity in the mink (Mustela vison Peale and Beauvois), a short-day mammal. *Biology of Reproduction*, *26*, 110-119.

Boklund, A., Hammer, A. S., Quaade, M. L., Rasmussen, T. B., Lohse, L., Strandbygaard, B., ... & Bøtner, A. (2021). SARS-CoV-2 in Danish mink farms: course of the epidemic and a descriptive analysis of the outbreaks in 2020. *Animals*, *11*(1), 164.

Bovo, S., Ribani, A., Muñoz, M., Alves, E., Araujo, J. P., Bozzi, R., & Fontanesi, L. (2020). Whole-genome sequencing of European autochthonous and commercial pig breeds allows the detection of signatures of selection for adaptation of genetic resources to different breeding and production systems. *Genetics Selection Evolution*, *52*, 1-19.

Bowman, J., Beauclerc, K., Farid, A. H., Fenton, H., Klütsch, C. F., & Schulte-Hostedde, A. I. (2017). Hybridization of domestic mink with wild American mink (*Neovison vison*) in eastern Canada. *Canadian Journal of Zoology*, *95*, 443-451.

Brito, L. F., Oliveira, H. R., Houlahan, K., Fonseca, P. A., Lam, S., Butty, A. M., & Schenkel, F. S. (2020). Genetic mechanisms underlying feed utilization and implementation of genomic selection for improved feed efficiency in dairy cattle. *Canadian Journal of Animal Science*, *100*, 587-604.

Brunes, L. C., Baldi, F., Lopes, F. B., Lôbo, R. B., Espigolan, R., Costa, M. F., & Magnabosco, C. U. (2021). Weighted single-step genome-wide association study and pathway analyses for feed efficiency traits in Nellore cattle. *Journal of Animal Breeding and Genetics*, *138*, 23-44.

Bu, D., Luo, H., Huo, P., Wang, Z., Zhang, S., He, Z., & Kong, L. (2021). KOBAS-i: intelligent prioritization and exploratory visualization of biological functions for gene enrichment analysis. *Nucleic Acids Research*, *49*, 317-325.

Burnicka-Turek, O., Shirneshan, K., Paprotta, I., Grzmil, P., Meinhardt, A., Engel, W., & Adham, I. M. (2009). Inactivation of insulin-like factor 6 disrupts the progression of spermatogenesis at late meiotic prophase. *Endocrinology*, *150*, 4348-4357.

Butler, D. G., Cullis, B. R., Gilmour, A. R., Gogel, B. J., & Thompson, R. (2017). ASReml-R reference manual version 4. *VSN International Ltd, Hemel Hempstead, HP1 1ES, UK*.

Butty, A. M., Chud, T. C., Miglior, F., Schenkel, F. S., Kommadath, A., Krivushin, K., & Baes, C. F. (2020). High confidence copy number variants identified in Holstein dairy cattle from whole genome sequence and genotype array data. *Scientific Reports*, *10*, 8044.

Butty, A. M., Chud, T. C., Cardoso, D. F., Lopes, L. S., Miglior, F., Schenkel, F. S., & Baes, C. F. (2021). Genome-wide association study between copy number variants and hoof health traits in Holstein dairy cattle. *Journal of Dairy Science*, *104*, 8050-8061.

Cammack, K. M., Leymaster, K. A., Jenkins, T. G., & Nielsen, M. K. (2005). Estimates of genetic parameters for feed intake, feeding behavior, and daily gain in composite ram lambs. *Journal of Animal Science*, *83*, 777-785.

Cantalapiedra-Hijar, G., Abo-Ismail, M., Carstens, G. E., Guan, L. L., Hegarty, R., Kenny, D. A., & Ortigues-Marty, I. (2018). Biological determinants of between-animal variation in feed efficiency of growing beef cattle. *Animal*, *12*, 321-335.

Carlson, M., Falcon, S., Pages, H., & Li, N. (2019). org. Hs. eg. db: Genome wide annotation for Human. *R package version*, *3*, 3.

Ceballos, F. C., Joshi, P. K., Clark, D. W., Ramsay, M., & Wilson, J. F. (2018). Runs of homozygosity: windows into population history and trait architecture. *Nature Reviews Genetics*, *19*, 220-234.

Celen, C., Chuang, J. C., Luo, X., Nijem, N., Walker, A. K., Chen, F., & Zhu, H. (2017). Arid1b haploinsufficient mice reveal neuropsychiatric phenotypes and reversible causes of growth impairment. *Elife*, *6*, e25730.

Cendron, F., Perini, F., Mastrangelo, S., Tolone, M., Criscione, A., Bordonaro, S., & Cassandro, M. (2020). Genome-wide SNP analysis reveals the population structure and the conservation status of 23 Italian chicken breeds. *Animals*, *10*, 1441.

Cesarani, A., Gaspa, G., Pauciullo, A., Degano, L., Vicario, D., & Macciotta, N. P. (2021). Genome-wide analysis of homozygosity regions in European Simmental bulls. *Journal of Animal Breeding and Genetics*, *138*, 69-79.

Chang, C. C., Chow, C. C., Tellier, L. C., Vattikuti, S., Purcell, S. M., & Lee, J. J. (2015). Second-generation PLINK: rising to the challenge of larger and richer datasets. *Gigascience*, *4*, 13742-015.

Chawla, A. S., Khalsa, J. K., Dhar, A., Gupta, S., Umar, D., Arimbasseri, G. A., & Rath, S. (2020). A role for cell-autocrine interleukin-2 in regulatory T-cell homeostasis. *Immunology*, *160*, 295-309.

Chen, F., Chen, H., Wang, J., Niu, H., Lan, X., Hua, L., & Fang, X. (2010). MEF2A gene polymorphisms are associated with growth traits in Chinese indigenous cattle breeds. *Journal of Animal and Veterinary Advances*, *9*, 814-819.

Chen, S., Guo, X., He, X., Di, R., Zhang, X., Zhang, J., & Chu, M. (2021). Transcriptome analysis reveals differentially expressed genes and long non-coding RNAs associated with fecundity in sheep hypothalamus with different FecB genotypes. *Frontiers in Cell and Developmental Biology*, *9*, 633747.

Chen, Y., Chen, Y., Shi, C., Huang, Z., Zhang, Y., Li, S., & Chen, Q. (2018). SOAPnuke: a MapReduce acceleration-supported software for integrated quality control and preprocessing of high-throughput sequencing data. *Gigascience*, *7*, 120.

Chen, Z., Zhang, Z., Wang, Z., Zhang, Z., Wang, Q., & Pan, Y. (2022). Heterozygosity and homozygosity regions affect reproductive success and the loss of reproduction: A case study with litter traits in pigs. *Computational and Structural Biotechnology Journal*, *20*, 4060-4071.

Chen, Z., Zhu, M., Wu, Q., Lu, H., Lei, C., Ahmed, Z., & Sun, J. (2023). Analysis of genetic diversity and selection characteristics using the whole genome sequencing data of five buffaloes, including Xilin buffalo, in Guangxi, China. *Frontiers in Genetics*, *13*, 1084824.

Chen, X., Schulz-Trieglaff, O., Shaw, R., Barnes, B., Schlesinger, F., Källberg, M., & Saunders, C. T. (2016). Manta: rapid detection of structural variants and indels for germline and cancer sequencing applications. *Bioinformatics*, *32*, 1220-1222.

Chen, Y., Hu, S., Mu, L., Zhao, B., Wang, M., Yang, N., & Wu, X. (2019). Slc7a11 modulated by POU2F1 is involved in pigmentation in rabbit. *International Journal of Molecular Sciences*, *20*, 2493.

Chen, Y., Samaraweera, P., Sun, T. T., Kreibich, G., & Orlow, S. J. (2002). Rab27b association with melanosomes: dominant negative mutants disrupt melanosomal movement. *Journal of Investigative Dermatology*, *118*, 933-940.

Chintala, S., Li, W., Lamoreux, M. L., Ito, S., Wakamatsu, K., Sviderskaya, E. V., & Swank, R. T. (2005). Slc7a11 gene controls production of pheomelanin pigment and proliferation of cultured cells. *Proceedings of the National Academy of Sciences*, *102*, 10964-10969.

Cho, S. H., Raybuck, A., Wei, M., Erickson, J., Nam, K. T., Cox, R. G., & Boothby, M. (2013). B Cell–Intrinsic and–Extrinsic Regulation of Antibody Responses by PARP14, an Intracellular (ADP-Ribosyl) Transferase. *The Journal of Immunology*, *191*, 3169-3178.

Choi, Y. J., Uehara, Y., Park, J. Y., Chung, K. W., Ha, Y. M., Kim, J. M., & Chung, H. Y. (2012). Suppression of melanogenesis by a newly synthesized compound, MHY966 via the nitric oxide/protein kinase G signaling pathway in murine skin. *Journal of Dermatological Science*, *68*, 164-171.

Christen, M., de le Roi, M., Jagannathan, V., Becker, K., & Leeb, T. (2021). Myo5a frameshift variant in a miniature dachshund with coat color dilution and neurological defects resembling human griscelli syndrome type 1. *Genes*, *12*, 1479.

Comba, A., Dunn, P. J., Argento, A. E., Kadiyala, P., Ventosa, M., Patel, P., & Lowenstein, P. R. (2020). Fyn tyrosine kinase, a downstream target of receptor tyrosine kinases, modulates antiglioma immune responses. *Neuro-oncology*, *22*, 806-818.

Crowley, J. J., McGee, M., Kenny, D. A., Crews Jr, D. H., Evans, R. D., & Berry, D. P. (2010). Phenotypic and genetic parameters for different measures of feed efficiency in

different breeds of Irish performance-tested beef bulls. *Journal of Animal Science*, *88*, 885-894.

Curik, I., Ferenčaković, M., & Sölkner, J. (2014). Inbreeding and runs of homozygosity: A possible solution to an old problem. *Livestock Science*, *166*, 26-34.

D'Orlando, O., Zhao, F., Kasper, B., Orinska, Z., Müller, J., Hermans-Borgmeyer, I., & Bulfone-Paus, S. (2013). Syntaxin 11 is required for NK and CD8+ T-cell cytotoxicity and neutrophil degranulation. *European journal of immunology*, *43*, 194-208.

Dai, S., Liu, M., Liu, M., Jiang, C., Yang, Y., Han, H., & Shen, Y. (2023). Population-based genetic analysis in infertile men reveals novel mutations of ADAD family members in patients with impaired spermatogenesis. *Human Molecular Genetics*, *32*, 1814-1825.

Davoudi, P., Do, D., Colombo, S. M., Rathgeber, B., Hu, G., Sargolzaei, M., & Miar, Y. (2022a). Genetic and phenotypic parameters for feed efficiency and component traits in American mink. *Journal of Animal Science*, *100*, skac216.

Davoudi, P., Do, D. N., Colombo, S. M., Rathgeber, B., & Miar, Y. (2022b). Application of Genetic, Genomic and Biological Pathways in Improvement of Swine Feed Efficiency. *Frontiers in Genetics*, *13*, 903733.

Davoudi, P., Do, D. N., Rathgeber, B., Colombo, S. M., Sargolzaei, M., Plastow, G., & Miar, Y. (2022c). Genome-wide detection of copy number variation in American mink using whole-genome sequencing. *BMC Genomics*, *23*(1), 649.

De Las Heras-Saldana, S., Lopez, B. I., Moghaddar, N., Park, W., Park, J. E., Chung, K. Y., ... & van Der Werf, J. H. (2020). Use of gene expression and whole-genome sequence information to improve the accuracy of genomic prediction for carcass traits in Hanwoo cattle. *Genetics Selection Evolution*, *52*, 1-16.

Deb-Choudhury, S. (2018). Crosslinking between trichocyte keratins and keratin associated proteins. *The Hair Fibre: Proteins, Structure and Development*, 173-183.

Deepa, S. S., & Dong, L. Q. (2009). APPL1: role in adiponectin signaling and beyond. *American Journal of Physiology-Endocrinology and Metabolism*, *296*, 22-36.

Ding, R., Yang, M., Wang, X., Quan, J., Zhuang, Z., Zhou, S., & Wu, Z. (2018). Genetic architecture of feeding behavior and feed efficiency in a Duroc pig population. *Frontiers in Genetics*, *9*, 220.

Ding, H., Zhao, H., Cheng, G., Yang, Y., Wang, X., Zhao, X., & Huang, D. (2019). Analyses of histological and transcriptome differences in the skin of short-hair and long-hair rabbits. *BMC Genomics*, *20*, 1-12.

Ding, R., Zhuang, Z., Qiu, Y., Wang, X., Wu, J., Zhou, S., & Yang, J. (2022). A composite strategy of genome-wide association study and copy number variation analysis for carcass traits in a Duroc pig population. *BMC genomics*, *23*, 1-16.

Diskin, S. J., Li, M., Hou, C., Yang, S., Glessner, J., Hakonarson, H., & Wang, K. (2008). Adjustment of genomic waves in signal intensities from whole-genome SNP genotyping platforms. *Nucleic Acids Research*, *36*, 126.

Dlamini, N. M., Dzomba, E. F., Magawana, M., Ngcamu, S., & Muchadeyi, F. C. (2022). Linkage disequilibrium, haplotype block structures, effective population size and genome-wide signatures of selection of two conservation herds of the south African nguni cattle. *Animals*, *12*, 2133.

Do, D. N., Strathe, A. B., Jensen, J., Mark, T., & Kadarmideen, H. N. (2013). Genetic parameters for different measures of feed efficiency and related traits in boars of three pig breeds. *Journal of Animal Science*, *91*, 4069-4079.

Do, D. N., Hu, G., Salek Ardestani, S., & Miar, Y. (2021a). Genetic and phenotypic parameters for body weights, harvest length, and growth curve parameters in American mink. *Journal of Animal Science*, *99*, skab049.

Do, D. N., Karimi, K., Hu, G., & Miar, Y. (2022). Candidate genes related to signatures of selection for body weight and harvest length in American mink. In *Proceedings of 12th World Congress on Genetics Applied to Livestock Production (WCGALP),* 837-840.

Do, D. N., Ostersen, T., Strathe, A. B., Mark, T., Jensen, J., & Kadarmideen, H. N. (2014). Genome-wide association and systems genetic analyses of residual feed intake, daily feed consumption, backfat and weight gain in pigs. *BMC Genetics*, *15*, 1-15.

Dong, L., Li, Y., Cao, J., Liu, F., Pier, E., Chen, J., & Cui, R. (2012). FGF2 regulates melanocytes viability through the STAT3-transactivated PAX3 transcription. *Cell Death & Differentiation*, *19*, 616-622.

Dong, S., Hou, B., Yang, C., Li, Y., Sun, B., Guo, Y., & Liu, G. (2023). Comparative Hypothalamic Transcriptome Analysis Reveals Crucial mRNAs, lncRNAs, and circRNAs Affecting Litter Size in Goats. *Genes*, *14*, 444.

Drouilhet, L., Gilbert, H., Balmisse, E., Ruesche, J., Tircazes, A., Larzul, C., & Garreau, H. (2013). Genetic parameters for two selection criteria for feed efficiency in rabbits. *Journal of Animal Science*, *91*, 3121-3128.

Dzomba, E. F., Van Der Nest, M. A., Mthembu, J. N. T., Soma, P., Snyman, M. A., Chimonyo, M., & Muchadeyi, F. C. (2023). Selection signature analysis and genome-wide divergence of South African Merino breeds from their founders. *Frontiers in Genetics*, *13*, 932272.

Emerson, K. J., Bradshaw, W. E., & Holzapfel, C. M. (2008). Concordance of the circadian clock with the environment is necessary to maximize fitness in natural populations. *Evolution*, *62*, 979-983.

Endo, C., Johnson, T. A., Morino, R., Nakazono, K., Kamitsuji, S., Akita, M., & Kawashima, M. (2018). Genome-wide association study in Japanese females identifies fifteen novel skin-related trait associations. *Scientific Reports*, *8*, 8974.

Enserink, M. (2020). Coronavirus rips through Dutch mink farms, triggering culls. *Science*, *368*, 1169.

Eriksson, S., Strandberg, E., & Johansson, A. M. (2023). Changes in genomic inbreeding and diversity over half a century in Swedish Red and Swedish Holstein dairy cattle. *Journal of Animal Breeding and Genetics*, *140*, 295-303.

Esfandyari, H., & Jensen, J. (2021). Simultaneous Bayesian estimation of genetic parameters for curves of weight, feed intake, and residual feed intake in beef cattle. *Journal of Animal Science*, *99*, skab231.

Estrada-Reyes, Z. M., Ogunade, I. M., Pech-Cervantes, A. A., & Terrill, T. H. (2022). Copy number variant-based genome wide association study reveals immune-related genes associated with parasite resistance in a heritage sheep breed from the United States. *Parasite Immunology*, *44*, e12943.

Falchi, L., Cesarani, A., Mastrangelo, S., Senczuk, G., Portolano, B., Pilla, F., & Macciotta, N. P. (2023). Analysis of runs of homozygosity of cattle living in different climate zones. *Journal of Animal Science*, *101*, skad061.

Falker-Gieske, C., Blaj, I., Preuß, S., Bennewitz, J., Thaller, G., & Tetens, J. (2019). GWAS for meat and carcass traits using imputed sequence level genotypes in pooled F2-designs in pigs. *G3: Genes, Genomes, Genetics*, *9*, 2823-2834.

Farid, A. H., Daftarian, P. M., & Fatehi, J. (2018). Transmission dynamics of Aleutian mink disease virus on a farm under test and removal scheme. *Journal of Veterinary Science & Medical Diagnosis*, *7*, 2-10.

Farid, A. H., Zillig, M. L., Finley, G. G., & Smith, G. C. (2012). Prevalence of the Aleutian mink disease virus infection in Nova Scotia, Canada. *Preventive Veterinary Medicine*, *106*, 332-338.

Farid, A. H., Hussain, I., Rupasinghe, P. P., Stephen, J., & Arju, I. (2022). Long-term antibody production and viremia in American mink (*Neovison vison*) challenged with Aleutian mink disease virus. *BMC Veterinary Research*, *18*, 364.

Feng, Z., Li, X., Cheng, J., Jiang, R., Huang, R., Wang, D., ... & Chen, H. (2020). Copy number variation of the PIGY gene in sheep and its association analysis with growth traits. *Animals*, *10*(4), 688.

Fernandes, A. C., da Silva, V. H., Goes, C. P., Moreira, G. C. M., Godoy, T. F., Ibelli, A. M. G., & Coutinho, L. L. (2021). Genome-wide detection of CNVs and their association with performance traits in broilers. *BMC Genomics*, *22*, 1-18.

Feske, S., Picard, C., & Fischer, A. (2010). Immunodeficiency due to mutations in ORAI1 and STIM1. *Clinical Immunology*, *135*, 169-182.

Fontanesi, L., Schiavo, G., Galimberti, G., Calò, D. G., & Russo, V. (2014). A genomewide association study for average daily gain in Italian Large White pigs. *Journal of Animal Science*, *92*, 1385-1394.

Fontanesi, L., Scotti, E., Dall'Olio, S., Oulmouden, A., & Russo, V. (2012). Identification and analysis of single nucleotide polymorphisms in the myosin VA (MYO5A) gene and its exclusion as the causative gene of the dilute coat colour locus in rabbit. *World Rabbit Science*, *20*, 35-41.

Fontanesi, L., Martelli, P. L., Scotti, E., Russo, V., Rogel-Gaillard, C., Casadio, R., & Vernesi, C. (2012). Exploring copy number variation in the rabbit (Oryctolagus cuniculus) genome by array comparative genome hybridization. *Genomics*, *100*, 245-251.

Foroutan, A., Devos, J., Wishart, D. S., Li, C., Colazo, M., Kastelic, J., & Fitzsimmons, C. (2021). Impact of prenatal maternal nutrition and parental residual feed intake (RFI) on mRNA abundance of metabolic drivers of growth and development in young Angus bulls. *Livestock Science*, *243*, 104365.

Fortes, M. R. S., Lehnert, S. A., Bolormaa, S., Reich, C., Fordyce, G., Corbet, N. J., & Reverter, A. (2012). Finding genes for economically important traits: Brahman cattle puberty. *Animal Production Science*, *52*, 143-150.

Frischknecht, M., Flury, C., Leeb, T., Rieder, S., & Neuditschko, M. (2016). Selection signatures in Shetland ponies. *Animal Genetics*, *47*, 370-372.

Fu, L., Jiang, Y., Wang, C., Mei, M., Zhou, Z., Jiang, Y., & Ding, X. (2020). A genome-wide association study on feed efficiency related traits in landrace pigs. *Frontiers in Genetics*, *11*, 692.

Furumai, R., Tamada, K., Liu, X., & Takumi, T. (2019). UBE3A regulates the transcription of IRF, an antiviral immunity. *Human Molecular Genetics*, *28*, 1947-1958.

Gaines, A. M., Peterson, B. A., & Mendoza, O. F. (2012). Herd management factors that influence whole herd feed efficiency. In *Feed Efficiency in Swine,* 15-39.

Gao, T., Han, Y., Yu, L., Ao, S., Li, Z., & Ji, J. (2014). CCNA2 is a prognostic biomarker for ER+ breast cancer and tamoxifen resistance. *PloS One*, *9*, e91771.

Garrick, D. J. (2017). The role of genomics in pig improvement. *Animal Production Science*, *57*, 2360-2365.

Garrick, D. J., Taylor, J. F., & Fernando, R. L. (2009). Deregressing estimated breeding values and weighting information for genomic regression analyses. *Genetics Selection Evolution*, *41*, 1-8.

Geistlinger, L., da Silva, V. H., Cesar, A. S. M., Tizioto, P. C., Waldron, L., Zimmer, R., & Coutinho, L. L. (2018). Widespread modulation of gene expression by copy number variation in skeletal muscle. *Scientific Reports*, *8*, 1399.

Genova, F., Longeri, M., Lyons, L. A., Bagnato, A., & Strillacci, M. G. (2018). First genome-wide CNV mapping in FELIS CATUS using next generation sequencing data. *BMC Genomics*, *19*, 1-13.

Georges, M., Nielsen, D., Mackinnon, M., Mishra, A., Okimoto, R., Pasquino, A. T., & Zhao, X. (1995). Mapping quantitative trait loci controlling milk production in dairy cattle by exploiting progeny testing. *Genetics*, *139*, 907-920.

Gezan, S., de Oliveira, A., & Murray, D. (2021). ASRgenomics: an R package with complementary genomic functions. *VSN International, Hemel Hempstead*.

Ghafouri-Kesbi, F., Abbasi, M. A., Afraz, F., Babaei, M., Baneh, H., & Abdollahi Arpanahi, R. (2011). Genetic analysis of growth rate and Kleiber ratio in Zandi sheep. *Tropical Animal Health and Production*, *43*, 1153-1159.

Ghosh, S., Qu, Z., Das, P. J., Fang, E., Juras, R., Cothran, E. G., & Raudsepp, T. (2014). Copy number variation in the horse genome. *PLoS Genetics*, *10*, e1004712.

Ghoreishifar, M., Vahedi, S. M., Salek Ardestani, S., Khansefid, M., & Pryce, J. E. (2023). Genome-wide assessment and mapping of inbreeding depression identifies candidate genes associated with semen traits in Holstein bulls. *BMC Genomics*, *24*, 1-11.

Ghoreishifar, S. M., Moradi-Shahrbabak, H., Fallahi, M. H., Jalil Sarghale, A., Moradi-Shahrbabak, M., Abdollahi-Arpanahi, R., & Khansefid, M. (2020). Genomic measures of inbreeding coefficients and genome-wide scan for runs of homozygosity islands in Iranian river buffalo, Bubalus bubalis. *BMC Genetics*, *21*, 1-12.

Ghoreishifar, S. M., Moradi-Shahrbabak, H., Parna, N., Davoudi, P., & Khansefid, M. (2019). Linkage disequilibrium and within-breed genetic diversity in Iranian Zandi sheep. *Archives Animal Breeding*, *62*, 143-151.

Gilbert, H., Billon, Y., Brossard, L., Faure, J., Gatellier, P., Gondret, F., & Noblet, J. (2017). Divergent selection for residual feed intake in the growing pig. *Animal*, *11*, 1427-1439.

Giuffra, E., Törnsten, A., Marklund, S., Bongcam-Rudloff, E., Chardon, P., Kijas, J. M., & Andersson, L. (2002). A large duplication associated with dominant white color in pigs

originated by homologous recombination between LINE elements flanking KIT. *Mammalian Genome*, *13*, 569-577.

Glessner, J. T., Li, J., & Hakonarson, H. (2013). ParseCNV integrative copy number variation association software with quality tracking. *Nucleic Acids Research*, *41*, 64.

Glessner, J. T., Li, J., Liu, Y., Khan, M., Chang, X., Sleiman, P. M., & Hakonarson, H. (2023). ParseCNV2: efficient sequencing tool for copy number variation genome-wide association studies. *European Journal of Human Genetics*, *31*, 304-312.

Gokhin, D. S., & Fowler, V. M. (2011). Tropomodulin capping of actin filaments in striated muscle development and physiology. *Journal of Biomedicine and Biotechnology*, *2011*.

Gomez, T. S., McCarney, S. D., Carrizosa, E., Labno, C. M., Comiskey, E. O., Nolz, J. C., & Burkhardt, J. K. (2006). HS1 functions as an essential actin-regulatory adaptor protein at the immune synapse. *Immunity*, *24*, 741-752.

Gorssen, W., Meyermans, R., Janssens, S., & Buys, N. (2021). A publicly available repository of ROH islands reveals signatures of selection in different livestock and pet species. *Genetics Selection Evolution*, *53*, 1-10.

Goshu, H. A., Chu, M., & Yan, P. (2018). Applications of genomic copy number variations on livestock: A review. *African Journal of Biotechnology*, *17*, 1313-1323.

Granholm, D. E., Reese, R. N., & Granholm, N. H. (1996). Agouti alleles alter cysteine and glutathione concentrations in hair follicles and serum of mice (Ay/a, AwJ/AwJ, and a/a). *Journal of Investigative Dermatology*, *106*, 559-563.

Griffin, D. K., Robertson, L. B., Tempest, H. G., Vignal, A., Fillon, V., Crooijmans, R. P., & Burt, D. W. (2008). Whole genome comparative studies between chicken and turkey and their implications for avian genome evolution. *BMC genomics*, *9*, 1-16.

Griffin, D., Liu, X., Pru, C., Pru, J. K., & Peluso, J. J. (2014). Expression of progesterone receptor membrane component-2 within the immature rat ovary and its role in regulating mitosis and apoptosis of spontaneously immortalized granulosa cells. *Biology of Reproduction*, *91*, 36-1.

Grigoletto, L., Brito, L. F., Mattos, E. C., Eler, J. P., Bussiman, F. O., Silva, B. D. C. A., & Ferraz, J. B. S. (2019). Genome-wide associations and detection of candidate genes for direct and maternal genetic effects influencing growth traits in the Montana Tropical® Composite population. *Livestock Science*, *229*, 64-76.

Grunewald, M. E., Chen, Y., Kuny, C., Maejima, T., Lease, R., Ferraris, D., & Fehr, A. R. (2019). The coronavirus macrodomain is required to prevent PARP-mediated inhibition of virus replication and enhancement of IFN expression. *PLoS Pathogens*, *15*, e1007756.

Gu, X., Feng, C., Ma, L., Song, C., Wang, Y., Da, Y., & Li, N. (2011). Genome-wide association study of body weight in chicken F2 resource population. *PloS One*, *6*, e21872.

Guan, D., Castelló, A., Luigi-Sierra, M. G., Landi, V., Delgado, J. V., Martínez, A., & Amills, M. (2021). Estimating the copy number of the agouti signaling protein (ASIP) gene in goat breeds with different color patterns. *Livestock Science*, *246*, 104440.

Yu, G. (2021). Enrichplot: visualization of functional enrichment result. *R package version*, *1*.

Gudbjartsson, D. F., Walters, G. B., Thorleifsson, G., Stefansson, H., Halldorsson, B. V., Zusmanovich, P., & Stefansson, K. (2008). Many sequence variants affecting diversity of adult human height. *Nature Genetics*, *40*, 609-615.

Gunsett, F. C. (1984). Linear index selection to improve traits defined as ratios. *Journal of Animal Science*, *59*, 1185-1193.Guo, Y. M., Zhang, Z. Y., Ma, J. W., Ai, H. S., Ren, J., & Huang, L. S. (2015). A genomewide association study of feed efficiency and feeding behaviors at two fattening stages in a white duroc× erhualian F2 population. *Journal of Animal Science*, *93*, 1481-1489.

Guo, J., Tao, H., Li, P., Li, L. I., Zhong, T., Wang, L., & Zhang, H. (2018). Whole-genome sequencing reveals selection signatures associated with important traits in six goat breeds. *Scientific Reports*, *8*, 10405.

Guo, J., Zhong, J., Liu, G. E., Yang, L., Li, L., Chen, G., & Zhang, H. (2020). Identification and population genetic analyses of copy number variations in six domestic goat breeds and Bezoar ibexes using next-generation sequencing. *BMC Genomics*, *21*, 1-13.

Han, J., Kraft, P., Nan, H., Guo, Q., Chen, C., Qureshi, A., & Hunter, D. J. (2008). A genome-wide association study identifies novel alleles associated with hair color and skin pigmentation. *PLoS Genetics*, *4*, e1000074.

Han, H., Randhawa, I. A., MacHugh, D. E., McGivney, B. A., Katz, L. M., Dugarjaviin, M., & Hill, E. W. (2023). Selection signatures for local and regional adaptation in Chinese Mongolian horse breeds reveal candidate genes for hoof health. *BMC Genomics*, *24*, 1-11.

Han, J., Kraft, P., Nan, H., Guo, Q., Chen, C., Qureshi, A., & Hunter, D. J. (2008). A genome-wide association study identifies novel alleles associated with hair color and skin pigmentation. *PLoS Genetics*, *4*, e1000074.

Hansen, B. K., & Berg, P. (2008). Reduced litter size and percent kits alive is a consequence of selecting for high body weight. *Scientifur*, *32*, 15.

Hansen, B. K., Su, G., & Berg, P. (2010). Genetic variation in litter size and kit survival of mink (Neovison vison). *Journal of Animal Breeding and Genetics*, *127*, 442-451.

Hartwig, J., Loebel, M., Steiner, S., Bauer, S., Karadeniz, Z., Roeger, C., & Sotzny, F. (2021). Metformin attenuates ROS via FOXO3 activation in immune cells. *Frontiers in Immunology*, *12*, 581799.

Hay, E. H. A., Utsunomiya, Y. T., Xu, L., Zhou, Y., Neves, H. H., Carvalheiro, R., & Liu, G. E. (2018). Genomic predictions combining SNP markers and copy number variations in Nellore cattle. *BMC Genomics*, *19*, 1-8.

He, X., Li, H., Zhou, Z., Zhao, Z., & Li, W. (2012). Production of brown/yellow patches in the SLC7A11 transgenic sheep via testicular injection of transgene. *Journal of Genetics and Genomics*, *39*, 281-285.

He, Z., Liu, R., Wang, M., Wang, Q., Zheng, J., Ding, J., & Zhao, G. (2023). Combined effect of microbially derived cecal SCFA and host genetics on feed efficiency in broiler chickens. *Microbiome*, *11*, 1-17.

Heimsath Jr, E. G., Yim, Y. I., Mustapha, M., Hammer, J. A., & Cheney, R. E. (2017). Myosin-X knockout is semi-lethal and demonstrates that myosin-X functions in neural tube closure, pigmentation, hyaloid vasculature regression, and filopodia formation. *Scientific Reports*, *7*, 17354.

Held, T., Paprotta, I., Khulan, J., Hemmerlein, B., Binder, L., Wolf, S., & Adham, I. M. (2006). Hspa4l-deficient mice display increased incidence of male infertility and hydronephrosis development. *Molecular and Cellular Biology*, *26*, 8099-8108.

Henrichsen, C. N., Chaignat, E., & Reymond, A. (2009). Copy number variants, diseases and gene expression. *Human Molecular Genetics*, *18*, 1-8.

Herd, R. M., Archer, J. A., & Arthur, P. F. (2003). Reducing the cost of beef production through genetic improvement in residual feed intake: Opportunity and challenges to application. *Journal of Animal Science*, *81*, 9-17.

Higgins, M. G., Fitzsimons, C., McClure, M. C., McKenna, C., Conroy, S., Kenny, D. A., & Morris, D. W. (2018). GWAS and eQTL analysis identifies a SNP associated with both residual feed intake and GFRA2 expression in beef cattle. *Scientific Reports*, *8*, 14301.

Hirobe, T. (2011). How are proliferation and differentiation of melanocytes regulated?. *Pigment Cell & Melanoma Research*, *24*, 462-478.

Hirschhorn, J. N., & Daly, M. J. (2005). Genome-wide association studies for common diseases and complex traits. *Nature Reviews Genetics*, *6*, 95-108.

Holzer, U., Reinhardt, K., Lang, P., Handgretinger, R., & Fischer, N. (2013). Influence of a mutation in IFN-γ receptor 2 (IFNGR2) in human cells on the generation of Th17 cells in memory T cells. *Human Immunology*, *74*, 693-700.

Hong, J. K., Lee, J. B., Ramayo-Caldas, Y., Kim, S. D., Cho, E. S., Kim, Y. S., ... & Park, H. B. (2020a). Single-step genome-wide association study for social genetic effects and direct genetic effects on growth in Landrace pigs. *Scientific Reports*, *10*, 14958.

Hong, R., Wang, Y., Dong, H., & Geng, R. (2020b). DTX3L/ARTD9 contributes to inflammation of fibroblast-like synoviocytes by increasing STAT1 translocation. *Tissue and Cell*, *64*, 101339.

Hong, J. K., Cho, K. H., Kim, Y. S., Chung, H. J., Baek, S. Y., Cho, E. S., & Sa, S. J. (2021). Genetic relationship between purebred and synthetic pigs for growth performance using single step method. *Animal Bioscience*, *34*, 967.

Hoopes, B. C., Rimbault, M., Liebers, D., Ostrander, E. A., & Sutter, N. B. (2012). The insulin-like growth factor 1 receptor (IGF1R) contributes to reduced size in dogs. *Mammalian Genome*, *23*, 780-790.

Hoque, M. A., & Suzuki, K. (2009). Genetics of residual feed intake in cattle and pigs: A review. *Asian-Australasian Journal of Animal Sciences*, *22*, 747-755.

Howrigan, D. P., Simonson, M. A., & Keller, M. C. (2011). Detecting autozygosity through runs of homozygosity: a comparison of three autozygosity detection algorithms. *BMC Genomics*, *12*, 1-15.

Hu, Y., Xia, H., Li, M., Xu, C., Ye, X., Su, R., & Zhou, Y. (2020). Comparative analyses of copy number variations between Bos taurus and Bos indicus. *BMC Genomics*, *21*, 1-11.

Hu, G., Do, D. N., Davoudi, P., Manafiazar, G., Kelvin, A. A., Plastow, G., & Miar, Y. (2022). Genetic and phenotypic correlations between Aleutian disease tests with body weight, growth, and feed efficiency traits in mink. *Journal of Animal Science*, *100*, skac346.

Hu, G., Do, D. N., Karimi, K., & Miar, Y. (2021). Genetic and phenotypic parameters for Aleutian disease tests and their correlations with pelt quality, reproductive performance, packed-cell volume, and harvest length in mink. *Journal of Animal Science*, *99*, skab216.

Hu, G., Do, D. N., Manafiazar, G., Kelvin, A. A., Sargolzaei, M., Plastow, G., & Miar, Y. (2023). Population genomics of American mink using genotype data. *Frontiers in Genetics*, *14*, 1175408.

Hu, J., Zhang, W., Xu, L., & Hu, L. (2022). JAK2 gene knockout inhibits corneal allograft rejection in mice by regulating dendritic cell-induced T cell immune tolerance. *Cell Death Discovery*, *8*, 289.

Huang, N., Zhao, L., Wang, J., Jiang, Q., Ju, Z., Wang, X., & Huang, J. (2023). Signatures of selection in indigenous Chinese cattle genomes reveal adaptive genes and genetic variations to cold climate. *Journal of Animal Science*, *101*, skad006.

Huang, X., Zhou, Y., Sun, Y., & Wang, Q. (2022). Intestinal fatty acid binding protein: A rising therapeutic target in lipid metabolism. *Progress in Lipid Research*, 101178.

Ibrahim, S., Al-Sharif, M., Younis, F., Ateya, A., Abdo, M., & Fericean, L. (2023). Analysis of Potential Genes and Economic Parameters Associated with Growth and Heat Tolerance in Sheep (Ovis aries). *Animals*, *13*, 353.

Ito, S., & Wakamatsu, K. (2003). Quantitative analysis of eumelanin and pheomelanin in humans, mice, and other animals: a comparative review. *Pigment Cell Research*, *16*, 523-531.

Islam, R., Liu, X., Gebreselassie, G., Abied, A., Ma, Q., & Ma, Y. (2020). Genome-wide association analysis reveals the genetic locus for high reproduction trait in Chinese Arbas Cashmere goat. *Genes & Genomics*, *42*, 893-899.

Ivell, R., & Grutzner, F. (2009). Evolution and male fertility: lessons from the insulin-like factor 6 gene (Insl6). *Endocrinology*, *150*, 3986–3990.

Jallageas, M., & Mas, N. (1996). Balance between opposite effects of short day stimulation and testicular steroid feedback inhibition on pituitary pulsatile LH release in male mink, Mustela vison. *Comparative Biochemistry and Physiology Part C: Pharmacology, Toxicology and Endocrinology*, *115*, 27-32.

Jeffares, D. C., Jolly, C., Hoti, M., Speed, D., Shaw, L., Rallis, C., & Sedlazeck, F. J. (2017). Transient structural variations have strong effects on quantitative traits and reproductive isolation in fission yeast. *Nature Communications*, *8*, 14061.

Jepsen, J. R., d'Amore, F., Baandrup, U., Clausen, M. R., Gottschalck, E., & Aasted, B. (2009). Aleutian mink disease virus and humans. *Emerging Infectious Diseases*, *15*, 2040.

Jiang, Y., Li, X., Liu, J., Zhang, W., Zhou, M., Wang, J., & Wang, C. (2022). Genome-wide detection of genetic structure and runs of homozygosity analysis in Anhui indigenous and Western commercial pig breeds using PorcineSNP80k data. *BMC Genomics*, *23*, 373.

Jiao, S., Maltecca, C., Gray, K. A., & Cassady, J. P. (2014). Feed intake, average daily gain, feed efficiency, and real-time ultrasound traits in Duroc pigs: I. Genetic parameter estimation and accuracy of genomic prediction. *Journal of Animal Science*, *92*, 2377-2386.

Johnson, R. C., Nelson, G. W., Troyer, J. L., Lautenberger, J. A., Kessing, B. D., Winkler, C. A., & O'Brien, S. J. (2010). Accounting for multiple comparisons in a genome-wide association study (GWAS). *BMC Genomics*, *11*, 1-6.

Juszczuk-Kubiak, E., Starzyński, R. R., Wicińska, K., & Flisikowski, K. (2012). Promoter variant-dependent mRNA expression of the MEF2A in longissimus dorsi muscle in cattle. *DNA and Cell Biology*, *31*, 1131-1135.

Jyotsana, N., Ta, K. T., & DelGiorno, K. E. (2022). The role of cystine/glutamate antiporter SLC7A11/xCT in the pathophysiology of cancer. *Frontiers in Oncology*, *12*, 858462.

Ka, M., Chopra, D. A., Dravid, S. M., & Kim, W. Y. (2016). Essential roles for ARID1B in dendritic arborization and spine morphology of developing pyramidal neurons. *Journal of Neuroscience*, *36*, 2723-2742.

Kaloğlu, C., Bulut, H. E., Hamutoğlu, R., Korkmaz, E. M., Önder, O., Dağdeviren, T., & Aydemir, M. N. (2020). Wingless ligands and beta-catenin expression in the rat endometrium: The role of Wnt3 and Wnt7a/beta-catenin pathway at the embryo–uterine interface. *Molecular Reproduction and Development*, *87*, 1159-1172.

Karaköse, E., Geiger, T., Flynn, K., Lorenz-Baath, K., Zent, R., Mann, M., & Fässler, R. (2015). The focal adhesion protein PINCH-1 associates with EPLIN at integrin adhesion sites. *Journal of Cell Science*, *128*, 1023-1033.

Karimi, K., Sargolzaei, M., Plastow, G. S., Wang, Z., & Miar, Y. (2018). Genetic and phenotypic parameters for litter size, survival rate, gestation length, and litter weight traits in American mink. *Journal of Animal Science*, *96*, 2596-2606.

Karimi, K., Sargolzaei, M., Plastow, G. S., Wang, Z., & Miar, Y. (2019). Opportunities for genomic selection in American mink: A simulation study. *PLoS One*, *14*, e0213873.

Karimi, K., Farid, A. H., Sargolzaei, M., Myles, S., & Miar, Y. (2020). Linkage disequilibrium, effective population size and genomic inbreeding rates in American mink using genotyping-by-sequencing data. *Frontiers in Genetics*, *11*, 223.

Karimi, K., Farid, A. H., Myles, S., & Miar, Y. (2021a). Detection of selection signatures for response to Aleutian mink disease virus infection in American mink. *Scientific Reports*, *11*, 2944.

Karimi, K., Ngoc Do, D., Sargolzaei, M., & Miar, Y. (2021b). Population genomics of American mink using whole genome sequencing data. *Genes*, *12*, 258.

Karimi, K., Do, D. N., Wang, J., Easley, J., Borzouie, S., Sargolzaei, M., & Miar, Y. (2022). A chromosome-level genome assembly reveals genomic characteristics of the American mink (Neogale vison). *Communications Biology*, *5*, 1381.

Karisa, B. K., Thomson, J., Wang, Z., Bruce, H. L., Plastow, G. S., & Moore, A. S. (2013). Candidate genes and biological pathways associated with carcass quality traits in beef cattle. *Canadian Journal of Animal Science*, *93*, 295-306.

Keller, M. C., Visscher, P. M., & Goddard, M. E. (2011). Quantification of inbreeding due to distant ancestors and its detection using dense single nucleotide polymorphism data. *Genetics*, *189*, 237-249.

Keel, B. N., Nonneman, D. J., Lindholm-Perry, A. K., Oliver, W. T., & Rohrer, G. A. (2019). A survey of copy number variation in the porcine genome detected from whole-genome sequence. *Frontiers in Genetics*, *10*, 737.

Kempe, R., Koskinen, N., Mäntysaari, E., & Strandén, I. (2010). The genetics of body condition and leg weakness in the blue fox (*Alopex lagopus*). *Acta Agriculturae Scand Section A*, *60*, 141-150.

Kendall, K. M., Rees, E., Bracher-Smith, M., Legge, S., Riglin, L., Zammit, S., & Walters, J. T. R. (2019). Association of rare copy number variants with risk of depression. *JAMA Psychiatry*, *76*, 818-825.

Kennedy, B. W., Van der Werf, J. H., & Meuwissen, T. H. (1993). Genetic and statistical properties of residual feed intake. *Journal of Animal Science*, *71*, 3239-3250.

Khan, M. Z., Wang, D., Liu, L., Usman, T., Wen, H., Zhang, R., & Yu, Y. (2019). Significant genetic effects of JAK2 and DGAT1 mutations on milk fat content and mastitis resistance in Holsteins. *Journal of Dairy Research*, *86*, 388-393.

Khatri, B., Kang, S., Shouse, S., Anthony, N., Kuenzel, W., & Kong, B. C. (2019). Copy number variation study in Japanese quail associated with stress related traits using whole genome re-sequencing data. *Plos One*, *14*, e0214543.

Kishimoto, J., Burgeson, R. E., & Morgan, B. A. (2000). Wnt signaling maintains the hair-inducing activity of the dermal papilla. *Genes & Development*, *14*, 1181-1185.

Kleiber, M. (1947). Body size and metabolic rate. *Physiological Reviews*, *27*, 511-541.

Koch, R. M., Swiger, L. A., Chambers, D., & Gregory, K. E. (1963). Efficiency of feed use in beef cattle. *Journal of Animal Science*, *22*, 486-494.

Knowles, H., Heizer, J. W., Li, Y., Chapman, K., Ogden, C. A., Andreasen, K., & Perraud, A. L. (2011). Transient Receptor Potential Melastatin 2 (TRPM2) ion channel is required for innate immunity against Listeria monocytogenes. *Proceedings of the National Academy of Sciences*, *108*, 11578-11583.

Kohl, M., Wiese, S., & Warscheid, B. (2011). Cytoscape: software for visualization and analysis of biological networks. *Data Mining in Proteomics: From Standards to Applications*, 291-303.

Koivula, M., Strandén, I., & Mäntysaari, E. A. (2010). Genetic and phenotypic parameters of age at first mating, litter size and animal size in Finnish mink. *Animal*, *4*, 183-188.

Kołodziejczyk, D., & Socha, S. (2011). Analysis of effectiveness of breeding work and estimation of genetic and phenotypic trends for reproductive traits in American mink. *Annals of Animal Science*, *11*, 273-282.

Kong, R. S., Liang, G., Chen, Y., Stothard, P., & Guan, L. L. (2016). Transcriptome profiling of the rumen epithelium of beef cattle differing in residual feed intake. *BMC Genomics*, *17*, 1-16.

Koopmans, M. (2021). SARS-CoV-2 and the human-animal interface: outbreaks on mink farms. *The Lancet Infectious Diseases*, *21*, 18-19.

Köster, E., Van der Westhuizen, J., & Erasmus, G. J. (1994). Heritability estimates for different Kleiber ratios obtained from growth performance data in a Hereford herd. *South African Journal of Animal Science*, *24*, 71-72.

Kovalevich, J., Tracy, B., & Langford, D. (2011). PINCH: More than just an adaptor protein in cellular response. *Journal of Cellular Physiology*, *226*, 940-947.

Kranis, A., Gheyas, A. A., Boschiero, C., Turner, F., Yu, L., Smith, S., & Burt, D. W. (2013). Development of a high density 600K SNP genotyping array for chicken. *BMC Genomics*, *14*, 1-13.

Kronenberg, F. (2008). Genome-wide association studies in aging-related processes such as diabetes mellitus, atherosclerosis and cancer. *Experimental Gerontology*, *43*, 39-43.

Krutskikh, A., Poliandri, A., Cabrera-Sharp, V., Dacheux, J. L., Poutanen, M., & Huhtaniemi, I. (2012). Epididymal protein Rnase10 is required for post-testicular sperm maturation and male fertility. *The FASEB Journal*, *26*, 4198.

Ku, C. S., Naidoo, N., Teo, S. M., & Pawitan, Y. (2011). Regions of homozygosity and their impact on complex diseases and traits. *Human Genetics*, *129*, 1-15.

Ku, K. E., Choi, N., & Sung, J. H. (2020). Inhibition of Rab27a and Rab27b has opposite effects on the regulation of hair cycle and hair growth. *International Journal of Molecular Sciences*, *21*, 5672.

Kuhn, R. M., Haussler, D., & Kent, W. J. (2013). The UCSC genome browser and associated tools. *Briefings in bioinformatics*, *14*, 144-161.

Kumar, C., Song, S., Dewani, P., Kumar, M., Parkash, O., Ma, Y., & Jiang, L. (2018). Population structure, genetic diversity and selection signatures within seven indigenous Pakistani goat populations. *Animal Genetics*, *49*, 592-604.

Ladeira, G. C., Pilonetto, F., Fernandes, A. C., Bóscollo, P. P., Dauria, B. D., Titto, C. G., & Mourão, G. B. (2022). CNV detection and their association with growth, efficiency and carcass traits in Santa Inês sheep. *Journal of Animal Breeding and Genetics*, *139*, 476-487.

Lagerkvist, G., Johansson, K., & Lundeheim, N. (1993). Selection for litter size, body weight, and pelt quality in mink (Mustela vison): experimental design and direct response of each trait. *Journal of Animal Science*, *71*, 3261-3272.

Lagerkvist, G., Johansson, K., & Lundeheim, N. (1993). Selection for litter size, body weight, and pelt quality in mink (Mustela vison): experimental design and direct response of each trait. *Journal of Animal Science*, *71*, 3261-3272.

Lango Allen, H., Estrada, K., Lettre, G., Berndt, S. I., Weedon, M. N., Rivadeneira, F., & Pietiläinen, K. H. (2010). Hundreds of variants clustered in genomic loci and biological pathways affect human height. *Nature*, *467*, 832-838.

Larzul, C., & De Rochambeau, H. (2005). Selection for residual feed consumption in the rabbit. *Livestock Production Science*, *95*, 67-72.

Le Goff, C., & Cormier-Daire, V. (2011). The ADAMTS (L) family and human genetic disorders. *Human Molecular Genetics*, *20*, 163-167.

Leaché, A. D., & Oaks, J. R. (2017). The utility of single nucleotide polymorphism (SNP) data in phylogenetics. *Annual Review of Ecology, Evolution, and Systematics*, *48*, 69-84.

Lee, S. H., Choi, B. H., Lim, D., Gondro, C., Cho, Y. M., Dang, C. G., & Hong, S. K. (2013). Genome-wide association study identifies major loci for carcass weight on BTA14 in Hanwoo (Korean cattle). *PloS One*, *8*, e74677.

Su, H., Wang, G., Wu, L., Ma, X., Ying, K., & Zhang, R. (2020). Transcriptome-wide map of m 6 A circRNAs identified in a rat model of hypoxia mediated pulmonary hypertension. *BMc Genomics*, *21*, 1-15.

Legate, K. R., Montañez, E., Kudlacek, O., & Füssler, R. (2006). ILK, PINCH and parvin: the tIPP of integrin signalling. *Nature reviews Molecular Cell Biology*, *7*, 20-31.

Lencz, T., Lambert, C., DeRosse, P., Burdick, K. E., Morgan, T. V., Kane, J. M., & Malhotra, A. K. (2007). Runs of homozygosity reveal highly penetrant recessive loci in schizophrenia. *Proceedings of the National Academy of Sciences*, *104*, 19942-19947.

Letaief, R., Rebours, E., Grohs, C., Meersseman, C., Fritz, S., Trouilh, L., & Boussaha, M. (2017). Identification of copy number variation in French dairy and beef breeds using next-generation sequencing. *Genetics Selection Evolution*, *49*, 1-15.

Lettre, G., Jackson, A. U., Gieger, C., Schumacher, F. R., Berndt, S. I., Sanna, S., & Hirschhorn, J. N. (2008). Identification of ten loci associated with height highlights new biological pathways in human growth. *Nature Genetics*, *40*, 584-591.

Li, C. H., Zhao, J. X., Sun, L., Yao, Z. Q., Deng, X. L., Liu, R., & Liu, X. Y. (2013). AG490 inhibits NFATc1 expression and STAT3 activation during RANKL induced osteoclastogenesis. *Biochemical and Biophysical Research Communications*, *435*, 533-539.

Li, H. (2013). Aligning sequence reads, clone sequences and assembly contigs with BWA-MEM. *ArXiv Preprint:1303.3997*.

Li, H., Handsaker, B., Wysoker, A., Fennell, T., Ruan, J., Homer, N., & 1000 Genome Project Data Processing Subgroup. (2009). The sequence alignment/map format and SAMtools. *Bioinformatics*, *25*, 2078-2079.

Li, M., Yin, C., Zhao, F., & Liu, Y. (2022). Copy number variation association studies for sheep tail-relevant traits in Hulunbuir sheep. *Animal Genetics*, *53*, 897-900.

Li, S., Xu, C., Tian, Y., Wang, X., Jiang, R., Zhang, M., & Li, W. D. (2017). TOX and ADIPOQ gene polymorphisms are associated with antipsychotic-induced weight gain in Han Chinese. *Scientific Reports*, *7*, 45203.

Li, Z., Wei, S., Li, H., Wu, K., Cai, Z., Li, D., & Zhang, L. (2017). Genome-wide genetic structure and differentially selected regions among Landrace, Erhualian, and Meishan pigs using specific-locus amplified fragment sequencing. *Scientific Reports*, *7*, 10063.

Liakath-Ali, K., Vancollie, V. E., Sequeira, I., Lelliott, C. J., & Watt, F. M. (2019). Myosin 10 is involved in murine pigmentation. *Experimental Dermatology*, *28*, 391-394.

Lin, Y. M. J., Hsin, I. L., Sun, H. S., Lin, S., Lai, Y. L., Chen, H. Y., & Wu, H. M. (2018). NTF3 is a novel target gene of the transcription factor POU3F2 and is required for neuronal differentiation. *Molecular Neurobiology*, *55*, 8403-8413.

Lin, S., Lin, X., Zhang, Z., Jiang, M., Rao, Y., Nie, Q., & Zhang, X. (2018). Copy number variation in SOX6 contributes to chicken muscle development. *Genes*, *9*, 42.

Lin, W. H., Xiang, L. J., Shi, H. X., Zhang, J., Jiang, L. P., Cai, P. T., & Xiao, J. (2015). Fibroblast growth factors stimulate hair growth through β-catenin and Shh expression in C57BL/6 mice. *BioMed Research International*, *2015*.

Lindholm-Perry, A. K., Meyer, A. M., Kern-Lunbery, R. J., Cunningham-Hollinger, H. C., Funk, T. H., & Keel, B. N. (2022). Genes involved in feed efficiency identified in a meta-analysis of rumen tissue from two populations of beef steers. *Animals*, *12*, 1514.

Liu, C., Ran, X., Yu, C., Xu, Q., Niu, X., Zhao, P., & Wang, J. (2019a). Whole-genome analysis of structural variations between Xiang pigs with larger litter sizes and those with smaller litter sizes. *Genomics*, *111*, 310-319.

Liu, H., Luo, Q., Zhang, J., Mo, C., Wang, Y., & Li, J. (2019b). Endothelins (EDN1, EDN2, EDN3) and their receptors (EDNRA, EDNRB, EDNRB2) in chickens: Functional analysis and tissue distribution. *General and Comparative Endocrinology*, *283*, 113231.

Liu, M., Fang, L., Liu, S., Pan, M. G., Seroussi, E., Cole, J. B., & Liu, G. E. (2019c). Array CGH-based detection of CNV regions and their potential association with reproduction and other economic traits in Holsteins. *BMC Genomics*, *20*(1), 1-10.

Liu, M., Zhou, Y., Rosen, B. D., Van Tassell, C. P., Stella, A., Tosser-Klopp, G., & ADAPTmap Consortium. (2019). Diversity of copy number variation in the worldwide goat population. *Heredity*, *122*, 636-646.

Liu, S. H., Ma, X. Y., Hassan, F. U., Gao, T. Y., & Deng, T. X. (2022). Genome-wide analysis of runs of homozygosity in Italian Mediterranean buffalo. *Journal of Dairy Science*, *105*, 4324-4334.

Liu, X., Wang, X., & Liu, F. (2019). Decreased expression of heat shock protein A4L in spermatozoa is positively related to poor human sperm quality. *Molecular Reproduction and Development*, *86*, 379-386.

Liu, Y., Liang, W. B., Gao, L. B., Pan, X. M., Chen, T. Y., Wang, Y. Y., & Zhang, L. (2010). CTLA4 and CD86 gene polymorphisms and susceptibility to chronic obstructive pulmonary disease. *Human Immunology*, *71*, 1141-1146.

Liu, G. E., & Bickhart, D. M. (2012). Copy number variation in the cattle genome. *Functional & Integrative Genomics*, *12*, 609-624.

Liu, Y., Zhao, Y., Wu, R., Chen, Y., Chen, W., Liu, Y., & Wang, X. (2021). mRNA m5C controls adipogenesis by promoting CDKN1A mRNA export and translation. *RNA Biology*, *18*, 711-721.

Liu, Z. Y., Liu, L. L., Song, X. C., Cong, B., & Yang, F. H. (2017). Heritability and genetic trends for growth and fur quality traits in silver blue mink. *Italian Journal of Animal Science*, *16*, 39-43.

Liu, M., Woodward-Greene, J., Kang, X., Pan, M. G., Rosen, B., Van Tassell, C. P., & Liu, G. E. (2020). Genome-wide CNV analysis revealed variants associated with growth traits in African indigenous goats. *Genomics*, *112*, 1477-1480.

Lo, P. K., Yao, Y., Lee, J. S., Zhang, Y., Huang, W., Kane, M. A., & Zhou, Q. (2018). LIPG signaling promotes tumor initiation and metastasis of human basal-like triple-negative breast cancer. *Elife*, *7*, e31334.

Lok, S., Johnston, D. S., Conklin, D., Lofton-Day, C. E., Adams, R. L., Jelmberg, A. C., & Jaspers, S. R. (2000). Identification of INSL6, a new member of the insulin family that is expressed in the testis of the human and rat. *Biology of Reproduction*, *62*, 1593-1599.

Locke, M. E. O., Milojevic, M., Eitutis, S. T., Patel, N., Wishart, A. E., Daley, M., & Hill, K. A. (2015). Genomic copy number variation in Mus musculus. *BMC Genomics*, *16*, 1-19.

Long, J. Z., & Cravatt, B. F. (2011). The metabolic serine hydrolases and their functions in mammalian physiology and disease. *Chemical Reviews*, *111*, 6022-6063.

Long, J., Delahanty, R. J., Li, G., Gao, Y. T., Lu, W., Cai, Q., & Zheng, W. (2013). A common deletion in the APOBEC3 genes and breast cancer risk. *Journal of the National Cancer Institute*, *105*, 573-579.

Lopes F. (2017) DRP R Package. In: *Availabe online: https://github.com/camult/DRP*

Lorenz, K., Grashoff, C., Torka, R., Sakai, T., Langbein, L., Bloch, W., & Fässler, R. (2007). Integrin-linked kinase is required for epidermal and hair follicle morphogenesis. *The Journal of Cell Biology*, *177*, 501-513.

Lu, D., Jiao, S., Tiezzi, F., Knauer, M., Huang, Y., Gray, K. A., & Maltecca, C. (2017). The relationship between different measures of feed efficiency and feeding behavior traits in Duroc pigs. *Journal of Animal Science*, *95*, 3370-3380.

Lu, Y., Vandehaar, M. J., Spurlock, D. M., Weigel, K. A., Armentano, L. E., Staples, C. R., & Tempelman, R. J. (2015). An alternative approach to modeling genetic merit of feed efficiency in dairy cattle. *Journal of Dairy Science*, *98*, 6535-6551.

Lv, X., Chen, W., Sun, W., Hussain, Z., Wang, S., & Wang, J. (2020). Analysis of lncRNAs expression profiles in hair follicle of Hu sheep lambskin. *Animals*, *10*, 1035.

Macciotta, N. P., Colli, L., Cesarani, A., Ajmone-Marsan, P., Low, W. Y., Tearle, R., & Williams, J. L. (2021). The distribution of runs of homozygosity in the genome of river and swamp buffaloes reveals a history of adaptation, migration and crossbred events. *Genetics Selection Evolution*, *53*, 1-21.

M Madsen, M. D., Villumsen, T. M., Hansen, B. K., Møller, S. H., Jensen, J., & Shirali, M. (2020). Combined analysis of group recorded feed intake and individually recorded body weight and litter size in mink. *Animal*, *14*, 1793-1801.

Maier, V., Jolicoeur, C., Rayburn, H., Takegahara, N., Kumanogoh, A., Kikutani, H., & Friedel, R. H. (2011). Semaphorin 4C and 4G are ligands of Plexin-B2 required in cerebellar development. *Molecular and Cellular Neuroscience*, *46*, 419-431.

Manakhov, A. D., Andreeva, T. V., Trapezov, O. V., Kolchanov, N. A., & Rogaev, E. I. (2019). Genome analysis identifies the mutant genes for common industrial Silverblue and Hedlund white coat colours in American mink. *Scientific Reports*, *9*, 4581.

Mancin, E., Tuliozi, B., Pegolo, S., Sartori, C., & Mantovani, R. (2022). Genome Wide Association Study of Beef Traits in Local Alpine Breed Reveals the Diversity of the Pathways Involved and the Role of Time Stratification. *Frontiers in Genetics*, *12*, 746665.

Mandal, A., Karunakaran, M., Sharma, D. K., Baneh, H., & Rout, P. K. (2015). Variance components and genetic parameters of growth traits and Kleiber ratio in Muzaffarnagari sheep. *Small Ruminant Research*, *132*, 79-85.

Manolio, T. A., Collins, F. S., Cox, N. J., Goldstein, D. B., Hindorff, L. A., Hunter, D. J., & Visscher, P. M. (2009). Finding the missing heritability of complex diseases. *Nature*, *461*, 747-753.

Manunza, A., Diaz, J. R., Sayre, B. L., Cozzi, P., Bobbo, T., Deniskova, T., & Stella, A. (2023). Discovering novel clues of natural selection on four worldwide goat breeds. *Scientific Reports*, *13*, 2110.

Manzanilla-Pech, C. I. V., Veerkamp, R. F., Tempelman, R. J., Van Pelt, M. L., Weigel, K. A., VandeHaar, M., & De Haas, Y. (2016). Genetic parameters between feed-intake-related traits and conformation in 2 separate dairy populations—the Netherlands and United States. *Journal of Dairy Science*, *99*, 443-457.

Marchesi, J. A. P., Buzanskas, M. E., Cantão, M. E., Ibelli, A. M. G., Peixoto, J. O., Joaquim, L. B., & Ledur, M. C. (2018). Relationship of runs of homozygosity with adaptive and production traits in a paternal broiler line. *Animal*, *12*, 1126-1134.

Marioni, J. C., Thorne, N. P., Valsesia, A., Fitzgerald, T., Redon, R., Fiegler, H., & Hurles, M. E. (2007). Breaking the waves: improved detection of copy number variation from microarray-based comparative genomic hybridization. *Genome Biology*, *8*, 1-14.

Martikainen, K., Koivula, M., & Uimari, P. (2020). Identification of runs of homozygosity affecting female fertility and milk production traits in Finnish Ayrshire cattle. *Scientific Reports*, *10*, 3804.

Martinet, L., Allain, D., & Meunier, M. (1983). Regulation in pregnant mink (*Mustela vison*) of plasma progesterone and prolactin concentrations and regulation of onset of the spring moult by daylight ratio and melatonin injections. *Canadian Journal of Zoology*, *61*, 1959-1963.

Martinet, L., Mondain-Monval, M., & Monnerie, R. (1992). Endogenous circannual rhythms and photorefractoriness of testis activity, moult and prolactin concentrations in mink (Mustela vison). *Reproduction*, *95*, 325-338.

Martínez-Montes, A. M., Muiños-Bühl, A., Fernández, A., Folch, J. M., Ibáñez-Escriche, N., & Fernández, A. I. (2017). Deciphering the regulation of porcine genes influencing growth, fatness and yield-related traits through genetical genomics. *Mammalian Genome*, *28*, 130-142.

Martínez, R. (2014). Genome-wide association studies for growth traits in Colombian Creole cattle using a single-step genomic best linear unbiased prediction (gBLUP). In *Proceedings, 10th World Congress of Genetics Applied to Livestock Production* 1-3.

Martinsen, K. H., Ødegård, J., Olsen, D., & Meuwissen, T. H. E. (2015). Genetic variation in efficiency to deposit fat and lean meat in Norwegian Landrace and Duroc pigs. *Journal of Animal Science*, *93*, 3794-3800.

Mattila, P. K., & Lappalainen, P. (2008). Filopodia: molecular architecture and cellular functions. *Nature Reviews Molecular Cell Biology*, *9*, 446-454.

McFadden, K., & Minshew, N. J. (2013). Evidence for dysregulation of axonal growth and guidance in the etiology of ASD. *Frontiers in Human Neuroscience*, *7*, 671.

Mebratie, W., Reyer, H., Wimmers, K., Bovenhuis, H., & Jensen, J. (2019). Genome wide association study of body weight and feed efficiency traits in a commercial broiler chicken population, a re-visitation. *Scientific Reports*, *9*, 922.

Mehrotra, P., Hollenbeck, A., Riley, J. P., Li, F., Patel, R. J., Akhtar, N., & Goenka, S. (2013). Poly (ADP-ribose) polymerase 14 and its enzyme activity regulates TH2 differentiation and allergic airway disease. *Journal of Allergy and Clinical Immunology*, *131*, 521-531.

Ménasché, G., Ho, C. H., Sanal, O., Feldmann, J., Tezcan, I., Ersoy, F., & de Saint Basile, G. (2003). Griscelli syndrome restricted to hypopigmentation results from a melanophilin defect (GS3) or a MYO5A F-exon deletion (GS1). *The Journal of Clinical Investigation*, *112*, 450-456.

Menzi, F., Keller, I., Reber, I., Beck, J., Brenig, B., Schütz, E., & Drögemüller, C. (2016). Genomic amplification of the caprine EDNRA locus might lead to a dose dependent loss of pigmentation. *Scientific Reports*, *6*, 28438.

Mermall, V., Post, P. L., & Mooseker, M. S. (1998). Unconventional myosins in cell movement, membrane traffic, and signal transduction. *Science*, *279*, 527-533.

Metzger, J., Rau, J., Naccache, F., Bas Conn, L., Lindgren, G., & Distl, O. (2018). Genome data uncover four synergistic key regulators for extremely small body size in horses. *BMC Genomics*, *19*, 1-15.

Meuwissen, T., Hayes, B., & Goddard, M. (2013). Accelerating improvement of livestock with genomic selection. *Annual Review of Animal Biosciences*, *1*, 221-237.

Meyers, S. N., McDaneld, T. G., Swist, S. L., Marron, B. M., Steffen, D. J., O'Toole, D., & Smith, T. P. (2010). A deletion mutation in bovine SLC4A2 is associated with osteopetrosis in Red Angus cattle. *BMC Genomics*, *11*, 1-14.

Meyer, O. S., Lunn, M. M., Garcia, S. L., Kjaerbye, A. B., Morling, N., Børsting, C., & Andersen, J. D. (2020). Association between brown eye colour in rs12913832: GG individuals and SNPs in TYR, TYRP1, and SLC24A4. *PLoS One*, *15*, e0239131.

Miao, Y., Mei, Q., Fu, C., Liao, M., Liu, Y., Xu, X., & Xiang, T. (2021). Genome-wide association and transcriptome studies identify candidate genes and pathways for feed conversion ratio in pigs. *BMC Genomics*, *22*, 1-11.

Miar, Y., Plastow, G. S., Bruce, H. L., Moore, S. S., Durunna, O. N., Nkrumah, J. D., & Wang, Z. (2014a). Estimation of genetic and phenotypic parameters for ultrasound and carcass merit traits in crossbred beef cattle. *Canadian Journal of Animal Science*, *94*, 273-280.

Miar, Y., Plastow, G. S., Moore, S. S., Manafiazar, G., Charagu, P., Kemp, R. A., & Wang, Z. (2014). Genetic and phenotypic parameters for carcass and meat quality traits in commercial crossbred pigs. *Journal of Animal Science*, *92*, 2869-2884.

Miar, Y., Plastow, G., & Wang, Z. (2015). Genomic selection, a new era for pork quality Improvement. *Springer Science Reviews*, *3*, 27-37.

Mignon-Grasteau, S., Muley, N., Bastianelli, D., Gomez, J., Péron, A., Sellier, N., & Carré, B. (2004). Heritability of digestibilities and divergent selection for digestion ability in growing chicks fed a wheat diet. *Poultry Science*, *83*, 860-867.

Millar, S. E., Willert, K., Salinas, P. C., Roelink, H., Nusse, R., Sussman, D. J., & Barsh, G. S. (1999). WNT signaling in the control of hair growth and structure. *Developmental Biology*, *207*(1), 133-149.

Mills, R. E., Walter, K., Stewart, C., Handsaker, R. E., Chen, K., Alkan, C., & 1000 Genomes Project. (2011). Mapping copy number variation by population-scale genome sequencing. *Nature*, *470*, 59-65.

Misztal, I. (2006). Challenges of application of marker assisted selection–a review. *Animal Science Papers and Reports, 24*, 5-10.

Mota, L. F., Santos, S. W., Júnior, G. A. F., Bresolin, T., Mercadante, M. E., Silva, J. A., & Albuquerque, L. G. (2022). Meta-analysis across Nellore cattle populations identifies common metabolic mechanisms that regulate feed efficiency-related traits. *BMC Genomics*, *23*, 1-12.

Montalbano, S., Sánchez, X. C., Vaez, M., Helenius, D., Werge, T., & Ingason, A. (2022). Accurate and Effective Detection of Recurrent Copy Number Variants in Large SNP Genotype Datasets. *Current protocols*, *2*, 621.

Mu, Y., Vander Voort, G., Abo-Ismail, M. K., Ventura, R., Jamrozik, J., & Miller, S. P. (2016). Genetic correlations between female fertility and postweaning growth and feed efficiency traits in multibreed beef cattle. *Canadian Journal of Animal Science*, *96*, 448-455.

Mulim, H. A., Brito, L. F., Pinto, L. F. B., Ferraz, J. B. S., Grigoletto, L., Silva, M. R., & Pedrosa, V. B. (2022). Characterization of runs of homozygosity, heterozygosity-enriched regions, and population structure in cattle populations selected for different breeding goals. *BMC Genomics*, *23*, 209.

Nandolo, W., Mészáros, G., Wurzinger, M., Banda, L. J., Gondwe, T. N., Mulindwa, H. A., & Sölkner, J. (2021). Detection of copy number variants in African goats using whole genome sequence data. *BMC Genomics*, *22*, 1-15.

Nani, J. P., & Peñagaricano, F. (2020). Whole-genome homozygosity mapping reveals candidate regions affecting bull fertility in US Holstein cattle. *BMC Genomics*, *21*, 1-9.

Ndung'u, C. W., Okeno, T. O., & Muasya, T. K. (2020). Pooled parameter estimates for traits of economic importance in indigenous chicken in the tropics. *Livestock Science*, *239*, 104102.

Negishi, M., Oinuma, I., & Katoh, H. (2005). Plexins: axon guidance and signal transduction. *Cellular and Molecular Life Sciences*, *62*, 1363-1371.

Nielsen, V., Henrik Møller, S., Krogh Hansen, B., & Berg, P. (2011). Response to selection and genotype–environment interaction in mink (Neovison vison) selected on ad libitum and restricted feeding. *Canadian Journal of Animal Science*, *91*, 231-237.

Nielsen, V. H., Møller, S. H., Hansen, B. K., & Berg, P. (2012). Genetic parameters and effect of selection for body weight in lines of mink (*Neovison vison*) on ad libitum and restricted feeding. *Acta Agriculturae Scandinavica, Section A–Animal Science*, *62*, 24-28.

Nishimura, Y., Shimojima, M., Miyazawa, T., Sato, E., Nakamura, K., Izumiya, Y., & Takahashi, E. (2000). Molecular cloning of the cDNAs encoding the feline B-lymphocyte activation antigen B7-1 (CD80) and B7-2 (CD86) homologues which interact with human CTLA4-Ig. *European Journal of Immunogenetics: Official Journal of the British Society for Histocompatibility and Immunogenetics*, *27*, 427-430.

Nkrumah, J. D., Basarab, J. A., Price, M. A., Okine, E. K., Ammoura, A., Guercio, S., & Moore, S. S. (2004). Different measures of energetic efficiency and their phenotypic relationships with growth, feed intake, and ultrasound and carcass merit in hybrid cattle. *Journal of Animal Science*, *82*, 2451-2459.

Nosrati, M., Asadollahpour Nanaei, H., Amiri Ghanatsaman, Z., & Esmailizadeh, A. (2019). Whole genome sequence analysis to detect signatures of positive selection for high fecundity in sheep. *Reproduction in Domestic Animals*, *54*, 358-364.

Nothnagel, M., Lu, T. T., Kayser, M., & Krawczak, M. (2010). Genomic and geographic distribution of SNP-defined runs of homozygosity in Europeans. *Human Molecular Genetics*, *19*, 2927-2935.

Novo, L. C., Gondo, A., Gomes, R. D. C., Junior, J. F., Ribas, M. N., Brito, L. F., & Menezes, G. R. O. (2021). Genetic parameters for performance, feed efficiency, and carcass traits in Senepol heifers. *Animal*, *15*, 100160.

Oliveira, T. T., Coutinho, L. G., de Oliveira, L. O. A., Timoteo, A. R. D. S., Farias, G. C., & Agnez-Lima, L. F. (2022). APE1/Ref-1 role in inflammation and immune response. *Frontiers in Immunology*, *13*, 793096.

Olivieri, B. F., Mercadante, M. E. Z., Cyrillo, J. N. D. S. G., Branco, R. H., Bonilha, S. F. M., de Albuquerque, L. G., & Baldi, F. (2016). Genomic regions associated with feed efficiency indicator traits in an experimental Nellore cattle population. *PLoS One*, *11*, e0164390.

Onteru, S. K., Gorbach, D. M., Young, J. M., Garrick, D. J., Dekkers, J. C., & Rothschild, M. F. (2013). Whole genome association studies of residual feed intake and related traits in the pig. *PloS One*, *8*, e61756.

Oreshkova, N., Molenaar, R. J., Vreman, S., Harders, F., Munnink, B. B. O., Hakze-van Der Honing, R. W., & Stegeman, A. (2020). SARS-CoV-2 infection in farmed minks, the Netherlands, April and May 2020. *Eurosurveillance*, *25*, 2001005.

Ornitz, D. M., & Itoh, N. (2015). The fibroblast growth factor signaling pathway. *Wiley Interdisciplinary Reviews: Developmental Biology*, *4*, 215-266.

Osada, A., Iwabuchi, T., Kishimoto, J., Hamazaki, T. S., & Okochi, H. (2007). Long-term culture of mouse vibrissal dermal papilla cells and de novo hair follicle induction. *Tissue Engineering*, *13*, 975-982.

Patience, J. F., Rossoni-Serão, M. C., & Gutiérrez, N. A. (2015). A review of feed efficiency in swine: biology and application. *Journal of Animal Science and Biotechnology*, *6*, 1-9.

Paudel, Y., Madsen, O., Megens, H. J., Frantz, L. A., Bosse, M., Bastiaansen, J. W., & Groenen, M. A. (2013). Evolutionary dynamics of copy number variation in pig genomes in the context of adaptation and domestication. *BMC Genomics*, *14*, 1-13.

Pailhoux, E., Vigier, B., Chaffaux, S., Servel, N., Taourit, S., Furet, J. P., & Vaiman, D. (2001). A 11.7-kb deletion triggers intersexuality and polledness in goats. *Nature Genetics*, *29*, 453-458.

Pakdel, A., Arendonk, J. V., Vereijken, A. L. J., & Bovenhuis, H. (2005). Genetic parameters of ascites-related traits in broilers: correlations with feed efficiency and carcase traits. *British Poultry Science*, *46*, 43-53.

Peripolli, E., Munari, D. P., Silva, M. V. G. B., Lima, A. L. F., Irgang, R., & Baldi, F. (2017). Runs of homozygosity: current knowledge and applications in livestock. *Animal Genetics*, *48*, 255-271.

Peripolli, E., Reimer, C., Ha, N. T., Geibel, J., Machado, M. A., Panetto, J. C. D. C., & da Silva, M. V. G. B. (2020). Genome-wide detection of signatures of selection in indicine and Brazilian locally adapted taurine cattle breeds using whole-genome re-sequencing data. *BMC Genomics*, *21*, 1-16.

Kolberg, L., Raudvere, U., Kuzmin, I., Vilo, J., & Peterson, H. (2020). gprofiler2--an R package for gene list functional enrichment analysis and namespace conversion toolset g: Profiler. *F1000Research*, *9*.

Picard, C., Gilles, A., Pontarotti, P., Olive, D., & Collette, Y. (2002). Cutting edge: recruitment of the ancestral fyn gene during emergence of the adaptive immune system. *The Journal of Immunology*, *168*, 2595-2598.

Pierce, M. D., Dzama, K., & Muchadeyi, F. C. (2018). Genetic diversity of seven cattle breeds inferred using copy number variations. *Frontiers in Genetics*, *9*, 163.

P Piles, M., & Blasco, A. (2003). Response to selection for growth rate in rabbits estimated by using a control cryopreserved population. *World Rabbit Science*, *11*(2), 53-62.

Piles, M., Gomez, E. A., Rafel, O., Ramon, J., & Blasco, A. (2004). Elliptical selection experiment for the estimation of genetic parameters of the growth rate and feed conversion ratio in rabbits. *Journal of Animal Science*, *82*, 654-660.

Piles, M., & Sánchez, J. P. (2019). Use of group records of feed intake to select for feed efficiency in rabbit. *Journal of Animal Breeding and Genetics*, *136*, 474-483.

Prakash, A., Saxena, V. K., & Singh, M. K. (2020). Genetic analysis of residual feed intake, feed conversion ratio and related growth parameters in broiler chicken: A review. *World's Poultry Science Journal*, *76*, 304-317.

Prekeris, R., Klumperman, J., & Scheller, R. H. (2000). Syntaxin 11 is an atypical SNARE abundant in the immune system. *European Journal of Cell Biology*, *79*, 771-780.

Price, A. L., Patterson, N. J., Plenge, R. M., Weinblatt, M. E., Shadick, N. A., & Reich, D. (2006). Principal components analysis corrects for stratification in genome-wide association studies. *Nature Genetics*, *38*, 904-909.

Prieto, A., Fernández-Antonio, R., Díaz-Cao, J. M., López, G., Díaz, P., Alonso, J. M., & Fernández, G. (2017). Distribution of Aleutian mink disease virus contamination in the environment of infected mink farms. *Veterinary Microbiology*, *204*, 59-63.

Pryce, J. E., Haile-Mariam, M., Goddard, M. E., & Hayes, B. J. (2014). Identification of genomic regions associated with inbreeding depression in Holstein and Jersey dairy cattle. *Genetics Selection Evolution*, *46*, 1-14.

Purcell, S., Neale, B., Todd-Brown, K., Thomas, L., Ferreira, M. A., Bender, D., & Sham, P. C. (2007). PLINK: a tool set for whole-genome association and population-based linkage analyses. *The American Journal of Human Genetics*, *81*, 559-575.

Purfield, D. C., McParland, S., Wall, E., & Berry, D. P. (2017). The distribution of runs of homozygosity and selection signatures in six commercial meat sheep breeds. *PLoS One*, *12*, e0176780.

Qian, Q., Li, Y., Fu, J., Leng, D., Dong, Z., Shi, J., & Liu, J. (2022). Switch-associated protein 70 protects against nonalcoholic fatty liver disease through suppression of TAK1. *Hepatology*, *75*, 1507-1522.

Qiu, Y., Ding, R., Zhuang, Z., Wu, J., Yang, M., Zhou, S., & Yang, J. (2021). Genome-wide detection of CNV regions and their potential association with growth and fatness traits in Duroc pigs. *BMC Genomics*, *22*, 332.

Quinlan, A. R., & Hall, I. M. (2010). BEDTools: a flexible suite of utilities for comparing genomic features. *Bioinformatics*, *26*, 841-842.

Quinton, C. D., Kause, A., Koskela, J., & Ritola, O. (2007). Breeding salmonids for feed efficiency in current fishmeal and future plant-based diet environments. *Genetics Selection Evolution*, *39*, 431-446.

R Core Team. (2010). R: A language and environment for statistical computing.

Raudvere, U., Kolberg, L., Kuzmin, I., Arak, T., Adler, P., Peterson, H., & Vilo, J. (2019). g: Profiler: a web server for functional enrichment analysis and conversions of gene lists (2019 update). *Nucleic Scids Research*, *47*, 191-198.

Rausch, T., Zichner, T., Schlattl, A., Stütz, A. M., Benes, V., & Korbel, J. O. (2012). DELLY: structural variant discovery by integrated paired-end and split-read analysis. *Bioinformatics*, *28*, i333-i339.

Redon, R., Ishikawa, S., Fitch, K. R., Feuk, L., Perry, G. H., Andrews, T. D., .& Hurles, M. E. (2006). Global variation in copy number in the human genome. *Nature*, *444*, 444-454.

Regis, G., Conti, L., Boselli, D., & Novelli, F. (2006). IFNγR2 trafficking tunes IFNγ–STAT1 signaling in T lymphocytes. *Trends in Immunology*, *27*, 96-101.

Rishikaysh, P., Dev, K., Diaz, D., Qureshi, W. M. S., Filip, S., & Mokry, J. (2014). Signaling involved in hair follicle morphogenesis and development. *International Journal of Molecular Sciences*, *15*, 1647-1670.

Reverter, A., Porto-Neto, L. R., Fortes, M. R. S., McCulloch, R., Lyons, R. E., Moore, S., & Lehnert, S. A. (2016). Genomic analyses of tropical beef cattle fertility based on genotyping pools of Brahman cows with unknown pedigree. *Journal of Animal Science*, *94*, 4096-4108.

Rizkalla, S. W., Prifti, E., Cotillard, A., Pelloux, V., Rouault, C., Allouche, R., & Clement, K. (2012). Differential effects of macronutrient content in 2 energy-restricted diets on cardiovascular risk factors and adipose tissue cell size in moderately obese individuals: a randomized controlled trial. *The American Journal of Clinical Nutrition*, *95*, 49-63.

Rocha, R. D. F. B., Garcia, A. O., Otto, P. I., da Silva, M. V. B., Martins, M. F., Machado, M. A., & Guimarães, S. E. F. (2023). Runs of homozygosity and signatures of selection for number of oocytes and embryos in the Gir Indicine cattle. *Mammalian Genome*, 1-15.

Rolf, M. M., Taylor, J. F., Schnabel, R. D., McKay, S. D., McClure, M. C., Northcutt, S. L., & Weaber, R. L. (2012). Genome-wide association analysis for feed efficiency in Angus cattle. *Animal Genetics*, *43*, 367-374.

Rose, J., Oldfield, J., & Stormshak, F. (1987). Apparent role of melatonin and prolactin in initiating winter fur growth in mink. *General and Comparative Endocrinology*, *65*, 212-215.

Rose, J., Stormshak, F., Oldfield, J., & Adair, J. (1984). Induction of winter fur growth in mink (Mustela vison) with melatonin. *Journal of Animal Science*, *58*, 57-61.

Rosengren Pielberg, G., Golovko, A., Sundström, E., Curik, I., Lennartsson, J., Seltenhammer, M. H., & Andersson, L. (2008). A cis-acting regulatory mutation causes premature hair graying and susceptibility to melanoma in the horse. *Nature Genetics*, *40*, 1004-1009.

Russo, L. C., Tomasin, R., Matos, I. A., Manucci, A. C., Sowa, S. T., Dale, K., & Hoch, N. C. (2021). The SARS-CoV-2 Nsp3 macrodomain reverses PARP9/DTX3L-dependent ADP-ribosylation induced by interferon signaling. *Journal of Biological Chemistry*, *297*.

Sahajpal, N. S., Lai, C. Y. J., Hastie, A., Mondal, A. K., Dehkordi, S. R., van der Made, C. I., & Kolhe, R. (2022). Optical genome mapping identifies rare structural variations as predisposition factors associated with severe COVID-19. *Iscience*, *25*.

Saitou, M., & Gokcumen, O. (2020). An evolutionary perspective on the impact of genomic copy number variation on human health. *Journal of Molecular Evolution*, *88*, 104-119.

Salehian-Dehkordi, H., Xu, Y. X., Xu, S. S., Li, X., Luo, L. Y., Liu, Y. J., & Lv, F. H. (2021). Genome-wide detection of copy number variations and their association with distinct phenotypes in the world's sheep. *Frontiers in Genetics*, *12*, 670582.

Sánchez, J. P., Legarra, A., Velasco-Galilea, M., Piles, M., Sánchez, A., Rafel, O., & Ballester, M. (2020). Genome-wide association study for feed efficiency in collective cage-raised rabbits under full and restricted feeding. *Animal Genetics*, *51*, 799-810.

Sandoval, A., Duran, P., Gandini, M. A., Andrade, A., Almanza, A., Kaja, S., & Felix, R. (2017). Regulation of L-type CaV1. 3 channel activity and insulin secretion by the cGMP-PKG signaling pathway. *Cell Calcium*, *66*, 1-9.

Sanglard, L. P., Huang, Y., Gray, K. A., Linhares, D. C., Dekkers, J., Niederwerder, M. C., & Serão, N. V. (2021). Further host-genomic characterization of total antibody response to PRRSV vaccination and its relationship with reproductive performance in commercial sows: genome-wide haplotype and zygosity analyses. *Genetics Selection Evolution*, *53*, 1-17.

Santiago, K. G., Kim, S. H., Lopez, B. I., Lee, D. H., Cho, Y. G., Song, Y. N., & Seo, K. S. (2021). Estimation of genetic parameters for feeding pattern traits and its relationship to feed efficiency and production traits in Duroc pigs. *Agriculture*, *11*, 850.

Sato, T., Kawamura, Y., Asai, R., Amano, T., Uchijima, Y., Dettlaff-Swiercz, D. A., & Kurihara, H. (2008). Recombinase-mediated cassette exchange reveals the selective use of

Gq/G11-dependent and-independent endothelin 1/endothelin type A receptor signaling in pharyngeal arch development. *Development, 135,* 755-765.

Schönauer, R., Jin, W., Findeisen, C., Valenzuela, I., Devlin, L. A., Murrell, J., & Halbritter, J. (2023). Monoallelic intragenic POU3F2 variants lead to neurodevelopmental delay and hyperphagic obesity, confirming the gene's candidacy in 6q16. 1 deletions. *The American Journal of Human Genetics*, *110*, 998-1007.

Schroder, K., Hertzog, P. J., Ravasi, T., & Hume, D. A. (2004). Interferon-γ: an overview of signals, mechanisms and functions. *Journal of Leucocyte Biology*, *75*, 163-189.

Schurink, A., da Silva, V. H., Velie, B. D., Dibbits, B. W., Crooijmans, R. P., François, L., & Ducro, B. J. (2018). Copy number variations in Friesian horses and genetic risk factors for insect bite hypersensitivity. *BMC Genetics*, *19*, 1-13.

Schweer, K. R., Kachman, S. D., Kuehn, L. A., Freetly, H. C., Pollak, J. E., & Spangler, M. L. (2018). Genome-wide association study for feed efficiency traits using SNP and haplotype models. *Journal of Animal Science*, *96*, 2086-2098.

Thermofisher Scientific. (2017) Axiom™ genotyping solution: data analysis guide. Pub. No. 702961 Rev 5.

Seabury, C. M., Oldeschulte, D. L., Saatchi, M., Beever, J. E., Decker, J. E., Halley, Y. A., & Taylor, J. F. (2017). Genome-wide association study for feed efficiency and growth traits in US beef cattle. *BMC Genomics*, *18*, 1-25.

Sell-Kubiak, E., Wimmers, K., Reyer, H., & Szwaczkowski, T. (2017). Genetic aspects of feed efficiency and reduction of environmental footprint in broilers: a review. *Journal of Applied Genetics*, *58*, 487-498.

Semenova, E. A., Zempo, H., Miyamoto-Mikami, E., Kumagai, H., Larin, A. K., Sultanov, R. I., & Ahmetov, I. I. (2022). Genome-wide association study identifies CDKN1A as a novel locus associated with muscle fiber composition. *Cells*, *11*, 3910.

Seol, D., Ko, B. J., Kim, B., Chai, H. H., Lim, D., & Kim, H. (2019). Identification of copy number variation in domestic chicken using whole-genome sequencing reveals evidence of selection in the genome. *Animals*, *9*, 809.

Serão, N. V., González-Peña, D., Beever, J. E., Faulkner, D. B., Southey, B. R., & Rodriguez-Zas, S. L. (2013). Single nucleotide polymorphisms and haplotypes associated with feed efficiency in beef cattle. *BMC Genetics*, *14*, 1-20.

Shah, T. M., Patel, J. G., Gohil, T. P., Blake, D. P., & Joshi, C. G. (2019). Host transcriptome and microbiome interaction modulates physiology of full-sibs broilers with divergent feed conversion ratio. *npj Biofilms and Microbiomes*, *5*, 24.

Sharma, A., Lee, J. S., Dang, C. G., Sudrajad, P., Kim, H. C., Yeon, S. H., & Lee, S. H. (2015). Stories and challenges of genome wide association studies in livestock—a review. *Asian-Australasian Journal of Animal Sciences*, *28*, 1371.

Shen, Y., Sun, Y., Zhang, L., & Liu, H. (2017). Effects of DTX3L on the cell proliferation, adhesion, and drug resistance of multiple myeloma cells. *Tumor Biology*, *39*, 1-10.

Shi, L., Wang, L., Liu, J., Deng, T., Yan, H., Zhang, L., & Zhao, F. (2020). Estimation of inbreeding and identification of regions under heavy selection based on runs of homozygosity in a Large White pig population. *Journal of Animal Science and Biotechnology*, *11*, 1-10.

Shi, S. Y., Li, L. J., Zhang, Z. J., Wang, E. Y., Wang, J., Xu, J. W., & Huang, Y. Z. (2020). Copy number variation of MYLK4 gene and its growth traits of Capra hircus (goat). *Animal Biotechnology*, *31*, 532-537.

Shimizu, H., & Morgan, B. A. (2004). Wnt signaling through the β-catenin pathway is sufficient to maintain, but not restore, anagen-phase characteristics of dermal papilla cells. *Journal of Investigative Dermatology*, *122*, 239-245.

Shimomura, Y., & Ito, M. (2005). Human hair keratin-associated proteins. *Journal of Investigative Dermatology Symposium Proceedings*, *10*, 230-233.

Shirali, M., Nielsen, V. H., Møller, S. H., & Jensen, J. (2015). Longitudinal analysis of residual feed intake and BW in mink using random regression with heterogeneous residual variance. *Animal*, *9*, 1597-1604.

Shirasaki, T., Yamagoe, S., Shimakami, T., Murai, K., Imamura, R., Ishii, K. A., & Honda, M. (2022). Leukocyte cell-derived chemotaxin 2 is an antiviral regulator acting through the proto-oncogene MET. *Nature Communications*, *13*, 3176.

Signer-Hasler, H., Henkel, J., Bangerter, E., Bulut, Z., Drögemüller, C., Leeb, T., & Flury, C. (2022). Runs of homozygosity in Swiss goats reveal genetic changes associated with domestication and modern selection. *Genetics Selection Evolution*, *54*, 1-11.

Signer-Hasler, H., Burren, A., Ammann, P., Drögemüller, C., & Flury, C. (2019). Runs of homozygosity and signatures of selection: a comparison among eight local Swiss sheep breeds. *Animal Genetics*, *50*, 512-525.

Fernandes, A. C., da Silva, V. H., Goes, C. P., Moreira, G. C. M., Godoy, T. F., Ibelli, A. M. G., & Coutinho, L. L. (2021). Genome-wide detection of CNVs and their association with performance traits in broilers. *BMC Genomics*, *22*, 1-18.

Singh, S. K., Kurfurst, R., Nizard, C., Schnebert, S., Perrier, E., & Tobin, D. J. (2010). Melanin transfer in human skin cells is mediated by filopodia—a model for homotypic and heterotypic lysosome-related organelle transfer. *The FASEB Journal*, *24*, 3756-3769.

Skinner-Noble, D. O., & Teeter, R. G. (2003). Components of feed efficiency in broiler breeding stock: energetics, performance, carcass composition, metabolism, and body temperature. *Poultry Science*, *82*, 1080-1090.

Ślaska, B., Rozempolska-Rucińska, I., & Jeżewska-Witkowska, G. (2009). Variation in some reproductive traits of mink (Neovison vison) according to their coat colour. *Annals of Animal Science*, *9*, 287-297.

Smith, S. N., Davis, M. E., & Loerch, S. C. (2010). Residual feed intake of Angus beef cattle divergently selected for feed conversion ratio. *Livestock Science*, *132*, 41-47.

Snyder, E., Chukrallah, L., Seltzer, K., Goodwin, L., & Braun, R. E. (2020). ADAD1 and ADAD2, testis-specific adenosine deaminase domain-containing proteins, are required for male fertility. *Scientific Reports*, *10*, 11536.

Sørensen, K. (2002). *Selection for feed efficiency in mink (Mustela vison)* (Doctoral dissertation, Royal Veterinary and Agricultural University, Department of Animal Science and Animal Health).

Sørensen, K., Grossman, M., & Koops, W. J. (2003). Multiphasic growth curves in mink (Mustela vison) selected for feed efficiency. *Acta Agriculturae Scandinavica, Section A—Animal Science*, *53*, 41-50.

Socha, S., Kołodziejczyk, D., & Konopna, E. (2008). Genetic parameters of animal size and fur quality in four colour types of mink (Mustela vison Sch.). *Journal of Agrobiology*, *25*, 65-67.

Song, X., Xu, C., Liu, Z., Yue, Z., Liu, L., Yang, T., & Yang, F. (2017). Comparative transcriptome analysis of mink (*Neovison vison*) skin reveals the key genes involved in the melanogenesis of black and white coat colour. *Scientific Reports*, *7*, 12461.

Song, X., Xu, C., Liu, Z., Yue, Z., Liu, L., Yang, T., & Yang, F. (2017). Comparative transcriptome analysis of mink (Neovison vison) skin reveals the key genes involved in the melanogenesis of black and white coat colour. *Scientific Reports*, *7*, 12461.

Sosa-Madrid, B. S., Varona, L., Blasco, A., Hernández, P., Casto-Rebollo, C., & Ibáñez-Escriche, N. (2020). The effect of divergent selection for intramuscular fat on the domestic rabbit genome. *Animal*, *14*, 2225-2235.

Spolski, R., & Leonard, W. J. (2008). Interleukin-21: basic biology and implications for cancer and autoimmunity. *Annual Review of Immunology*, *26*, 57-79.

Stafuzza, N. B., Silva, R. M. D. O., Fragomeni, B. D. O., Masuda, Y., Huang, Y., Gray, K., & Lourenco, D. A. L. (2019). A genome-wide single nucleotide polymorphism and copy number variation analysis for number of piglets born alive. *BMC Genomics*, *20*, 1-11.

Steyn, Y., van Marle-Köster, E., & Theron, H. E. (2014). Residual feed intake as selection tool in South African Bonsmara cattle. *Livestock Science*, *164*, 35-38.

Strillacci, M. G., Cozzi, M. C., Gorla, E., Mosca, F., Schiavini, F., Román-Ponce, S. I., & Bagnato, A. (2017). Genomic and genetic variability of six chicken populations using single nucleotide polymorphism and copy number variants as markers. *Animal*, *11*, 737-745.

Strillacci, M. G., Gorla, E., Cozzi, M. C., Vevey, M., Genova, F., Scienski, K., & Bagnato, A. (2018). A copy number variant scan in the autochthonous Valdostana Red Pied cattle breed and comparison with specialized dairy populations. *PLoS One*, *13*, e0204669.

Strillacci, M. G., Gorla, E., Ríos-Utrera, A., Vega-Murillo, V. E., Montaño-Bermudez, M., Garcia-Ruiz, A., & Bagnato, A. (2019). Copy number variation mapping and genomic variation of autochthonous and commercial turkey populations. *Frontiers in Genetics*, *10*, 982.

Strillacci, M. G., Marelli, S. P., Milanesi, R., Zaniboni, L., Punturiero, C., & Cerolini, S. (2021). Copy number variants in four Italian turkey breeds. *Animals*, *11*, 391.

Strillacci, M. G., Moradi-Shahrbabak, H., Davoudi, P., Ghoreishifar, S. M., Mokhber, M., Masroure, A. J., & Bagnato, A. (2021). A genome-wide scan of copy number variants in three Iranian indigenous river buffaloes. *BMC Genomics*, *22*, 1-14.

Sulem, P., Gudbjartsson, D. F., Stacey, S. N., Helgason, A., Rafnar, T., Magnusson, K. P., & Stefansson, K. (2007). Genetic determinants of hair, eye and skin pigmentation in Europeans. *Nature Genetics*, *39*, 1443-1452.

Sun, X., Guo, J., Li, L., Zhong, T., Wang, L., Zhan, S., & Zhang, H. (2022). Genetic diversity and selection signatures in Jianchang black goats revealed by whole-genome sequencing data. *Animals*, *12*, 2365.

Sun, Y., Zhao, G., Liu, R., Zheng, M., Hu, Y., Wu, D., & Wen, J. (2013). The identification of 14 new genes for meat quality traits in chicken using a genome-wide association study. *BMC Genomics*, *14*, 1-11.

Suvakov, M., Panda, A., Diesh, C., Holmes, I., & Abyzov, A. (2021). CNVpytor: a tool for copy number variation detection and analysis from read depth and allele imbalance in whole-genome sequencing. *Gigascience*, *10*, 1-9.

Taghizadeh, S., Gholizadeh, M., Rahimi-Mianji, G., Moradi, M. H., Costilla, R., Moore, S., & Di Gerlando, R. (2022). Genome-wide identification of copy number variation and association with fat deposition in thin and fat-tailed sheep breeds. *Scientific Reports*, *12*, 8834.

Tahir, M. S., Porto-Neto, L. R., Gondro, C., Shittu, O. B., Wockner, K., Tan, A. W., & Fortes, M. R. (2021). Meta-analysis of heifer traits identified reproductive pathways in Bos indicus cattle. *Genes*, *12*, 768.

Tang, J., Ouyang, H., Chen, X., Jiang, D., Tian, Y., Huang, Y., & Shen, X. (2023). Comparative Transcriptome Analyses of Leg Muscle during Early Growth between Geese (Anser cygnoides) Breeds Differing in Body Size Characteristics. *Genes*, *14*, 1048.

Taussat, S., Boussaha, M., Ramayo-Caldas, Y., Martin, P., Venot, E., Cantalapiedra-Hijar, G., & Renand, G. (2020). Gene networks for three feed efficiency criteria reveal shared and specific biological processes. *Genetics Selection Evolution*, *52*, 1-14.

Teo, S. M., Pawitan, Y., Ku, C. S., Chia, K. S., & Salim, A. (2012). Statistical challenges associated with detecting copy number variations with next-generation sequencing. *Bioinformatics*, *28*, 2711-2718.

Thirstrup, J. P., Ruiz-Gonzalez, A., Pujolar, J. M., Larsen, P. F., Jensen, J., Randi, E., & Pertoldi, C. (2015). Population genetic structure in farm and feral American mink (*Neovison vison*) inferred from RAD sequencing-generated single nucleotide polymorphisms. *Journal of Animal Science*, *93*, 3773-3782.

Thirstrup, J. P., Jensen, J., & Lund, M. S. (2017). Genetic parameters for fur quality graded on live animals and dried pelts of American mink (*Neovison vison*). *Journal of Animal Breeding and Genetics*, *134*, 322-331.

Tian, X., Meng, X., Wang, L., Song, Y., Zhang, D., Ji, Y., & Dong, C. (2015). Molecular cloning, mRNA expression and tissue distribution analysis of Slc7a11 gene in alpaca (Lama paco) skins associated with different coat colors. *Gene*, *555*, 88-94.

Ticli, G., Cazzalini, O., Stivala, L. A., & Prosperi, E. (2022). Revisiting the function of p21CDKN1A in DNA repair: The influence of protein interactions and stability. *International Journal of Molecular Sciences*, *23*, 7058.

Tokuo, H., Bhawan, J., & Coluccio, L. M. (2018). Myosin X is required for efficient melanoblast migration and melanoma initiation and metastasis. *Scientific Reports*, *8*, 10449.

Toolkit, P. (2019). Picard Toolkit. Broad Institute, GitHub Repository.

Tortereau, F., Marie-Etancelin, C., Weisbecker, J. L., Marcon, D., Bouvier, F., Moreno-Romieux, C., & François, D. (2020). Genetic parameters for feed efficiency in Romane rams and responses to single-generation selection. *Animal*, *14*, 681-687.

Tsurusaki, Y., Okamoto, N., Ohashi, H., Kosho, T., Imai, Y., Hibi-Ko, Y., & Matsumoto, N. (2012). Mutations affecting components of the SWI/SNF complex cause Coffin-Siris syndrome. *Nature Genetics*, *44*, 376-378.

Turner, P., Buijs, S., Rommers, J. M., & Tessier, M. (2013). The code of practice for the care and handling of farmed mink. *National. Farm Animal. Care Council. Rexdale ON Can*, *58*.

Upadhyay, M., da Silva, V. H., Megens, H. J., Visker, M. H., Ajmone-Marsan, P., Bâlteanu, V. A., & Crooijmans, R. P. (2017). Distribution and functionality of copy number variation across European cattle populations. *Frontiers in Genetics*, *8*, 108.

Usman, T., Yu, Y., Liu, C., Wang, X., Zhang, Q., & Wang, Y. (2014). Genetic effects of single nucleotide polymorphisms in JAK2 and STAT5A genes on susceptibility of Chinese Holsteins to mastitis. *Molecular Biology Reports*, *41*, 8293-8301.

Valipour, S., Karimi, K., Barrett, D., Do, D. N., Hu, G., Sargolzaei, M., & Miar, Y. (2022a). Genetic and Phenotypic Parameters for Pelt Quality and Body Length and Weight Traits in American Mink. *Animals*, *12*, 3184.

Valipour, S., Karimi, K., Do, D. N., Barrett, D., Sargolzaei, M., Plastow, G., & Miar, Y. (2022b). Genome-wide detection of selection signatures for pelt quality traits and coat color using whole-genome sequencing data in American Mink. *Genes*, *13*, 1939.

Vallimont, J. E., Dechow, C. D., Daubert, J. M., Dekleva, M. W., Blum, J. W., Barlieb, C. M., & Baumrucker, C. R. (2011). Heritability of gross feed efficiency and associations with yield, intake, residual intake, body weight, and body condition score in 11 commercial Pennsylvania tie stalls. *Journal of Dairy Science*, *94*, 2108-2113.

Van den Berg, I., Boichard, D., & Lund, M. S. (2016). Sequence variants selected from a multi-breed GWAS can improve the reliability of genomic predictions in dairy cattle. *Genetics Selection Evolution*, *48*, 1-18.

Van der Werf, J. H. J. (2004). Is it useful to define residual feed intake as a trait in animal breeding programs? *Australian Journal of Experimental Agriculture*, *44*, 405-409.

Van Duyvenvoorde, H. A., Lui, J. C., Kant, S. G., Oostdijk, W., Gijsbers, A. C., Hoffer, M. J., & Wit, J. M. (2014). Copy number variants in patients with short stature. *European Journal of Human Genetics*, *22*, 602-609.

VanRaden, P. M. (2008). Efficient methods to compute genomic predictions. *Journal of Dairy Science*, *91*, 4414-4423.

Veerkamp, R. F., & Thompson, R. (1999). A covariance function for feed intake, live weight, and milk yield estimated using a random regression model. *Journal of Dairy Science*, *82*, 1565-1573.

Verardo, L. L., Silva, F. F., Varona, L., Resende, M. D. V., Bastiaansen, J. W. M., Lopes, P. S., & Guimarães, S. E. F. (2015). Bayesian GWAS and network analysis revealed new candidate genes for number of teats in pigs. *Journal of Applied Genetics*, *56*, 123-132.

Verardo, L. L., Silva, F. F., Lopes, M. S., Madsen, O., Bastiaansen, J. W., Knol, E. F., & Guimarães, S. E. (2016). Revealing new candidate genes for reproductive traits in pigs: combining Bayesian GWAS and functional pathways. *Genetics Selection Evolution*, *48*, 1-13.

Vigors, S., O'Doherty, J. V., Bryan, K., & Sweeney, T. (2019). A comparative analysis of the transcriptome profiles of liver and muscle tissue in pigs divergent for feed efficiency. *Bmc Genomics*, *20*, 1-12.

Visscher, P. M., Hill, W. G., & Wray, N. R. (2008). Heritability in the genomics era—concepts and misconceptions. *Nature Reviews Genetics*, *9*, 255-266.

Von Felde, A., Roehe, R., Looft, H., & Kalm, E. (1996). Genetic association between feed intake and feed intake behaviour at different stages of growth of group-housed boars. *Livestock Production Science*, *47*, 11-22.

Wan, X., Jing, J. N., Wang, D. F., & Lv, F. H. (2023). Whole-genome selective scans detect genes associated with important phenotypic traits in goat (*Capra hircus*). *Frontiers in Genetics*, *14*, 1173017.

Wang, K., Li, M., Hadley, D., Liu, R., Glessner, J., Grant, S. F., & Bucan, M. (2007). PennCNV: an integrated hidden Markov model designed for high-resolution copy number variation detection in whole-genome SNP genotyping data. *Genome Research*, *17*, 1665-1674.

Wang, X., Nahashon, S., Feaster, T. K., Bohannon-Stewart, A., & Adefope, N. (2010). An initial map of chromosomal segmental copy number variations in the chicken. *BMC Genomics*, *11*, 1-10.

Wang, K. S., Liu, X., Zheng, S., Zeng, M., Pan, Y., & Callahan, K. (2012). A novel locus for body mass index on 5p15. 2: a meta-analysis of two genome-wide association studies. *Gene*, *500*, 80-84.

Wang, Y., Gu, X., Feng, C., Song, C., Hu, X., & Li, N. (2012). A genome-wide survey of copy number variation regions in various chicken breeds by array comparative genomic hybridization method. *Animal Genetics*, *43*, 282-289.

Wang, L., Zhang, L., Yan, H., Liu, X., Li, N., Liang, J., ... & Wang, L. (2014). Genome-wide association studies identify the loci for 5 exterior traits in a Large White× Minzhu pig population. *PLoS One*, *9*(8), e103766.

Wang, H., Wang, C., Yang, K., Liu, J., Zhang, Y., Wang, Y., & Liu, B. (2015). Genome wide distributions and functional characterization of copy number variations between Chinese and Western pigs. *PLoS One*, *10*, e0131522.

Wang, K., Ouyang, H., Xie, Z., Yao, C., Guo, N., Li, M., & Pang, D. (2015). Efficient generation of myostatin mutations in pigs using the CRISPR/Cas9 system. *Scientific Reports*, *5*, 16623.

Wang, M. S., Huo, Y. X., Li, Y., Otecko, N. O., Su, L. Y., Xu, H. B., & Zhang, Y. P. (2016). Comparative population genomics reveals genetic basis underlying body size of domestic chickens. *Journal of Molecular Cell Biology*, *8*, 542-552.

Wang, Y. N., Yang, W. C., Li, P. W., Wang, H. B., Zhang, Y. Y., & Zan, L. S. (2018). Myocyte enhancer factor 2A promotes proliferation and its inhibition attenuates myogenic differentiation via myozenin 2 in bovine skeletal muscle myoblast. *PLoS One*, *13*, e0196255.

Wang, H., Chai, Z., Hu, D., Ji, Q., Xin, J., Zhang, C., & Zhong, J. (2019). A global analysis of CNVs in diverse yak populations using whole-genome resequencing. *BMC Genomics*, *20*, 1-12.

Wang, F., Hou, H., Luo, Y., Tang, G., Wu, S., Huang, M., & Sun, Z. (2020). The laboratory tests and host immunity of COVID-19 patients with different severity of illness. *JCI Insight*, *5*.

Wang, L. M., Bu, H. Y., Song, F. B., Zhu, W. B., Fu, J. J., & Dong, Z. J. (2019). Characterization and functional analysis of slc7a11 gene, involved in skin color differentiation in the red tilapia. *Comparative Biochemistry and Physiology Part A: Molecular & Integrative Physiology*, *236*, 110529.

Wang, Z., Guo, J., Guo, Y., Yang, Y., Teng, T., Yu, Q., & Yang, H. (2020). Genome-wide detection of CNVs and association with body weight in sheep based on 600K SNP arrays. *Frontiers in Genetics*, *11*, 558.

Wang, F. H., Zhang, L., Gong, G., Yan, X. C., Zhang, L. T., Zhang, F. T., & Li, J. Q. (2021). Genome-wide association study of fleece traits in Inner Mongolia Cashmere goats. *Animal Genetics*, *52*, 375-379.

Wang, Z., Guo, Y., Liu, S., & Meng, Q. (2021). Genome-wide assessment characteristics of genes overlapping copy number variation regions in Duroc purebred population. *Frontiers in Genetics*, *12*, 753748.

Wang, X., Li, G., Ruan, D., Zhuang, Z., Ding, R., Quan, J., & Yang, J. (2022). Runs of homozygosity uncover potential functional-altering mutation associated with body weight and length in two Duroc pig lines. *Frontiers in Veterinary Science*, *9*, 832633.

Wang, Q., Zhang, J., Wang, H., Wang, Z., Li, Q., Zhao, G., & Wen, J. (2023). Estimates of genomic inbreeding and identification of candidate regions in Beijing-You chicken populations. *Animal Genetics*, *54*, 155-165.

Warland, A., Kendall, K. M., Rees, E., Kirov, G., & Caseras, X. (2020). Schizophrenia-associated genomic copy number variants and subcortical brain volumes in the UK Biobank. *Molecular Psychiatry*, *25*, 854-862.

Westbroek, W., Lambert, J., Schepper, S. D., Kleta, R., Bossche, K. V. D., Seabra, M. C., & Naeyaert, J. M. (2004). Rab27b is up-regulated in human Griscelli syndrome type II melanocytes and linked to the actin cytoskeleton via exon F-Myosin Va transcripts. *Pigment Cell Research*, *17*, 498-505.

Westphal, D. S., Riedhammer, K. M., Kovacs-Nagy, R., Meitinger, T., Hoefele, J., & Wagner, M. (2018). A de novo missense variant in POU3F2 identified in a child with global developmental delay. *Neuropediatrics*, *49*, 401-404.

Widmann, P., Reverter, A., Fortes, M. R., Weikard, R., Suhre, K., Hammon, H., & Kuehn, C. (2013). A systems biology approach using metabolomic data reveals genes and pathways interacting to modulate divergent growth in cattle. *BMC Genomics*, *14*, 1-17.

Willems, O. W., Miller, S. P., & Wood, B. J. (2013). Assessment of residual body weight gain and residual intake and body weight gain as feed efficiency traits in the turkey (Meleagris gallopavo). *Genetics Selection Evolution*, *45*, 1-8.

Wilkinson, B., Chen, J. Y. F., Han, P., Rufner, K. M., Goularte, O. D., & Kaye, J. (2002). TOX: an HMG box protein implicated in the regulation of thymocyte selection. *Nature Immunology*, *3*, 272-280.

Winheim, E., Rinke, L., Lutz, K., Reischer, A., Leutbecher, A., Wolfram, L., & Krug, A. B. (2021). Impaired function and delayed regeneration of dendritic cells in COVID-19. *PLoS pathogens*, *17*, e1009742.

Wu, J., Wang, X., Ding, R., Quan, J., Ye, Y., Gu, T., & Yang, J. (2020). Identification of important proteins and pathways affecting feed efficiency in DLY pigs by iTRAQ-based proteomic analysis. *Animals*, *10*, 189.

Wu, X. J., Williams, M. J., Patel, P. R., Kew, K. A., & Zhu, Y. (2019). Subfertility and reduced progestin synthesis in Pgrmc2 knockout zebrafish. *General and Comparative Endocrinology*, *282*, 113218.

Wu, X., Zhou, R., Wang, Y., Zhang, W., Zheng, X., Zhao, G., & Ding, Y. (2022). Genome-wide scan for runs of homozygosity in Asian wild boars and Anqing six-end-white pigs. *Animal Genetics*, *53*, 867-871.

Xie, R., Shi, L., Liu, J., Deng, T., Wang, L., Liu, Y., & Zhao, F. (2019). Genome-wide scan for runs of homozygosity identifies candidate genes in three pig breeds. *Animals*, *9*, 518.

Xing, J., Zhang, A., Du, Y., Fang, M., Minze, L. J., Liu, Y. J., & Zhang, Z. (2021). Identification of poly (ADP-ribose) polymerase 9 (PARP9) as a noncanonical sensor for RNA virus in dendritic cells. *Nature Communications*, *12*, 2681.

Xu, C., Wang, X., Zhou, S., Wu, J., Geng, Q., Ruan, D., & Yang, J. (2021). Brain transcriptome analysis reveals potential transcription factors and biological pathways

associated with feed efficiency in commercial DLY pigs. *DNA and Cell Biology*, *40*, 272-282.

Xu, H., Chai, S., Wang, Y., Wang, J., Xiao, D., Li, J., & Xiong, N. (2020). Molecular and clinical characterization of PARP9 in gliomas: a potential immunotherapeutic target. *CNS Neuroscience & Therapeutics*, *26*, 804-814.

Xu, L., Yang, L., Wang, L., Zhu, B., Chen, Y., Gao, H., & Li, J. (2019). Probe-based association analysis identifies several deletions associated with average daily gain in beef cattle. *BMC Genomics*, *20*, 1-10.

Xue, Y., Zhou, S., Xie, W., Meng, M., Ma, N., Zhang, H., & Shen, X. (2022). STIM1–Orai1 interaction exacerbates lps-induced inflammation and endoplasmic reticulum stress in bovine hepatocytes through store-operated calcium entry. *Genes*, *13*, 874.

Yamauchi, K., & Kurosaka, A. (2009). Inhibition of glycogen synthase kinase-3 enhances the expression of alkaline phosphatase and insulin-like growth factor-1 in human primary dermal papilla cell culture and maintains mouse hair bulbs in organ culture. *Archives of Dermatological Research*, *301*, 357-365.

Yamamoto, S., Shimizu, S., Kiyonaka, S., Takahashi, N., Wajima, T., Hara, Y., & Mori, Y. (2008). TRPM2-mediated Ca2+ influx induces chemokine production in monocytes that aggravates inflammatory neutrophil infiltration. *Nature Medicine*, *14*, 738-747.

Yan, H., Wu, L., Shih, C., Hou, S., Shi, J., Mao, T., & Qi, H. (2017). Plexin B2 and semaphorin 4C guide T cell recruitment and function in the germinal center. *Cell Reports*, *19*, 995-1007.

Yan, Q., Xu, R., Zhu, L., Cheng, X., Wang, Z., Manis, J., & Shipp, M. A. (2013). BAL1 and its partner E3 ligase, BBAP, link Poly (ADP-ribose) activation, ubiquitylation, and double-strand DNA repair independent of ATM, MDC1, and RNF8. *Molecular and Cellular Biology*, *33*, 845-857.

Yang, F., Gong, J., Wang, G., Chen, P., Yang, L., & Wang, Z. (2016). Waltonitone inhibits proliferation of hepatoma cells and tumorigenesis via FXR-miR-22-CCNA2 signaling pathway. *Oncotarget*, *7*, 75165.

Yang, J., Lee, S. H., Goddard, M. E., & Visscher, P. M. (2011). GCTA: a tool for genome-wide complex trait analysis. *The American Journal of Human Genetics*, *88*, 76-82.

Yang, J. I., Li, W. R., Lv, F. H., He, S. G., Tian, S. L., Peng, W. F., & Liu, M. J. (2016). Whole-genome sequencing of native sheep provides insights into rapid adaptations to extreme environments. *Molecular Biology and Evolution*, *33*, 2576-2592.

Yang, L., Niu, Q., Zhang, T., Zhao, G., Zhu, B., Chen, Y., & Xu, L. (2021). Genomic sequencing analysis reveals copy number variations and their associations with economically important traits in beef cattle. *Genomics*, *113*, 812-820.

Yang, Y., Hui, Y., Guo, Z., Song, X., Zhu, H., Pan, C., & Lan, X. (2022). Investigation of the association between goat DNMT3B gene polymorphism and growth traits. *Animal Biotechnology*, 1-7.

Yin, S., Song, G., Gao, N., Gao, H., Zeng, Q., Lu, P., & He, J. (2023). Identifying Genetic Architecture of Carcass and Meat Quality Traits in a Ningxiang Indigenous Pig Population. *Genes*, *14*, 1308.

Yin, X., Wu, Y., Zhang, S., Zhang, T., Zhang, G., & Wang, J. (2021). Transcriptomic profile of leg muscle during early growth and development in Haiyang yellow chicken. *Archives Animal Breeding*, *64*, 405-416.

Yu, G., Wang, L. G., Han, Y., & He, Q. Y. (2012). clusterProfiler: an R package for comparing biological themes among gene clusters. *Omics: A Journal of Integrative Biology*, *16*, 284-287.

Yu, Y., Yao, R., Wang, L., Fan, Y., Huang, X., Hirschhorn, J., & Shen, Y. (2015). De novo mutations in ARID1B associated with both syndromic and non-syndromic short stature. *BMC Genomics*, *16*, 1-10.

Yuan, C., Lu, Z., Guo, T., Yue, Y., Wang, X., Wang, T., & Yang, B. (2021). A global analysis of CNVs in Chinese indigenous fine-wool sheep populations using whole-genome resequencing. *BMC Genomics*, *22*, 1-10.

Yuan, J., Dou, T., Ma, M., Yi, G., Chen, S., Qu, L., & Yang, N. (2015). Genetic parameters of feed efficiency traits in laying period of chickens. *Poultry Science*, *94*(7), 1470-1475.

Yuan, J., Li, S., Sheng, Z., Zhang, M., Liu, X., Yuan, Z., & Chen, J. (2022). Genome-wide run of homozygosity analysis reveals candidate genomic regions associated with environmental adaptations of Tibetan native chickens. *BMC Genomics*, *23*(1), 91.

Yoon, S., Xuan, Z., Makarov, V., Ye, K., & Sebat, J. (2009). Sensitive and accurate detection of copy number variants using read depth of coverage. *Genome Research*, *19*, 1586-1592.

Zanella, R., Gava, D., de Oliveira Peixoto, J., Schaefer, R., Ciacci-Zanella, J. R., Biondo, N., & Ledur, M. C. (2015). Unravelling the genetic components involved in the immune response of pigs vaccinated against influenza virus. *Virus Research*, *210*, 327-336.

Zhang, F., Gu, W., Hurles, M. E., & Lupski, J. R. (2009). Copy number variation in human health, disease, and evolution. *Annual Review of Genomics and Human Genetics*, *10*, 451-481.

Zhang, H., Wang, Z., Wang, S., & Li, H. (2012). Progress of genome wide association study in domestic animals. *Journal of Animal Science and Biotechnology*, *3*, 1-10.

Zhang, J. M., Hoffmann, R., & Sieber-Blum, M. (1997). Mitogenic and anti-proliferative signals for neural crest cells and the neurogenic action of TGF-β1. *Developmental Dynamics: An Official Publication of the American Association of Anatomists*, *208*, 375-386.

Zhang, L., Wang, Y., Wu, G., Rao, L., Wei, Y., Yue, H., & Wang, C. Y. (2020). Blockade of JAK2 protects mice against hypoxia-induced pulmonary arterial hypertension by repressing pulmonary arterial smooth muscle cell proliferation. *Cell Proliferation*, *53*, e12742.

Zhang, N., Shen, J., Gou, L., Cao, M., Ding, W., Luo, P., & Zhang, J. (2022). UBE3A deletion enhances the efficiency of immunotherapy in non-small-cell lung cancer. *Bioengineered*, *13*, 11577-11592.

Zhang, Q., Guldbrandtsen, B., Bosse, M., Lund, M. S., & Sahana, G. (2015). Runs of homozygosity and distribution of functional variants in the cattle genome. *BMC Genomics*, *16*, 1-16.

Zhang, H., Wu, Z., Yang, L., Zhang, Z., Chen, H., & Ren, J. (2021). Novel mutations in the Myo5a gene cause a dilute coat color phenotype in mice. *The FASEB Journal*, *35*, e21261.

Zhang, X., Wang, K., Wang, L., Yang, Y., Ni, Z., Xie, X., & Qiu, Q. (2016). Genome-wide patterns of copy number variation in the Chinese yak genome. *BMC Genomics*, *17*, 1-12.

Zhang, T., Li, H., Larsen, P. F., Ba, H., Shi, H., Zhang, H., & Liu, Z. (2023). The Genetic Diversity of Mink (Neovison vison) Populations in China. *Animals*, *13*, 1497.

Zhao, G., Liu, Y., Niu, Q., Zheng, X., Zhang, T., Wang, Z., & Xu, L. (2021). Runs of homozygosity analysis reveals consensus homozygous regions affecting production traits in Chinese Simmental beef cattle. *BMC Genomics*, *22*, 1-12.

Zhao, M., Wang, Q., Wang, Q., Jia, P., & Zhao, Z. (2013). Computational tools for copy number variation (CNV) detection using next-generation sequencing data: features and perspectives. *BMC Bioinformatics*, *14*, 1-16.

Zheng, L. I., Zhang, G. M., Dong, Y. P., Wen, Y. F., Dong, D., Lei, C. Z., & Huang, Y. Z. (2019). Genetic variant of MYLK4 gene and its association with growth traits in Chinese cattle. *Animal Biotechnology*, *30*, 30-35.

Zheng, X., Zhao, P., Yang, K., Ning, C., Wang, H., Zhou, L., & Liu, J. (2020). CNV analysis of Meishan pig by next-generation sequencing and effects of AHR gene CNV on pig reproductive traits. *Journal of Animal Science and Biotechnology*, *11*, 1-11.

Zhong, Z. Q., Li, R., Wang, Z., Tian, S. S., Xie, X. F., Wang, Z. Y., & Xiao, Q. (2023). Genome-wide scans for selection signatures in indigenous pigs revealed candidate genes relating to heat tolerance. *Animal*, 100882.

Zhou, J., Hu, M., He, M., Wang, X., Sun, D., Huang, Y., & Zhang, P. (2021). TNFAIP3 Interacting Protein 3 Is an Activator of Hippo-YAP Signaling Protecting Against Hepatic Ischemia/Reperfusion Injury. *Hepatology*, *74*, 2133-2153.

Zhou, R., To, K. K. W., Wong, Y. C., Liu, L., Zhou, B., Li, X., & Chen, Z. (2020). Acute SARS-CoV-2 infection impairs dendritic cell and T cell responses. *Immunity*, *53*(4), 864-877.

Zhou, Y., Connor, E. E., Wiggans, G. R., Lu, Y., Tempelman, R. J., Schroeder, S. G., & Liu, G. E. (2018). Genome-wide copy number variant analysis reveals variants associated with 10 diverse production traits in Holstein cattle. *BMC Genomics*, *19*, 1-9.

Zhou, Y., Liu, Y., Jiang, X., Du, H., Li, X., & Zhu, Q. (2010). Polymorphism of chicken myocyte-specific enhancer-binding factor 2A gene and its association with chicken carcass traits. *Molecular Biology Reports*, *37*, 587-594.

Zhu, H., & Zheng, C. (2021). When PARPs meet antiviral innate immunity. *Trends in Microbiology*, *29*, 776-778.

Zhu, M., Zhang, H., Yang, H., Zhao, Z., Blair, H. T., Zhai, M., & Xie, M. (2022a). Polymorphisms and association of GRM1, GNAQ and HCRTR1 genes with seasonal reproduction and litter size in three sheep breeds. *Reproduction in Domestic Animals*, *57*, 532-540.

Zhu, Y., Liu, X., Wang, Y., Liu, L., Wang, Y., Zhao, G., & Cui, H. (2022). Genome-Wide Association Study Revealed the Effect of rs312715211 in ZNF652 Gene on Abdominal Fat Percentage of Chickens. *Biology*, *11*, 1849.

Ziegler, T. E., Molina, A., Ramón, M., Sanchez, M., Muñoz-Mejías, E., Antonini, A., & Demyda-Peyrás, S. (2023). Analysis of the genomic landscape of inbreeding in two divergent groups of Spanish Florida goats. *Journal of Animal Breeding and Genetics*, *140*, 316-329.

Zinovieva, N. A., Dotsev, A. V., Sermyagin, A. A., Deniskova, T. E., Abdelmanova, A. S., Kharzinova, V. R., & Brem, G. (2020). Selection signatures in two oldest Russian native cattle breeds revealed using high-density single nucleotide polymorphism analysis. *PLoS One*, *15*, e0242200.

Zschille, J., Stier, N., & Roth, M. (2010). Gender differences in activity patterns of American mink *Neovison vison* in Germany. *European Journal of Wildlife Research*, *56*, 187-194.

APPENDIX 1. List of publications and conference presentations (as of 19 December 2023)

1. Based on chapter 2:

   Davoudi, P., Do, D., Colombo, S., Rathgeber, B., & Miar, Y. (2022). Application of genetic, genomic, and biological pathways in improvement of swine feed efficiency. **PUBLISHED** in **Frontiers in Genetics**, 13:903733.

2. Based on chapter 3:

   Davoudi, P., Do, D., Colombo, S., Rathgeber, B., Hu, G., Sargolzaei, M., Wang, Z., Plastow, G., & Miar, Y. (2022). Genetic and phenotypic parameters for feed efficiency and component traits in American mink. **PUBLISHED** in **Journal of Animal Science,** 216:1-10.

3. Based on chapter 4:

   Davoudi, P., Do, D., Colombo, S., Rathgeber, B., Sargolzaei, M., Wang, Z., Plastow, G., Karimi, K., Hu, G., Valipour, S., & Miar, Y. (2022). Genome-wide detection of copy number variation in American mink using whole-genome sequencing. **PUBLISHED** in **BMC Genomics***,* 23:649.

4. Based on chapter 5:

   Davoudi, P., Do, D., Rathgeber, B., Colombo, S., Sargolzaei, M., Wang, Z., Plastow, G., Hu, G., Valipour, S., & Miar, Y. (2023). CNV-based association study of feed efficiency, growth traits, pelt quality traits, and Aleutian disease in American mink. **SUBMITTED** in **Scientific Reports.**

   AND

Davoudi, P., Do, D., Sargolzaei, M., Wang, Z., Plastow, & Miar, Y. (2023). Genome-wide association study between copy number variations and economically important traits in American mink. *International Society for Animal Genetics.* Cape Town, South Africa*,* July 2-7.

5. Based on chapter 6:

   Davoudi, P., Do, D., Rathgeber, B., Colombo, S., Sargolzaei, M., Wang, Z., Plastow, & Miar, Y. (2023). Characterization of runs of homozygosity islands in American mink using whole-genome sequencing data. **SUBMITTED** in **Journal of Animal Breeding and Genetics.**

   AND

   Davoudi, P., Do, D., Sargolzaei, M., Wang, Z., Plastow, & Miar, Y. (2023). Characterization of runs of homozygosity islands in American mink using whole-genome sequencing data. *ASAS-CSAS Annual Meeting and Trade Show.* Albuquerque, USA, July 16-20.

6. Based on chapter 7:

   Davoudi, P., Do, D., Rathgeber, B., Colombo, S., Sargolzaei, M., Wang, Z., Plastow, & Miar, Y. (2023). Identification of consensus homozygous regions and their associations with growth and feed efficiency traits in American mink. **SUBMITTED** in **PLOS One.**

   AND

   Davoudi, P., Do, D., Sargolzaei, M., Wang, Z., Plastow, & Miar, Y. (2023). Identification of consensus homozygous regions and their associations with growth and feed efficiency traits in American mink. *International Society for Animal Genetics.* Cape Town, South Africa*,* July 2-7.

7. Based on chapter 8:

   Davoudi, P., Do, D., Colombo, S., Rathgeber, B., Sargolzaei, M., Wang, Z., Plastow, & Miar, Y. (2023). Genome-wide association studies for growth and feed

efficiency traits in American mink. **SUBMITTED** in **Canadian Journal of Animal Science.**

AND

Davoudi, P., Do, D., Sargolzaei, M., Wang, Z., Plastow, G., Hu, G., Valipour, S., & Miar, Y. (2023). Genome-wide association study for feed efficiency and growth traits in American mink. *ASAS-CSAS Annual Meeting and Trade Show.* Albuquerque, USA, July 16-20.